How did mammals evolve into their ecological niches through time? Quantitative tests for classic macroevolutionary questions

Gemma Louise Benevento

The Queen's College
Department of Earth Sciences
University of Oxford



Submitted to the University of Oxford for the degree
Doctor of Philosophy in Earth Sciences
Trinity 2018

Supervised by Professor Matt Friedman and
Professor Roger B.J. Benson

Declaration

The contents of this thesis are all my own work, except where otherwise stated. The views and opinions expressed herein are mine and not necessarily those of any other person or body unless so attributed.



Gemma Louise Benevento

Acknowledgements

I would like to thank my two supervisors Roger Benson and Matt Friedman, without whom none of this would have been possible. Throughout my time here I have learnt more from them both than I could ever express, and their continued guidance and mentoring has allowed me to arrive at a completed thesis a more confident and competent palaeontologist. I couldn't have hoped for a better supervisory team, or two more inspiring scientists.

I'm also grateful to the following people for offering help with analyses and methods when needed: Neil Brocklehurst, John Clarke, Roger Close, Luke Parry, and David Bapst. Science is a collaborative subject, and without the help of my colleagues I would have been lost numerous times. I would additionally like to thank my thesis examiners, Erin Saupe and Guillaume Billet, for their thoughtful comments and guidance, and for an enjoyable viva experience.

During my time here at Oxford, I've benefitted academically and personally from the presence of a large and social palaeontological community. Their collective wisdom has enlightened and challenged me, and their friendship has been invaluable. I am hugely grateful for their readiness to offer both. Listed hereafter are all of the people that are, or have been, a part of this wider palaeo lab during my time at Oxford: Roger Benson, Matt Friedman, Erin Saupe, John Clarke, James Neenan, Donald Davesne, Sam Giles, Neil Brockelhurst, Roger Close, Andrzej Wolniewicz, Laura Soul, Dan Delbarre, Valantin Fischer, Mimi

Harrison, David Ford, Serjoscha Evers, César Augusto Espinoza Campuzano, Marie-Claire Koschowitz, Imran Raman, Claire Dobson, Alberto Martín Serra, Felipe De La Parra, Ricardo Pérez-de la Fuente, Duncan Murdock, Brooke Johnson, Harrie Drage, Steve Pates, George Fernandez, Alex Bjarnason, and Armin Schmitt.

Four of these lab members have played a special role in my time at Oxford. Myself, Mimi, David, Serjoscha, and Harrie all started on the DTP in 2014, and have made this journey together. On top of this, Mimi, Dave, Serjoscha and I have shared an office for the last 4 years, along with Tom Lamont, our long-suffering hard rock geologist office mate. I am especially thankful to all of these guys for providing support throughout, and apologies to Tom for 4 years of listening to us talk about palaeontology.

As well as being part of a fantastic lab and a great office, I am privileged to be part of the wider Earth Science department as well. Thanks to everyone that has been part of this department over the last four years. Thanks also for the opportunities I was given to demonstrate in undergraduate labs and on field trips. I am particularly grateful to all of the members of my own year group across the Earth Science disciplines, there are too many individuals to name but many of you have been an important part of my time at Oxford.

Throughout my DPhil I undertook numerous collections visits, and I would like to thank the following people for hosting me at their institutions and/or arranging access to specimens in their care: Hilary Ketchum (OUMNH), Judy

Galkin (AMNH), Ken Rose (Johns Hopkins University), Amy Henrici (Carnegie Museum), Chris Norris & Dan Brinkman (Yale Peabody Museum), Amanda Millhouse (Smithsonian Institution NMNH), Bill Simpson, Adrienne Stroup & Susumu Tomiya (Chicago Field Museum), Thomas Lehmann & Elvira Brahm (Naturmuseum Senckenburg), and Norbert Micklich (Hessisches Landesmuseum Darmstadt).

During these collections visits I also benefited socially and financially from staying with friends on three occasions, and I am grateful for their hospitality and friendship; thanks to former lab member Laura Soul for having me to stay in Washington DC, to colleague Rachel Frigot for her hospitality in Baltimore, and to my childhood friend Cara Myers for letting me stay with her in New York.

As well as being a former lab member and providing methodological help on occasion, I further thank John Clarke for his patience, care and support as my partner throughout the near entirety of my DPhil. As a palaeontologist himself, he was able to support me academically in ways that many other couples cannot enjoy, but most important is his personal encouragement and love on a daily basis, and I continue to feel privileged to have met him.

Special thanks to my parents and siblings for continuous support in everything I do, and further thanks to my parents for considerable financial support during large periods of my academic career. From a young age my parents have encouraged mine and my younger brother Toby's interest in science and the Earth Sciences, and did all they could to foster this interest with trips to

museums, science fairs, and geologically impressive locations across the world. I know that Toby's Masters in Geology and my completion of a DPhil makes them proud and I hope that it shows them that their dedication was appreciated and worthwhile.

Many people have been important in furthering my academic career over the past 10 years, but a small number have been instrumental. I consider the following people, alongside my current supervisors, among the latter. After being taught by Richard Twitchett during my undergraduate degree, he has been pushing me to pursue my dreams ever since, and has consistently provided good advice and encouragement. Graeme Lloyd provided me with my first opportunity to undertake macroevolutionary research by taking me on as a student for my MSc thesis. Graeme introduced me to a number of macroevolutionary methods and taught me to program in R, a skill which has proved invaluable during my DPhil.

Lastly, I would like to thank all of the people that were involved in giving me this opportunity to study here at Oxford on the Environmental DTP and my funders NERC for making it financially possible. Palaeontology has been my passion since I was young, and studying for a PhD had been a life-goal. I couldn't have ever hoped to complete it among the dreaming spires.

Abstract

Observations that the taxonomic and ecomorphological diversity of mammals increased across the Cretaceous/Paleocene (K/Pg) boundary led to the model of adaptive radiation. These rapid and large-scale increases in diversity and disparity are thought to have resulted from unprecedented ecological opportunity for mammals in the wake of the K/Pg event, during which numerous niches previously occupied by the non-avian dinosaurs and other components of the Mesozoic fauna were cleared. Although patterns of increased body size and body size disparity have been thoroughly explored, fundamental questions remain regarding both the magnitude and exact nature of mammalian ecomorphological change across the K/Pg boundary. It has long been established that Cenozoic mammals appear to exhibit a wider range of ecomorphotypes associated with feeding ecology in comparison to the Mesozoic. Here I use a dataset of six functionally-relevant traits made up of ten continuous character measurements across 276 fossil and 730 modern (including 23 recently extinct Pleistocene megafauna) mammal jaws to quantify and explore patterns of jaw ecomorphological disparity from the Late Triassic–end-Eocene and Pleistocene–Recent. I further explore the evolutionary rate across the K/Pg boundary by analysing six functional jaw traits for 69 Jurassic-Eocene mammals in a phylogenetic framework. The results presented herein demonstrate that, despite an immediate increase in therian mammal jaw ecomorphological disparity across the K/Pg boundary, mammals as a whole did

not show an increase until the Paleocene/Eocene boundary. This lag of ~10 My is interpreted as an interval of ecological recovery, during which high rates of mandibular ecomorphological trait evolution are detected. Much of the Paleocene/Eocene increase in disparity can be attributed to mammals with larger body sizes. My results are indicative of an adaptive radiation of placental mammals in the early Paleogene, in response to large-scale niche clearing.

Extended Abstract

Extant mammals are a taxonomically diverse clade and exhibit an incredible diversity of skeletal form and function. They inhabit almost all regions of the Earth and occupy a body size range spanning almost seven orders of magnitude and highly disparate ecologies. In particular, mammals exhibit a wide range of feeding and locomotor ecologies. These include, but are not limited to, the volant, nocturnal lifestyle of bats, the fully aquatic, suspension-feeding baleen whales, the arboreal primates, the fossorial moles, golden moles and marsupial moles, ungulates and carnivorans with cursorially-adapted forelimbs, and the hypercarnivorous felids. Each of these unique modes of life influence skeletal ecomorphology, resulting in a diverse range of skeletal adaptations among mammals.

Despite a long evolutionary history dating back some 240 million years, the fossil record suggests that much of the taxonomic and morphological diversity seen among extant mammals accumulated since the Cretaceous/Paleogene (K/Pg) extinction event. Mammals that lived prior to the extinction event during the Mesozoic have been categorised as small, generalised, shrew-like organisms, and are often referred to as having lived 'in the shadow of the dinosaurs'. It is generally hypothesized that the dinosaurs, which dominated ecosystems throughout the Mesozoic, suppressed mammalian ecomorphological disparity by excluding them from particular habitats and resources. Under this model, the extinction of non-avian dinosaurs at the end of the Cretaceous is taken to represent an 'ecological release' that opened up niche

space, providing opportunities for clades that survived the mass extinction event. This ecological opportunity was taken by mammals, and in particular therian mammals, the clade that comprises the last common ancestor of placentals and marsupials and all of their descendants. Confronted with a less constrained ecological landscape, mammals appear to radiate into numerous novel ecomorphologies, exhibiting previously-unrecognised body sizes and ecological adaptations.

Complicating this classic story, however, are a number of new fossil mammal specimens from the Mesozoic, which appear to exhibit ecomorphologies previously thought to have been suppressed prior to the K/Pg boundary. Fossorial, arboreal, semiaquatic, carnivorous, gumnivorous, and even gliding adaptations are now recognised among Mesozoic mammals, and a mid-Jurassic radiation has subsequently been proposed, calling into question this classic narrative of pre-Cenozoic conservatism.

Although it is now clear that this hypothesis of Mesozoic suppression may be more complicated than once thought, it is nevertheless true that mammals known from the earliest Cenozoic exhibit many functional traits not known for Mesozoic mammals. Most obvious is a discrepancy in mean and maximum body size between Mesozoic and Cenozoic mammals, but there are also locomotor modes and feeding ecologies unique to post-K/Pg faunas, such as cursoriality, fully aquatic, flying, hypercarnivory, and specialist herbivores. This rapid and substantial increase in mammalian maximum body size and body size disparity, ecomorphological disparity, and associated taxonomic diversity was the basis of the theory of adaptive radiation, where clades may undergo an

early burst of taxonomic and morphological evolution in response to ecological opportunity.

Two main explanations for the way in which ecomorphological disparity accumulated along lineages across the K/Pg boundary have been proposed. The first is an increase in evolutionary *rate*, such that disparity accumulates more quickly among lineages. Adaptive radiation is predicted to be accompanied by elevated rates of trait evolution, and may be central in producing evolutionarily successful clades. The second is a change in the *mode* of evolution at the K/Pg boundary. This hypothesizes that competition from the dinosaurs acted as a constraint on Mesozoic mammal evolution, resulting in an Ornstein-Uhlenbeck-like evolutionary mode, whereby mammals were unable to diverge substantially from a trait optimum. Once the competition was removed, however, mammals were able to evolve under a diffusive Brownian motion evolutionary mode without such constraints, accumulating disparity as a function of time.

Historically these ideas were laid out in qualitative terms, and more recently quantitative studies have begun to investigate the patterns and processes associated with the accumulation of ecomorphological disparity in Mesozoic/Cenozoic mammals. Despite substantial interest in these classic macroevolutionary questions, much of the previous work has focused on changes in body size in mammals, or quantified ecomorphological disparity along different axes across a restricted taxonomic sample or on a short temporal scale.

In light of this, I produced an extensive dataset of functionally-relevant continuous character traits for the mandibles of 1006 fossil and extant

mammals, spanning the entire mammalian clade and including fossil specimens from the Late Triassic – end-Eocene. This is the largest dataset of functionally-relevant mandibular traits currently compiled for mammals, and allows me to quantitatively assess mandibular ecomorphological disparity patterns among all mammals throughout the Mesozoic, Cenozoic, and Recent, and in particular across the K/Pg boundary. The mandible was used because it has good preservation potential in comparison to other skeletal elements, it contains a large amount of taxonomic information, and, most importantly, its morphology is intrinsically linked to feeding ecology, an important biological trait.

First, I assess patterns of mandibular disparity throughout the Mesozoic and early Paleogene using a subset of 272 fossil terrestrial mammal mandibles. Six functionally relevant mandibular ratios consisting of ten continuous character traits were subjected to a principal components analysis and function space was plotted through time using Mesozoic epochs and Cenozoic North American Land Mammal Ages (NALMAs) as time bins. Additionally, disparity through time was calculated using a number of variance- and range- based metrics (minimum spanning tree (MST) length, sum of variance, sum of ranges, mean pairwise distances, and mean distance from centroid). My results show low overall jaw ecomorphological disparity throughout the Mesozoic, as well as across the K/Pg boundary, with total mammal disparity increasing significantly for the first time across the Paleocene/Eocene boundary. Conversely, therian mammals (marsupials + placentals) show a consistent increase in disparity from the Cretaceous onward. This pattern of therian increase but overall stasis in mammalian ecomorphological disparity indicates a period of therian

replacement during the Paleocene, whereby therian mammals occupy regions of function space previously occupied by non-therians during the Mesozoic. By the Paleocene/Eocene boundary, however, therian mammals had explored regions of function space that had not previously been occupied, increasing overall mammal disparity above Mesozoic levels.

Second, I test whether suppressed body size restricted the mandibular ecomorphological disparity of Mesozoic mammals. A clear increase in maximum body mass and body mass disparity is associated with a suite of novel ecomorphologies across the K/Pg boundary. Body mass correlates with almost every aspect of an organism's biology, and it has been proposed that large-bodied mammals require more eccentric skeletal morphologies to perform specialised ecological tasks. I therefore test whether all of the expansion of jaw functional disparity seen in mammals after the K/Pg boundary can be explained by the origin of large-bodied mammals, larger than those known from the Mesozoic. In other words, did the release of body size constraint result in increased jaw disparity among early Cenozoic mammals. To do so, I use the full dataset of 1006 mammalian mandibles, comprising 276 terrestrial and aquatic fossil mammals from the Late Triassic – end Eocene, and 730 extant and recently extinct mammals (26 of which are members of the Pleistocene megafauna). Principal components analyses were again conducted for this full dataset, and disparity through time for small and large mammals was calculated (using a number of small-to-large cut off values). My results suggest that mammals with body sizes in the upper 80th percentile of Mesozoic mammal (and larger) do exhibit higher mandibular ecomorphological from the Eocene

onward. This finding suggests that the small body sizes of most Mesozoic mammals explains their relatively conservative ecomorphologies, and that larger-bodied Mesozoic mammals were too scarce to fully explore the available function space. The pattern of increased disparity among larger-bodied Cenozoic mammals is driven primarily by patterns in artiodactyls, horses, and proboscideans.

Third and finally, I test the rate of mandibular ecomorphological trait evolution across a comprehensive supertree of mammals produced from two published phylogenies. This supertree spans all mammalian clades and includes mammals from the Late Triassic–end-Eocene. In order to remain consistent with the previous chapters, I use the six principal components axes from chapter 1 to assess rate though time. The supertree was timescaled under the Fossil Birth Death model, and evolutionary rate along branches were calculated. My analysis identifies three periods of increased rate across the mammal tree; one at the origin of the mammaliaform clade, one during the mid-Jurassic radiation of stem therian mammals, and one associated with the appearance of placental mammals. Rates were high among the earliest branching mammaliaforms, likely due to the initial evolution of traits associated with the mammal-like jaw. Analysing rates across Jurassic and Cretaceous/Paleogene mammals together allows for direct comparison between the two proposed radiations for the first time. As is suggested by the fossil record, I find evidence to suggest that the Jurassic radiation concerned fewer mammal clades and the evolution of fewer functional traits than did the placental radiation. Here, the placental radiation is associated with a rate increase of at least three times

background levels, consistent with the hypothesis that placental mammals underwent a substantial adaptive radiation.

Contents

Acknowledgements……iii

Abstract……vii

Extended Abstract……ix

Introduction to Thesis……1

Chapter 1: **Patterns of mammalian jaw ecomorphology during the Mesozoic/Cenozoic transition**

Introduction……33

Methods……36

Results……41

Discussion……48

Conclusion……56

Chapter 2: **The effects of size on jaw functional disparity through time in mammals**

Introduction……59

Methods……64

Results……72

Discussion……92

Conclusion……100

Chapter 3: **Rates of jaw functional trait evolution among Mesozoic and early Cenozoic mammals**

Introduction……103

Methods……107

Results……119

Discussion……127

Conclusion……132

Thesis Conclusions……133

Future Directions……137

References……141

Supplementary Materials

Sup. Mat. For Chapter 1……169

Sup. Mat. For Chapter 2……201

Sup. Mat. For Chapter 3……219

Supplementary References……245

Introduction to Thesis

"It is as if the curtain were rung down suddenly on a stage where all the leading roles were taken by reptiles, especially dinosaurs, in great numbers and bewildering variety, and rose again immediately to reveal the same setting but an entirely new cast, a cast in which the dinosaurs do not appear at all, other reptiles are mere supernumeraries, and the leading parts are all played by mammals of sorts barely hinted at in the preceding acts."

George Gaylord Simpson, 1937

So contrasted are the fossil tetrapod faunas either side of the Mesozoic/Cenozoic boundary that GG Simpson was moved to write the preceding passage, which eloquently highlights this dramatic nature of turnover at the Cretaceous/Paleogene (K/Pg) boundary (Simpson, 1937). The mass extinction event at the end of the Cretaceous closed the door on a world dominated by dinosaurs and other reptiles and ushered in a new age: the 'age of mammals' (Simpson, 1937). This worldwide appearance of countless new mammal species exhibiting previously-unrecognised morphologies in the aftermath of the K/Pg mass extinction event (66 Ma) (Osborn, 1902, Simpson, 1937, Rose, 2006) occurred so abruptly that the then pre-existing evolutionary theories did not provide an adequate explanation. The theory of adaptive radiation was therefore erected to explain the way in which clades may radiate rapidly into many disparate and novel niches and associated ecomorphologies

in response to large-scale ecological opportunity (Osborn, 1902). This thesis is dedicated to furthering our understanding of the evolutionary patterns and processes associated with the mammalian radiation.

The Evolutionary History of Mammaliformes

The earliest Mammaliaformes occur in the fossil record in the Late Triassic, and are nested within a group of 'mammal-like reptiles' (synapsids) known as cynodonts (Hopson & Kitchling, 2001, Kielan-Jaworowska et al, 2004, Kemp, 2005). Mammaliaformes are a stem-based group united by a series of derived features. Mammaliaformes includes the mammal crown group plus a series of crownward radiations on the mammalian stem lineage. *Adelobasileus* from the Late Triassic of Texas (Lucas & Hunt, 1990) and *Sinoconodon* from the Early Jurassic of China (Zhang et al, 1998, Kielan-Jaworowska et al, 2004) are generally accepted to be among the most basally branching mammaliaforms (Lucas & Hunt, 1990, Lucas & Luo, 1993). The morganucodontids, known from the Middle Triassic – Middle Jurassic of Europe, Asia, North America, and Africa, are also resolved as early diverging mammaliaforms. The position of a clade known as the haramiyidans (consisting of the haramiyids and eleutherodontids) continues to be heavily debated (Luo et al, 2015, Han et al, 2017). Recent studies from two groups of authors have found evidence for the placement of haramiyidans both among the earliest mammaliaforms (Luo et al, 2015, Meng et al, 2017) and as close relatives of the multituberculates (Han et al, 2017, Zheng et al, 2013). The position of the haramiyidans has implications for the early evolution of mammaliaforms, as the placement of this clade closer to the

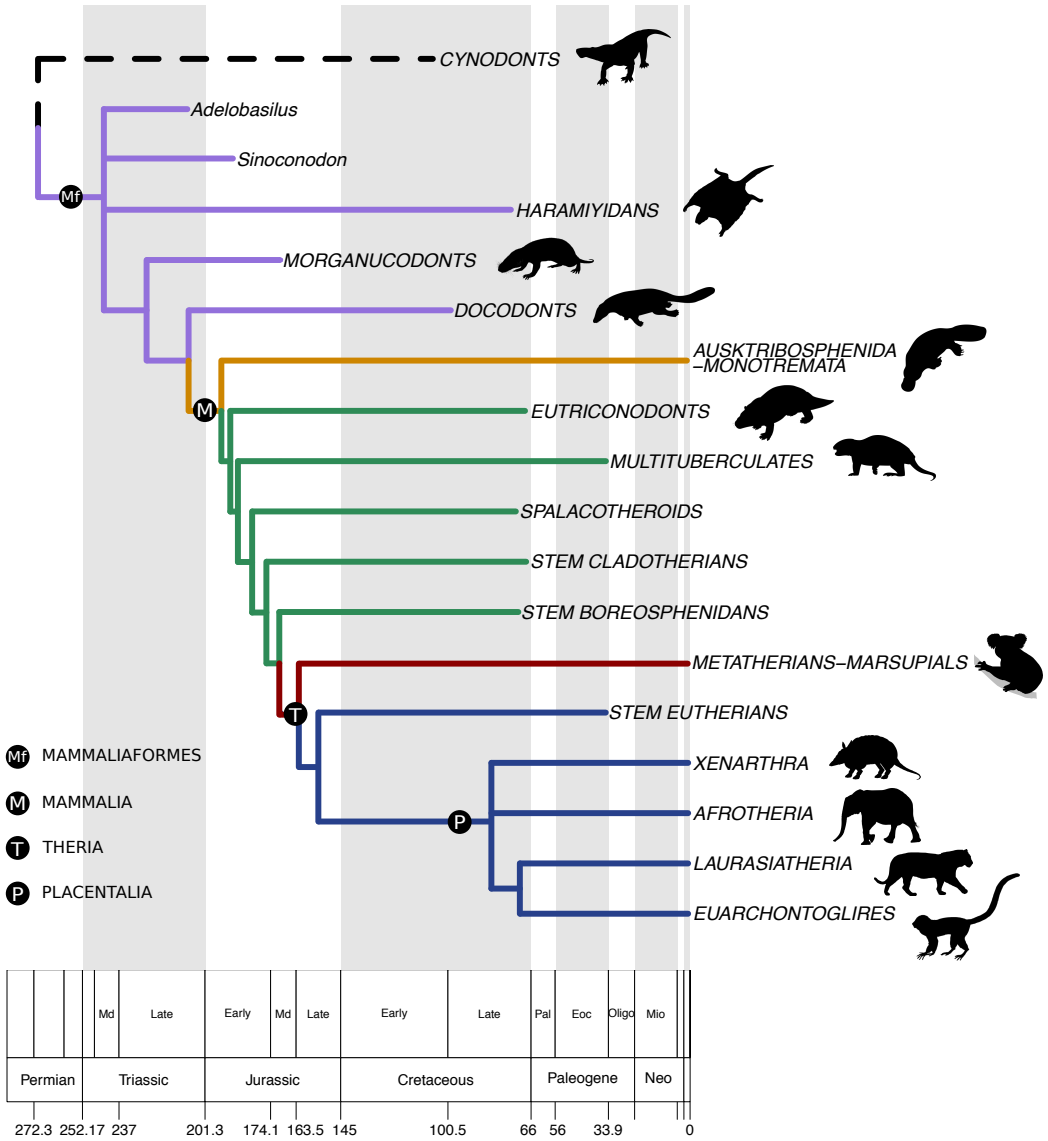


Figure i.1. Summary cladogram of Mammaliaformes, showing an overview of likely relationships between clades. Black dashed line depicts the mammaliaform outgroup. Purple shows stem mammals, orange the lineage leading to monotremes. Green branches are stem therian mammals. The red branch is the lineage leading to marsupials, and the blue branches indicate crown and stem eutherian mammals. Divergence and extinction ages are approximations. Based primarily on the cladograms presented in Luo (2007; figure 1b) and Macdonald (2006).

multituberculates moves them into the crown group of mammals, and out of the stem. Haramiyidans exhibit a suite of different ecomorphologies that have been suggested to relate to disparate ecologies within the group (Zheng et al, 2013, Bi et al, 2014, Han et al, 2017, Meng et al, 2017; outlined below under heading 'The

Mammalian Adaptive Radiation'). Placement of these taxa among basally branching mammaliaforms would be the first evidence for gliding outside of the mammal crown (Meng et al, 2017, Han et al, 2017), and would indicate that derived locomotor modes were present in some of the earliest mammaliaforms. The studies presented in this thesis include all mammaliaforms from *Adelobasileus* and *Sinoconodon* lineages onward, and consider haramiyidans among the early mammaliaforms, in accordance with Luo et al (2015).

The Middle Jurassic – Early Cretaceous docodonts represent another successful mammaliaform radiation (but see also Sigogneau-Russell and Godefroit (1997) for a contested Late Triassic occurrence (Butler, 1997)). Docodonts exhibit arguably the widest range of ecomorphologies among early mammaliaforms (see discussion below in 'The Mammalian Adaptive Radiation'), including fossorial, terrestrial, semiaquatic, and arboreal taxa (Ji, 2006, Luo, 2015, Meng, 2015). They are known from Europe, North America and Asia (Kielan-Jaworowska et al, 2004).

Crown Mammalia consist of the most recent common ancestor of placentals, marsupials (together crown Theria), and monotremes, plus all of its descendants, fossil and living. The australosphenidans are the earliest branching of these extant clades, and represent the group consisting of all taxa more closely related to living monotremes than to therian mammals. Despite restriction of modern australosphenidans (i.e. monotremes) to Australia, Tasmania and New Guinea, the oldest fossil australosphenidans (Middle Jurassic) are from Madagascar (Luo et al, 2001) and South America (Marti & Rauhut 2005). Their fossils are also known from the Late Jurassic – Paleocene of

South America, and have an Australian fossil record since the Early Cretaceous (Rich and Vickers-Rich, 2004, Kielan-Jaworowska et al, 2004). As well as being geographically restricted, extant monotremes are taxonomically conservative, with only five species belonging to two families: one species of short-beaked echidna (*Tachyglossus aculeatus*) and three species of long-beaked echidna (*Zaglossus*) within Tachyglossidae, and one species of platypus (*Ornithorynchus anatinus*) within Ornithorhynchidae (Nowak, 2006). Extant monotremes exhibit many physiological traits, particularly concerning reproductive strategy, that are unique to the group among mammals. They are the only extant mammals to lay eggs (oviparous), poses a cloaca, and lack nipples (lactating instead through glands in the skin). Although these traits seem peculiar in comparison to other living mammals, it is likely that at least some of these aspects of monotreme biology reflect primitive traits of the ancestral mammal. Until very recently, little conclusive evidence existed for reproductive strategy among mammal ancestors, however a newly discovered fossil of the cynodont *Kayentatherium wellesi*, was reported with a minimum of 38 perinates, substantially more than any living mammal species (Hoffman and Rowe, 2018). No eggshell was found associated with the fossil, but due to a poor preservation potential of monotreme-like eggshell it is still unclear whether *Kayentatherium* was viviparous or oviparous (Hoffman and Rowe, 2018).

There are more than 5000 extant species of therian mammals, making up more than 99% of all extant mammalian species and hugely outnumbering monotremes (Nowak, 2006). Stem therian mammals also played an important role in Mesozoic mammal faunas. The earliest branching stem therian

mammals are the eutriconodonts. Eutriconodonts comprise amphilestids, gobiconodonts, triconodonts, and other well-known eutriconodonts of uncertain familial affiliation such as the Early Cretaceous *Jeholodens jenkinsi*. They are known from the Middle Jurassic – mid Late Cretaceous of Europe, Asia, North America and Africa (Fox, 1969, Broderip, 1828, Fox, 1969).

Multituberculates are a speciose and long-lived clade of stem therian mammals which are immediately recognisable due to their highly derived dentition. Their fossils are known from the Middle Jurassic – Eocene, surviving the K/Pg extinction event. Multituberculates in fact reached their highest levels of diversity during the Paleocene (Wilson et al, 2012), and are prominent members of both Mesozoic and early Cenozoic mammal faunas. Multituberculates can be separated into two suborders, the plagiaulacids and the cimolodontans. Phylogenetic hypotheses for the relationships among multituberculates are somewhat poorly supported, with the more basally branching plagiaulacid taxa likely paraphyletic with respect to cimolodontans (McKenna and Bell, 1997). Kielan-Jaworowska and Hurum (2001) recognised three separate clades within Plagiaulacida; the allodontids, the paulchoffatiids and the plagiaulacids. Plagiaulacid multituberculates are known from the Middle Jurassic to the Early Cretaceous, and are found across Europe, North America, Asia and Africa. Cimolodontans (including djadochtatherids, taeniolabids, and ptilodontids) are known from the Early Cretaceous – Eocene of North America, Europe and Asia, with a tooth fragment recovered from South America (*Argentodite coloniensis*; Kielan-Jaworowska et al, 2007). The enigmatic gondwanatheres may also be

multituberculates (Gurovich & Beck 2009) or their sister taxon (Krausse et al. 2017).

Spalacotheroids (including zhangheotheriids) are defined by traits pertaining to the triangular arrangement of the principle cusps of the molars (Kielan-Jarowoska, 2004). Stem cladotherians (including the dryolestids), and stem boreosphenidans (those mammals more closely related to therians than to monotremes that possess tribosphenic molars (Luo et al, 2001)) are successively more crownward members of the therian mammal stem.

Theria (i.e. crown-group therian mammals) are subdivided into Metatheria, the total-group of Marsupialia, and Eutheria, the total-group of Placentalia. The age of divergence between Metatheria and Eutheria is debated but *Juramaia sinensis*, an early Late Jurassic mammal from China, has been proposed to belong to Eutheria (Luo et al, 2011, Bi et al, 2018, but see also Krause et al, 2014 for an opposing view), suggesting that this divergence occurred by the Middle Jurassic (Luo et al, 2011).

Extant metatherians (i.e. marsupials) are much less speciose than placentals, and are also more geographically restricted. According to recent studies, there are approximately 300 extant marsupials (Nowak, 2006), two-thirds of which are restricted to Australia and the surrounding islands from the Australasian region. The remaining marsupials can be found primarily in Central and South America, with the genus *Didelphis* also native to and widespread in North America. Metatherians have a somewhat poor Mesozoic record, but are known from the Cretaceous of Asia, Europe and North America (Kielan-Jarowoska, 2004, Benson et al, 2013). Deltatheroidean

mammals have been historically recovered as metatherians (Kielan-Jaworowska and Nessov, 1990), eutherians, and as stem therians (Lillegraven et al, 1979), but more recent studies consider them among the earliest branching metatherians (Williamson et al, 2014). Very few metatherian mammals are well-preserved, but the oldest fossil *Sinodelphys szalayi* and *Asiatherium reshetovi* are exceptions (Szalay and Trofimov, 1996, Luo et al, 2003). New research suggests that metatherian mammals underwent taxonomic increases in the wake of the K/Pg mass extinction, particularly in South America, and continued to radiate taxonomically until the Eocene. Australian metatherians show an increase in diversity during the Eocene/Oligocene (Bennett et al, 2018).

Placental mammals, the crown-group of Eutheria, today total more than 4500 species (Nowak, 2006), and are known from all corners of the world. They can be divided into the following clades (Macdonald, 2006): (a) Afrotheria a largely African radiation, including the paenungulates (elephants, hyraxes and dugongs) aardvarks, tenrecs and sengis; (b) Xenarthra, consisting of anteaters, sloths and armadilos, and primitively South American in distribution; (c) Laurasiatheria, a clade that originated on the northern supercontinent Laurasia and that unites cetartiodactyls, perissodactyls, carnivores, pangolins, bats, and eulipotyphylans (solenodons, hedgehogs, gymnures, moles and shrews); (d) Euarchontoglires, including rodents, lagomorphs, primates, tree shrews and colugos. Together Laurasiatheria and Euarchontoglires comprise Boreoeutheria.

The oldest eutherian mammal is debated. Most studies agree that *Eomaia scansorius* (~124 Ma) and the recently-described *Ambolestes zhoui* should be considered among eutherians (Ji et al, 2002, Bi et al, 2018), but the position of the considerably older *Juramaia sinensis* (~160 Ma) as the oldest eutherian is more debated (Averianov and Archibald, 2016, Luo et al, 2011). More basally branching eutherian clades include the zalambdalestids and the asioryctitherids from the Late Cretaceous of Asia. In the early Paleocene, eutherian mammals undergo rapid and substantial taxonomic (and ecomorphological; see below) radiation.

Cimolestids are a clade of either stem or crown placental mammals (see Halliday et al, 2017 for discussion of their proposed relationships) known from the Cretaceous of North America, and are also present in Paleocene faunas from North America and Europe (Rose, 2006, Grande, 2013). They exhibit considerable diversity of form, including the semi-aquatic pantolestids *Palaeosinopa didelphoides and Buxolestes piscator,* and a remarkable undescribed arboreal cimolested with an elongate, prehensile tail (Grande, 2013). Important among Paleocene mammals faunas are a group of mammals known as the 'condylarths', or 'archaic ungulates'. The 'condylarths', consisting of a number of subgroups such as the well-known arctocyonids, the phenacodontids, and the hyopsodontids, are now considered polyphyletic (Halliday et al, 2017). Phylogenetic placement of these mammals has been difficult, but a recent and comprehensive study of Paleocene mammal phylogeny by Halliday et al (2015; see also for an extensive review of alternative phylogenetic hypotheses for fossil eutherian

clades) recovered all 'condylarths' within the crown placental clade Laurasiatheria. Pantodonts are also relatively common in the Paleocene and Eocene, and appear to belong to Laurasistheria (Halliday et al, 2017). Pantodonts are among the first large-bodied omnivorous-herbivorous mammals, and are known throughout Asia and the Americas.

Although no overall consensus exists for the phylogenetic placement of all clades (or even individual species) of mammaliaforms, a long history of extensive work on this subject has advanced our understanding of the evolution of mammals substantially. Particular progress was made for relationships of living species with the advent of DNA sequencing techniques, which allowed for molecular phylogenies (Murphy et al, 2001, Springer et al, 2004). Although this thesis is not primarily concerned with the relationships among mammaliaforms, understanding the phylogenetic relationships of a clade is of utmost importance to enable well-informed phylogenetic comparative research to be carried out. In order to understand how traits change through time, and assess evolutionary tempo and mode, accurate phylogenies are needed.

The Mammalian fossil record

Mammals have a highly variable fossil record both geographically and temporally. Despite this, they are relatively well documented from the Jurassic onwards. Mesozoic mammal fossils are known from all continents except Antarctica (Kielan-Jaworowska et al, 2004), but the best preserved and arguably

the most scientifically important specimens are known from China and Europe (Broderip, 1828, Meng, 2014, Hahn and Hahn, 1998a, Hahn and Hahn, 1998b). The Mesozoic mammal fossil record is dominated by the preservation of isolated fossil teeth and jaw fragments, but mammals from the Jurassic and Cretaceous of China in particular can exhibit excellent preservation of more complete skeletons with articulated postcrania. Numerous formations from the Liaoning Province of China represent Konservat-Lagerstätten yielding fossils beautifully preserved on limestone slabs, even retaining traces of skin and integument (e.g. *Eomaia scansorious* (Ji et al, 2002), *Volaticotherium antiquum* (Meng et al, 2006)). These exceptional fossils grant an opportunity to examine the skeletal anatomy of small and therefore delicate Mesozoic mammals that would have otherwise been destroyed, immeasurably advancing our understanding of Mesozoic mammal ecomorphology and phylogeny. The Kimmeridgian (Late Jurassic) Guimarota site from Portugal has also yielded exceptionally preserved fossil mammals, including skulls, mandibles, and postcranial elements (e.g. *Henkelotherium guimarotae* (Krebs, 1991)). Barremian (Early Cretaceous) *Spinolestes xenarthrosus* (Martin, 2015) is also preserved in detail, and is from the Las Hoyas formation of Spain. Numerous multituberculates and two eutherian mammals have been recovered from the Late Cretaceous Barum Goyot and Djadokhta formations from the Gobi desert (Kielan-Jaworowska, 1975).

Konservat-Lagerstätten are also important for our understanding of mammalian faunas in the Eocene. The most famous Lagerstätte of the Eocene is arguably the Messel Pit in Germany. The Messel fossils were preserved 47

million years ago, when the lake, which formed inside a maar volcano vent, was part of a forest ecosystem (Gruber and Michlich, 2007). Preserved in oil-shale, the Messel fossil mammals are truly spectacular; they are numerous, uncrushed, articulated, and exceptionally complete. Although preserved in lake sediments, the mammals recovered are from a range of terrestrial and semi-aquatic niches. Fossil mammals known from Messel include (but are not limited to) chiropterans, perissodactyls, pholidotans, plesiadapiforms, artiodactyls, as well as stem placental cimolestid mammals (e.g. Storch, 1996, Simmons and Geisler, 1998, Delsuc et al, 2001, Gruber and Michlich, 2007, Franzen et al, 2009).

Eocene cimolestids, condylarths, perissodactyls, and chiropterans are known from the Fossil Butte Member of the Green River Formation, North America (Grande, 2013). These fossils are again preserved on slabs, and are almost exclusively complete and articulated. Many more Eocene fossil mammals are recovered from North America. The badlands of the North American interior, including (but not limited to) the Chadronian Formation, Brider Formation, Wasatch Formation, and Fort Union Formation, yield numerous well-preserved mammal fossils, including jaw, skull, and limb material. Preserved in riverine deposits, these fossils are less frequently articulated or complete, but have produced many important specimens nonetheless.

Less well preserved, but nevertheless noteworthy, mammal specimens are known from the Eocene Geiseltal Lagerstätte in Germany. Creodonts,

condylarths, artiodactyls and perissodactyls, chiropterans and primates are all known from complete or near complete jaws (Krumbiegel et al, 1983).

Fewer mammal-dominated Lagerstätten are known from the Paleocene, which is unfortunate considering this is exactly the time period during which the adaptive radiation of mammals is hypothesized to have occurred. Nevertheless, a handful of well-preserved and relatively complete fossil mammals are known from Tiupampa, Bolivia, examples of which are the near-complete pantodont *Alcidedorbignya inopinata* (Muizon et al, 2015) and numerous individuals of the species *Pucadelphys andinus* preserved as a familial group (Ladeveze et al, 2011).

Geographically, mammal fossils, along with almost all terrestrial tetrapod fossils (see 'Mammaliaformes' search at https://paleobiodb.org/navigator/), are known in much higher numbers in the Northern Hemisphere. During the early Cenozoic, the southern continents were largely separated both from each other and the Northern continents. This means that many clades of mammals (and other tetrapods) were in effect evolving in isolation from one another, unable to migrate due to geographic barriers. The poor record of Southern Hemisphere mammal fossils likely means that a substantial amount of taxonomic and morphological diversity is missing from the record. Patterns of diversity and disparity derived from largely Northern Hemisphere fossil occurrences should be interpreted as such, and their limitations acknowledged.

The Mammalian Adaptive Radiation

For the first two-thirds of their evolution, mammals shared the Earth with the dinosaurs. Despite evidence of higher regional species richness among Jurassic and Cretaceous mammals compared to dinosaurs (Benson et al, 2016), Mesozoic mammals were typically regarded as living 'in the shadow of the dinosaurs' (Kielan-Jaworowska et al, 2004), exhibiting only conservative ecomorphologies as exclusively small body sizes in faunas dominated by dinosaurs. The conservatism of Mesozoic mammals has been called into question however, due to numerous examples of exceptionally preserved fossils from the Mesozoic being recovered in just the last two decades (e.g. Meng, 2006, Ji, 2006, Luo, 2015, Meng, 2015, Martin, 2015, Han et al, 2017). These mammals appear to exhibit disparate morphologies not previously recognised among Mesozoic taxa. Moreover, many of these ecomorphologies that appear among early mammals have evolved convergently in different clades, different regions of the world, and different time periods. Whereas early mammals may have previously been considered almost exclusively scansorial insectivores (e.g. Lillegraven et al, 1979), clear examples of more disparate phenotypes now exist. As previously mentioned, the early Late Jurassic haramiyidans *Maiopatagium furculiferum* (Meng et al, 2017) and *Arboroharamiya allinhopsoni* (Han et al, 2017) show evidence of a gliding locomotor mode, as does the Mid-Late Jurassic eutriconodont *Volaticotherium antiquum* (Meng et al, 2006, but see Luo, 2007 and Gaetano & Rougier, 2011 for phylogenetic affiliation). The docodont *Castorocauda lutrasimilis* has a number of adaptations associated with swimming, such as a wide paddle-shaped scaly tail and powerful limbs much

like the modern beaver (*Castor*; Nowak, 2006), and is therefore considered semi-aquatic. Docodont *Agilodocodon scansorius* from the Middle Jurassic of China possesses arboreal ecomorphological traits such as slender digits and a gracile skeleton (Meng et al, 2015), and it has also been suggested that dental adaptations resulting in spoon-shaped teeth indicate a gumnivorous diet (Meng et al, 2015, although see also Wibble & Burrows, 2016 for a contrasting view). *Docofossor brachydactylus*, also a docodont from the Middle Jurassic of China, on the other hand displays many adaptations seen today in burrowing or fossorial mammals (Luo et al, 2015). *Docofossor* possessed a very large and robust olecranon process on the ulna and flattened, spade-like hands, which would have resulting in strong forelimbs for digging. *Repenomamus giganticus* (Hu, 2005) from the Early Cretaceous of China was shown to have the remains of a juvenile *Psittacosaurus* dinosaur in its stomach, demonstrating that *Repenomamus* was carnivorous. Increases in ecomorphological diversity have been shown to occur among mammaliaforms during the Middle Jurassic at a time when the group was undergoing substantial lineage diversification (Close et al, 2015). Further, increases in the ecomorphological disparity of teeth among multituberculates have been demonstrated during the Late Cretaceous (Wilson et al, 2012), likely as a response to the evolution of angiosperms. These radiations indicate that Mesozoic mammals were able to evolve to exploit opportunity, and that these mammals were not as evolutionarily constrained by competition from the dinosaurs as was once thought.

Despite advances in our understanding of ecomorphology among Mesozoic mammals, it is still clear that extant mammals poses a much wider

range of both body sizes and ecomorphologies. While Mesozoic mammals are all estimated to be less than 15 kg (Hu et al, 2006), and the vast majority of them under 100g (Alroy, 1998), extant mammals range in size from the bumblebee bat (*Craseonycteris thonglongyai*), weighing just 2 g, to the largest animal to ever live, the blue whale (*Balaenoptera musculus*), at ~190,000 kg (Jones et al, 2009). Alongside increased body size and body size disparity are an almost bewildering array of ecomorphologies possessed by mammals occupying disparate niches. Extant mammals have evolved to inhabit almost every corner of the Earth and every niche available to them. Their feeding strategies range from hypercarnivory (e.g. lions (*Panthera leo*)) to highly specialised herbivory (e.g. the koala (*Phascolarctos cinereus*), feeding solely on eucalyptus leaves). Their locomotor ecologies include powered flight in bats, tree climbing and dwelling (e.g. arboreal primates and sloths), swimming (e.g. whales, otters),

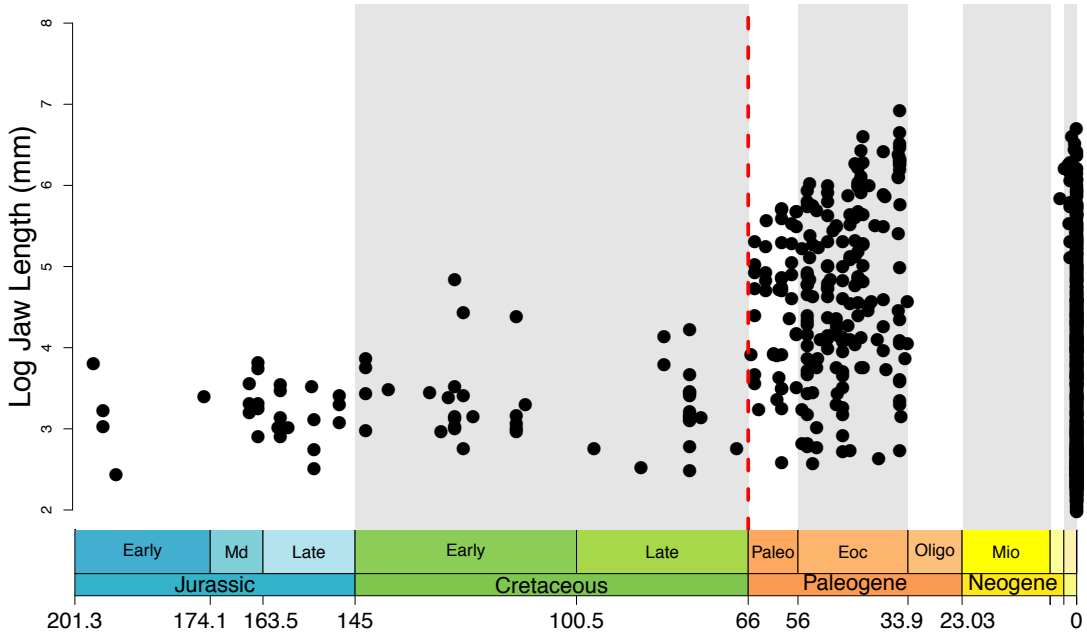


Figure i.2. Log jaw length through time for all terrestrial and marine mammals included in my dataset.

running (e.g. horses), jumping (e.g. kangaroos) and gliding (e.g. sugar gliders and colugos).

The fossil record clearly indicates that substantial increases in the maximum body sizes of mammals occurred for the first time immediately after the K/Pg boundary 66 Ma, resulting in substantial increases of mammalian body size disparity (Figure i.2, and see also Alroy 1998, Smith 2010).

Furthermore, although recent fossil discoveries have indicated that many Mesozoic mammals were not 'conservative' shrew-like creatures, there are still a number of ecomorphologies that were only realised after the K/Pg boundary. For example, no Mesozoic mammals can be considered cursorial, fully aquatic or volant, or exhibit any of the ecomorphological traits that are associated with a browsing or a grazing feeding strategy, and no mammal is large enough to fill a hypercarnivorous niche. This sudden appearance of novel body sizes and ecomorphologies immediately after the K/Pg boundary has attracted considerable attention since Osborn's (1902) seminal contribution on the subject. Osborn's work identified three main areas of ecomorphological trait evolution in the wake of the K/Pg mass extinction. These were body size, traits associated with feeding such as the teeth and lower jaw, and traits associated with locomotion such as limb bone shape and arrangement.

In more recent years, considerable effort has been put into attempting to quantify aspects of ecomorphological disparity, focusing on some subset of the trait categories highlighted by Osborn over a century ago. The first studies focused on changes in maximum body size across the K/Pg boundary (Alroy, 1998, Alroy, 1999, Smith, 2010). These studies found unequivocal evidence for

increased body mass across the K/Pg boundary. Maximum body mass increased dramatically across the boundary, and continued to increase until the Eocene when it plateaued (Alroy, 1998, Smith, 2010). Patterns of ecomorphological disparity and trait evolution through time among other traits are less clear, however, although several studies have quantified mammal disparity in the Mesozoic, Cenozoic, or both (Wilson, 2013, Grossnickle and Polly, 2013, Grossnickle and Newham, 2016, Wilson et al, 2012, Halliday and Goswami, 2015). These studies are summarised in Table i1.

Wilson et al (2012) used a measure of dental complexity known as orientation patch count (OPC) to assess herbivory among multuberculate mammals. Higher OPC values indicate a more complex tooth surface with a larger number of surfaces in different orientations. OPC values among extant mammals are low for more carnivorous mammals and increase with increased herbivory (Evans et al, 2007). This study suggests a radiation of multutuberculates into novel herbivorous niches approximately 20 million years before the K/Pg boundary, and the authors hypothesized that this increased herbivory tracked the evolution of angiosperms during the Cretaceous.

Grosnickle and Polly (2013), who applied geometric morphometric (GMM) techniques to measure shape variation in mammal jaws, also found a shift toward more herbivorous diets among multituberculates in possible response to angiosperm radiation and environmental perturbation. They additionally find a shift toward insectivory in non-multituberculate Cretaceous

mammals. Further decrease in the number of dental types alongside these shifts result in a decrease in mammalian disparity during the Cretaceous.

Authors	Clade	Study Period	Data used	Result
Halliday & Goswami, 2016	Placentalia	Cretaceous - Recent	Discrete and continuous characters of entire skeleton	Increased sum of ranges across the K/Pg boundary
Grossnickle & Polly, 2013	Mammalia-formes	Mesozoic	GMM of lower jaws	Decreased disparity during Cretaceous angiosperm radiation, with a move toward more herbivorous diets
Wilson et al, 2012	Multituberc-ulata	Cretaceous – Paleocene	Orientation Patch Count (OPC) of tooth row (dental complexity)	Increased disparity during Cretaceous angiosperm radiation, with an expansion into more herbivorous diets
Grossnickle & Newham, 2017	Theria	Cretaceous – early Paleocene	GMM of lower molars	Late Cretaceous radiation and K/Pg decline
Wilson, 2013	Multituberc-ulates and Therian mammals	Cretaceous - Paleocene	GMM of lower molars	Higher disparity among Cretaceous forms than expected, slower start to post-K/Pg radiation
Close et al, 2016	Mammalia-formes	Mesozoic	Discrete characters	Mid-Jurassic adaptive radiation

Table i1. Summary of previous work investigating the patterns of mammalian morphological diversity during the Mesozoic/Cenozoic.

Grosnickle and Polly (2013), who applied geometric morphometric (GMM) techniques to measure shape variation in mammal jaws, also found a shift toward more herbivorous diets among multituberculates in possible response to angiosperm radiation and environmental perturbation. They

additionally find a shift toward insectivory in non-multituberculate Cretaceous mammals. Further decrease in the number of dental types alongside these shifts result in a decrease in mammalian disparity during the Cretaceous.

Grossnickle and Newham (2016) analysed therian mammal tooth morphology using GMM, and found evidence for a radiation of therian mammals prior to the K/Pg boundary, and a decrease in disparity during the first 4.4 million years of the Paleocene. This decrease in disparity, they conclude, was likely due to selective extinction of ecological specialists during the mass extinction event.

Using a geometric morphometric analysis of mammal teeth, Wilson (2013) found evidence for a decrease in local-scale disparity in the immediate aftermath of the K/Pg extinction event, with Cretaceous mammals occupying regions of function space associated with distinct feeding ecologies. Wilson (2013) concluded that this decrease in disparity resulted from the selective extinction of larger mammals with more specialised diets.

Halliday and Goswami (2016) used total-skeletal discrete morphological characters to assess eutherian disparity through time. They found an increase in disparity in the aftermath of the K/Pg boundary, but no increase from the Maastrichtian to the Puercan (early Paleocene), despite a drop in disparity immediately prior to the K/Pg.

The timing of the mammalian radiation into novel feeding ecologies was also dated recently by a study which analysed the presence of genes coding for insect carapace digestion. Codon evolution models suggest that a number of mammals began losing copies of a suite of genes responsible for carapace

digestion in the immediate aftermath of the K/Pg boundary, indicating evolution into novel, non-insectivorous niches during the Paleocene (Emerling et al, 2018).

Additionally, Chen and Wilson (2014), although not directly measuring disparity levels during the Mesozoic, sought to quantitatively assess the locomotor mode of a number of Jurassic and Cretaceous mammals known from exceptionally preserved fossils. Using continuous character ratios from limb bones and an extant dataset for comparison, Chen and Wilson categorised these Mesozoic mammals into a number different locomotor modes.

Discrepancies between the patterns of ecomorphological disparity through time recovered by these studies likely result from substantial differences in the measure of morphological disparity implemented (e.g. 3D (Grossnickle & Newham, 2017) and 2D (Grossnickle and Polly, 2012) morphological data, OPC (Wilson et al, 2012) and discrete character data (Halliday and Goswami, 2015)), the clades examined (e.g. Theria (Grossnickle & Newham, 2017), Eutheria (Halliday and Goswami, 2015) and multituberculates (Wilson et al, 2012)), the period of time analysed (e.g. the time periods immediately surrounding the K/Pg boundary (Grossnickle & Newham, 2017), the Mesozoic (Grossnickle and Polly, 2012), or longer time periods, including the K/Pg boundary (Halliday and Goswami, 2015, Wilson et al, 2012)) or the geographic region studied (e.g. individual sites in North America (Wilson, 2013) and global (Wilson et al, 2012)).

Dating the Mammalian Radiation

Considerable research effort has also been given to understanding the timing of the radiation of crown marsupial and placental clades. Adaptive radiations predict rapid increases in clade diversity and disparity, and therefore the timing of mammalian diversification has implications for how important the K/Pg extinction event was in the radiation of mammals. The fossil record suggests an

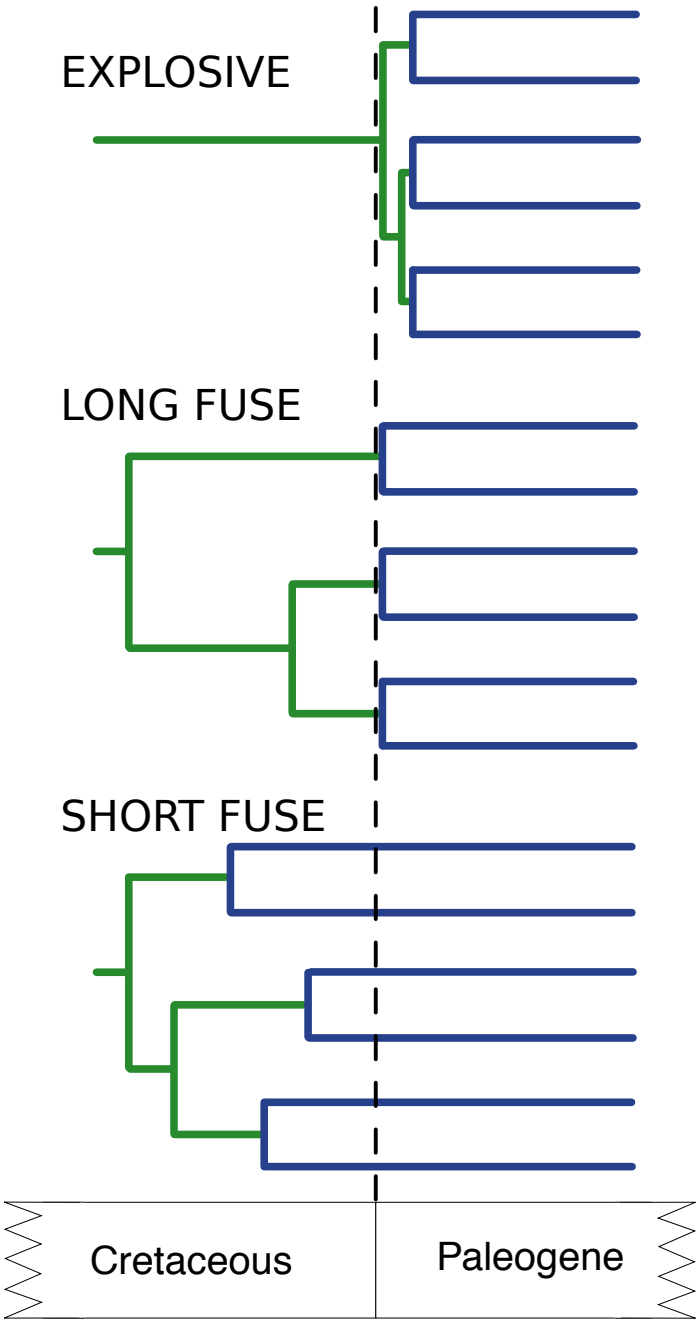


Figure i.3. Three hypotheses for the timing of divergences, relative to the K/Pg boundary, among placental mammals. Figure based primarily on figure 1 from Springer et al (2003).

explosion of taxonomic diversity, particularly within the placental mammals, alongside ecomorphological disparity in the wake of the K/Pg boundary (this viewpoint is exemplified by O'Leary et al, 2013). The fossil record is known to be incomplete however, and species or clade first occurrences can only place minimum constraints on the age of cladogenesis. This abrupt appearance of many species of mammal from diverse placental clades in the immediate aftermath of the K/Pg boundary raises questions about divergence times for placental mammals in relation to the extinction event. Three hypotheses for diversification were proposed for mammalian cladogenesis which would result in high diversity by the early Paleocene (Archibald and Deutschman, 2001). These are laid out in Figure i.3. The explosive model shows diversification among and within orders after the K/Pg boundary. The long fuse model shows interordinal diversification prior to the K/Pg boundary, but intraordinal diversification during the Cenozoic. The short fuse model hypothesizes both interordinal and intraordinal diversification before the K/Pg boundary.

Literal reading of the mammalian fossil record suggests that placental mammals diversified under the explosive model in the immediate aftermath of the K/Pg boundary. No unequivocal placental mammal fossils are known from the Mesozoic, but it is possible that placental mammals did exist during the Cretaceous but have not yet been recovered or accurately identified (Foote et al, 1999). Molecular clock analyses have recovered much older ages for the diversification of placental mammal orders (Kumar & Hedges 1998; Murphy et al, 2001, Bininda-Emonds et al, 2007, Meredith et al, 2011). Older age estimates for clade diversification when using molecular clock analyses are not unusual

however, and this pattern is repeated across study systems (e.g. Meredeth et al, 2011 vs O'Leary et al, 2013).

Nevertheless, many recent molecular studies agree that at least interordinal diversification of placental mammals likely took place prior to the K/Pg boundary during the Cretaceous (e.g. dos Reis et al, 2012; crown placental origination estimated between 88-90 Ma, Tarver et al, 2015; crown placental origination estimated between 87-100 Ma) but that the majority of intraordinal diversification occurred during the first few million years of the Paleogene, more similar to the long fuse model (named the 'soft explosive model' by Phillips, 2016, and see also Springer et al, 2003 dos Reis, 2012, Halliday et al, 2016), although O'Leary et al concluded that ordinal diversification of placentals took place after the end-Cretaceous, more consistent with the explosive model.

If older (often molecular) divergence dates and a long fuse model for the origin of crown placental mammals are correct, this indicates that palaeontologists have to date either not recovered any Mesozoic placental fossils, or have misidentified them. Non-recovery would likely be the result of rare, or biogeographically and environmentally constrained organisms, while misidentification may result from non-typical morphologies among more stemwardly-branching placental mammals. In each of these scenarios, a substantial taxonomic and morphological radiation may still have occurred as a result of the K/Pg mass extinction event. Ultimately, future fossil discoveries of Mesozoic mammals may help to bridge the gap between molecular divergence date estimates and the fossil record.

Quantifying patterns of taxonomic and morphological evolution in mammals during the Mesozoic and Cenozoic is not enough to fully understand the evolutionary processes at play during the adaptive radiation of mammals. A number of studies aiming to assess the tempo and mode of evolution exist. These studies include investigations of the rate of body size (Venditti et al, 2011) and discrete character evolution (Close et al, 2015, Halliday et al, 2016), as well as one study which investigated changes in the mode of evolution across the K/Pg boundary (Slater, 2013).

In light of numerous Mesozoic mammal discoveries highlighting previously-unrecognised ecomorphologies during the Jurassic and Cretaceous, Close et al (2015) analysed rates of discrete character evolution among Mesozoic mammals. They find evidence for increased rates of morphological evolution during the Middle Jurassic, and conclude that mid-Jurassic mammals underwent an adaptive radiation, increasing their ecomorphological disparity and taxonomic diversity.

Using the newly-published and comprehensive Late Cretaceous-Paleogene placental mammal tree, Halliday et al (2016) analysed rates of evolution during the proposed adaptive radiation of placental mammals across the K/Pg boundary. They reported increased rates of continuous character morphological evolution among Paleocene placental mammals.

Slater (2013), rather than analysing evolutionary rate through time, tested for a change in evolutionary mode across the K/Pg boundary. Slater (2013) found that body size among Mesozoic mammals was evolving under an Ornstein-Uhlenbeck mode of evolution, where body size was continuously

pulled back toward an optimum value. This small-bodied optimum and strong central tendency reflects the low body size disparity of Mesozoic mammals. Model fitting revealed a shift in evolutionary mode to a diffusive Brownian motion model after the K-Pg extinction, under which body-size disparity accrued in an unconstrained way over evolutionary time. This latter study by Slater (2013) in particular, lends weight to the idea that mammals experienced a release of constraint after the dinosaurs went extinct. This release of constraint from competition from the dinosaurs likely allowed mammals to radiated into novel body sizes for the first time during the early Paleogene.

Goals of the Current Work

In order to quantitatively test changes in the ecomorphological disparity through time and across the K/Pg boundary for the first time, I use an overall dataset of six ratios made up of ten continuous character traits taken from 1006 fossil and extant mammal jaws. In Chapter 1, I quantify mandibular ecomorphological disparity through time using a subset of 272 terrestrial fossil mammals, ranging in age from the Late Triassic – Eocene. The localities of the fossils used are shown in Figure i4. I conduct a principal components analysis and investigate function space occupation throughout the Mesozoic and early Paleogene, as well as calculating disparity through time using five variance- and range-based metrics (minimum spanning tree length [MST], sum of variance, sum of ranges, mean distance from centroid, and mean euclidean distance).

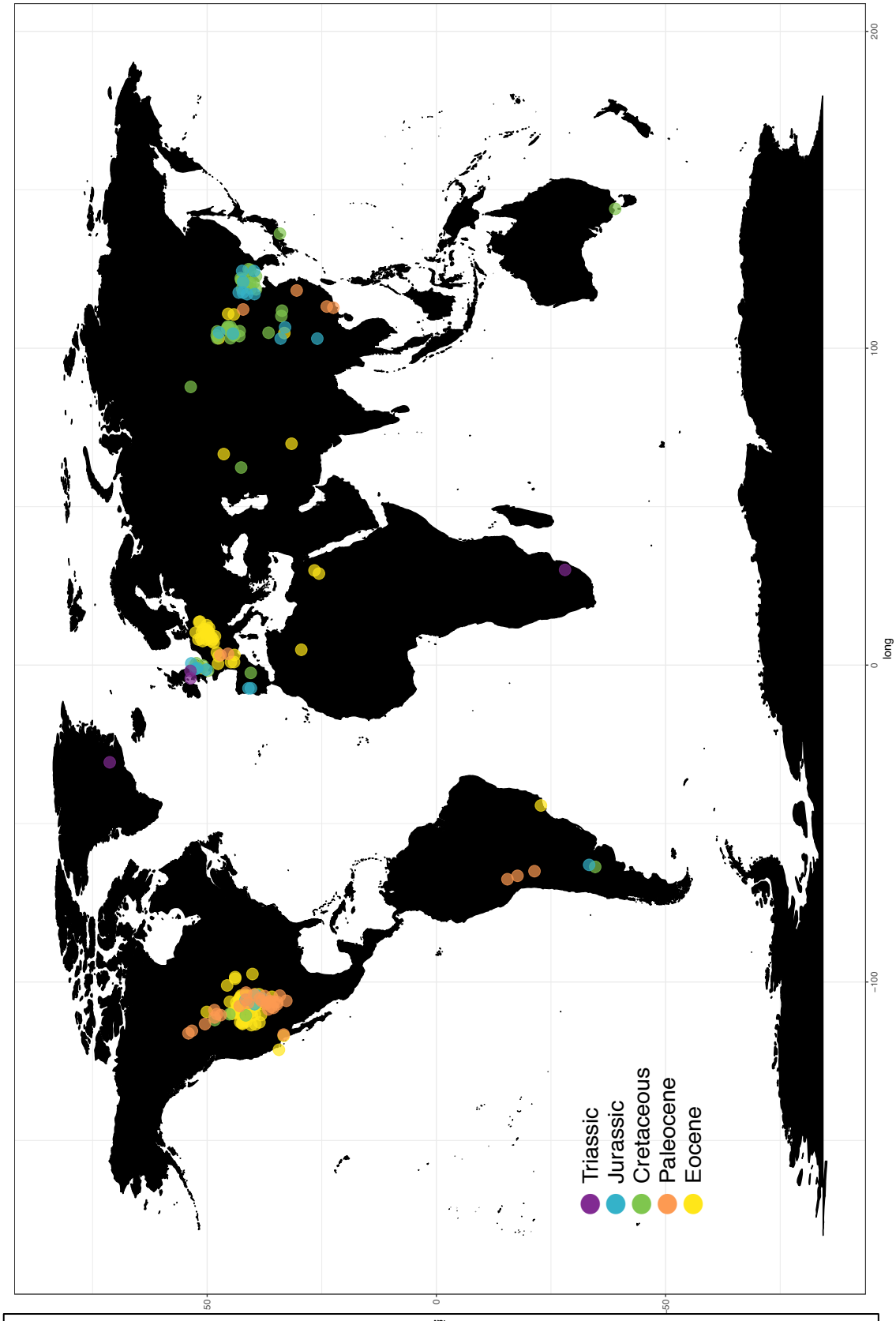


Figure i4. Map of fossil mammal (Triassic – Eocene) specimen localities included in this study.

In Chapter 2, function space occupation and disparity through time is investigated for small- and large-bodied mammals separately. A full dataset of six functionally relevant mandibular ratios for 276 fossil mammals and 730 Pleistocene-Recent mammals (n = 1006) are used in a principal components analysis. The aims of this chapter are to understand whether increased Cenozoic disparity detected among mammals is the result of a release of body size constraint.

In Chapter 3, I use a comprehensive timescaled supertree (initially comprising 272 taxa and later pruned to include the 69 taxa with available mandibular ecomorphological data) to calculate mandibular functional evolutionary rate among Late Triassic – Eocene mammals. This allows me to assess the way in which ecomorphological disparity accumulated along lineages through time.

The Use of Continuous Character Jaw Data

Mammalian mandibles were used for a number of reasons: (a) they consist of only one, flat, bone, meaning that they have higher taxonomic potential in comparison to skull or limb material, particularly among smaller individuals; (b) they can be readily used to infer evolutionary relationships (high taxonomic information content); and (c) their structure and form directly relates to feeding ecology, a central aspect of organismal biology.

Ratios produced from continuous measurements are used in preference to other measures of ecomorphology in an attempt to capture functional morphology more directly. A direct link between mandibular ratios and jaw

function have been demonstrated (Greaves, 2012, Lazagabaster et al, 2016) and therefore capturing these traits may enable me to directly assess the range of ecomorphologies present at any given time among mammals, rather than capturing the range of morphologies alone. Further, ratios may be available from incomplete jaws where other measures of shape (such as GMM) are not. This allows me to include a larger number of fossil mammals in my dataset.

The Use of a Supertree

Hypotheses of relatedness among organisms are integral when conducting analyses regarding evolutionary tempo and mode. Patterns of morphological diversification generated by different processes can look near-identical, and therefore in the absence of a phylogeny it is not possible to distinguish between different evolutionary processes (Foote, 1996). Although considerable effort has been given to producing comprehensive phylogenetic hypotheses for fossil and Recent mammals, no one tree covers the range of taxa included in this study. For this reason, I construct a supertree which includes both stem and crown Mammalia, and spans the K/Pg boundary. Supertrees are extremely useful tool for phylogenetic comparative methods, because they allow for large trees to be produced without the need to combine the character matrices that these partial trees are produced from. Combining matrices or creating one large matrix for all of the taxa included in this study would take years of research effort, and while a supertree is likely to be less accurate, the recovered relationships are often sufficient to run analyses of evolutionary rate

and mode tempo and mode, given that even less resolved taxonomies alone have been shown to be sufficient for this purpose (Soul and Friedman, 2015). I used the matrix representation parsimony (MRP) method (Baum 1992, Ragan 1992) to construct the supertree presented here, combining two relatively large trees previously published for mammals (Close et al, 2015 (which used the matrix of Zhou et al, 2013), Halliday et al, 2017).

Mammals as a study system for adaptive radiations

Being the type example (Osborn, 1902), mammals provide a key study system to explore the evolutionary processes associated with adaptive radiations. By definition, the evolutionary processes that underpin the taxonomic and morphological expansion of mammals in the early Paleogene are those that describe an adaptive radiation. Among biologists, the term adaptive radiation is often used to describe the way in which a given clade may populate a new island and radiate to occupy a wide range of available niches, subsequently exhibiting a suite of disparate ecomorphologies (e.g. Schluter, 2000, Pinto et al, 2008). A classic example of this is the radiation of *Anolis* lizards in the Caribbean. Caribbean *Anolis* lizards have evolved rapidly on the islands from possibly as few as two original colonisers (Jackman et al, 1997, Losos and Thorpe, 2004). Today they show considerable diversity and ecomorphological disparity, occupying a wide range of niches. There are clear parallels between radiations of clades onto new islands and adaptive radiations of clades in the fossil record such as mammals and birds, but there are also large differences. Adaptive radiations seen in the fossil record are often worldwide

events, and result in the speciation and ecomorphological diversification of entire orders. Although they appear to happen instantaneously in geological terms, they occur over much longer time scales and concern near-global colonisation. As such island radiations may exhibit different evolutionary patterns than true adaptive radiation that shape global ecosystems and result in whole-scale faunal turnover.

Chapter 1

Patterns of mammalian jaw ecomorphology during the Mesozoic/Cenozoic transition

Introduction

Cenozoic mammals are the 'type' example of an adaptive radiation. Adaptive radiations have assumed a central position in macroevolutionary theory, and were originally proposed from a qualitative observation that high taxonomic diversity and ecomorphological disparity of mammals appeared abruptly in the earliest Cenozoic (Osborn, 1902). This has been interpreted as resulting from ecological release of mammals following from the extinction of many species, including all non-avian dinosaurs, during the Cretaceous/Palaeogene (K/Pg) mass extinction event (Archibald, 2011, Slater, 2013).

Throughout the Mesozoic, representing the first two-thirds of their evolutionary history, mammals were thought to occupy few niches, and have often been described as small-bodied ecological generalists (e.g. Osborn, 1902, Simpson, 1937, Kielan-Jaworowska et al, 2004). Nevertheless, fossil discoveries from the last two decades have revealed greater ecomorphological diversity than was previously recognised, as early as the Jurassic, including swimming (*Castorocauda*; Ji et al, 2006), digging (e.g. *Fruitafossor*; Luo & Wible, 2005),

arboreal (e.g. *Eomaia*; Ji et al, 2002), and gliding (e.g. *Volaticotheriam*; Meng et al, 2006) mammals, and adaptations to carnivory in the badger-sized (estimated 12-14kg) *Repenomamus* (Hu et al, 2005). Indeed, quantitative comparative analyses indicate ecomorphological radiation among early mammals in the Early/Middle Jurassic (Close et al, 2015), more than 100 million years before the extinction of dinosaurs at the end of the Cretaceous. These observations demand a revised appraisal of the ways in which mammals increased their ecomorphological and functional disparity across the K/Pg boundary.

Abrupt and substantial increases in mammalian species richness occurred within the first few million years of the Palaeogene (Alroy, 1999, Wilson, 2013, Benson et al. 2016). The maximum body size and total range of mammalian body sizes also increased across the K/Pg boundary, initiating in the earliest Palaeocene and reaching more modern sizes in the Eocene (Alroy, 1998, Alroy, 1999, Smith et al, 2010, Slater, 2013). Studies of other aspects of morphological variation, however, have yielded distinct, and sometimes contradictory, results. Geometric morphometric analyses of teeth show decreases in therian disparity during the earliest Paleogene, on both regional (North America; Wilson, 2013, Grossnickle & Newham, 2016) and global (Grossnickle & Newham, 2016) scales, whereas dental complexity (orientation patch counts) suggests that multituberculates underwent a radiation into herbivorous niches at least 20 Myr before the K/Pg boundary (Wilson et al, 2012). In contrast, discrete character data and reconstructed ancestral states of the entire skeleton (cranial, dental, and postcranial) suggest that disparity in eutherian mammals did increase across the K/Pg boundary (Halliday &

Goswami, 2016). In addition, genomic evidence for parallel post-Cretaceous losses of ancestral genes for cuticle-specific digestive enzymes in placentals point to the origins of new, divergent trophic roles from a primitive insectivorous ecology in the early Cenozoic (Emerling et al, 2018). These studies have advanced our understanding of ecomorphological disparity in some groups of mammals and in during time intervals adjacent to the K/Pg mass extinction event. However, their focus on individual subclades, varying time scales of analysis, and analysis of different types of data limit our ability to detect broader patterns of ecomorphological disparity through time (Slater & Friscia, 2018(preprint)), or to compare patterns across the K/Pg boundary to longer 'background' intervals of both the Mesozoic and early Cenozoic. This may be resolved by more inclusive studies, spanning longer time intervals and encompassing all mammal groups.

In contrast to previous studies, I include species from all clades of Mammaliaformes, from the Early Jurassic–end-Eocene. I focus on a set of six functional ratios made up of nine continuous character traits of the mandible, a proxy for feeding ecology, and one of the axes along which mammals were originally hypothesized to increase their ecomorphological disparity across the K/Pg (Osborn, 1902; who observed differences in adaptations to the teeth (feeding ecology) and limbs and feet (locomotor ecology)). The dataset includes 271 species, from which I quantify patterns of jaw functional disparity through time for Mammaliaformes as a whole, as well as for Theria. I aim to establish the scope of expansion in mammalian jaw functional morphology, and identify how

the patterns of jaw morphological disparity compare to patterns of increasing body mass disparity across the K/Pg boundary.

Methods

Functional data

Six mechanically-relevant jaw ratios (described in Sup. Mat. S1.1; and see Anderson et al, 2013, Lazagabaster et al, 2016) were collected from 271 species representing all major terrestrial mammalian groups, from the Middle Jurassic to the end-Eocene. Jaw measurements were collected from images of jaws in the literature (n = 157), as well as first hand from fossil mammal collections. Specimen measurements were recorded using digital callipers correct to 0.1mm, and images from the literature and specimen photographs were measured using the program GIMP to place landmarks on images, and distances between these landmarks were calculated in R.

This study begins in the Middle Jurassic, because sampling of this epoch is sufficient to allow analysis of mammalian disparity, unlike earlier intervals. It continues to the end-Eocene because ecomorphotypes recognised in the Eocene are suggested to mirror, to a greater or lesser extent, those of modern mammal faunas (Simpson, 1937). Moreover, mammalian maximum body masses reached modern levels by the middle Eocene (~40Ma; Smith et al, 2010). Investigating patterns of mammalian morphological diversity until the end-Eocene therefore

enabled a thorough investigation of mammalian disparity during the protracted increase following the K/Pg boundary (66 Ma).

Dating and binning specimens

Time bins used are based on Mesozoic stages and North American Land Mammal Ages (NALMAs) to reflect known changes in mammal faunas through time. Stages and NALMAs were amalgamated where bin length was particularly short, or where sampling of mandibles was low, to enable a more consistent analysis of disparity through time. The shortest time bin included in disparity analyses is 6.5 My (Clarkforkian-Wasatchian) and the longest time bins are 13 My (Aptian and Albian). The most poorly sampled bins included in my disparity analyses contain 6 species (Oxfordian and Albian), and the best sampled contains 79 (Bridgerian-Uintan). To further increase sample size, and to allow meaningful rarefaction of the time series data, Mesozoic stages were used where appropriate to conduct disparity through time analyses.

Ages, where possible, were assigned to specimens preferentially using the formation age given by primary publications, or using the stage or NALMA (Gradstein et al, 2012). Where ages from formations, stages or NALMAs are not available, estimates were obtained from Fossilworks (http://fossilworks.org) using the genus or species range. Midpoint ages were used to assign fossils to time bins when their age range spanned multiple bins. Duplicate species are removed from the same time bins, but different specimens representing the same species may be included in different time bins.

Principal components analysis (PCA)

All six functional traits for all 271 mammals were subjected to a principal components analysis (PCA). Where appropriate, proportional ratios were subjected to a logit transformation. This spreads out the tails of the distribution for proportions to correct for a tendency for ratios to not fall within the entire range of theoretically possible values (0-1). All data were then *z*-transformed. This scales all traits to have equal variances and a mean of 0, giving each trait equal weight in the PCA. All analyses were conducted in R (version 1.1.456). Ordination space was examined by epoch, to determine changes in occupation of function space among my focal time bins (e.g. Foote, 1997). Ordination spaces plotted against finer time bins (matching those used for disparity through time curves (Figure 1.2) can be viewed in Figures S1.3-S1.5.

Disparity analysis

Disparity, the spread of species in ecomorphological space (Foote, 1997), was calculated for each time bin using all six PC axes. Minimum spanning tree length was used as the primary measure of disparity in this study (Gower & Ross, 1969) and various other indices are presented in the supplement (Figures S6, S7). Minimum spanning tree length was preferred because it captures the spread of points in space as well as the distances between clusters of points, without being biased by bimodal data. Variance is an unbiased estimator of spread only when data are unimodal, but many of the intervals have bimodal distributions. Therefore, although a commonly-used variance-based metric was computed (sum of variance; Foote, 1992, Wills et al, 1994), the results are

presented only in the supplement (Figures S1.6). This measure shows artificially increased disparity within time bins containing bimodal data distributions (e.g. Campanian) compared to other bins, even when they appear to cover a similar function space area. Range based metrics (e.g. sum of ranges) attempt to capture a different element of disparity: how far apart the most disparate species are. However, they are highly susceptible to both sample size variation and the occurrence of outliers (Ciampaglio et al, 2001), and therefore may not describe incompletely-sampled fossil data in a biologically meaningful way. Mean pairwise distance was also calculated and presented in the supplementary material (Figures S1.7).

The minimum spanning tree (MST) was calculated based on the distance between occupied grid cells across function space. PC scores were rounded to the nearest round number (0 decimal places) to obtain these grids. Although the results obtained using grid cells are primarily presented here (Figure 1.2), MST length was also calculated without grouping taxa into grid cells (i.e. using rarefaction only), the results of which can be seen in Figures S1.8 (5000 are used show the same patterns of disparity through time for both all mammals and therian mammals (compare Figure 1.2 to Figures S1.8 and S1.9, and see supplementary materials for further discussion of the use of grid cells). The function dist2mst() was used in R (Close et al, 2017) to find the minimum spanning tree length. Bins were then rarefied so that each bin contained the same number of species in an attempt to mitigate the effects of uneven sampling through time. Data within each bin were rarefied to six species via sampling with replacement for 5000 iterations to produce the disparity curve seen in

Figure 1.2. As this number is relatively low, a second disparity curve was produced using fewer time bins but allowing for a higher quota of 15 species (Figure S1.7a). Overall patterns of mammal disparity across the K/Pg boundary were found to be the same at both quotas. The patterns shown in Figure 2 (using a quota of six species) are therefore robust. Error bars represent 95% confidence intervals calculated from sampling six species with replacement from each bin 5000 times. Other disparity measures, as well as disparity for subclades, were calculated for comparison and details about these alternative measures and their results can be found in Sup. Mat S1.3 (Figures S1.6-S1.7). All analyses were conducted in R.

Collection of taxonomic information

Taxonomic information was collected from the primary literature, as well as Fossilworks (http://fossilworks.org). Taxonomic affiliation was based primarily on the phylogenies of Luo (2007; based on Luo & Wibble, 2005 and Luo et al, 2007), Close et al (2015; based on Zhou et al, 2013) and taxonomic information in Kielan-Jaworowska et al (2004) and Rose (2006). The following clades were employed: Stem Mammalia, Stem Theria, Australosphenida-Prototheria-Monotremata, Metatheria-Marsupalia, Eutheria-Placentalia, Carnivora + Creodonta, Multituberculata, Pantodonta, Primates + Plesiadapiformes, Rodentia, and 'ungulate'. 'Ungulate' is used here to refer to the likely polyphyletic grouping of the following hoofed mammal clades: Cetartiodactyla, Perissodactyla, Notoungulata, Dinocerata and Mesonychida. These groups were chosen to represent mammals with close phylogenetic affiliation (e.g. Rodentia),

and/or ecomorphological attribution ('ungulate'). For discussion on the placement of taxonomically contested genera or clades, please refer to Sup. Mat. S1.4.

Results

Relative to the intervals of the Cenozoic included in this study, mammalian jaw disparity (measured as Euclidean minimum spanning tree length) was low throughout the Mesozoic. Jaw functional disparity for mammaliaformes as a whole remained constant across the K/Pg boundary, but increased across the Paleocene/Eocene boundary, and again in the late Eocene (Duchesnean-Chadronian), the final interval of this study (Figure 1.2). Despite no change in total disparity across the K/Pg boundary, therian mammals underwent consistent interval-to-interval increases from the Paleocene to the late Eocene. As early as the Paleocene, therians had entered regions of function space that were left vacant by K/Pg extinctions, and as well as those that were never occupied by Mesozoic mammals (Figure 1.1a; high positive values of PC2).

Here, I primarily discuss patterns on the first four principal component axes (PC1–PC4), which together summarize 87% of shape variance. Further discussion of the traits correlating to each principal component (PC) axis and the extreme morphologies associated with positive and negative PC axes scores can be found in Sup. Mat. S1.2.

Jaw functional disparity of Mesozoic mammals

Jaw functional disparity was consistently low throughout the Jurassic and Cretaceous, with broad overlap between confidence intervals for different Mesozoic time bins (Figure 1.2). This stability arises from relatively low function space occupation on principal components (PCs) 1-4 (Figure 1.1), suggesting a restricted range of jaw functional morphologies. Jaw function space occupation increased from the Late Triassic to the Late Cretaceous (Figure 1.1). Prior to the Late Jurassic, mammals were largely restricted to positive PC1 scores, indicating a predominance of mammals with dorsoventrally slender jaws with longer relative molar rows, little or no diastema, anterioposteriorly wider coronoid processes, and less vertical offset between the jaw hinge and tooth row for Late Triassic–Middle Jurassic mammaliaformes. From the Late Jurassic onwards, mammals increased their occupation into areas of negative PC1 function space. This reflects the addition of species of mostly multituberculate such as *Liaobaatar* and *Catopsbaatar* (labelled; Figure S1.1), which have dorsoventrally deep jaws with relatively larger diastemas and anteroposteriorly wide coronoid processes.

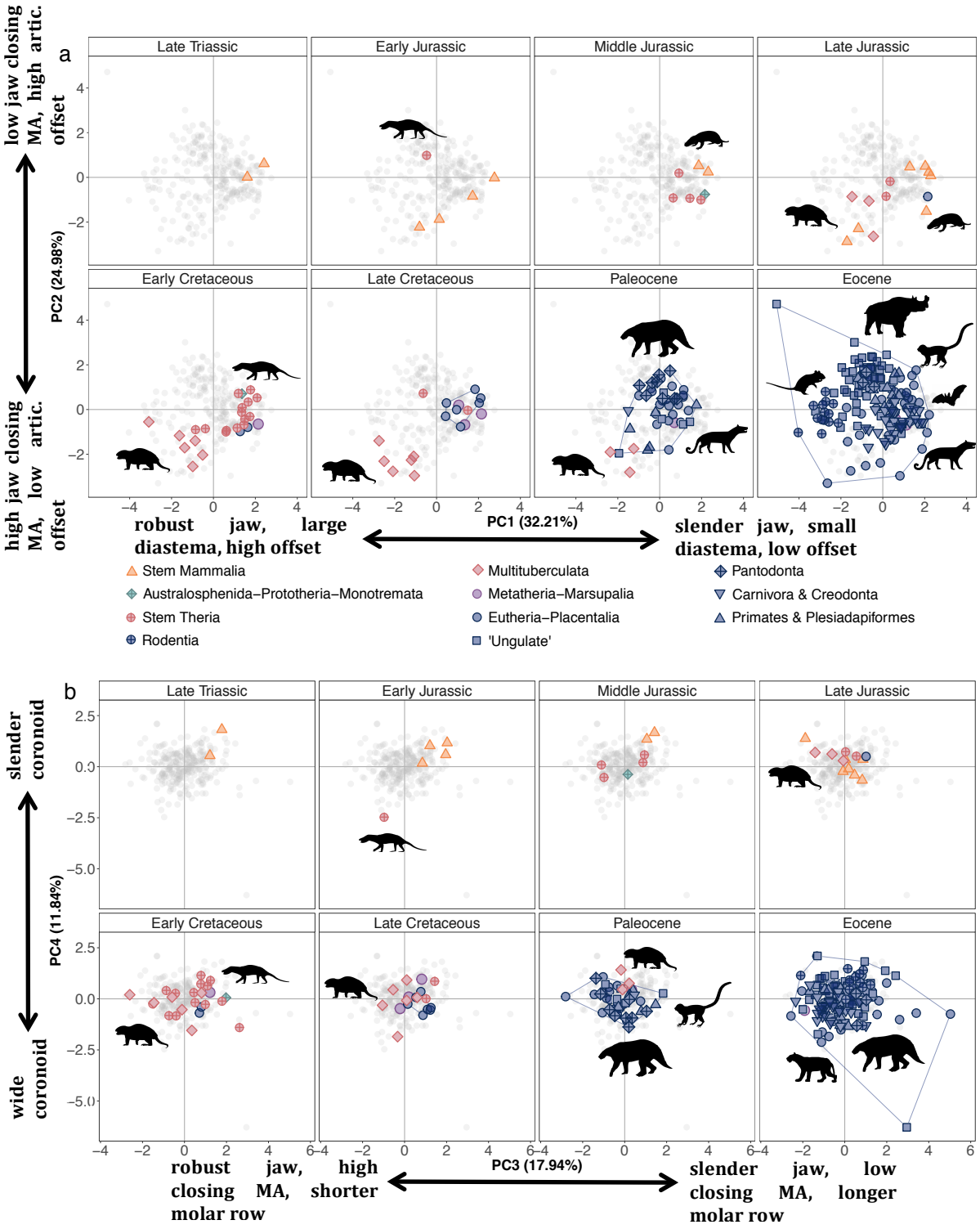


Figure 1.1. Jaw disparity function space across 8 epochs from the Late Triassic–Eocene split between (a) PC1-PC2 and (b) PC3-PC4. Different colours and symbols represent mammal clades (see key within Figure). The blue polygon depicts the total spread of Eutheria-Placentalia mammals in the Late Cretaceous, Paleocene, and Eocene. Figure S1.1 shows a copy of this Figure but with the addition of species labels for mammals that occupy extreme regions of function space across all epochs. The grey points represent the spread of all data points across the total study time interval. PC5-6 is shown in Figure S1.2.

Jaw functional disparity of Cenozoic mammals

Early Palaeocene mammals occupy a wider range of jaw function space than those of the latest Cretaceous (Figure 1.1a,b). However, this results from increases in the number of species sampled: when rarefied to equal counts of species per time bin, overall mammalian functional disparity is relatively constant across the K/Pg boundary (Figure 1.2; purple curve). Disparity increased across the Paleocene/Eocene boundary, and then continued to rise throughout the Eocene, peaking in the late Eocene, the last time bin included in this study. Late Cretaceous mammals show a bimodal distribution in function space. This is lost in the Paleocene due to the appearance of plesiadapiformes such as *Plesiadapis cookei* (labelled; Figure S1.1) possessing intermediate PC1 morphologies (intermediate jaw depths and diastema lengths). The novel appearance of jaws that plot more positively on PC2 during the Paleocene results from the appearance of pantodonts, eutherians that represent the first relatively large-bodied herbivorous mammals. Pantodont mandibles are characterized by smaller values of jaw closing mechanical advantage, more anteroposteriorly slender coronoid processes, greater vertical offset between the jaw hinge and tooth row, and larger relative molar row lengths. The Paleocene shows a small reduction in the occupied range of PC1 compared to the Cretaceous. This occurs because of the disappearance of taxa showing the highest positive PC1 jaw morphologies of the Mesozoic, those mammals with the most slender jaws and the smallest diastemas, such as *Sinodelphys*, *Amblotherium*, and *Alphadon* (labelled; Figure S1.1) (Figure 1.1a). On PC3-4,

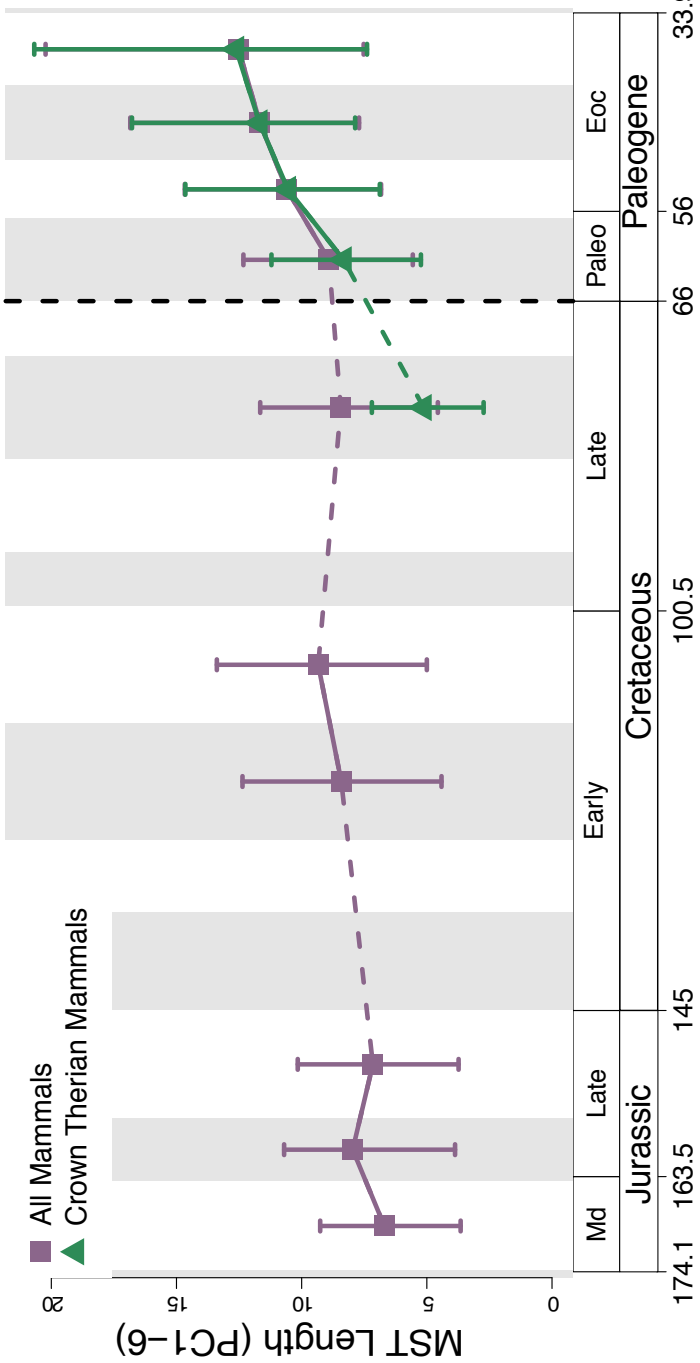


Figure 1.2. Jaw function minimum spanning tree length through time. The purple curve represents all mammals, and the green curve represents therian mammals only. Amalgamated stages (Mesozoic) and NALMAs (Cenozoic) with six or more individuals are used as time bins (see methods). Data is rarefied ($n = 6$) and sampled with replacement to enable fairer comparison between bins with differing sample sizes. The 95% confidence intervals represent uncertainty produced by sampling six individuals at random with replacement across each time bin, for 5000 iterations. The points represent the mean values of these 5000 runs. A solid line indicates changes between consecutive time bins. Dashed lines indicate changes across two or more time bin boundaries. Although these curves represent rarefaction to six, total mammal minimum spanning tree length rarefied to fifteen (across fewer bins) can be seen in Fig. S1.7a, and analysis using this higher rarefaction number recovers the same pattern across the K/Pg boundary and into the Cenozoic. Curves representing other methods of calculating disparity (see methods) can also be found in the supplement (Figs. S1.6-S1.7) and are discussed in Sup. Mat. S1.3.

Paleocene function space occupation is similar to that for the Cretaceous (Figure 1.1b).

The Eocene shows further expansion into areas with more extreme positive values on PC2, general expansion into wider ranges of PC1-2 scores (Figure 1.1a), and population of areas further from the PC3-4 centroid (Figure 1.1b). Among large-bodied herbivorous mammals, 'ungulates' (used here to refer to artiodactyls and perissodactyls) occupy a greater volume of PC2 function space than did Paleocene–Eocene pantodonts. The late Eocene artiodactyl *Hypisodus* shows a particularly divergent ecomorphology relative to other Eocene and earlier mammals. It plots in the uppermost part of the left quadrant in PC1-2 function space (Figure 1.1a) and the lowermost region of the right quadrant in PC3-4 function space (Figure 1.1b), exhibiting a rare combination of traits for pre-Oligocene mammals, including a large diastema, large articulation offset, and a slender coronoid process.

Jaw functional disparity of eutherians

Eutherians constitute an increasingly large subset of total mammalian diversity through the studied interval, and show a distinct, expanding pattern of disparity through time from the Late Jurassic–Eocene (blue in Figure 1.1a,b: PCs 1.1-1.4, and Figure S1.2: PCs 1.5-1.6). During this time, they originated at positive PC1 values, around positive 3, subsequently expanding to lower and more negative PC1 scores and across a wider range of PC2-4 scores, representing the introduction of species with larger diastemas and dorsoventrally deeper jaw ramus as well as species with larger ranges of a jaw

traits associated with PC3-4 (e.g., jaw slenderness, jaw closing mechanical advantage, molar row length, and coronoid anteroposterior slenderness.

Eutherian mammals appear in this dataset in the Late Jurassic (*Juramaia*; Luo et al, 2011), and increase in taxonomic number and proportion between time bins in this dataset until the Eocene. Mesozoic eutherians are almost exclusively confined to regions of function space already occupied by stem mammals and stem therian mammals on PCs 1-4, but in general do not overlap with the stem therian group Multituberculata. The Paleocene is the first time eutherians explore function spaces not previously occupied by any other mammal groups, as well as that previously occupied exclusively by multituberculates. On PC1-2, pantodonts (including *Leptolambda* and *Alcidedorbignya* (labelled; Figure S1.1)) plot in a completely novel area of function space, and plesiadapiforms, the palaeanodont *Ernanodon*, and the dinoceratan *Probathyopsis* occupy regions that had previously been occupied almost exclusively by multituberculates throughout the Mesozoic (larger relative diastema, slender jaw ramus, shorter relative molar row).

During the Eocene, eutherians are responsible for the further spread into areas of function space not occupied by Mesozoic mammals. 'Ungulates' occupy a large range of PC1-4 scores in the Eocene. Rodents also spread into function space that was sparsely populated before the Cenozoic, exhibiting jaws with intermediate values for coronoid and jaw ramus slenderness, combined with relatively large diastemas and relatively short molars. Although rodents are missing from the Paleocene in this dataset, fragmentary remains indicate their presence in the Paleocene (Jepsen, 1937, Ivy, 1990, Dawson, 2003, Rose, 2005),

suggesting that this area of function space was populated earlier than is shown (Figure 1.1a).

Crown therian disparity increased across the K/Pg boundary (Figure 1.2; green curve). Although the therian crown includes eutherians and metatherians, very few metatherians can be included in this dataset (n = 6). Therefore this increase in crown therian disparity is evidence for an increase in eutherian jaw ecomorphological disparity across the K/Pg boundary.

Discussion

Patterns of Mesozoic jaw functional disparity

I find evidence of consistently low jaw functional disparity among Mesozoic mammals compared to post-Paleocene mammals. This pattern emerges despite strong evidence that mammals occupied more ecomorphological roles in the Mesozoic than previously recognised (Hu, 2005, Ji et al, 2006, Meng, 2006, Luo, 2008, Zheng, 2013, Meng et al, 2015, Han et al, 2017), and underwent an early adaptive radiation during the Early/Middle Jurassic (Close et al. 2015). This early radiation entailed both dietary and locomotory innovations (Luo 2007, Close et al. 2015). Nevertheless, I conclude that the ecological breadth of the Paleogene radiation was ultimately much greater, at least in respect of dietary ecomorphology (and body size; e.g. Alroy, 1999; Slater 2013).

Wilson et al (2012) and Grossnickle and Polly (2013) reported a shift in mean multituberculate ecomorphology toward more herbivorous diets, or toward omnivorous diets with a larger reliance on plant-based foods, beginning ~ 100 Ma and increasing throughout the remainder of the Late Cretaceous. This shift represents the origin and radiation of cimolodontan multituberculates. I also find a change in occupation of jaw functional space by multituberculates from the Late Jurassic to the Late Cretaceous, with a move toward more extreme negative PC1 and PC2 scores representing the appearance of species with larger diastemas and a greater vertical offset between the jaw articulation and tooth row. These traits are often associated with more herbivorous diets (Lazagabaster et al, 2016), and are well-developed in many modern grazers. The consistent pattern recovered by studies measuring different aspects of the feeding apparatus (dental complexity using orientation patch count (OPC) analysis (Wilson et al, 2012), jaw morphology using geometric morphometric (GMM) analyses (Grossnickle & Polly, 2013), and jaw functional morphology using continuous character trait ratios (current study)) lends weight to the hypothesis that multituberculates responded to environmental changes such as the Cretaceous angiosperm radiation (Dilcher, 2000, Grossnickle & Polly, 2013) by adapting multiple aspects of jaw and tooth morphology to a more plant-rich diet.

Despite this broad agreement, previous studies recovered fluctuations in multituberculate (Wilson et al, 2012, Grossnickle & Polly, 2013) and overall mammal (Grossnickle & Polly, 2013) disparity during the Cretaceous that are not apparent in my results. Those studies recovered a decline in

multituberculate or overall mammalian jaw ecomorphological disparity during the late Early and early Late Cretaceous. Disparity then appears to have rebounded (Grossnickle & Polly, 2013) or increased (Wilson et al, 2012) in the latest Cretaceous. Although my study recovers a small increase in disparity in the Campanian (latest Cretaceous), I do not find direct evidence of a decline in jaw functional disparity in the late Early Cretaceous–early Late Cretaceous in non-multituberculate mammals. These discrepancies may result from low sampling of complete jaws available to this study during this time period. For example, it is not possible to estimate early Late Cretaceous jaw disparity due to lack of data, with poor sampling of mandibles for this time also apparent in Grossnickle & Polly (2013). Multituberculate teeth, however, are much more numerous than complete multituberculate jaws during the Cretaceous and early Cenozoic. This suggests that finer scale patterns of disparity in multituberculates recovered using OPC analyses for the Cretaceous, Paleocene, and Eocene may be more robust. It is alternatively possible that tooth characters and jaw characters show fundamentally different patterns of ecomorphological disparity through time due to differing constraints on morphology. Future discoveries of Cretaceous mammals will provide a test of the early Late Cetaceous decline of mammalian ecomorphology by increasing all sample sizes. The current rarity of Paleocene and Eocene multituberculate jaws also explains the dip in disparity found for multituberculates in this dataset across the K/Pg, a pattern that is not consistently recovered in other studies (e.g. Wilson et al, 2013).

Patterns of Cenozoic Jaw Functional Disparity

The results presented here suggest an approximately 10 million year delay between the Cretaceous/Paleogene extinction event and an increase in mammalian jaw functional disparity across the Paleocene/Eocene boundary. This is not the case for changes in mammalian body size across the K/Pg, which have been shown to increase in the immediate aftermath of the extinction (Alroy, 1998, Alroy, 1999, Smith et al,, 2010, Slater, 2013). This lag in an increase in morphological jaw disparity does not necessarily mean that there was no expansion in feeding ecology during the Paleocene. Because of the importance of body size for jaw function (e.g. absolute jaw closing force, gape width) and digestive physiology, it is likely that this does indicate changes in dietary breadth among mammals from earlier in the Paleogene. Size has been suggested to be more liable to evolutionary change than morphology due to increased selection pressures (Stanley & Yang, 1989, Hunt, 2007). The rate at which smaller or larger size can be achieved while overall morphology remains in stasis is demonstrated by numerous examples of gigantism or dwarfism in mammals (e.g. dwarf elephant *Palaeoloxodon cypriotes* from the Pleistocene of Cyprus (Davies & Lister, 2001)).

Therian mammals provide an exception to this general pattern, showing an increase in disparity immediately across the K/Pg boundary followed by continuing rises in disparity in the Eocene. This rise in therian jaw functional disparity, coupled with an apparent stasis in overall mammalian jaw disparity until the Eocene suggests that therian mammals may have taken advantage of niches once occupied by non-therian or stem-therian mammal lineages that

became extinct at the end of the Cretaceous. In this respect, it appears likely that therians were beneficiaries of the K/Pg extinction event, showing evidence of preferential diversification during the recovery phase.

Most studies have shown increases in measures of body size disparity in the immediate wake of the K/Pg boundary (Alroy, 1998, Alroy, 1999, Smith et al, 2010, Slater, 2013). Nevertheless, a few recent studies showed either no increase in disparity across the K/Pg, or in fact reported a drop in disparity in the early Cenozoic on the basis of tooth morphology (Wilson, 2013, Grossnickle & Newham, 2016). Grossnickle & Newham (2016) interpreted an increase in therian disparity during the Late Cretaceous, coupled with a decrease in therian disparity in the immediate aftermath of the K/Pg extinction as being inconsistent with the hypothesis of ecological release during the early Cenozoic. Instead they suggested that mammals underwent selective extinction across the boundary. However, selective extinction across the K/Pg boundary, leading to a short-lived decline in disparity across the K/Pg, is not necessarily inconsistent with the hypothesis of ecological release.

Grossnickle & Newham (2016) focused only on the first 4.4 million years of the Paleocene, and showed that disparity had begun to increase after 1.4 million years, although it still did not exceed Mesozoic levels. In context of my findings over a longer study interval, I instead interpret their results as demonstrating that the timescale required for ecological release to result in disparity exceeding pre-extinction levels was longer. Ecological recovery after an extinction event does not occur instantaneously, and may even take up to 10 million years on average for complete ecological recovery and for opportunistic

taxa found in the wake of an extinction event to be replaced by taxa exploiting novel or vacated ecologies (Erwin, 1998, Kirchner & Well, 2000, Erwin, 2001). This lag in ecological recovery likely explains the short-term decrease in therian disparity recovered by Grossnickle & Newham (2016), and may also explain the longer-term delayed increase in total mammal disparity in my data.

The drop in therian disparity found across the K/Pg reported by Grossnickle & Newham (2016) appears to have been driven by the loss of bimodality in eutherian function space occupation and the removal of two metatherian outliers present in their latest Cretaceous time bin. Although the distance between distinct groups of species in function space and the range of function space occupation appears to have been reduced, the overall 'footprint' of function space occupation appears to increase. Mammalian jaw ecomorphological disparity may have decreased immediately across the K/Pg boundary (Wilson, 2013, Grossnickle & Newham, 2016; see also Figures S1.6-S1.7 and Sup. Mat. S1.3), but therian mammal disparity shows an increase by the end of the Paleocene in comparison to Campanian levels, and overall mammal disparity had recovered to pre-extinction levels by the early Eocene (Figure 1.2a,b).

Eutherian Disparity Patterns

Eutherian function space occupation increased from the Late Jurassic/Early Cretaceous to the Late Cretaceous, and then across the K/Pg boundary, and again across the Paleocene/Eocene boundary. Mesozoic eutherians achieved their highest function space occupation in the Late Cretaceous (Figure 1.1a, b).

It is therefore possible that eutherian jaw disparity, and with it overall mammalian jaw disparity, may have continued to rise after the Cretaceous even without the K/Pg extinction. The Paleocene, however, also represents the first occurrence of mammal species, all of which are eutherians, plotting in a completely novel area of PC1-2 function space, and with it likely novel dietary ecomorphologies, consistent with the findings of Halliday et al (2016) and Emerling et al (2018). This suggests that the K/Pg boundary and the early Cenozoic likely does represent a period of unprecedented ecomorphological opportunity for eutherian mammals. In particular it appears that, in the Eocene, hoofed mammals and their decedents, the large majority of which are herbivorous, occupied large and disparate regions of function space (Figure 1.1a,b).

Metatherian disparity patterns

Recent metatherians are much less diverse than eutherians, but nevertheless exhibit a wide range of ecomorphologies, are important today in Australian ecosystems, and were more abundant in South American ecosystems for much of their evolutionary history (Nowak, 2006, Goswami et al, 2011). Metatherian jaws are rare and often fragmentary in the Mesozoic and early Cenozoic fossil record (Croft et al, 2017). These fragmentary remains, however, show that metatherians had substantially higher diversity through time than shown here (Grossnickle & Newham, 2016, Bennett et al, 2018, Croft et al, 2017). It is likely, therefore, that these analyses underestimate the role that metatherians have played in increasing mammalian disparity in certain geographic regions, most

notably South America and Australia. A more reliable appraisal of metatherian disparity will necessarily draw on fragmentary material and teeth (e.g. Grossnickle & Newham, 2016, Croft et al, 2017).

Comparison with Patterns of Body Size Disparity Through Time

Patterns of mammalian body size evolution throughout the Mesozoic and early Cenozoic (Alroy, 1998, Alroy, 1999, Smith et al, 2010, Slater, 2013) indicate a similar pattern to that recovered here for therian jaw function, showing long-term constraint to low disparity during the Mesozoic, followed by increases from early in the Cenozoic (Paleocene). Both differ from the overall pattern of total mammalian jaw disparity across the K/Pg, which shows a delayed increase until some time in the Eocene, suggesting that mammals as a whole initially increased their jaw disparity only to pre-extinction levels, taking ~10Ma to further increase disparity to previously-unattained levels. During both phases, increases in disparity largely resulted from the radiation of therians.

Previous studies have shown that body size disparity stabilised from the Eocene onward, with later Cenozoic and Recent disparity levels comparable to those recovered from the Eocene (Alroy, 1998, Smith et al, 2010). Studies concerned with mammalian feeding ecology disparity (including the current study), have typically not measured post-Eocene disparity (Grossnickle & Polly, 2012, Wilson et al, 2013, Grossnickle & Newham, 2017). A more complete survey of post-Eocene species is needed to determine whether patterns of diversity in feeding ecology stabilized in the Cenozoic.

Conclusion

My survey of jaw functional measurements from representatives across the mammalian tree allows us to quantify large-scale patterns of disparity through time along an important axis of ecomorphological variation. Discrepancies in recovered patterns of disparity among previous studies, as well as between previous studies and the current study, are due primarily to the focus on different traits, mammalian subclades, and geographic regions. Although these studies are integral in quantifying disparity patterns at finer scales, they do not provide a clear picture of mammalian disparity overall.

The pattern recovered here shows continually low jaw functional disparity among Mesozoic mammals. This was followed by an expansion of therian, and particularly eutherian, mammals into novel niches across the K/Pg boundary. Initially these novel functional morphologies and ecologies explored by therian mammals did not increase disparity enough to exceed levels seen during the Mesozoic, when non-therian and stem-therian mammals were more abundant. Paleocene therians predominantly explored regions of function space that were previously occupied by stem-therians, indicating a pattern of turnover involving the replacement of non-therians by therians. I suggest therefore that the initial radiation of therian mammals resulted not only from ecological release enabled by extinctions of dinosaurs, but also from those of non-therian mammals. By the Paleocene/Eocene boundary, however, therians had exceeded the total disparity of all Mesozoic mammals, and continued to increase in disparity and function space occupation throughout the Eocene.

Although the current study cannot directly test evolutionary mode or rate throughout mammalian evolution (Foote 1996), the results presented here are consistent with a release of jaw ecomorphological constraint at or immediately after the K/Pg boundary (Slater, 2013), with therian mammals taking advantage of these newly available niches.

So far, our quantitative understanding of the adaptive radiation of Cenozoic mammals is incomplete, and does not capture the ecomorphological complexity of the mammalian skeleton in total. Nevertheless, patterns of jaw ecomorphological disparity presented here are broadly congruent with patterns of body size evolution. I suggest therefore that they place fundamental constraints on our knowledge of the timing and mode of the ecomorphological expansion. They also suggest a pattern replacement of non-therian mammals by therians over the K/Pg. Investigating patterns of ecomorphological disparity across a wider variety of traits can help us to more fully understand the ways in which organisms may accumulate novel traits during an adaptive radiation.

Chapter 2

The effects of size on jaw functional disparity through time in mammals

Introduction

Among the most widely recognised and well-documented macroevolutionary changes to occur during the history of mammalian evolution is an apparently rapid and substantial increase in maximum body size across the Cretaceous/Paleogene (K/Pg) boundary. Initially put forward as a qualitative observation (Osborn, 1902, Simpson, 1937), this pattern of increased maximum body size, resulting in an increase in total body size disparity, is now quantitatively well-established (Alroy, 1998, Smith et al, 2010, Slater, 2013). These changes in mammalian body size occurred at a time of widespread faunal turnover and reorganisation in the wake of the end-Cretaceous mass extinction event 66 ma, during which ~70%-80% of species (Sepkoski 1996, Jablonski, 1994), including all non-avian dinosaurs and many established clades of Mesozoic mammals went extinct (Wilson et al, 2013). This mass extinction event and in particular the removal of non-avian dinosaurs from a wide variety of terrestrial niches has been identified as a likely cause of increases in maximum body mass among early Cenozoic mammals (Archibald,

2011, Slater, 2013). According to this hypothesis, early Cenozoic mammals were able to access niches that were unavailable to them in the Mesozoic due to competition from incumbent, and larger-bodied dinosaurs (e.g. Slater, 2013).

Increases in phenotypic disparity among early Cenozoic mammals are also seen in traits other than body size. Placental mammals make their first appearances in the fossil record in the early Cenozoic (O'Leary, 2013, Halliday et al, 2016), although many molecular studies suggest that placental mammals may have originated prior to the K/Pg boundary, durning the Cretaceous (dos Reis et al, 2012, Tarver et al, 2015, Phillips, 2016, Liu et al, 2017, Springer et al, 2018). Nevertheless, once placentals appear in the fossil record in the wake of the K/Pg extinction event, they possess many highly distinct aspects of skeletal morphology and inferred ecology. In particular, mammals known from early Cenozoic assemblages have novel limb, jaw, and teeth ecomorphologies compared to those known from the Mesozoic (Osborn, 1902, Simpson, 1937). These novel traits are ecomorphologically significant, and likely imply increasing locomotory and dietary disparity (e.g. Hu et al, 2005, Ji et al, 2006, Chen and Wilson, 2015, Luo et al, 2015, Meng et al, 2015, Meng et al, 2017). Halliday & Goswami (2016) have documented increased disparity of cladistic character states among early Cenozoic mammals, and Chapter 1 of this thesis showed that disparity of mammalian jaw ecomorphology had increased to levels greater than those of the Mesozoic by the early Eocene (Chapter 1; Figure 1.2). Here, I test one possible explanation for the proposed increase in phenotypic disparity among early Cenozoic mammals, specifically that it is

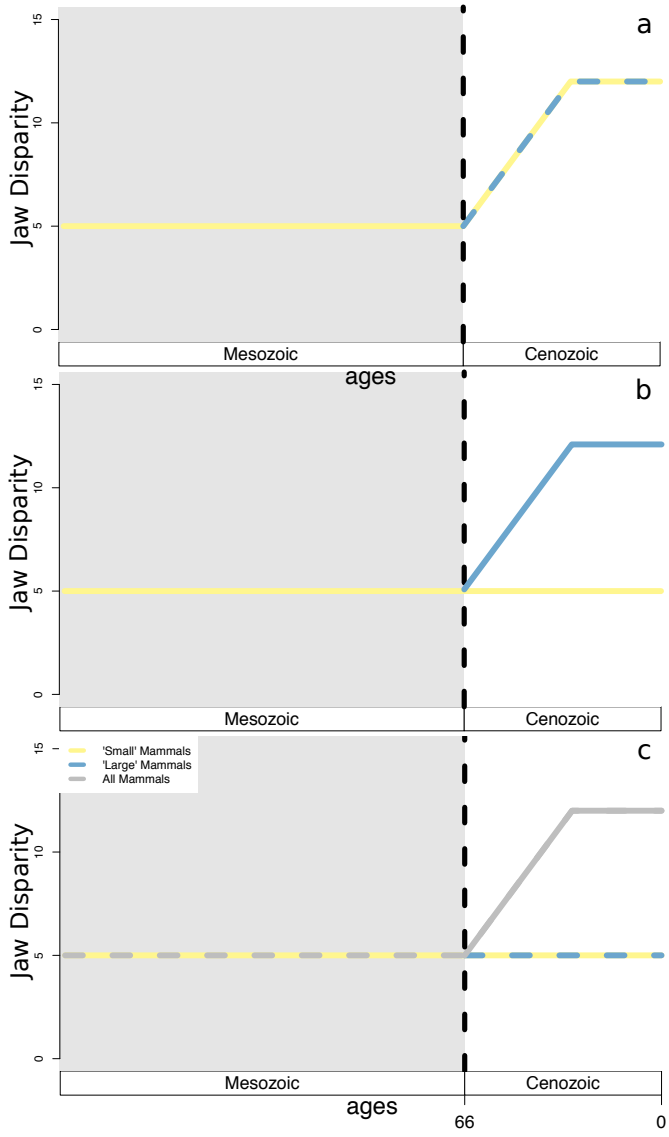


Figure 2.1. Three alternative hypotheses of how body mass may interact with jaw ecomorphological disparity through time. 2.1a. Scenario A - No interaction between body size and jaw ecomorphological disparity, with the pattern of increased mammal jaw ecomorphological disparity seen across both size classes. 2.1b. Scenario B - A pattern of high ecomorphological disparity among larger mammals and low ecomorphological disparity among smaller mammals. 2.1c. Scenario C – Low ecomorphological disparity among small and large mammals respectively, but high overall disparity during the Cenozoic due to little or no overlap between small mammal and large mammal jaw ecomorphologies.

linked to their evolutionary expansion into larger body sizes that permitted the exploration of new feeding roles.

Although maximum body size (and body size disparity) and the ecomorphological disparity of mammalian jaws both increased in the wake of the K/Pg mass extinction, the relative timings of these increases appear to vary. Jaw ecomorphological disparity lagged behind increases in body size disparity by up to 10 million years (Chapter 1). Nevertheless, body mass correlates with almost every aspect of mammalian, and wider organismal, biology (e.g. Calder, 1984, Sibly and Brown, 2007, Cooper & Purvis, 2010). These include aspects of functional morphology such as digestive physiology, locomotory efficiency, and feeding ecology

(quantitative evidence suggests that herbivores have a larger optimal mass than carnivores or omnivores among terrestrial mammals (Price & Hopkins, 2015), and it has been suggested that larger-bodied animals have more extreme and therefore disparate morphologies (Van Soest, 1996). This suggests the possibility of links between body mass disparity and ecomorphological disparity. The idea that the small maximum size of Mesozoic mammals (relative to Cenozoic mammals) might have prevented these early mammals occupying a more disparate range of feeding ecologies resulting in lower overall disparity has been suggested but not fully explored (e.g. Lillegraven et al, 1979, Smith, 2010).

To test the hypothesis that evolutionary expansion into larger maximum body sizes explains increases in ecomorphological disparity of mammalian jaws during the early Cenozoic, I suggest three conceptual models describing patterns of jaw ecomorphology among mammalian body size classes. These scenarios are laid out in Figure 2.1a-c. Figure 2.1a depicts a hypothesis of higher disparity among both 'small' and 'large' (size class cut-offs chosen are discussed below in methods) mammals in the Cenozoic compared to the Mesozoic. This is the result that might be expected if body size were to show no correlation with jaw ecomorphological disparity, with mammals of all sizes exploring novel ecomorphologies after the K/Pg boundary and overall increases in mandibular ecomorphological disparity increase being the result of increased disparity across all size classes. Scenario 2 (Figure 2.1b) shows a hypothesis of low disparity among small mammals both before and after the K/Pg boundary, and higher disparity among larger mammals, which are known only from the

Cenozoic. This pattern might reflect a wider range of ecomorphologies realized by mammals at larger body sizes than at smaller ones. This pattern is consistent with a hypothesis in which the release of body size constraint at the K/Pg boundary enabled a radiation of mammals into novel ecomorphologies resulting in higher levels of disparity due to the appearance of large-bodied mammals for the first time. Figure 2.1c shows a third hypothesis, in which disparity among small mammals stayed at the same level throughout the Mesozoic and Cenozoic, and larger Cenozoic mammals also show similarly low levels of disparity, but overall disparity is higher that for either group individually. This pattern suggests a relationship between body size and jaw ecomorphology where large mammals have different ecomorphologies to small mammals that are not more disparate, but show little overlap so that mammals exhibit higher overall disparity when mammals of all size classes are considered together.

I test these hypotheses using six functional continuous character traits from 276 Late Triassic – Eocene fossil mammals and 730 Pleistocene–Recent mammals. To do this, I examined at disparity and function space occupation across different size classes; 'smaller' sized mammals, more similar to body sizes realised in the Mesozoic, and 'larger' sized mammals, more similar those body sizes that were explored by mammals after the K/Pg boundary. The dataset analysed here differs from that in Chapter 1 by the inclusion of 730 Pleistocene-Recent mammal species, and the inclusion of marine fossil and Recent mammals.

Methods

Functional data

The same six mechanically relevant jaw ratios described in Chapter 1 are also used here. These ratios and the raw measurements used to construct them are outlined in Sup. Mat. S1.1. As with Chapter 1, measurements were taken either first hand from the specimen using calipers correct to 0.01 mm, or from 2D images in lateral view from the primary literature using tpsDig (Rohlf, 2018). The statistical programming language R was then used to measure Euclidean distances between these landmarks in order to obtain the linear measurements used for the functional ratios.

This chapter includes a sample of 1006 mammal species, expanded from that of Chapter 1 (n = 272) due to inclusion of Pleistocene-Recent specimens. The dataset includes both terrestrial and marine mammals from the Jurassic-Eocene, and from the Recent. Members of the recently-extinct Pleistocene megafauna were included together with Recent mammals, and as such our final time bin is referred to as Pleistocene-Recent. I include the Pleistocene-Recent time bin in this analysis to assess the disparity levels among modern faunas in comparison to the Mesozoic and early Cenozoic. In particular I wish to assess jaw functional disparity levels among all mammals and among larger mammals in the Pleistocene-Recent compared to the Eocene, because previous studies have suggested a plateau in maximum body size disparity from the Eocene to the Recent. Pleistocene megafauna were included in our recent sample due to the nature of our question. I seek to understand the impact of body size on

mammal jaw functional morphology, and as such I find it necessary to include members of the pre-human megafauna. I also aim to establish whether some or all of these Pleistocene megafauna species occupied unique or currently vacant regions of function space. Of the 730 Pleistocene-Recent mammals included in this study, 23 are Pleistocene in age.

Data for fossil mammals were collected from the primary literature and from museum specimens. Although some Recent mammal specimens were also collected from the primary literature and museum specimens, most Recent specimen images were taken from the online resource Animal Diversity Web (https://animaldiversity.org/accounts/Mammalia/specimens) and the Museum Victoria specimen image repository (http://museumvictoria.com.au/bioinformatics/mammals).

Binning schemes and dating specimens

I use a coarser time binning scheme in these analyses compared to Chapter 1. This is because I test disparity among small mammals and large mammals separately, producing smaller within-group sample sizes that would have resulted in sample sizes that were too low to robustly calculate disparity levels under the binning scheme of Chapter 1. The time bins for this chapter therefore are Mesozoic Periods (Jurassic (201-145Ma) and Cretaceous (145-66Ma)), Cenozoic Epochs (Paleocene (66-56Ma) and Eocene (56-33.9Ma)) and the Pleistocene-Recent (2.5-0Ma). As in Chapter 1, ages were preferentially assigned to specimens based on formation age or using the Stage or North American Land Mammal Age (NALMA). Where ages could not be assigned in this

way, genus or preferably species ranges were instead obtained from Fossilworks (http://fossilworks.org). As in Chapter 1, duplicate species were removed from time bins, but different specimens assigned to the same species may be included in different time bins.

Principal components analysis

I subjected all 1006 Jurassic-Eocene and Pleistocene-Recent mammals to a principal components analysis. As in Chapter 1, the logit transformation was used to correct proportional ratios. Function space is analysed through time using Mesozoic Periods, Cenozoic epochs, and a final Pleistocene-Recent time bin.

Euclidean distances for PC1-6 from both overall centroids and from individual time bin centroids were calculated separately for each size bin, and was done for each of the five size bin divisions used (see 'Choice of cut odd sizes for body size classes' below).

Significance tests

T-tests were used to determine the statistical significance of differences between small and large mammals, and were conducted in R. These tests were conducted in the following ways:

(i) Two multivariate PC1-6 centroids were calculated per time bin, one for small mammals and a second for large mammals. For each time bin, the Euclidean distances of small and large mammals from their own centroids were then calculated (i.e. distance from centroid). A t-

test was then used to test for significant differences between the mean distances from centroid for small mammals compared to that of large mammals. This tests for statistically significant differences in the spreads of datapoints for small and large mammals.

(ii) T-tests were used to compare the distribution of small mammals to the distribution of large mammals along each of the six principal component axes (PC1-6) and across each time bin. This allowed me to test for significant differences in the mean scores on individual PC axes between small mammals and large mammals.

The results of these tests can be viewed in Sup. Tables 2.1-2.5.

Disparity analysis

Jaw functional disparity was calculated using principal components 1-6 for each time bin. Minimum spanning tree length, calculated using distances from the centre of populated grid cells, was used to calculate disparity (see 'Methods; Disparity Analysis'; Chapter 1).

Disparity curves were calculated based on rarefaction via sampling with replacement for 5000 iterations to ensure that differences in disparity among size classes and time intervals were not artificially inflated by sample size. These 5000 replicate samples were used to then calculate 95 per cent confidence intervals, and are represented by error bars on the disparity curves shown in Figures 2.3 and 2.4 and Figures S2.1-S2.3. Rarefaction sample size was chosen to be equal to the number of species present within the most poorly sampled size class in its most poorly sampled time bin.

Because the counts of species assigned to the 'small-bodied' and 'large-bodied' categories varied depending on choice of cut-off size (see below), the rarefaction quota (*n*) varies across data treatments (in total, five different cut-off sizes were compared). The largest rarefaction number used in any of these five analyses was 19 and the smallest was eight. Rarefaction quotas for each individual size bin division analysis are indicated in the relevant figure captions (Figures 2.3 and 2.4, and Figures S2.1-S2.3).

Choice of cut-off sizes for body size classes

To test the effects of body size on jaw functional disparity and functional ecomorphology, species were binned into one of two size classes representing 'smaller' mammals and 'larger' mammals. Dividing the continuum of sampled body sizes into two discrete categories representing 'small' and 'large' mammals is not straightforward, and requires an arbitrary choice of cut-off size. For this reason, and to test the robustness of our results, I use five different division points, outlined below.

I use maximum jaw length, measured in a straight line from the tip of the first incisor (i_1) to the most posterior part of the mandible (see Sup. Mat. S1.1; measurement M1), as a proxy for body size. I use jaw length rather than estimated body mass or other body size proxies because jaw lengths can be collected directly from the data I studied when the mandible is well preserved. In contrast, body mass can only be observed in our modern sample and must be estimated for fossil mammals. Using jaw length as a proxy for body size

therefore allows us to more reliably and fairly compare between fossil and extant mammals.

Size class divisions used to bin mammals into discrete size bins

Five different size class divisions were used to analyse potential differences in jaw functional disparity and function space occupation between 'small' and 'large' mammals through time. All of the jaw lengths chosen as the cut-off value for placement in either size category were chosen based on the distribution of mammal jaw lengths during the Mesozoic. This is because we know that small body size is a characteristic of Mesozoic mammals (Lillegraven et al, 1979, Alroy, 1998, Kielan-Jaworowska et al, 2004), and maximum body size increases among mammals soon after the K/Pg boundary (Alroy, 1998, Smith et al, 2010).

Figures 2.2a-b show the distribution of jaw lengths among Mesozoic mammals and the five jaw lengths used to divide small and large mammals.

Size class division 1: The first and most conservative upper limit of small mammals used in this study included only those mammals with jaw lengths of less than 37 mm. More than eighty per cent (81.81%) of Mesozoic mammals fall within this most conservative size bin (dashed red line D1 on Figures 2.2a-b).

Size class division 2. The second division value chosen (dashed red line D2 on Figure 2.2a-b) includes all mammals with a jaw length of less than 50 mm. Over ninety per cent (92.42%) of Mesozoic mammals exhibit jaw lengths of 50 mm or smaller. The first natural break in the Mesozoic data included in this study also occurs at around 50 mm (dashed red line on Figure 2.2b). Mammals

with jaws lengths of more than 50 mm in the Mesozoic may be considered among a population of outliers in terms of body size.

Size class division 3. Division three (dashed red line D3 on Figures 2.2a-b) includes mammals with jaw lengths of less than 68.4 mm. A second natural

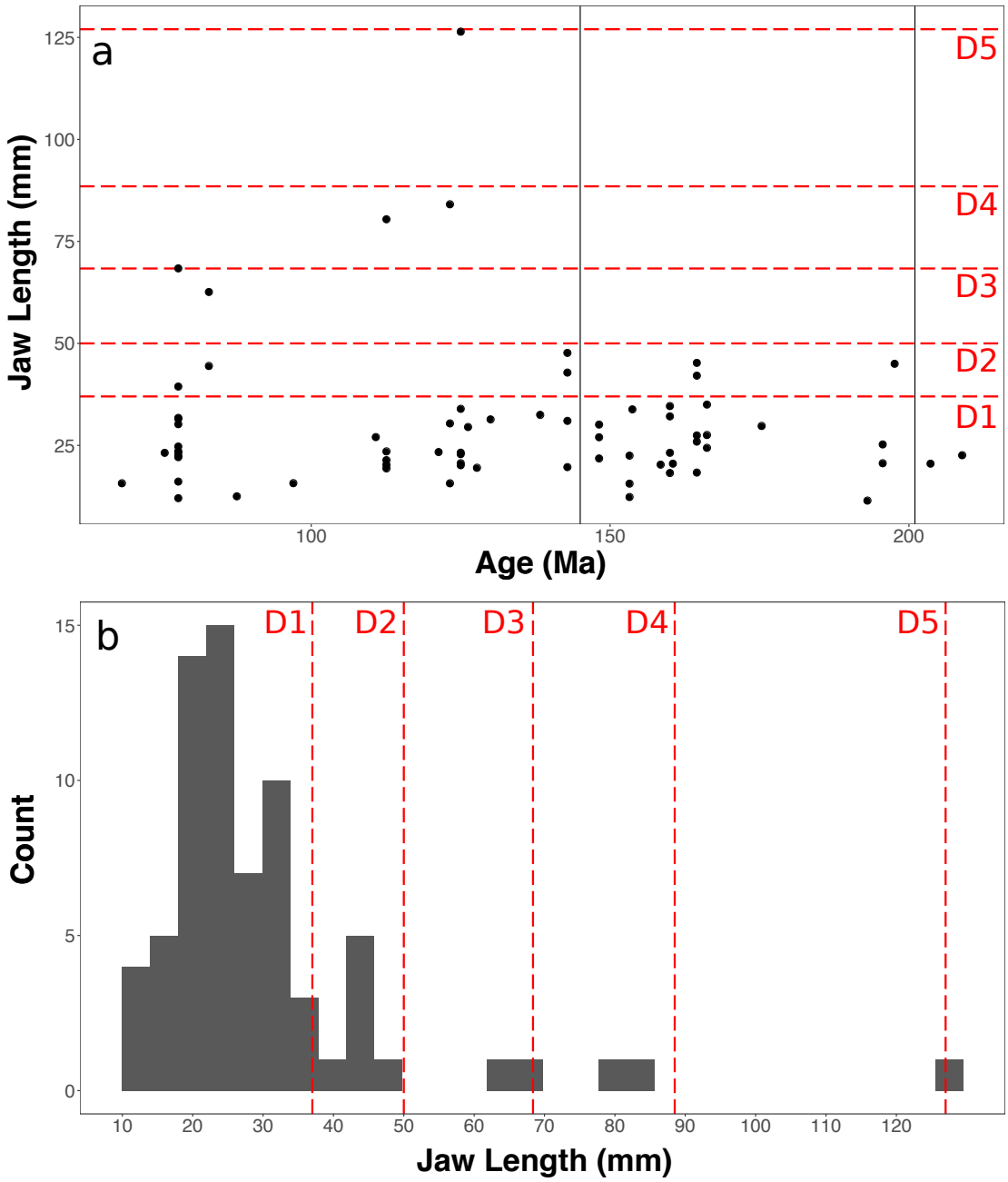


Figure 2.2. Mesozoic jaw length (a) through time, and (b) frequencies. Red dashed lines (horizontal in (a) and vertical in (b)) indicate the jaw lengths used as division values (labelled D1-5) between 'small' mammals and 'large' mammals and their relationship to Mesozoic mammal jaw length distribution.

break in the data occurs around this value (dashed red line D3 on Figure 2.2b). Over ninety per cent (93.93%) of Mesozoic mammals exhibit jaw lengths of 68.4 mm or smaller.

Size class division 4. The fourth division length used was 88.5 mm (dashed red line D3 on Figures 2.2a-b) and marks the third natural break in the Mesozoic data (dashed red line D4 on Figure 2.2b). This upper value for small mammals includes 98.48% of Mesozoic mammals and excludes only one mammal from our Mesozoic sample; *Repenomamus giganticus*. *Repenomamus giganticus* is well established as a Cretaceous mammal exhibiting a substantially larger body size than any other mammal currently known from the Mesozoic (Hu et al, 2006) and is a clear body size outlier.

Size class division 5. My fifth and final 'small mammal' upper limit (dashed red line D5 on Figure 2.2b) used is chosen to reflect the total jaw length recovered for mammaliaformes during the Mesozoic (and therefore includes 100% of our Mesozoic mammal sample). Although *Repenomamus giganticus* is clearly an outlier in possessing a jaw of 127 mm long during the Mesozoic, its presence in Mesozoic faunas is nevertheless evidence that, although rare, it was possible for mammals to evolve to this larger size before the K/Pg boundary. Including this fifth division therefore allows us to assess differences between disparity among all Mesozoic mammals and Cenozoic mammals that exhibit sizes up to that of the largest currently known from the Mesozoic.

Collection of taxonomic and ecological information

Information regarding the feeding ecology and higher taxonomic affiliation of each specimen included in our dataset was collected from the primary literature and Animal Diversity Web (https://animaldiversity.org/accounts/Mammalia).

Results

Size-partitioned disparity through time

Patterns of jaw functional disparity through the Mesozoic and early Cenozoic for the total sample of mammals are similar to those shown in Chapter 1, with the addition of new data for Pleistocene–Recent species. Pleistocene–Recent mammals (small- and large-bodied species analysed together) show remarkably similar disparity to those of the Eocene. This occurs despite a relative decrease in small mammal disparity and an increase in large mammal disparity recovered using all five size class cut-off values (Figure 2.3, 2.4 and Figures S2.1-S2.3).

The smallest mammals (jaw length < 37 mm; 'size division 1') show relatively low disparity throughout the Mesozoic, early Paleogene and in the Pleistocene-Recent (Figure 2.3). They exhibit a decrease in disparity across the K/Pg boundary, resulting in their lowest disparity during the Paleocene. Eocene small mammals exhibit the highest levels. It is striking that Eocene and Pleistocene–Recent mammals of these small body sizes show similar disparities

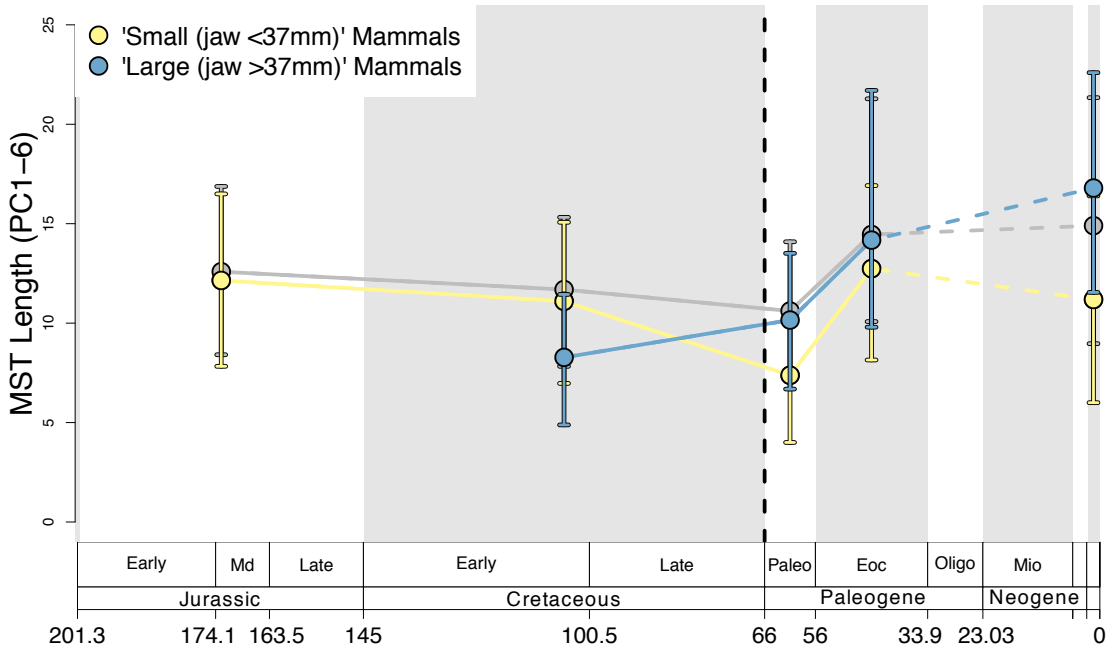


Figure 2.3. Jaw functional disparity through time, calculated as minimum spanning tree length across 5000 rarefied (*n* = 8) bootstrap replicates. The yellow curve depicts disparity levels through time among mammals within a small size class (defined here as any mammals that has a jaw length of 37mm or less). The blue curve shows disparity levels among mammals with a larger size class (with mammals exhibiting a jaw length of more than 37mm). The grey line depicts overall jaw functional disparity though time. A solid line connecting points indicates bin-to-bin disparity changes, while a dashed line indicates unsampled bins in between the disparity estimates.

to those of the Mesozoic, with strongly overlapping error bars. Larger mammals (jaw length > 37 mm) show a continuous increase in disparity through time from the Cretaceous to Recent, with a particularly large increase from the Paleocene to the Eocene (Figure 2.3). The disparity of these larger mammals is higher than that of smaller mammals (jaw length < 37 mm) in all Cenozoic intervals. Furthermore, and in contrast to both small mammal disparity (yellow curve; Figure 2.3) and overall mammal disparity (grey curve; Figure 2.3), larger mammals show higher jaw functional disparity in the Pleistocene–Recent than in the Eocene (blue curve; Figure 2.3). Throughout the early Paleogene and in the Pleistocene-Recent, mammals with jaws lengths of less than 37 mm

contribute very little to overall disparity. This is because mammals of this size do not occupy regions of function space that are not also occupied by mammals with jaw lengths of more than 37 mm.

Figure 2.4 shows patterns of jaw functional disparity for small- and large-bodied mammals when using a cut-off of 127 mm ('size class division 5'). This cut-off categorises larger numbers of species as being small-bodied, and is based on the maximal jaw size of Mesozoic mammals (*Repenomamus gianteus*; 126.4 mm). This results in the recovery of substantially greater disparity among 'small' mammals (jaw length < 127 mm) during the Eocene and Pleistocene-Recent than in the Mesozoic or Paleocene (Figure 2.4), and contrasts with the pattern obtained for mammals with jaw lengths < 37 mm (Figure 2.3). Small mammal disparity still decreases across the K/Pg boundary, and rises between the Paleocene and Eocene. However, unlike in Figure 2.3, this Paleocene-Eocene disparity increase raises small mammal disparity to levels higher than those recovered for the Mesozoic. Using size class division 5, overall mammal disparity in the Paleocene is higher than either small mammal disparity or large mammal disparity individually, suggesting that this higher overall disparity is caused primarily by differences between the occupation of function space by small mammals compared to large mammals. This can be seen in Figure 2.6c, in which small mammals alone occupy the upper left quadrant of Paleocene function space. Large mammals (jaw lengths > 127 mm) show a pattern of increasing disparity throughout the early Paleogene and into the Pleistocene-Recent (blue curve; Figure 2.4) and show higher jaw functional disparity in the Pleistocene-Recent compared to the Eocene. This is similar to the result

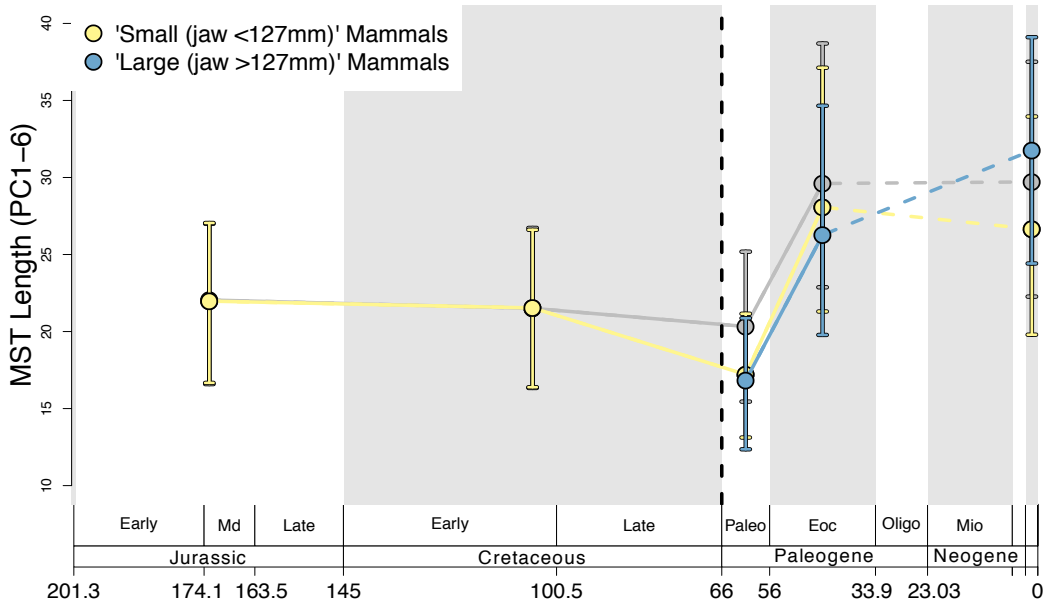


Figure 2.4. Jaw functional disparity through time, calculated as minimum spanning tree length across 5000 rarefied (n = 19) bootstrap replicates. The yellow curve depicts disparity levels through time among mammals within a small size class (defined here as any mammals that has a jaw length of 127 mm or less). The blue curve shows disparity levels among mammals with a larger size class (with mammals exhibiting a jaw length of more than 37 mm). The grey line depicts overall jaw functional disparity though time. A solid line connecting points indicates bin-to-bin disparity changes, while a dashed line indicates unsampled bins in between the disparity estimates.

obtained using all other cut-off values for body size categories (Figures 2.3 and Figures S2.1-S2.3). Futhermore, it occurs despite overall body size disparity and maximum size of Peistocene–Recent mammals being similar to that of the Eocene (Alroy, 1998, Smith, 2010, and see Figure S1.2).

Patterns of jaw functional disparity of small mammals vary depending on selection of cut-off value for body size categories. Size class divisions 2-4 recover high disparity of small mammals during the Eocene (i.e. substantially higher than in the Mesozoic; Figures S1-S3), similar to those recovered for size class division 5 (Figure 2.4). In fact, when using size class divisions 3-5 (Figure 2.4 and Figures S2.2 and S2.3), Eocene small mammal disparity is higher than Eocene large mammal disparity. Nevertheless, results for divisions 2-4 differ from those from division 5, and are similar to those from division 1 in finding

that small mammal disparity in the Pleistocene-Recent is similar to that of the Mesozoic (Figure S2.1 and S2.3).

Function space resulting from principal component analysis (PCA)

Figures 2.5a-e and 2.6a-e and Figures S2.4a-e-S2.5a-e show the spread of mammal species in PC1-PC6 function space through time, with points coloured according to body size. The frequency of mammal species from each size class distributed along PC1-PC6 are shown above (x-axes) and to the right (y-axes) of each function space. PC1 summarizes 34.38% of the variance, and relative diastema length (Sup. Mat. S1.1, T1) and relative molar length (Sup. Mat. S1.1, T2) have high loadings on this axis. Mammals that plot more negatively on PC1 have, on average, larger diastemas and smaller molar rows relative to overall jaw length. PC2 summarizes 23.35% of the variance and correlates well with jaw closing mechanical advantage (Sup. Mat. S1.1, T3), jaw slenderness (Sup. Mat. S1.1, T4), and coronoid process slenderness (Sup. Mat. S1.1, T5). Mammals plotting more negatively on PC2 have, on average, a smaller jaw closing mechanical advantage, an anteroposteriorly slender coronoid, and a more dorsoventrally slender jaw. PC3 explains 19.75% of the variance and correlates well with the jaw articulation offset (Sup. Mat. S1.1, T6), so that mammals that have more positive PC3 scores have a smaller articulation offset in relation to overall jaw length. PC4 summarizes 11.5% of the overall variance and correlates primarily with anteriorposterior slenderness of the coronoid process (Sup. Mat. S1.1, T5), with more positive scores on PC4 indicating a more anteriorposteriorly slender coronoid process. PC5 summarizes just 7.5% of the

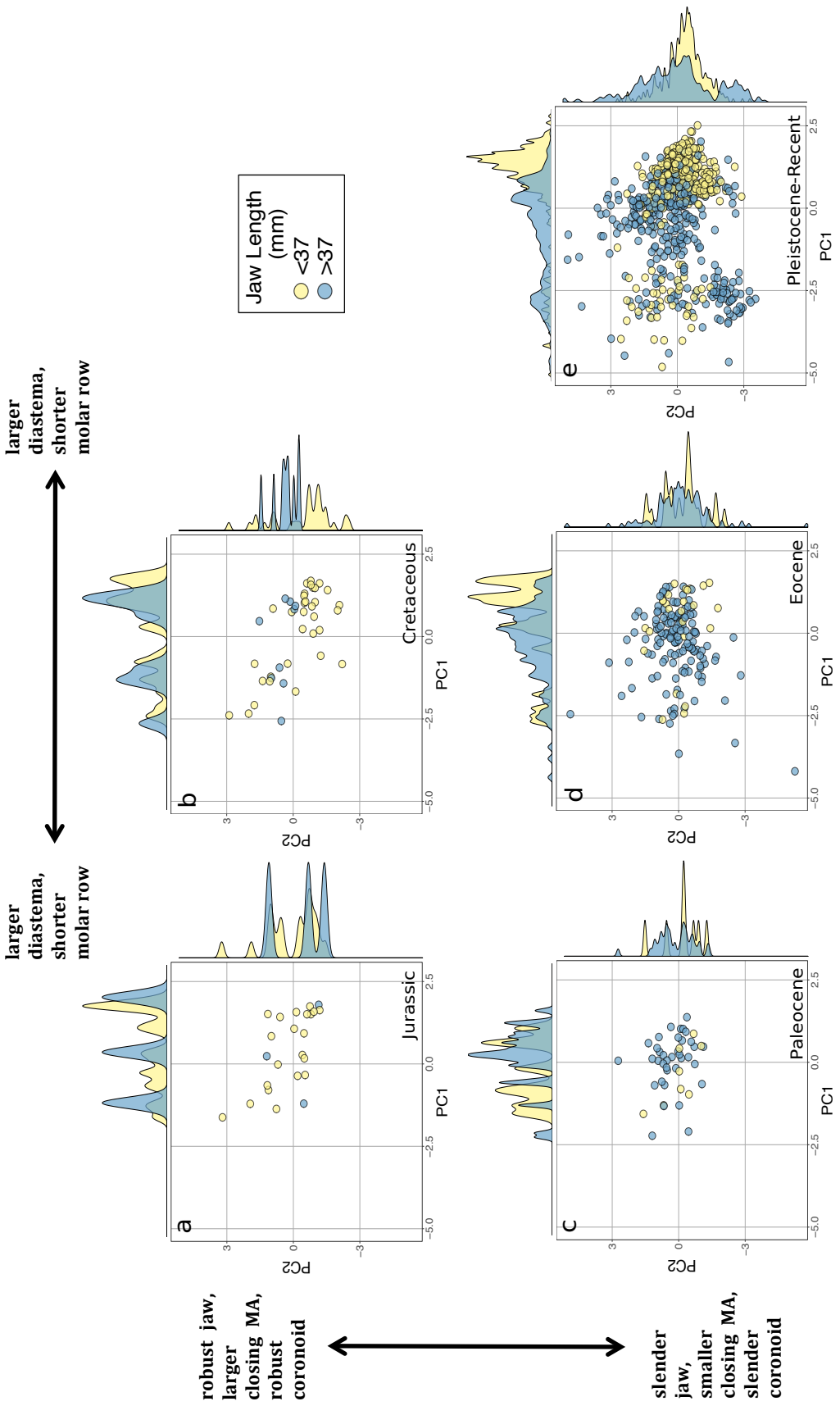


Figure 2.5. PC1-2 function space, split by Mesozoic periods, Cenozoic epoch, and the Recent, including Pleistocene megafauna. Points are coloured by size class (see legend). For this analysis, the size classes were based on mammals with jaw lengths of either below (small) or above (large) 37 mm. On each function space plot, frequencies of points in each size class along PC1 (top) and PC2 (right) are shown.

variance but nevertheless correlates with both the slenderness of the jaw ramus (Sup. Mat. S1.1, T4) and the articulation offset ratio (Sup. Mat. S1.1, T6). More positive PC5 scores indicate a more robust jaw ramus and a larger offset between the tooth row and the mandible articulation. PC6 summarizes the final 3.5% of the variance. It correlates primarily with relative molar length (Sup. Mat. S1.1, T2) and relative diastema length (Sup. Mat. S1.1, T1). Mammals plotting more positively on this axis have broadly shorter relative diastemas and longer relative molar rows.

Description of function space occupancy through time among small- and large-bodied mammals

Figure 2.5a-e shows PC1-PC2 jaw function space through time using the smallest size class cut-off value of 37 mm (size class division 1). Using this smallest maximum size class value, it is worth noting that in our Pleistocene-Recent sample (Figure 2.5e), small mammals and large mammals make up relatively even proportions of the overall sample of species. In the Paleocene and Eocene, however, large mammals (blue points; Figures 2.5c-d) make up a much larger proportion of the overall sample for each time bin. This difference in size class frequencies between extinct and extant mammals may be an artefact of preservation biases negatively affecting the preservation potential of smaller more fragile mammal specimens (Kidwell, 2001). Of course there are proportionally fewer mammals in the large category in the Jurassic and Cretaceous. This is somewhat because the cut-off of 37 mm was explicitly chosen based on the observation that jaws larger than 37 mm were rare in the

Mesozoic. Larger Mesozoic mammals with jaw lengths between 37 mm - 127 mm did occur, but the maximum jaw length of Cenozoic mammals is much greater (1017 mm).

Changes in function space occupation from the Mesozoic to the early Cenozoic have been discussed in detail in Chapter 1, and therefore will not be the focus of this chapter. Instead I will examine differences in function space occupation between small and large mammals through time.

Small (jaw length < 37 mm) Cretaceous mammals show notably different distributions in function space to those of larger species along PC2 (Figure 2.5b), PC4 (Figure S2.4b) and PC5 (Figure S2.5b, Table S2.1). Large Cretaceous species (jaw length > 37 mm) include almost exclusively members of the gobiconodontid clade. On PC2, large mammals exhibit scores close to the axis centroid, and for PC4 exhibit more positive values, whereas most small mammals exhibit more negative scores, producing distributions which do not fully overlap in range. On PC5, large mammals overlap with small mammals primarily at more negative values (a more slender jaw ramus, and coronoid process slenderness).

Paleocene mammals show no significant difference in the function space occupation of small and large species along five of the six principal components axes (Table S2.1). PC3 (Figure S2.4c) shows a significant difference, with small mammals clustering more densely in the lower right quadrant of PC3-4 function space and large mammals cluster more densely in the upper-left region of function space.

Eocene mammals show a significant difference in the function space occupation of small and large species along PC1, PC3 and PC6 (Table S2.1). On PC1 (Figure 2.5d) small mammals show a slightly bimodal distribution, with a lack of small mammals exhibiting intermediate PC1 values. Although bimodal, many fewer small mammals exhibit negative PC1 values than positive. Large mammals show a wider range of PC1 scores than small mammals, encompassing the PC1 small mammal range. Within this range, larger mammals populate positive PC1 values more densely. Eocene small mammals exhibit more positive PC3 scores than large mammals and the most extreme positive scores known for the Eocene are exclusively seen in smaller mammals. Conversely, the most extreme negative PC3 scores represent larger mammals. For PC6, more negative values are populated more densely by larger mammals, producing different frequency curves.

In the Pleistocene-Recent, small and large mammals (split using size class division 1) exhibit significantly different distributions across all principal components axes (PCs 1-6; Table S2.1). Aspects of their distributions are similar to those of the Eocene, as follows: (1) Small mammals of the Pleistocene–Recent have a bimodal distribution of PC1 scores, however this separation between the two areas of function space occupied by small mammals is more apparent than in the Eocene. (2) Small mammals populate positive PC1 scores more densely than they populate negative PC1 scores. Large mammals on the other hand more densely populate intermediate and more negative PC1 scores. For PC2, small mammals have a more restricted range of values, and intermediate values are more densely populated. Large mammals have a wider range of PC2 values

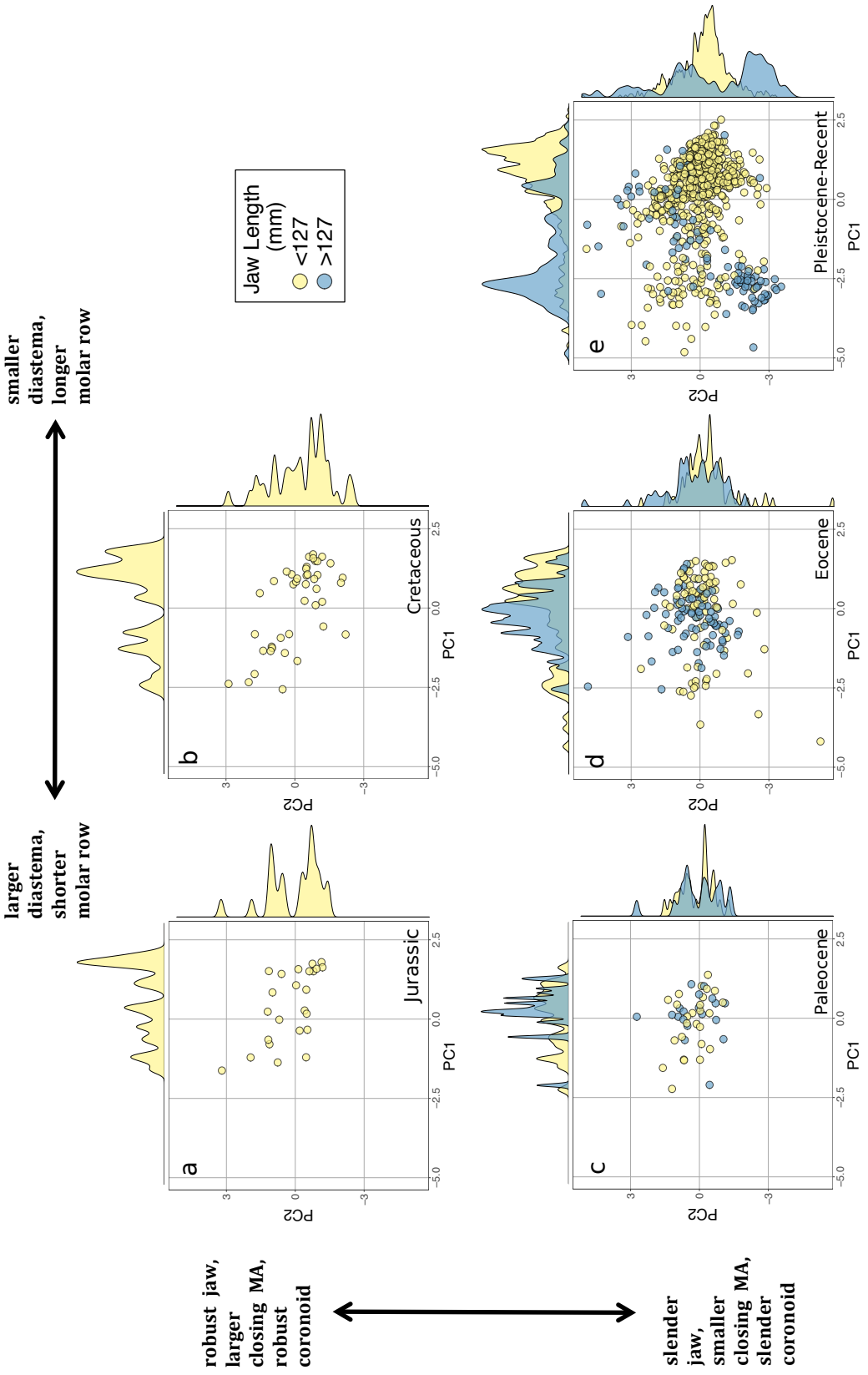


Figure 2.6. PC1-2 function space, split by Mesozoic periods, Cenozoic epoch, and the Recent, including Pleistocene megafauna. Points are coloured by size class (see legend). For this analysis, the size classes were based on mammals with jaw lengths of either below (small) or above (large) 127mm. On each function space plot, frequencies of points in each size class along PC1 (top) and PC2 (right) are shown.

and are more evenly distributed. In PC1-2 function space, there are areas which are populated either primarily or exclusively by either large or small mammals (Figure 2.5e). Most notably, large mammals exclusively inhabit the left-lower quadrant of function space. Large mammals also inhabit the middle region of PC1 function space, an area unoccupied by the bimodal distribution of small mammals. Pleistocene-Recent large mammals exhibit more negative PC3 scores, and do not overlap with small mammals in this region of function space using size class division 1 (Figure S2.4e). Small and large mammals have a more similar distribution across PC4, but small mammals cluster closer to central PC4 values. In PC5-6 function space, almost all mammals are closely clustered as PC5-6 only summarize just over 10% of the data when combined. Nevertheless, small mammals plot more densely in the lower-left quadrant, and large mammals in the lower-left quadrant (Figure S2.5e). Small mammals therefore more often plot more positively on PC5 and more negatively on PC6 in comparison to large mammals.

Figures 2.6a-e and Figures S2.6a-e and S2.7a-e show function space using size class division 5. As a result fewer mammals (and zero Mesozoic mammals) are included in the large size class (here mammals with jaw lengths >37 mm). In the Paleocene, this reclassification results in no significant difference being recovered between small and large mammals on any principal components axes. Among Eocene mammals, PC2, PC3, PC5, and PC6 show significant differences between small and large species. In Eocene PC1-2 function space, all of the mammals that plot further from the centroid in the lower-left quadrant are mammals with jaw lengths between 37 mm - 127 mm. In PC5-6 function

space Eocene mammals show a more obvious split between small mammals in the upper-right quadrant and large mammals in the lower-left quadrant. In the Pleistocene-Recent all but PC5 show a significant difference between small and large mammals (Table S2.5). The number of large mammals falling close to the centroid of PC1-2 function space is greatly reduced compared to size class division 1 (Figure 2.5e), indicating that the large majority of mammals in this region of function space have jaws between 37 mm – 127 mm.

For the other three size class divisions examined (size class divisions 2-4), the Paleocene shows no significant difference across any axes, the same as for size class division 5. Results for significance tests on Eocene PC1-6 yield the same results as size class division 1 using size class divisions 2-4 (Table S2.2-S2.4). Conversely, the Pleistocene-Recent shows significant differences between small and large mammals across PC1, and PC3-6 for size class divisions 2 and 3, and across PC1, PC3, PC4 and PC6 for size class division 4.

Despite these subtle differences, the following patterns are repeated across all size class divisions.

(i) Some Cretaceous mammals have jaw lengths exceeding 37 mm and are classified as 'large' under some of the schemes (e.g. division 1). These larger Cretaceous mammals show significant differences in function space occupation along PC2, PC4, and PC5, resulting from their limited range of ecomorphologies.

(ii) Paleocene mammals show almost no difference in occupation of function space between small- and large-bodied species.

(iii) Eocene mammals show significant differences between small and large species along up to four principal components axes, but never along PC1, the axis that explains the largest amount of variance.

(iv) Pleistocene-Recent mammals show a significant difference in size class across at least four and more often five or all six principal components across size class divisions 1-5. In contrast to the Eocene time bin, a significant difference is always recovered along PC1, which explains approximately 35% of the variance.

In summary, there is a pattern of increasing differentiation of the jaw ecomorphologies of small mammals and large mammals throughout the Cenozoic, with the largest differences in function space occupation recovered in the Pleistocene-Recent sample.

This result is also supported by the significant difference in multivariate spread (mean Euclidean distance from centroid in a space defined by PC1-6) between small and large species during the Pleistocene–Recent, unlike other intervals (Figures S2.9 and S2.10, Table S2.6). This indicates that large mammals are considerably more disparate than small mammals during the Pleistocene–Recent (size class division 1; Figure S2.9, size class division 5; Figure S2.10, Table S2.6). This result is also obtained when Pleistocene mammals are removed and Recent mammals are analysed alone (Table S2.7).

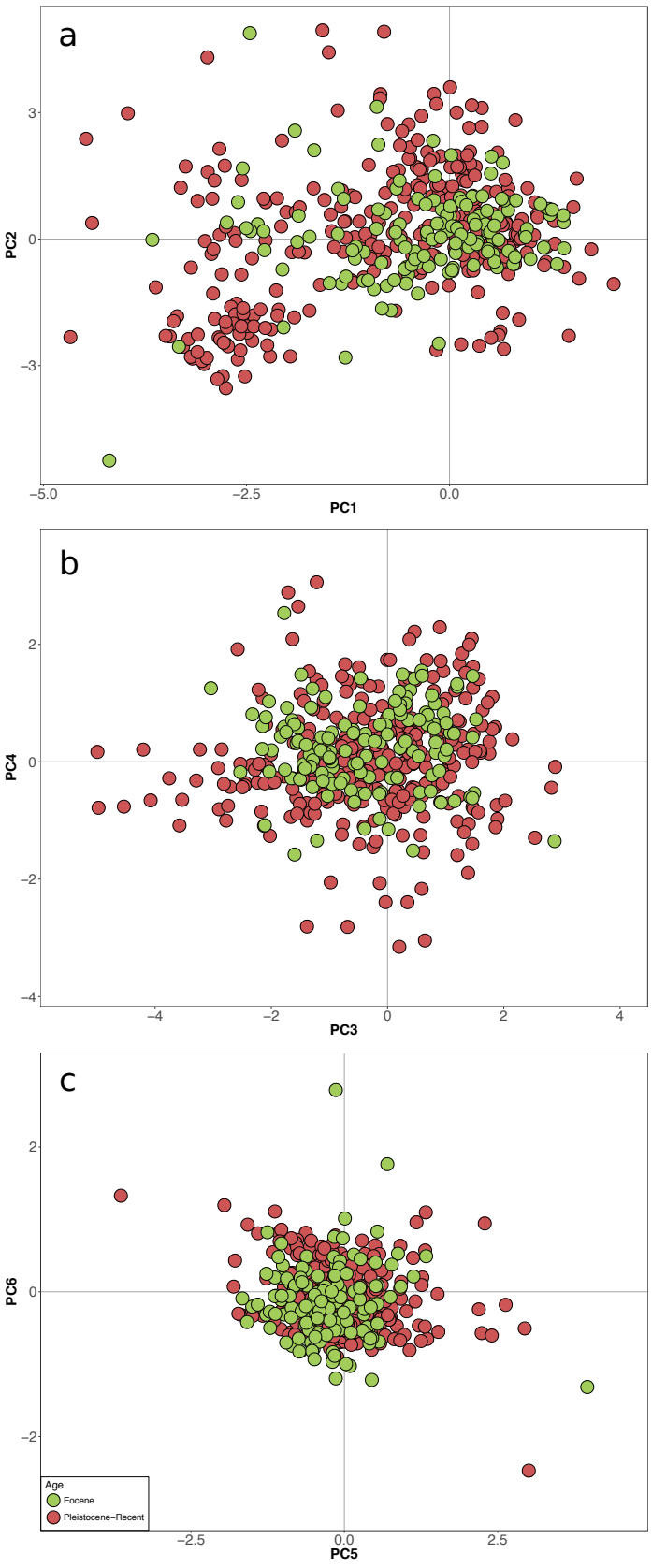


Figure 2.7. The overlap between species of Eocene (green points) and Pleistocene-Recent (red points) mammals in the large size class in (a) PC1-PC2 (b) PC3-PC4 and (c) PC5-PC6 function space. Size class division 1 was used (37 mm).

Increases in large mammal function space occupation from the Eocene to the Pleistocene-Recent

Despite previous evidence that maximum body size levelled off from the Eocene onwards (Smith, 2010), mean distance from size class centroid is higher among large Pleistocene-Recent mammals than in the Eocene. This, coupled with increased function space separation of small and large mammals from the Eocene to the Pleistocene-Recent, warrants closer inspection.

Figure 2.7a-c show the overlap of large Eocene (green) and large Pleistocene-Recent (red) mammals in PC1-2 (Figure 2.7a), PC3-4 (Figure

2.7b) and PC5-6 (Figure 2.7c) function space using size class division 1. The same plot but using size class division 5 can be seen in figure S2.8a-c. On all axes except PC6, large Pleistocene-Recent mammals have expanded their jaw function space occupation to some extent in both directions when compared to large Eocene mammals (Figure 2.7a-c, Figure S2.8a-c). The fact that some areas of function space which are expanded into in the Pleistocene-Recent are lost when using the largest size class division (size class division 5; excluding mammals with jaw lengths of between 37 mm – 127 mm from the large size class) demonstrates that some of these more disparate Pleistocene-Recent mammals are among those 'medium sized' mammals which get reclassified across size class divisions used. These mammals plotting more disparately in function space are therefore comparable in size to the largest outliers known from the Mesozoic.

Figure 2.8a-b shows PC1-2 large mammal function space for the Eocene (green, Figure 2.8a) and for the Pleistocene-Recent (red, Figure 2.8b). Silhouettes indicate the types of mammal species occupying different regions of function space. Figures 2.9a-b and 2.10a-b show the same Eocene and Pleistocene-Recent large mammals but for PC3-4 (Figure 2.9a-b) and PC5-6 (Figure 2.10a-b).

One pattern that is clearly recovered regardless of the size class division used (Figures 2.7a and S2.8a) is a clustering of larger mammals in the lower left quadrant of PC1-PC2 Pleistocene-Recent function space, indicating larger diastemas, slender jaws, and a shorter relative molar row length. Mammals enter this region of function space for the first time in the Eocene, and no

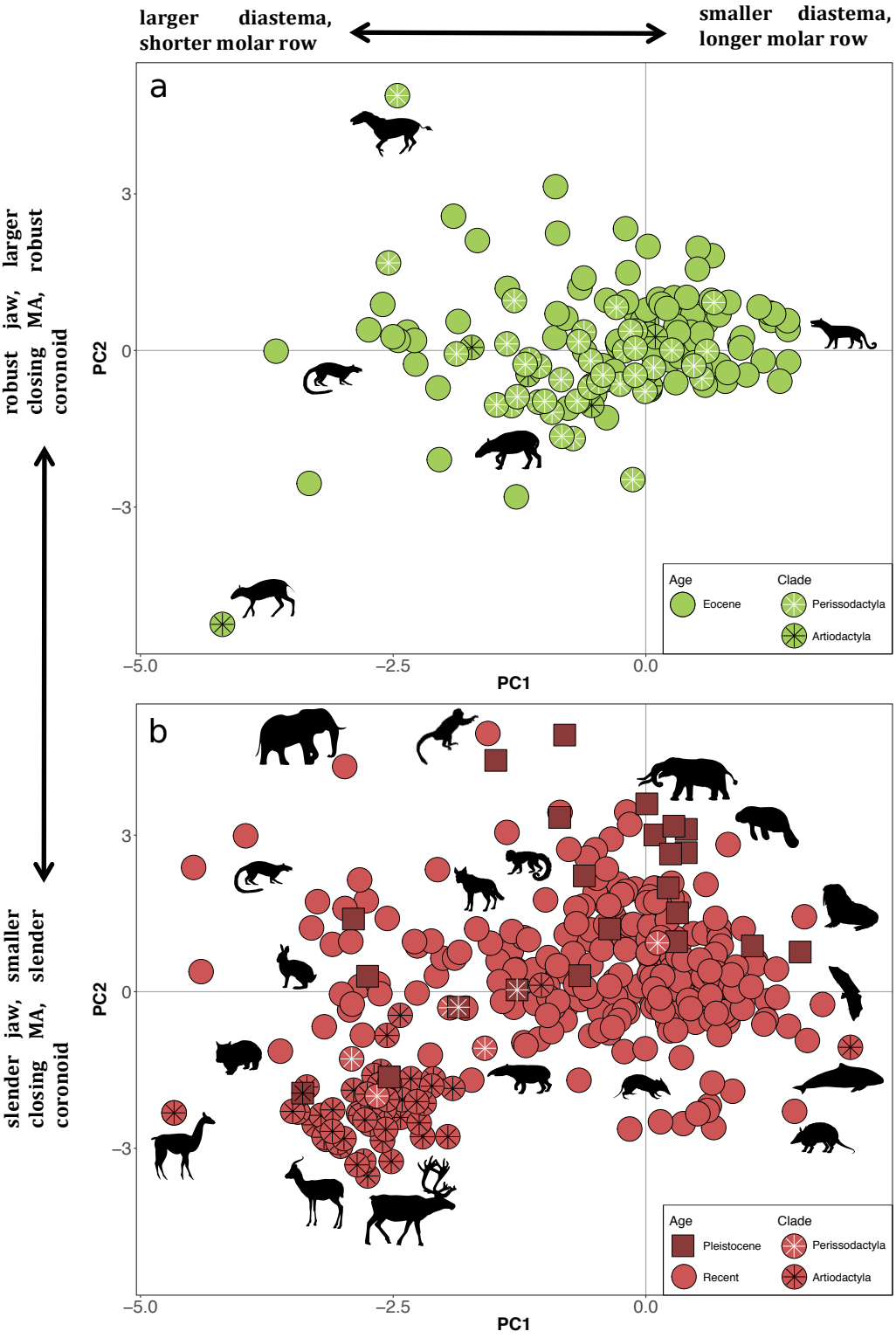


Figure 2.8. Large mammal PC1-2 function space in (a) the Eocene (shown in green) and (b) the Pleistocene-Recent (shown in two shades of red). The lowest threshold of 37mm is used here, and all mammals with a jaw length larger than 37mm are included. Pleistocene mammals are highlighted in graph b using a square data point and a deeper colour of red (see key for b). In both (a) and (b), members of Perissodactyla are identified with a white star, and members of Artiodactyla are identified with a black star. Silhouettes indicate which mammals the data points represent. All silhouettes were taken from phylopic (Keesey, 2018).

mammals with jaws smaller than 37 mm fall within this region of function space in any of the sampled time bins (Figure 2.5). During the Eocene, all three of the mammals that plotted within this region of function space (two species of the palaeanodont *Metacheiromys* and the hypertragulid artiodactyl *Hypisodus minimus*) had jaws comparable in size to the largest 18.19% of mammals in the Mesozoic sample (between 37 mm – 127 mm) (Figure 2.5d). In the Pleistocene-Recent, however, many mammals with jaws larger than 127 mm densely occupy this region of function space. These Recent mammals are almost exclusively artiodactyls plus and two horse species (Perissodactyla; *Equus grevyi* and *Equus caballus*). *Llama glama* and *Gazella gazella* represent two extreme PC1-2 jaw ecomorphologies among artiodactyls (Figure 2.8b). The artiodactyls plotting in this region of function space exhibit a large relative diastema, a short relative molar row, and a slender mandibular ramus.

Artiodactyls with more extreme morphologies are also clearly separated from other Pleistocene-Recent mammals and all Eocene mammals except for the perissodactyl *Protitanops curryi* along PC3 (Figure 2.9). This distribution of perissodactyls and artiodactyls overlap substantially in regions of Eocene function space. More species of perissodactyl than artiodactyl are known from the Eocene, whereas Recent artiodactyls are far more speciose than perissodactyls. If we believe that this discrepancy is not a product of differential preservation potential, this increased diversity of artiodactyls comes alongside a shift in their jaw functional ecology and a separation of artiodactyls and perissodactyls in function space.

Proboscideans also occupy a distinct region of Pleistocene-Recent

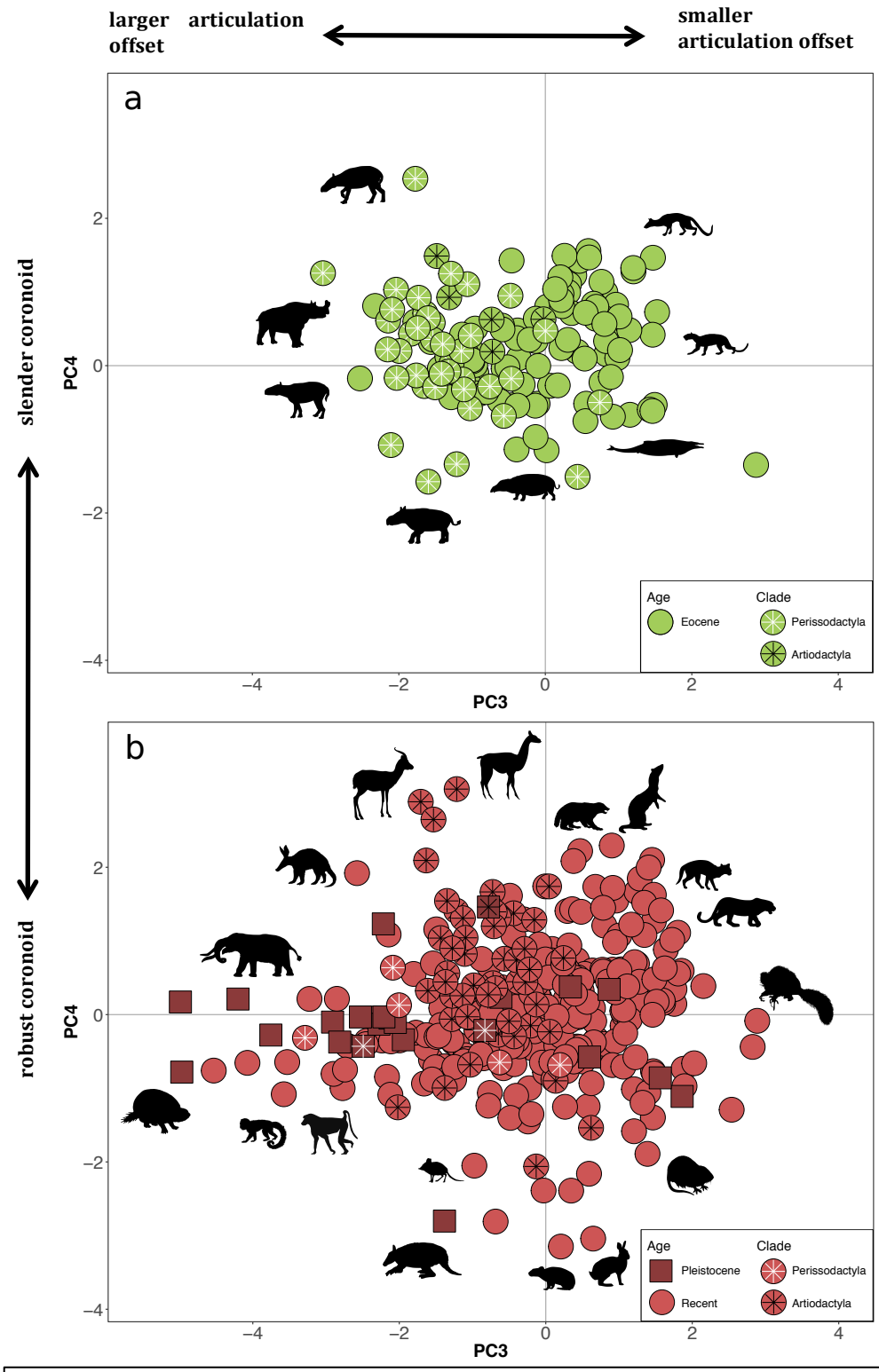


Figure 2.9. Large mammal PC3-4 function space in (a) the Eocene (shown in green) and (b) the Pleistocene-Recent (shown in two shades of red). The lowest threshold of 37mm is used here, and all mammals with a jaw length larger than 37mm are included. Pleistocene mammals are highlighted in graph b using a square data point and a deeper colour of red (see key for b). In both (a) and (b), members of Perissodactyla are identified with a white star, and members of Artiodactyla are identified with a black star. Silhouettes indicate which mammals the data points represent. All silhouettes were taken from phylopic (Keesey, 2018).

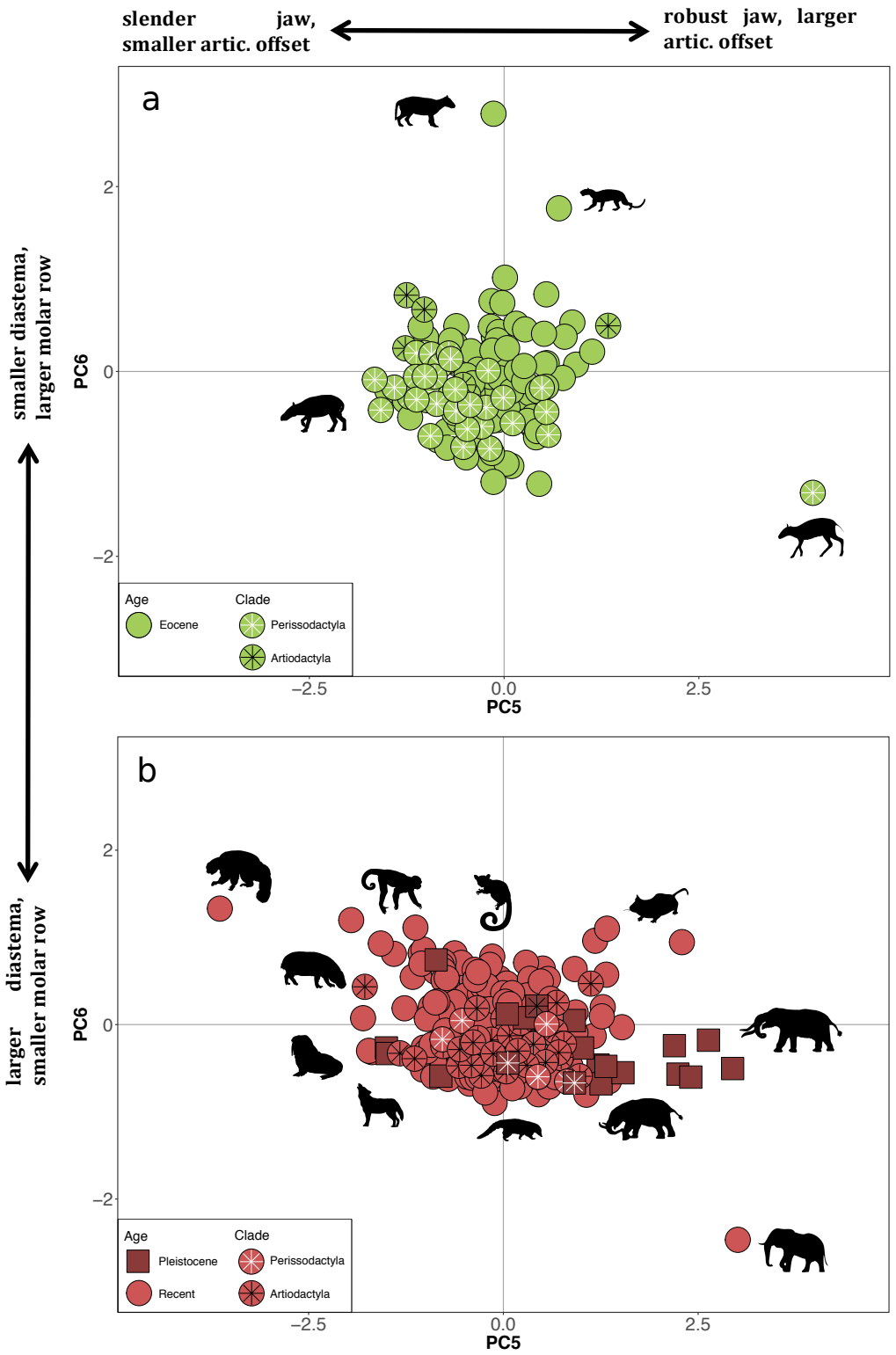


Figure 2.10. Large mammal PC5-6 function space in (a) the Eocene (shown in green) and (b) the Pleistocene-Recent (shown in two shades of red). The lowest threshold of 37mm is used here, and all mammals with a jaw length larger than 37mm are included. Pleistocene mammals are highlighted in graph b using a square data point and a deeper colour of red (see key for b). In both (a) and (b), members of Perissodactyla are identified with a white star, and members of Artiodactyla are identified with a black star. Silhouettes indicate which mammals the data points represent. All silhouettes were taken from phylopic (Keesey, 2018).

function space, a pattern that is clearly visible across multiple principal components analyses and all size class divisions. In PC1-2 function space, proboscideans exhibit a range of PC1 values, but all plot among the most positive values for PC2, indicating a more robust and deeper jaw ramus, a more robust coronoid process, and a larger jaw closing mechanical advantage. The extant *Elephas maximus* is separated from Pleistocene proboscideans by exhibiting a more negative PC1 value (larger relative diastema, shorter relative molar row). Pleistocene *Mammuthus primigenius* and *Palaeoloxodon mnaidriensis* also plot more negatively on PC1, separating them from species with more positive PC1 scores such as Pleistocene *Stegomastodon aftoniae* and *Haplomastodon chimborazi*. This represents a range of relative molar row lengths, with the extant *Elephas* having a relatively smaller length of grinding surface than do Pleistocene members of the clade. In PC3-4 function space (Figure 2.9) all members of Proboscidea occupy a distinct region of function space characterised by a large relative distance between the tooth row and the jaw articulation (negative PC3 values). For PC5-6, all Pleistocene proboscidean species cluster together, but *Elephas* is separated once again showing a more negative PC6 score (Figure 2.10). This again appears to reflect a shorter relative molar row in *Elephas maximus*. On all axes, *Dugong dugong*, a close relative of proboscideans (and the only sirenian included in this dataset), falls within a similar region of function space (Figures 2.8-2.10).

For PC1-2, an area of function space representing the most extreme morphologies found in the lower right quadrant is populated in the Pleistocene-Recent but not in the Eocene (Figure 2.8a). These mammals have jaws of

between 37 mm – 127 mm in length, and are therefore comparable in size to Mesozoic outliers. Species plotting here largely belong to the marsupial clade Peramelemorphia (bandicoots), exhibiting the following unique set of traits: a slender jaw ramus, a smaller jaw closing mechanical advantage, a more anteriorposteriorally slender coronoid, a long relative molar length and a short relative diastema length.

Some rodents such as *Castor canadensis* (beaver) and *Pedetes capensis* (springhare) the lagomorphs *Ochotona sp* (pika) and *Lepus americanus* (hare) and the primate *Daubentonia madagascarensis* (aye-aye) also occupy unique regions of Pleistocene-Recent function space when using size class divisions that include mammals with jaw lengths of 37 mm – 127 mm. For PC1-2 these mammals plot in the upper left quadrant of function space (Figure 8a), and posess longer relative diastemas, smaller relative molar rows, a larger jaw closing mechanical advantage, a more anteriorposteriorally robust coronoid process, and a more dorsoventrally robust jaw ramus.

Discussion

Size-partitioned jaw ecomorphological disparity in the Mesozoic and Cenozoic

Increases in both maximum body size (Alroy, 1998, Smith, 2010, Slater, 2013) and morphological disparity (Halliday and Goswami, 2016) alongside increases in diversity (McKenna and Bell, 1997, Alroy, 1999, Archibald and

Deutschman, 2001, Benson et al, 2016), characterise the mammalian adaptive radiation of the early Cenozoic (Osborn, 1902, O'Leary et al, 2013, Slater, 2013, Halliday & Goswami, 2016). In order to better understand the mechanisms that drive these changes in disparity, I tested the relationship between increased Cenozoic body size and jaw ecomorphological disparity. Small mammals with jaw lengths shorter than 37 mm, comparable in size to over eighty per cent of Mesozoic mammals, do show relatively low disparity in comparison to mammals with jaw lengths of more than 37 mm and remained essentially static throughout the Jurassic, Cretaceous and Cenozoic (Figure 2.3). This finding that small mammals may be restricted in their morphologies could indicate a restricted range of feeding ecologies among smaller mammals (Lillegraven et al, 1979, Smith, 2010). It is also possible, however, that small mammals need less extreme morphologies than large mammals to achieve disparate ecologies (Stanley 1973). If the latter is true, small mammals could display lower phenotypic disparity than large mammalsF, but nevertheless occupy more disparate ecologies.

Two modern clades consisting largely of small mammals, rodents (Rodentia) and bats (Chiroptera), are today extremely speciose (Nowak, 2006). Despite this, these clades form clusters in function space, making them anatomically conservative. These clusters persist despite the existence of different observed feeding ecologies within each clade. In particular bat jaws exhibit very similar morphologies when considered among mammals as a whole despite distinct feeding strategies including insectivory, frugivory, piscivory and sanguivory (Nowak, 2006). This suggests that separation between rodents and

bats, and the clustering of closely related species could largely be a phylogenetic signal.

Throughout time, there are very few regions of function space populated exclusively by the smallest mammals (with jaw lengths of less than 37 mm) (Figures 2.5a-e and S2.4a-e and S2.5a-e). Large mammals on the other hand occupy spaces that never appear to be colonized by small mammals (Figures 2.5a-e and S2.4a-e and S2.5a-e).

Despite a clear and consistent pattern of lower disparity among mammals which are comparable in size to the vast majority of Mesozoic mammals (Figure 2.3), a small number of Mesozoic mammals did reach larger sizes. In the Cenozoic and Pleistocene-Recent, mammals comparable to these larger mammals do achieve higher levels of jaw ecomorphological disparity (Figure 2.4). These mammals exhibit jaw lengths of between 37 mm and 127 mm. When mammals with jaws of this size are included in my small mammal subset (size class division 5; Figure 2.4) small mammal disparity does then increase across the K/Pg boundary and into the Cenozoic. Although analyses are carried out both including and excluding mammals with these jaw sizes in the small mammal sample, I feel more confident with the analyses where these are categorised as large mammals (size class division 1). This is because these mammals exhibit disparity patterns more similar to larger mammals than to smaller mammals. For this reason the results from size class division 1 are considered more reliable (Figure 2.3 and Figure 2.5a-e).

Regardless of this, the results indicate that Mesozoic mammals were able to achieve sizes at which Cenozoic mammals were able to exploit more

disparate and novel morphologies. This suggests that constrained size was not the sole factor in keeping Mesozoic mammals conservative in jaw ecomorphology. It is likely, however, that the rarity of these larger Mesozoic mammal species resulted in poor exploration of function space prior to the K/Pg. In fact Mesozoic mammals included in the large subset show lower disparity than small Mesozoic mammals, despite reports of novel Mesozoic ecologies among mammals in this size class (e.g. *Repenomamus giganticus* is reported as being carnivorous (Hu et al, 2005)). In the Cenozoic and Pleistocene-Recent mammals with jaw lengths of between 37 mm – 127 mm have a much larger and more disparate function space occupation, but also retain morphologies similar to these Mesozoic species.

During the Mesozoic, the vast majority of these mammals with jaw lengths of 37 mm – 127 mm are members of the Gobiconodontidae, suggesting that only one clade managed to consistently sustain these larger body sizes prior to the K/Pg mass extinction event.

Evidence for a lag in exploration of available function space by larger mammals is further supported by an increase in both large and overall mammal disparity across the Paleocene/Eocene boundary. In contrast, Paleocene large mammals explore only areas already previously occupied by small mammals, resulting in an increase in large mammal disparity across the K/Pg, but not in overall disparity. Changes in large and small mammal disparity levels and function space occupation across the Paleocene/Eocene boundary, as well as a plateauing of maximum body mass from the Eocene onward, backs up ideas that the Eocene was a period of large scale reorganisation (immigration into novel

regions) and evolution among mammals (Gervais, 1877, Clyde and Gingerich, 1998, Rose, 2005). Extrinsic factors such as changes in vegetation and habitat (Wing et al, 2005, Jaramillo et al, 2010) in response to climate perturbations (the Paleocene/Eocene thermal maximum (PETM) (as identified by a global carbon isotope excursion; Sloan and Thomas, 1998, Aubrey et al, 2003) likely contributed to this.

Disparity increases in Pleistocene-Recent large mammals

Despite a plateau in maximum body mass since the Eocene (Alroy, 1998, Alroy, 1999, Smith, 2010), Pleistocene-Recent large mammals exhibit higher levels of jaw function disparity in comparison to the Eocene (Figure 2.3, Figure 2.4, F2.5a-e and 2.6a-e). In the Pleistocene-Recent, large mammals explore more disparate regions of function space while small mammals reduce their function space occupation. This results in a constant disparity level in the Eocene and the Pleistocene-Recent, but a reorganisation of function space.

Among modern mammals, artiodactyls (Artiodactyla) and horses (*Equus*) populate an area of function space only populated previously by three other mammals in the dataset: two species of the mid-Eocene paleanodont *Metacheiromys,* and the latest Eocene-Oligocene artiodactyl *Hypisodus mimimus*. Although *Metacheiromys* overlaps with terrestrial artiodactyls in PC1-2 function space, they differ in overall form of their jaw in ways not easily captured by functional measures used here. Despite sharing functional characters such as a slender mandibular ramus, a short relative molar row, a long relative diastema, and a slender coronoid process, it seems probable that they had contrasting

ecologies. *Metacheiromys* and other paleanodonts are stem pangolins (Rose et al, 2005, O'leary et al, 2013), with reduction in dentition likely reflecting an increasing specialisation on insect prey. Modern pangolins and other ant- and termite-eating mammals have either completely (pangolins, echidnas, ant-eaters) or largely (aardvarks, aardwolves) reduced their teeth (Nowak, 2006). Consequently, these modern toothless mammals were not included in this analysis due to a lack of analogous tooth row traits. Nevertheless, these mammals clearly possess disparate ecomorphologies which have been present from at least the Eocene.

The Eocene *Hypisodus* on the other hand is also an artiodactyl. *Hypisodus minimus* is one of the youngest mammals in the Eocene sample, and is known from the latest Eocene and Oligocene. *Hypisodus* is smaller than most modern artiodactlys (Matthew, 1902, Nowak, 2006), but is more similar in size to members of Tragulidae (chevrotains), which represent its closest living relative (Janis and Theodor, 2014). *Hypisodus* exhibits a mandibular morphology very similar to that of extant artiodactyls, and in fact plots further from the centroid of PC1-2 function space than all Recent artiodactyls. As well as having a number of traits that are associated with the specialised jaw morphology of artiodactyls captured by these functional traits (e.g. a large relative diastema length, a slender jaw ramus, a slender coronoid process, and a large articulation offset (e.g. Radinski, 1985)), *Hypisodus* also exhibits hypsodont-like dentition (Matthew, 1902, Meehan and Martin, 2004).

Modern ungulates that exhibit this combination of traits are grazing mammals (Janis et al, 2000), and include perissodactyl *Equus* and the

artiodactyls *Bos* and *Camelus*. It is worth pointing out, however, that artiodactlys with the same jaw functional traits and overall morphology but lacking the high crowns of hypsodont teeth (brachydont; e.g. *Sus*, *Giraffa*) are today recognised as browsers, and plot alongside these hypsodont mammals in function space. In fact, many more artiodactyl exhibited brachydont dentition, and have therefore been interpreted as grazers, in the Miocene compared to modern faunas (Janis et al, 2000). Nevertheless, the presence of these traits in association with hypsodonty in mammals prior to the widespread evolution of grasslands clearly shows that they did not evolve as a response to the proliferation of grasslands. Despite this, this derived jaw ecomorphology does not appear to have evolved until around 30 million years after the K/Pg boundary. Although rare in the Eocene and common in the Pleistocene-Recent, it appears that many more artiodactyls and horses evolved this ecomorphology separately during the Oligocene (e.g. protoceratid artiodactyl *Protoceras* (Scott, 1940), hypertragulid artiodactyl *Hypertragulus* (Scott, 1940, Meehan and Martin, 2004), leptomerycid artiodactyl *Leptomeryx* (Korth and Diamond, 2002) and the camelid artiodactyl Poebrotherium (Scott, 1891)), and was more common from the Oligocene onward, a time period not captured by the current study. Prior to the Eocene/Oligocene boundary, artiodactyls and perissodactyls did not occupy this region of function space, but rather overlapped in a region of function space still occupied by non-equid perissodactyls in the Recent. It is clear that this morphology evolved in response to ecological changes that occurred around the late Eocene. More recent studies have suggested that a possible increase in levels of grit ingested from when feeding resulted in the

need for more wear-resistant hypsodont teeth (e.g. Jardine et al, 2012). Lagomorphs and some rodent clades also have hypsodont molars, and species from these two clades also show disparate morphologies on some principal components axes.

Recent and Pleistocene proboscideans occupy novel regions of Pleistocene-Recent function space. One species, *Moeritherium lyonsi*, is included in our Eocene sample. In comparison to Pleistocene-Recent proboscideans, *Moeritherium* does not plot as far from the centroid. Pleistocene-Recent probosideans have an extremely derived jaw morphology. They have a robust mandibular ramus and a large articulation offset, and poses large, primarily flat grinding teeth with lophs. Extant elephants are today the largest terrestrial mammals (Nowak, 2006).

On multiple principal components axes, extant proboscidean species do not share the same region of function space as Pleistocene proboscidean. On PC1-2, gomphotheres (e.g. *Stegomastodon*, *Haplomastodon*, *Notomastodon*) cluster in function space. Extinct elephantids (e.g. *Mammuthus*, *Palaeoloxodon*) also cluster in function space, but are separated from the gomphotheres, and from the extant *Elephas,* which does not overlap in function space with any of the aforementioned proboscideans. This suggests that the loss of Pleistocene megafaunas did remove a distinct ecomorphology from Recent mammal function space. Past studies suggest that gompotheres were primarily browsers, different from the more generalized feeding ecology of elephantids which includes components of browsing and grazing (Zhang et al, 2017).

Among groups of slightly smaller mammals in our large sample (many with jaw lengths between 37 mm – 127 mm), bandicoots occupy a novel region of Pleistocene-Recent function space. Bandicoots are insectivorous marsupial mammals, and exhibit jaws with a particularly slender jaw ramus, a long relative molar row, and a small relative diastema. They are the only marsupial mammals to carve out their own novel region of function space among Recent mammals in our dataset. These marsupial mammals exhibiting more disparate and unique morphologies is noteworthy, as marsupial mammals are more than ten times less speciose than extant placental mammals (Nowak, 2006).

Conclusion

With clear evidence that maximum body size and body size disparity increase across the K/Pg boundary, I aimed to test whether increases in ecomorphological disparity could be attributed to the appearance of larger mammals in the wake of the K/Pg boundary.

Small mammals do appear to have lower levels of jaw functional disparity than large mammals. Increases in Cenozoic jaw functional disparity were generated by higher overall disparity among large mammals and differences in ecomorphology between small and large mammals, more similar to scenario two outlined in the introduction (Figure 2.1b). It is hypothesized that Mesozoic mammals occupied body size ranges too small to explore many of the niches available to larger mammals. This is likely the result of physiological

and biological differences between small and large mammals, for example in their digestive physiology (Van Soest, 1996). Mesozoic species, and in particular species belonging to the clade Gobiconodontidae, did however reach body sizes at which post-K/Pg mammals were able to occupy a wider range of niches. Despite this it appears that there were too few larger Mesozoic mammals to fully explore large mammal function space. Further, feeding ecologies open to large Cenozoic mammals were likely more similar to ecologies already occupied by dinosaurs in the Mesozoic, (e.g. grazing herbivores), suggesting that the competitive exclusion hypothesis, although not solely responsible for low jaw ecomorphology in the Mesozoic, likely did play a role.

Although large mammals increase their jaw ecomorphological disparity consistently throughout our sampled time period, an expansion into regions of function space unavailable to small mammals did not happen until the Eocene, and continued into the Oligocene and the Pleistocene-Recent. The Eocene and the Oligocene both represent periods of mammalian faunal turnover (e.g. Badgley and Gingerich, 1988, Hooker et al, 2004, Rose, 2005, Hooker and Collinson, 2012). With the appearance and disappearance of numerous mammal lineages, these turnovers likely enabled new lineages to explore under-populated or vacant regions of jaw ecomorphological function space.

Among more modern mammals, the clades most responsible for the increase in jaw functional disparity among large mammals are artiodactyls, horses, and proboscideans. These clades contain primarily large-bodied herbivores (largest terrestrial Artiodactlya: Hippopotamus, ~4,500kg; largest modern proboscidean: ~7,500kg (Nowak, 2006)) with specialised jaw

morphologies evolved for either browsing or grazing, or both. It is unsurprising that all of the most disparate mammals are herbivores. Plant matter has changed its properties through time, whereas the properties of animal flesh has stayed constant (Wesley-Hunt, 2005), resulting in a need for herbivores to adapt while carnivores can continue to use the same basic jaw morphology through time.

Chapter 3

Rates of jaw functional trait evolution among Mesozoic and early Cenozoic mammals

Introduction

Patterns of jaw ecomorphological disparity during the proposed adaptive radiation of mammals after the Cretaceous/Paleogene (K/Pg) mass extinction have been thoroughly explored in the first two chapters of this thesis. However, documenting jaw functional disparity alone cannot answer fundamental questions regarding the pattern of evolution along phylogenetic lineages that gave rise to them. This is because patterns of morphological disparity produced from contrasting evolutionary dynamics can look nearly identical (Foote, 1996).

Modern mammals, and in particular eutherian mammals, are incredibly speciose and anatomically disparate, numbering approximately 5000 species (Nowak, 2006) and displaying a broad range of morphologies (Nowak, 2006). Acquisition of these novel ecologies and an associated burst of taxonomic diversification among eutherian mammals have generally been traced back to the K/Pg adaptive radiation (e.g. Osborn, 1902, Simpson, 1937, Rose, 2006,

O'Leary et al, 2013, Halliday and Goswami, 2016). The hypothesis of adaptive radiation was formulated to describe this pattern in mammals (Osborn 1902, Simpson, 1953), and has been applied more widely to describe a process by which an entire clade may radiate to fill available niches and associated ecomorphologies rapidly (eg. Schluter, 2000, Etienne and Haegeman, 2012). These niche-filling radiations are predicted to be accompanied by elevated rates of trait evolution (e.g. Harmon et al, 2010), and may in fact be a central mechanism for producing taxonomically and ecologically successful clades (Simpson, 1953, Schluter, 2000, Alfaro et al, 2009, Rabosky et al, 2013, Benson et al, 2014).

Inferring patterns of variation in the rate of trait acquisition through time and among lineages has become a popular theme in phylogenetic palaeobiology (Slater et al, 2010, Lloyd et al, 2012, Benson & Choiniere, 2013, Hopkins and Smith, 2015, Wright, 2017). Nevertheless, relatively few studies have assessed the rate of phenotypic or morphological evolution among mammals, despite the centrality of that group in formulating many classic macroevolutionary hypotheses (e.g. Simpson, 1944). Notable exceptions include two recent analyses that used discrete morphological characters to assess morphological evolutionary rate through time (Close et al, 2015, Halliday et al, 2016). Close et al (2015) analysed rates among Mesozoic mammals and reported higher rates of morphological character evolution during the Early – Middle Jurassic, supporting the hypothesis that stem therian mammals underwent a mid-Jurassic adaptive radiation (Kielan-Jaworowska et al, 2004, Luo, 2007, Luo, 2007, Meng, 2014, Close et al, 2015). In a second study, analysed

on a phylogeny of Late Cretaceous and Paleocene placental mammals, Halliday et al (2016) found increased rates of morphological evolution among Paleocene placental mammals. These two analyses concern different mammal taxa and time scales. To date, rate across these two proposed radiations has not been analysed across a more inclusive phylogeny, which would allow for direct comparisons between them.

Another analysis also directly tests for the patterns of mammalian evolution across the K/Pg boundary, but rather than assessing evolutionary rate focuses on changes in evolutionary mode (Slater, 2013). This study used body mass to evaluate mode of evolution among mammals both before and after the K/Pg boundary. In this study Slater (2013) found evidence that evolutionary mode changed from an Ornstein-Uhlenbeck mode of constrained evolution to a diffusive, Brownian motion (unconstrained) mode of evolution. By relaxing constraints on body size evolution, this model allows disparity to accumulate after the K/Pg boundary without the need to invoke higher evolutionary rates. Unfortunately, methods for inferring mode of evolution using multivariate data are limited, and they cannot easily be applied to the data presented earlier in this thesis. However, see Adams & Collyer (2018) for advice on some methods that may better deal with multivariate data in certain circumstances, and I note that the development of truly multivariate approaches is a rapidly developing field in comparative biology (Clavel et al, 2015, Clavel et al, 2018).

To build upon these previous efforts, I test for variation in evolutionary rate along univariate trait axes through time, using multivariate continuous character jaw functional data, to assess whether rates of jaw trait evolution are

increased at any given time during the Mesozoic and early Paleogene, but in particular associated with the proposed radiation of placental mammals. Although this has been investigated previously using discrete characters, my more taxonomically inclusive dataset allows for tests of rate across a larger timescale. Furthermore, the use of functionally relevant jaw ecomorphological traits has a closer relationship to the hypothesis of adaptive radiation, which involves phenotypic divergence along ecological lines (Simpson, 1944, Slater and Friscia, 2018 (Preprint)). This contrasts with matrices of discrete characters, which have most commonly been designed for the production of phylogenies, and there is evidence to suggest that they show only a weak correspondence to functional variety (Anderson and Friedman, 2011). Discrete character matrices can be highly variable across clades and from one researcher to another, depending on which subclades and skeletal elements have been studied the most. Analyses of rate based on the same taxa but using different discrete character matrices have in the past yielded disparate results (Benson 2018, describing discrepancies between the analyses of Lee et al, 2014 and Brusatte et al, 2014).

This emphasises the need for purpose-built datasets of functional traits for questions concerning ecomorphological evolution (Anderson & Friedman 2011; and see Slater & Friscia, 2018 (Preprint)). Functionally relevant traits allow for an assessment of evolutionary rate through time based on a set of traits that can be collected in a standardised way for all mammaliaforms, and which can be clearly tied back to aspects of organismal function. In particular, I quantify rates of jaw evolution for each ordination axis of functional jaw

characters in order to test: (a) whether there is evidence of a Middle Jurassic increase in rates of ecomorphological evolution; and (b) whether there are elevated rates associated with the diversification of crown placental mammals.

Methods

Supertree construction

In order to test rates of jaw functional evolution across the K/Pg boundary in a phylogenetic framework, I constructed a supertree using the phylogenetic hypotheses from two published analyses as source trees. These trees differ in their stratigraphic and taxonomic scope, but together give broad coverage for my functional dataset. The first tree is that of Close et al (2015), which conducted a Bayesian analysis of the morphological matrix of Zhou et al (2013). This phylogeny includes Mesozoic, Cenozoic, and Recent mammals, but is focused primarily on Mesozoic taxa. The second source tree is a comprehensive phylogeny of Paleocene (but also includes Cretaceous, Eocene and Recent) mammals produced using parsimony by Halliday et al (2017). Here I use the phylogenetic hypotheses resulting from Halliday et al's (2017) fully constrained analysis of discrete character data only (see Halliday et al's 'Descrete Full' (DF) analysis methods; Halliday et al, 2017). Together these two phylogenies allow for a sample of mammaliaforms that span much of the Mesozoic, the K/Pg boundary, and the radiation of therian mammals.

A backbone constraint tree was also included (Figure S3.1a-f), to enforce relationships within the supertree that are well-established from morphological

and molecular data. This was used primarily to mitigate the effects of having little or no overlap between taxa from some clades in the two phylogenies (e.g. Rodentia).

Supertree construction was carried out in R using mrp.supertree() in the R package phytools (Revell, 2012). This method of supertree construction uses matrix representation of parsimony (Baum, 1992, Ragen, 1992). Matrix representation of parsimony (MRP) converts a tree structure to a matrix, where clades are represented as characters (Ragen, 1992, Bininda-Emonds, 2004).

Rate analyses were conducted on a subsample of 20 supertrees, to allow for inclusion of phylogenetic uncertainty in mammal relationships. Each of these 20 trees represent one tree drawn at random from (a) the 1000 posterior trees sampled by Close et al (2015) and (b) a dataset comprising the one optimal and a subset of 200 of the suboptimal (+1 step) most parsimonious trees from Halliday et al (2017). These two randomly chosen trees were then submitted to mrp.supertree() along with the backbone tree which was chosen to be the starting tree using the command 'start'. The resulting supertrees have 272 tips and span taxa from the Early Triassic (cynodont outgroup taxon *Thrinaxodon*) to the Recent, with more even sampling from the Late Triassic – end-Paleocene. An example of one of the resulting mrp supertrees is shown in Figures 3.1a-f and Figure 3.2 (timescaled).

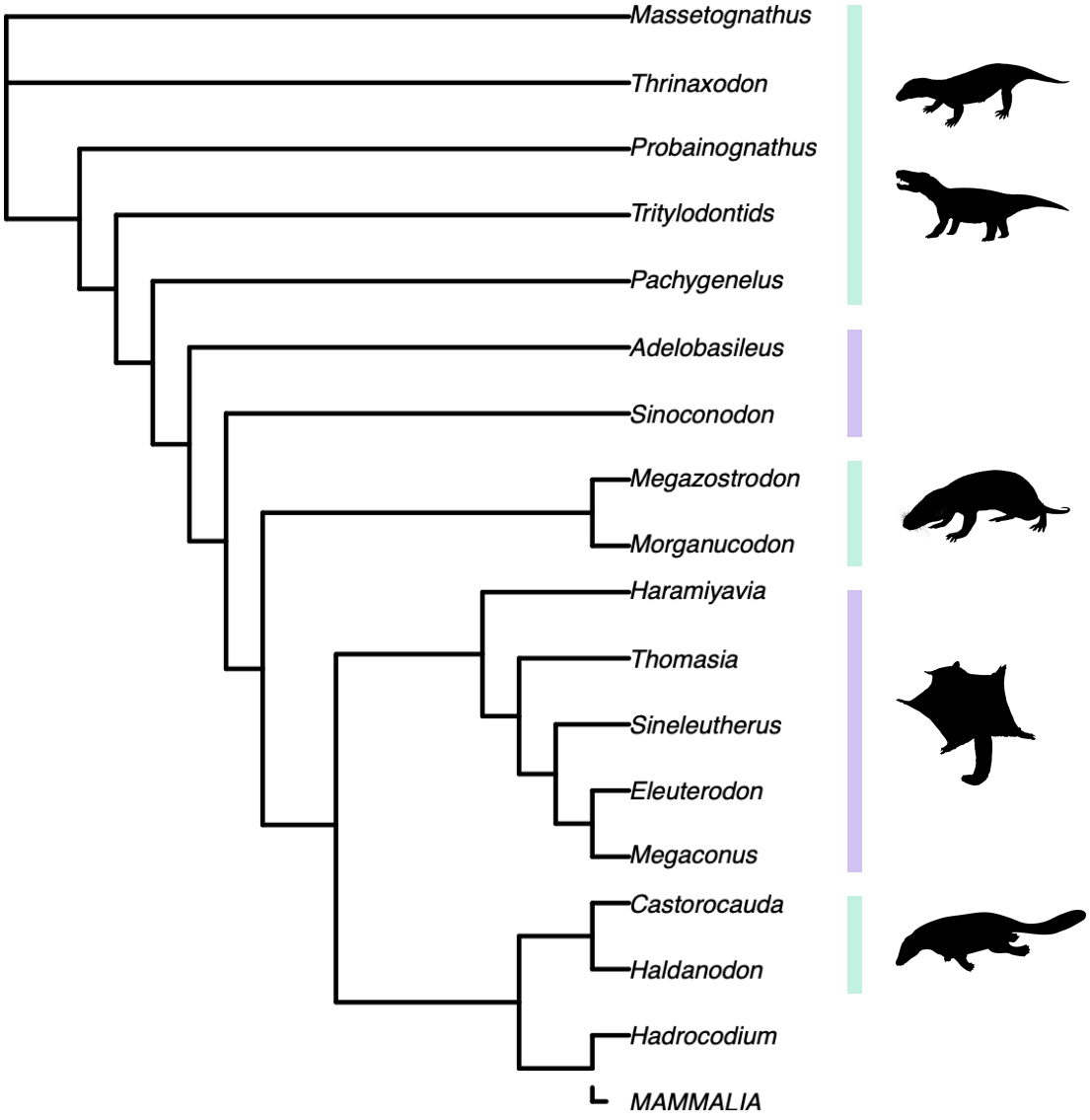


Figure 3.1a. Representative supertree (supertree 7), part (a), consisting of mammaliaform outgroups (*Massetognathus, Thrinaxodon, Probainognathus, Tritylodontids,* and *Pachygenelus*), mammaliaformes, and their branching relationship to crown Mammalia. Supertree 7 was chosen because the pruned version was also used in Figure 3.

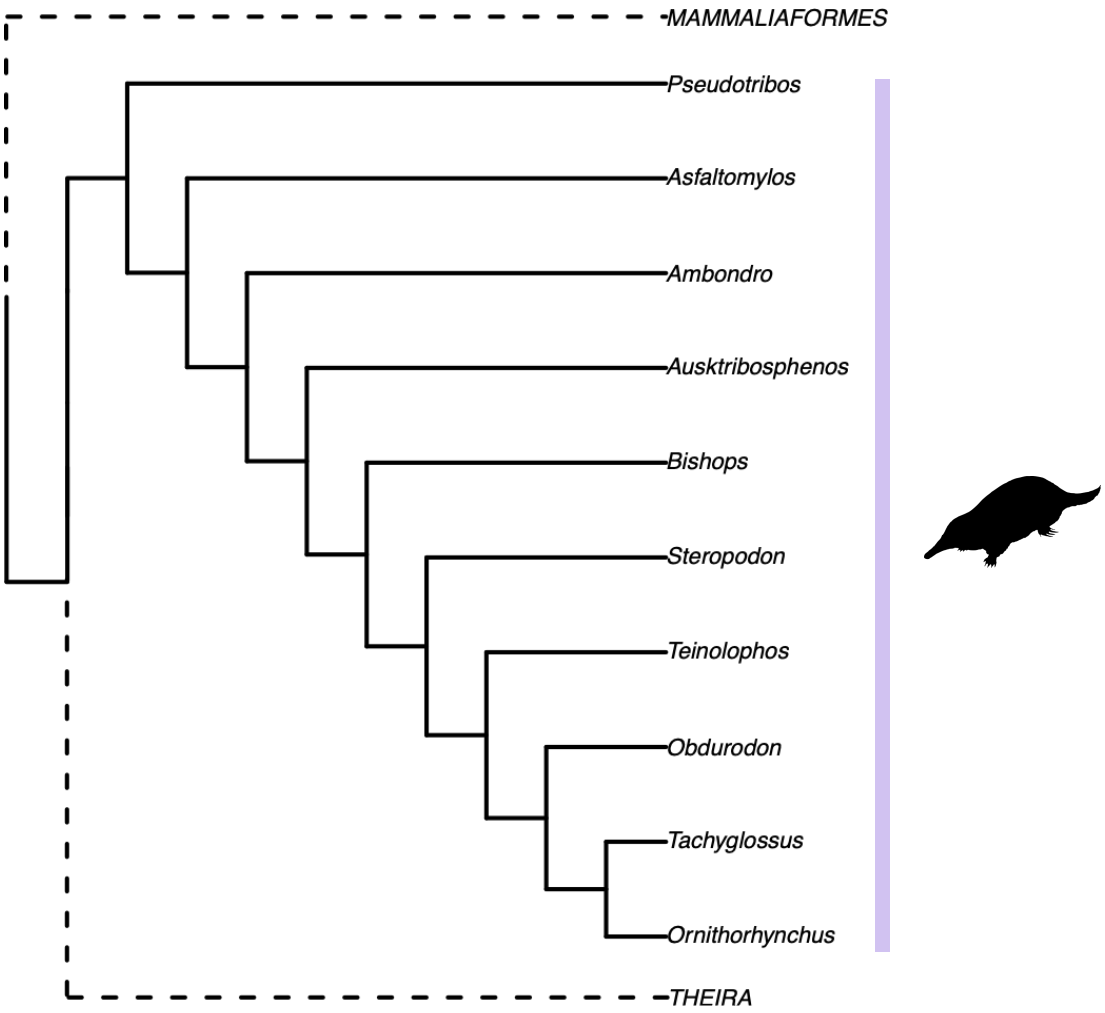


Figure 3.1b. Representative supertree continued, part (b), consisting of Ausktribosphenida-Marsupialia and their branching relationship to

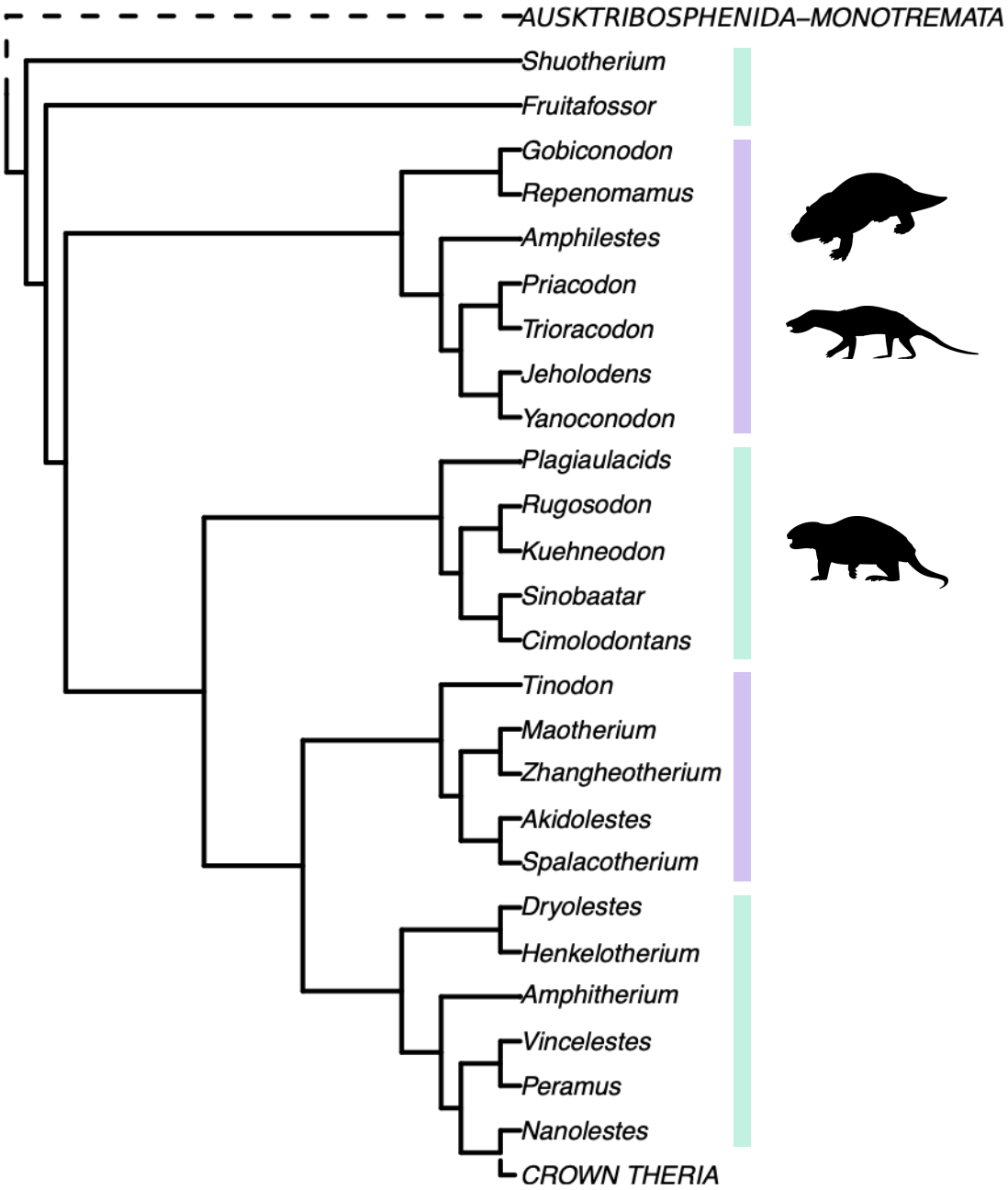


Figure 3.1c. Representative supertree, part (c), showing stem Theria, and their relationship to the montoremes and to crown Theria.

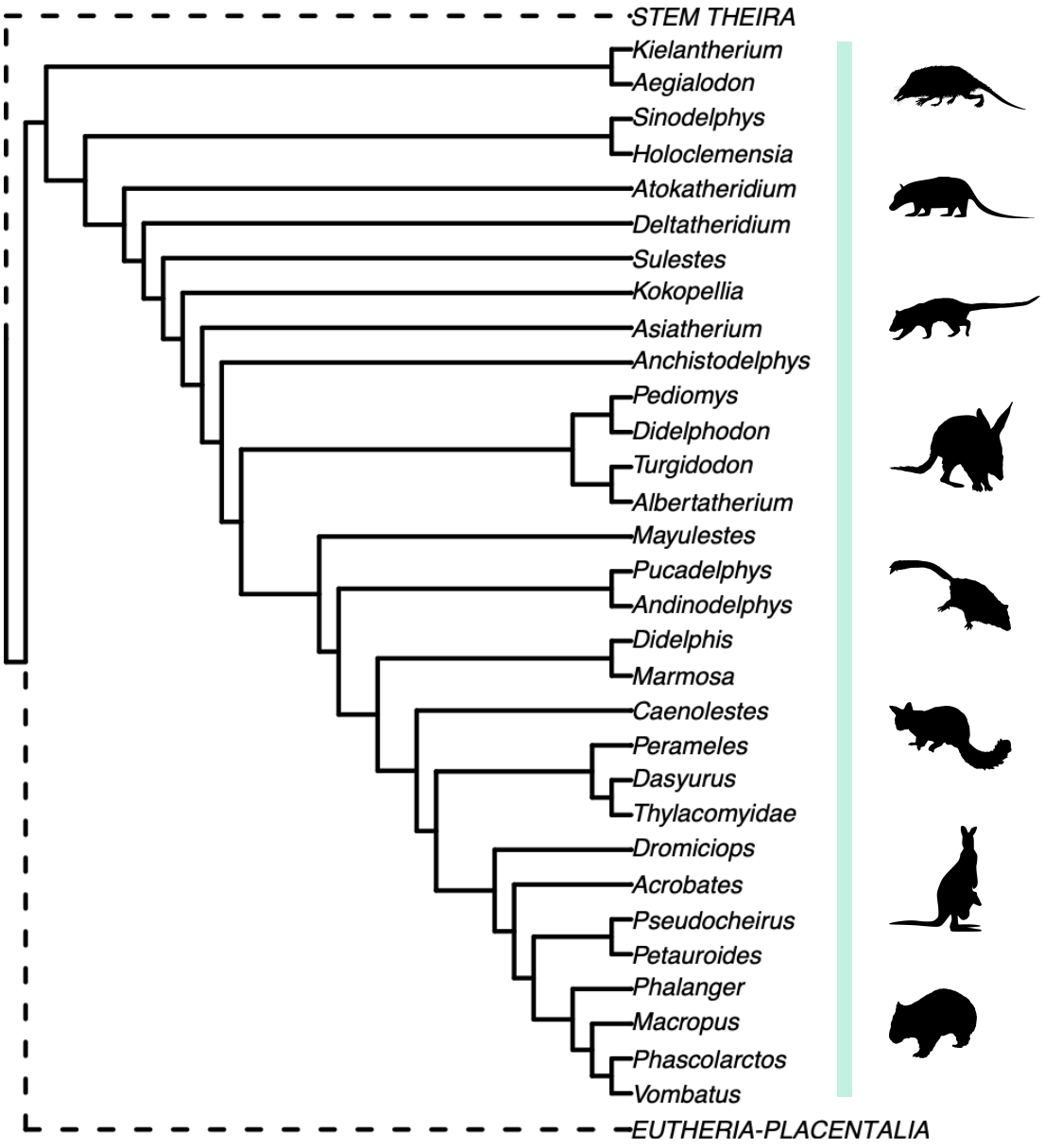


Figure 3.1d. Representative supertree, part (d), showing Metatheria-Marsupalia and their relationship to stem theria and to eutherian-placentals.

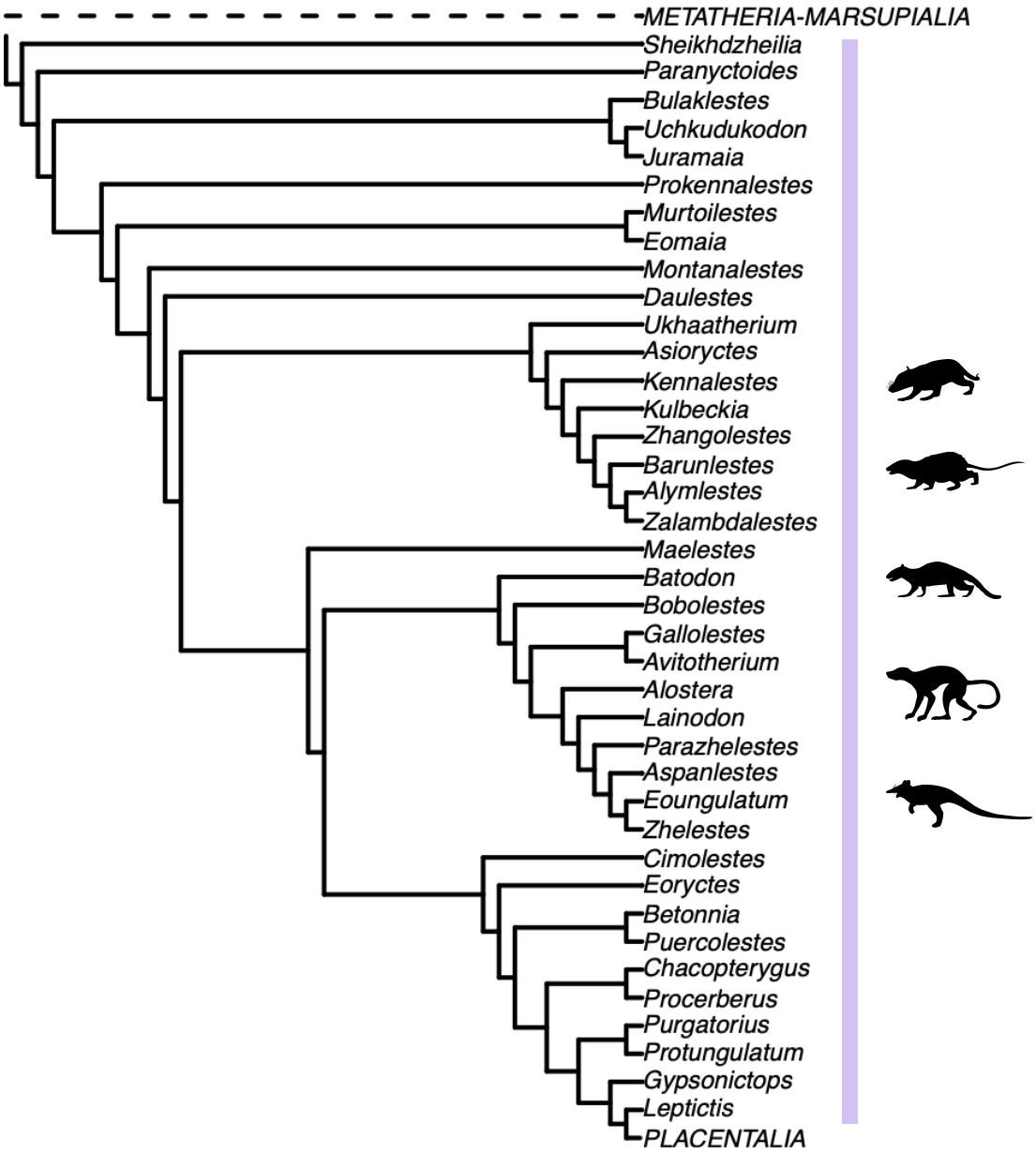


Figure 3.1e. Representative supertree, part (e), showing stem placental mammals, and their relationship to Metatheria-Marsupalia and to crown placentals.

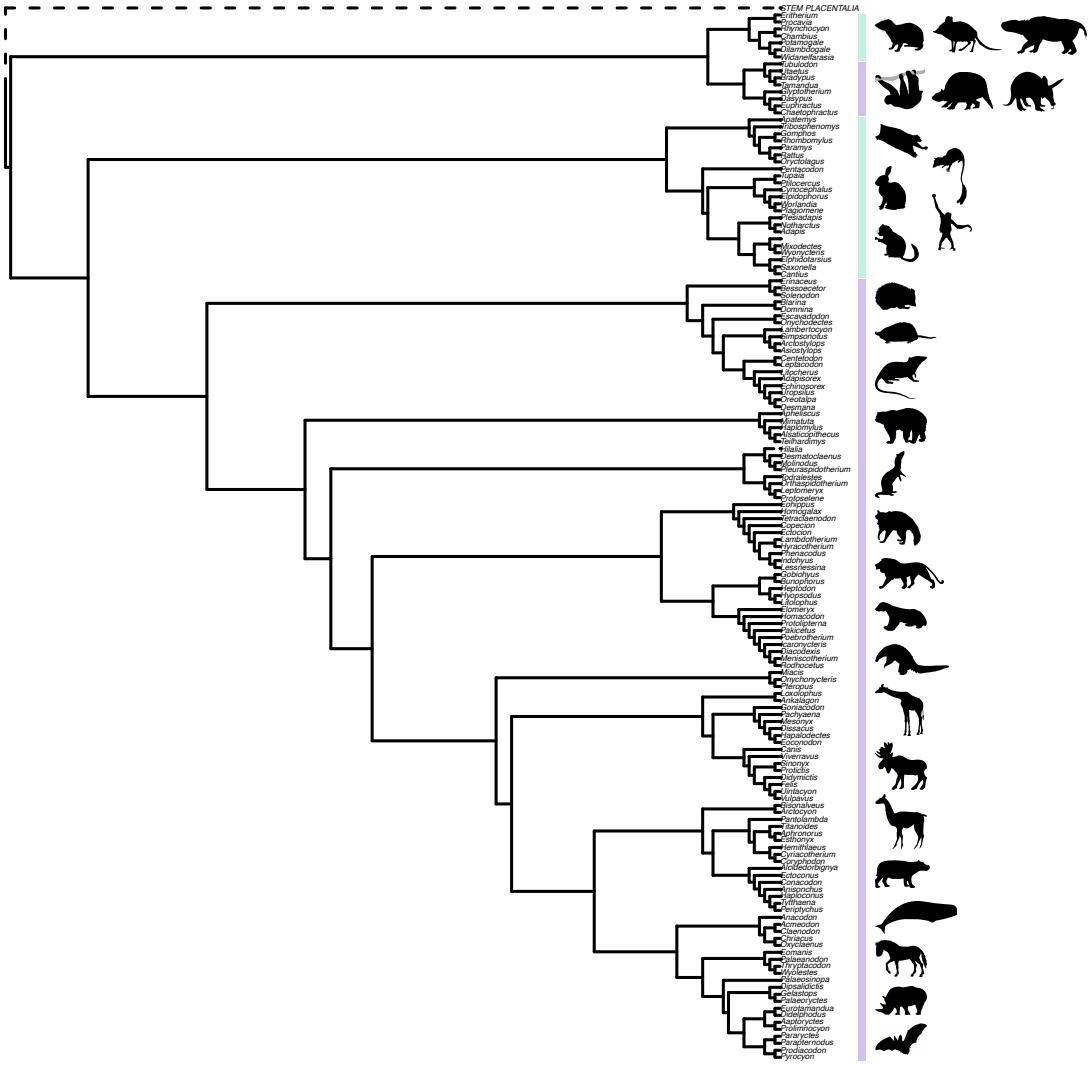


Figure 3.1f. Representative supertree, part (f), showing crown placental mammals and their relationship to stem placentals.

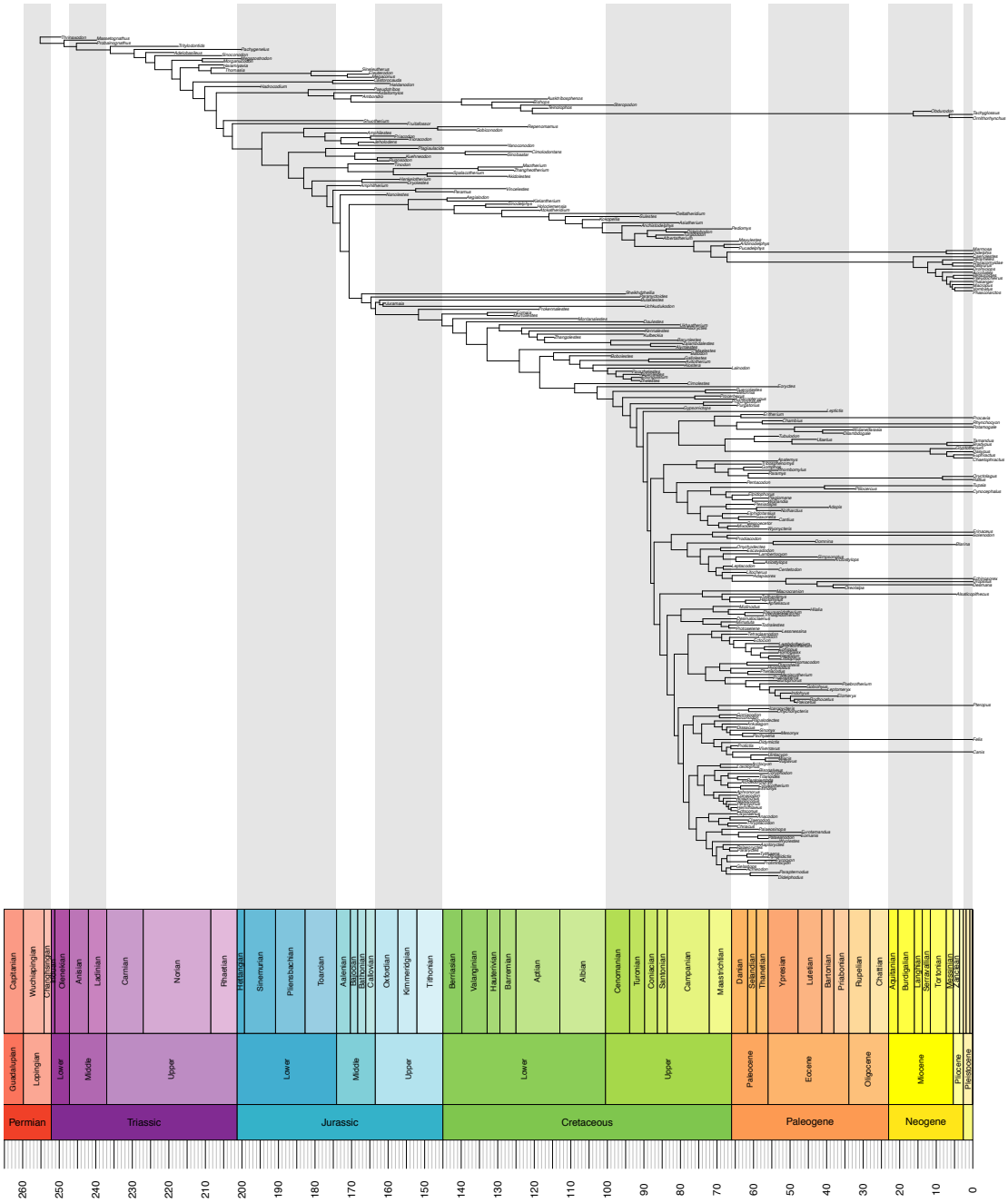


Figure 3.2. Entire representative supertree (supertree 7) showing divergence age estimates calculated from my fossil birth death model.

Timescaling the supertree

A fossilized birth death model (FBD) (Heath et al, 2014), run for 1,000,000 generations, was used to timescale each of the twenty supertrees in MrBayes (Ronquist et al, 2012). Because there is no character data associated with these supertrees, the model was run in MrBayes with no character data and with a fully constrained topology. Tip ages were assigned uniform priors, using the minimum and maximum age associated with the first occurrence of each taxon. The minimum and maximum ages were defined by the beginning and ending of the narrowest stratigraphic interval to which the genus can be assigned. The root of the tree was calibrated using a uniform prior where the youngest age was the maximum occurrence age for the oldest taxon in my tree (the cynodont *Thrinaxodon*) and the oldest age was a reasonable estimate of the age of divergence between cyndonts and mammaliaforms. Additionally, the internal nodes uniting Theria, Marsupialia, and Placentalia were all calibrated using a uniform prior where the input minimum and maximum age data was entered as the 95 per cent confidence intervals for the age of each clade taken from the time-calibrated molecular phylogeny presented by dos Reis et al (2012). I constrained these ages tightly based on the results of the combined (nuclear and mitochondrial) analysis from dos Reis et al (2012) because I consider the results obtained by their study using genomic data and a Bayesian dating method to be more reliable and robust than results that could be achieved by dating a supertree without character or molecular data. Theira was constrained between 177.8 Ma – 168.4 Ma, Placentalia was constrained between 90.4 Ma – 87.9 Ma, and Marsupalia was constrained between 84 Ma – 64.4 Ma.

My application of this approach allows divergence times to be inferred based on the shape of the tree and ages of terminals. This is achieved through estimation of the parameters of the FBD model: (1) the 'net speciation' rate (equivalent to diversification rate of some studies, and equal to speciation rate minus extinction rate); (2) the relative extinction rate (equal to extinction rate / speciation rate), and (3) the fossilisation rate. With reasonable node age constraints, application of the FBD model to topologies can give a reasonable hypothesis for the timescales of diversification even in the absence of character data. In each case, the consensus tree for all of the age estimates sampled across the 1,000,000 Bayesian generations was used. An example of the full timescaled supertree (supertree 7) is shown in Figure 3.2.

Pruning the full supertree

The initial tree contains 272 species ranging in age from the Late Permian – Recent. Pre-Late Triassic species are outgroup taxa. The best and most evenly sampled time period is from the Late Triassic – Eocene, and therefore mammal species plotting from the Eocene/Oligocene boundary onward were not included in the pruned supertree which was used to run rate analyses (see following section). Jaw functional data was available for 69 of the remaining fossil mammals.

Running evolutionary rate analyses

The rate of jaw phenotypic evolution across the pruned (n = 69) supertree was calculated in BayesTraits (e.g. see Venditti et al, 2012, available from

www.evolution.rdg.ac.uk). The six functionally relevant jaw ratios that are used throughout this thesis are again used here (relative diastema length, relative molar row length, coronoid process slenderness, jaw ramus slenderness, relative articulation offset, and jaw closing mechanical advantage). A principal components analysis (PCA) was conducted using 272 terrestrial Late Triassic – end-Eocene fossil jaws (the same dataset and analysis presented in Chapter 1 of this thesis). PC axes were used here rather than raw ratios so that the results of this chapter could be more easily linked to the previous two chapters in this thesis. There are limitations to using PC axes for rate analyses however, namely that, because each axis comprises multiple traits, they can prove a little harder to interpret biologically. Further, some studies have shown that PC axes that explain the most variance may capture trait differences that occurred early on in the initial tree, which can result in early burst models being favoured (Uyeda et al, 2015). PC axes are as in Chapter 1. All species without PC data that are included in the supertree were dropped in R using drop.tips(). Evolutionary rates were calculated under a variable rates MCMC model, and analyses were run using all six PC axes simultaneously across all twenty timescaled supertrees, as well as for each PC axis individually, using one representative timescaled supertree; supertree 7. Supertree 7 was used as the representative timescale throughout this chapter because patterns of mean rate through time for this individual tree are similar to patterns of the mean of the mean rate through time across all trees.

Rate through time analyses

Rate through time was calculated in two separate sets of analyses. The first set of analyses uses pooled PC axis, and the second tests rates across each PC axes separately. The variable-rates model is implemented in BayesTraits [version 2.1], available at http://www.evolution.rdg.ac.uk/BayesTraits.html.

Mesozoic stages and Cenozoic North American Land Mammal Ages (NALMAs) were used as time bins. These time bins were chosen because stages and NALMAs reflect the average error on a fossil occurrence and therefore the average error included in my supertree calibrations. The mean (Figure 3.3) and the median (Figure 3.4) of mean branch rate for each branch present in a given time bin was calculated for each of the 20 trees using PC1-6. The mean branch rate was also calculated for each PC axis separately (Figures 3.4-3.6).

Results

Rates of mandibular ecomorphological trait evolution vary throughout the Jurassic – Eocene. Figure 3.3 (and Figures S3.2-S3.20) shows a spectrum of colours from warm (faster rates of evolution) to cool (slower rates of evolution). Each supertree shows a small amount of variation in the patterns of rate across branches, due to small differences in both the topology captured by each tree and estimated divergence times. Despite these variations, several common patterns in evolutionary rate emerge across all trees. First, higher

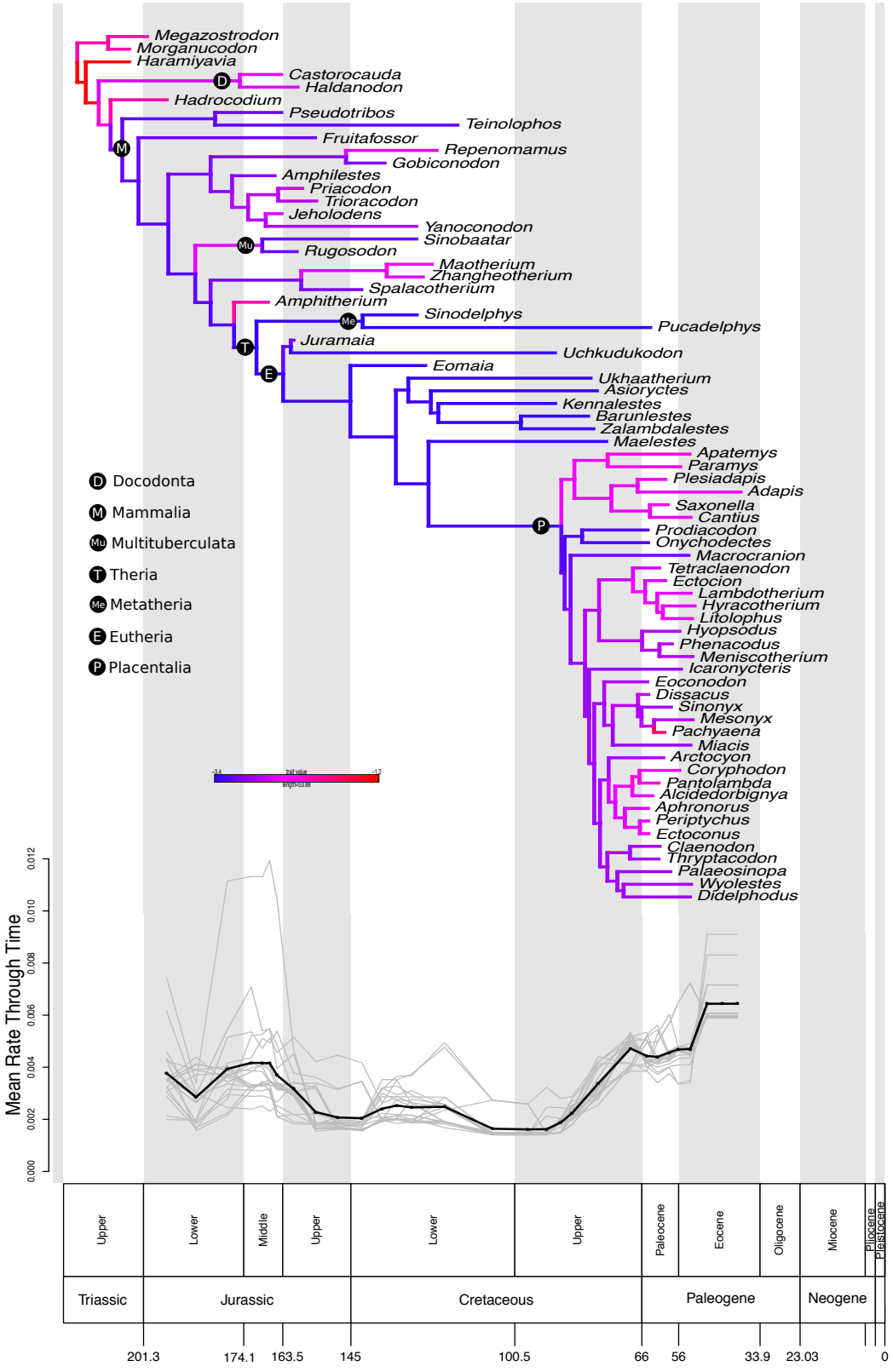


Figure 3.3. Example supertree (a) (supertree 7) showing rates of jaw functional trait change across all six PC axes through time. Warmer colours depict higher rate, and cooler colours indicate cooler rates. Mean rate through time for each supertree is shown below the rates tree (b). Individual tree results are shown in grey, and a mean rate across all trees is calculated and shown in black.

rates of jaw functional trait change among the earliest mammaliaform branches, leading to *Morganucodon*, *Megazostrodon* (morganucodontids), *Castorocauda*, *Haldanodon* (docodonts), haramyids, and *Hadrocodium*. Rates among early mammalians (i.e. descendants of the node Mammalia) are on average slower than those among the earlier mammaliaforms included in this analysis. Nevertheless, various stem-group therian mammals show elevated rates in comparison to the stem monotreme, metatherian and early eutherian mammals included in this study. In all of the rate trees, the lineages leading to *Maotherium* and *Zhangheotherium* show elevated rates among stem therian mammals, and in all but one tree (Figure S3.5; supertree 4) *Amphitherium* also shows elevated rates. The lineage leading to the multituburculates included in this study (*Sinobaatar* and *Rugosodon*), the gobiconodontid *Repenomamus*, and the eutriconodonts also show higher rates.

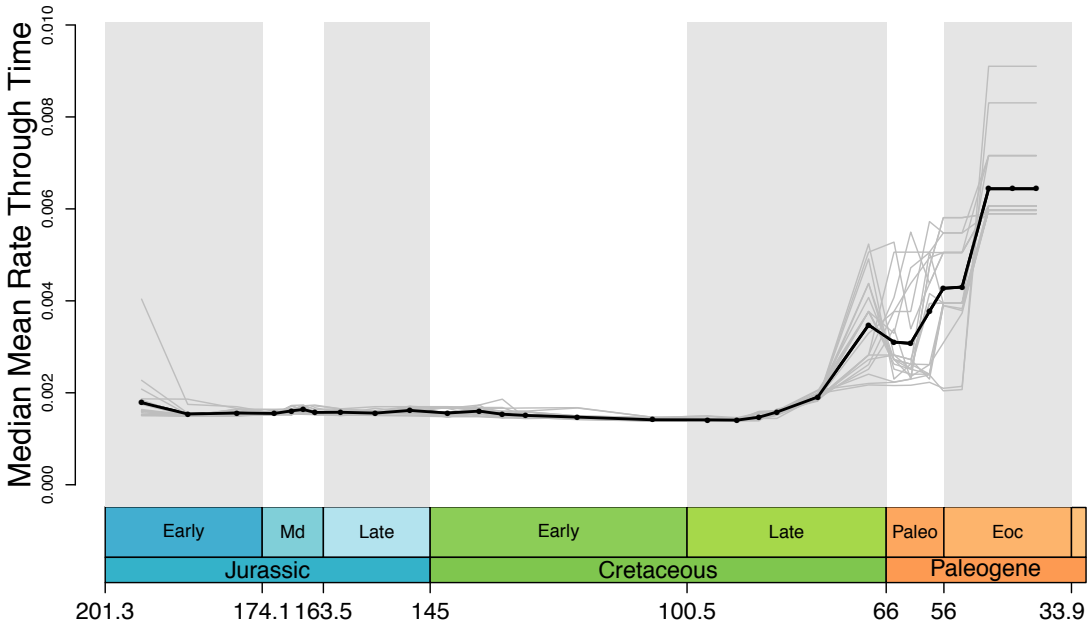


Figure 3.4. Median rate through time is shown for each supertree in grey. Mean median rate across all trees is shown in black.

Each PC axis shows a similar pattern to that described above, with a little variation. In all trees, the crown-group therian node represents the start of a period with uniformly low rates. Rates of jaw functional trait evolution remain low until the origin of placentals. Rates among these branches is not uniform, but almost all branches show increased rates compared to stem eutherian mammals. Mean rate through time across all trees (black line; Figure 3.3a) for all PC axes analysed together (PC1-6) shows higher rates during the Early to Middle Jurassic. This period of elevated rates is produced by the higher rates recovered for some stem-group therian mammals, as discussed above. Peak mean rates in the Jurassic are approximately 1.5 times higher than Early and early Late Cretaceous values. Mean rates begin to decrease after their Middle Jurassic high, staying primarily low (with small perturbations) until the middle Late Cretaceous.

Rates begin to increase after the middle Late Cretaceous due to the entire placental mammal clade. These rates plateau across the K/Pg boundary and throughout the Paleocene, and then continue to increase into the Eocene. The early Cenozoic increase in rates of mandibular evolution exceeds that of the Middle Jurassic: the highest mean rates through time from the Jurassic-end Eocene are during the Eocene in almost all of the trees tested. Rates are at least two times higher from the middle Late Cretaceous onward compared to the Early and early Late Cretaceous. This middle Late Cretaceous – Eocene rate increase through time reflects higher rates among placental mammals in comparison to other groups. Median rate through time (calculated as the median from the mean rate along each branch in a given tree) is consistently

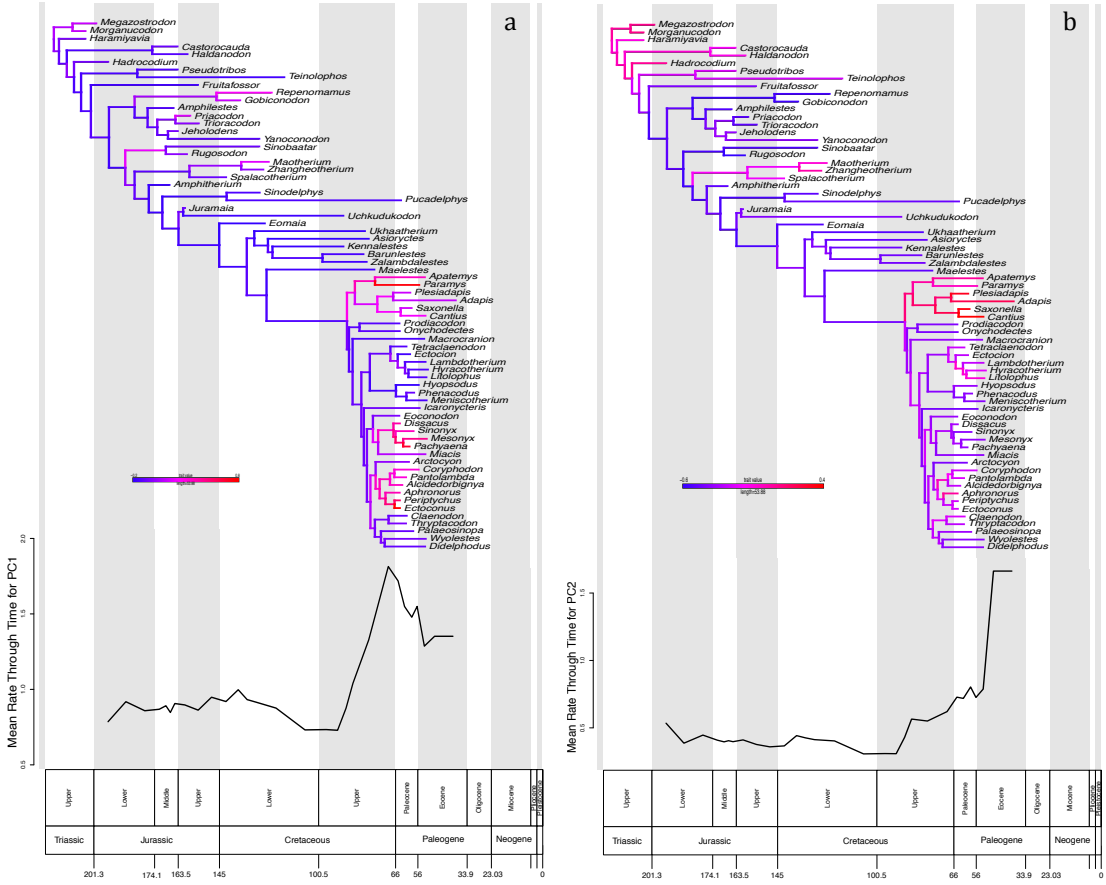


Figure 3.5. Example supertree (supertree 7) showing rates of jaw functional trait change through time along PC1 (3.5a) (correlates with relative diastema length, relative molar row length, the slenderness of the jaw ramus, and relative articulation offset) and PC2 (3.5b) (correlates with articulation offset ratio, jaw closing mechanical advantage, coronoid slenderness, and molar row length). Mean mean branch rate through time for PC1 (3.5a) and PC2 (3.5b) is shown below.

low until the mid-late Late Cretaceous. Median rate then increases from the late Late Cretaceous until the Eocene (Figure 3.4).

PC1 describes 32.21 per cent of overall variance and correlates with relative diastema length, relative molar row length, the slenderness of the jaw ramus, and relative articulation offset. Rate of jaw morphological evolution for PC1 are shown in Figure 3.5a. The same pattern of increased rates among mammaliaforms, some stem therians, and crown placentals is recovered, but the magnitude of the increase among mammaliaforms and the stem theiran

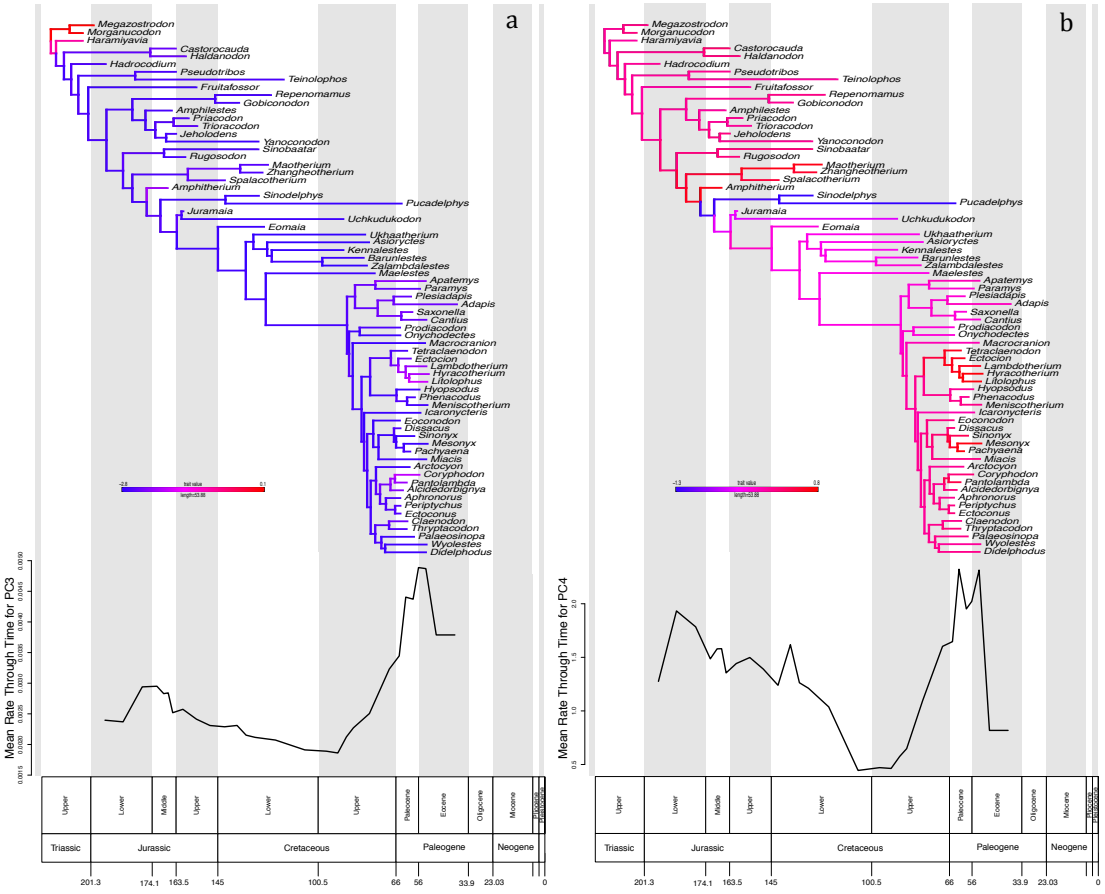


Figure 3.6. Example supertree (supertree 7) showing rates of jaw functional trait change through time along PC3 (3.6a) (correlates with jaw ramus slenderness, jaw closing mechanical advantage, and relative molar row length) and PC4 (3.5b) (correlates with coronoid slenderness ratio). Mean mean branch rate through time for PC3 (3.6a) and PC4 (3.6b) is shown below.

mammals are less pronounced. Increased rates among some clades of placental mammals are particularly pronounced. Rate through time for PC1 shows a slightly different pattern to that recovered for all PC axes (Figure 3.3b). Rate is consistently low throughout the Jurassic and Cretaceous, dropping to its lowest rates across the Early Cretaceous/Late Cretaceous boundary. Rate increases rapidly during the Late Cretaceous. It then declines during the Paleocene and plateaus in the Eocene, but never drops as low as Jurassic and Cretaceous mean rates.

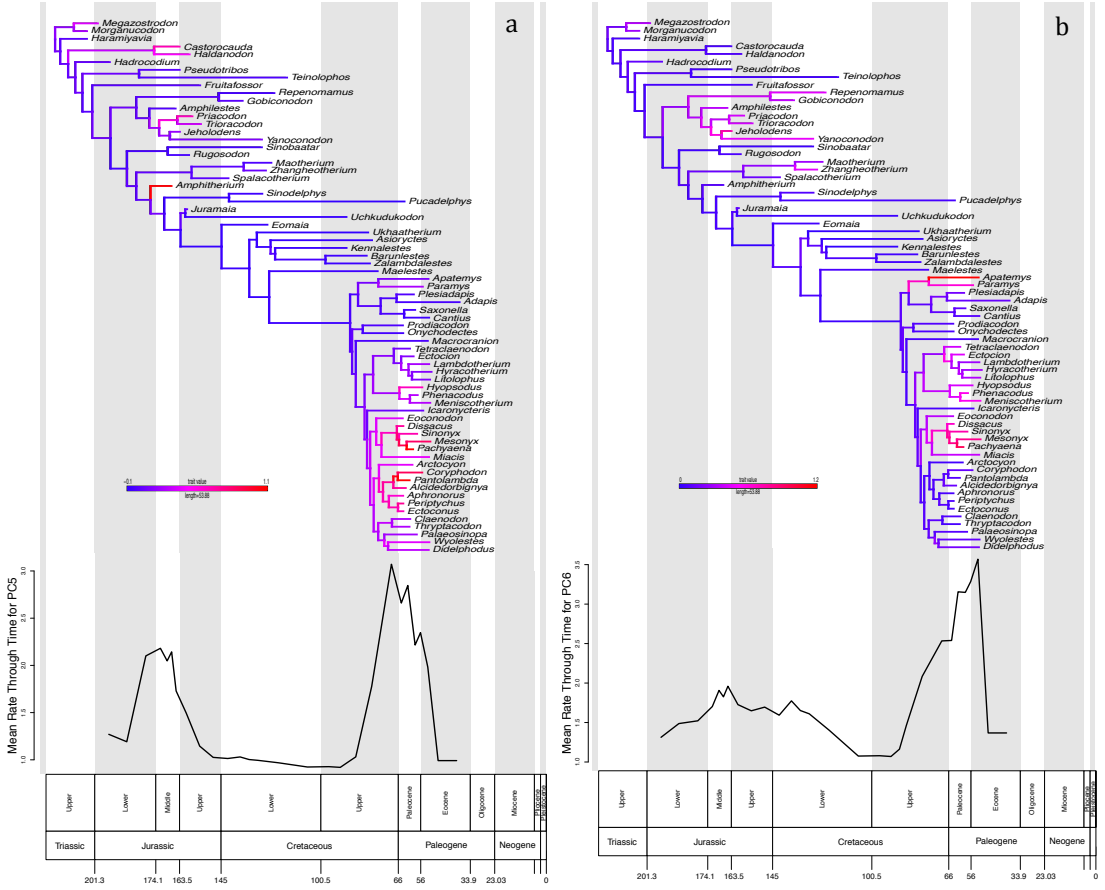


Figure 3.7. Example supertree (supertree 7) showing rates of jaw functional trait change through time along PC5 (3.7a) (correlates with articulation offset ratio, relative jaw ramus slenderness, and jaw closing mechanical advantage) and PC6 (3.7b) (diastema length and relative molar length). Mean mean branch rate through time for PC5 (3.7a) and PC6 (3.7b) is shown below.

PC2 describes 24.98 per cent of overall variance. The articulation offset ratio, jaw closing mechanical advantage, coronoid slenderness, and molar row length correlate well with this axis. Rates of evolution along PC2 are shown in Figure 3.5b. Mean rate through time is shown below. Branches leading to mammaliaforms, eutriconodonts, and placental mammals exhibit higher warmer colours and therefore higher rates. Mean rate through time indicates that rates were low throughout the Jurassic and Early-early Late Cretaceous in comparison to Paleocene and Eocene rates. Rates begin to increase in the Late

Cretaceous and continue to increase until their peak in the Eocene, by which time mean rates are approximately two times higher than Jurassic and Early Cretaceous levels.

PC3 describes 17.94 per cent of the variance and correlates primarily with jaw ramus slenderness, jaw closing mechanical advantage, and relative molar row length. The results of the rate analysis using PC3 are shown in Figure 3.6a. Rate among early mammaliaforms is higher than across the rest of the tree. Rates from the docodont lineage onward seem low, but there is a very small amount of change on the branches leading to *Amphitherium* and certain placental mammals. Rate through time shows a small increase in the late Early – Middle Jurassic, associated with small rate increases among stem therian mammals. Paleocene-Eocene rates are approximately double compared to those of the Early – early Late Cretaceous.

PC4 describes 11.84 per cent of the variance, and the rate analysis associated with this PC axis can be seen in Figure 3.6b. PC4 correlates with coronoid slenderness ratio. Rates are notably low among metatherian mammals, and higher rates are detected among the most crownward branching stem therian mammals and among a number of placental lineages. PC4 shows increased mean rates throughout the Jurassic and early Early Cretaceous compared to the late Early – early Late Cretaceous. Placental mammals also show higher rates, comparable to those seen in the Jurassic.

PC5 describes 7.06 per cent of the data, and the results can be seen in Figure 3.7a. PC5 correlates weakly with the articulation offset ratio, relative jaw ramus slenderness, and jaw closing mechanical advantage. PC5 shows a similar

pattern of rate variation as all axes analysed together (Figure 3.3). Mean rate through time is again elevated during the Early – Middle Jurassic, and low throughout the first half of the Cretaceous. Peak rates are seen just prior to the K/Pg boundary, after a sharp increase during the late Late Cretaceous. Rates then drop again throughout the Eocene.

PC6 describes just 5.91 per cent of the overall variance, and correlates best with diastema length and relative molar length, but does not correlate strongly with any individual trait. The distribution of rate for PC6 (Figure 3.7a) is again similar to those seen in Figure 3.3. The same pattern of Early – Middle Jurassic increase, middle Cretaceous low and Late Cretaceous – Paleocene rise is again recovered.

Overall, results from the analysis of separate PC axes indicates that all axes underwent high rates of evolution in the early Cenozoic, whereas only PC3-6 show high rates during the Middle Jurassic. This suggests that the early Cenozoic radiation involved more distinct types of shape and functional change in the mammalian mandible.

Discussion

Despite considerable interest in the mechanisms of adaptive radiation and the evolution of novel ecomorphology in mammals, this represents the first analysis of functionally relevant continuous character trait evolution across a comprehensive Mesozoic - early Cenozoic mammal phylogeny. I recover

evidence of elevated rates of ecomorphological evolution among three mammalian clades, representing distinct periods of radiation. High rates are recovered for stem mammals (mammaliaforms), for some stem therian mammals, and for placental mammals.

Elevated rates among the earliest mammaliafoms

Early mammaliaforms, which were likely diversifying during the Late Triassic, show the highest rates of jaw morphological evolution on almost every tree tested (Figure 3.3 and Figures S3.2-S3.20). This suggests rapid morphological diversification early on for the entire mammaliaform clade. An initial wave of radiation among the earliest mammaliaforms has been recognised previously, with the origination of a number of clades with distinct dental characteristics (Lautenschlager et al, 2018) and locomotor modes (e.g. Haramyidans). This may reflect the initial evolution of traits associated with a more mammal-like jaw. In this analysis, these elevated rates are associated with the morganucodontids *Morganucodon* and *Megazostradon*, the haramyidan *Haramyavia*, the docodonts *Castorocauda* and *Haldanodon*, and the enigmatic *Hadrocodium wui*.

Elevated rates among stem therian mammals

Evolutionary rate among a number of jaw functional traits was high during the Early – Middle Jurassic. This mirrors qualitative evidence that Jurassic mammals were exploring novel ecomorphologies associated with more disparate feeding ecologies (e.g. Hu, 2005, Meng, 2015) and locomotor ecologies (e.g. Meng et al, 2015, Luo et al, 2015, Meng et al, 2017), as well as quantitative evidence that

discrete character evolution rate and rates of diversification were higher during the Early – Middle Jurassic (Close et al, 2015).

Increased rates among Jurassic mammals are detected when analysing all six PC axes simultaneously as well as when analysing PC3, PC4, PC5, and PC6 separately. Notably, no increased rates are found along PC1 or PC2, the two axes which explain the highest percentage of variance. Also, median mean rate through time does not show increased rates during the Jurassic. This suggests that these increased rates are associated with a subset of stem therian branches, as well as a subset of jaw functional character traits.

Low rates among early eutherian mammals

Compared to almost all other areas of the mammal phylogeny, stem placental mammals show uniformly low rates of jaw morphological evolution. Low rates among Cretaceous eutherian mammals were also recovered by Close et al (2015), who noted that low rates among stem placental mammals may be expected if placental mammals diversified under a long fuse model.

Elevated rates among placental mammals

Jaw morphological evolutionary rates were high among placental mammals, mirroring results obtained using discrete character data (Halliday et al, 2016). In contrast to the radiation detected during the Jurassic, this rate increase is apparent across all PC axes, and median rate through time also shows an increase in rate associated with the diversification of placental mammals. This suggests that multiple traits evolved quickly and simultaneously along a

number of placental branches. Unlike Halliday et al (2016), I find evidence for increased morphological rates among Euarchontoglires, and therefore do not find the same pattern of lauasiatherian-driven rate increases. This most likely results from the different datasets used to quantify morphology in each study.

The results presented here suggest that evolutionary rates began to increase during the Late Cretaceous. This is entirely the result of increased rate of jaw functional trait evolution along the branches of placental mammals, which have no definite fossils from before the Paleocene. The timing of this placental radiation has attracted considerable attention. The fossil record suggests that placental mammals radiated largely or completely after the K/Pg boundary (O'leary et al, 2013), but fossils provide only minimum constraints on clade ages, due to the possibility that older fossils for a clade remain undiscovered (Foote et al, 1999). The fossil record is incomplete, and the absence of uncontested Cretaceous placental mammals does not necessarily mean that they could not have existed. Indeed, molecular and morphological clock models have in the past found much older ages for the diversification of Placentalia, favouring the short fuse model (see Introduction to Thesis) (e.g. Springer, 1997, Murphy et al, 2001). However newer, more methodologically robust analyses with more reliable calibrations move divergence estimates closer to the K/Pg boundary and shorten the gap between fossils and molecules, giving dates more congruent with the long fuse model of interordinal and some intraorfinal diversification prior to the K/Pg, but the majority of intraordinal diversification taking place post-K/Pg (Springer et al, 2003, Halliday et al, 2016, dos Reis et al, 2012). Therefore the results presented here regarding the timing

of the diversification and rate increases of placental mammals should be interpreted in light of this uncertainty. The FBD model used here pulls many intraordinal divergences into the Late Cretaceous, and as such an increase in rate is recovered from the Late Cretaceous onward. Compared to recent studies, this overestimates the age of splits, which would underestimate the rates of jaw functional trait evolution along these branches. If much of the placental radiation did indeed occurred after the K/Pg boundary, as seems most likely, placental rates would be higher still. The current analysis finds placental rates that are up to two times faster than those seen among stem placental mammals. This is comparable to rate increases detected by Halliday et al (2016), who recovered rate increases of around three times higher than background rates.

Rates leading to Palaeocene mammals are high across the majority of placental branches, despite a plateau of overall mammal disparity across the K/Pg boundary and throughout the Paleocene (see Chapter 2). Therian mammals do increase their disparity across the K/Pg boundary (see Chapter 2; see also Halliday and Goswami, 2016), and these results suggest that a number of clades radiated rapidly into regions of function space that were previously held primarily by stem therian mammals.

These analyses provide evidence that the dynamic of high rates of mandibular evolution along phylogenetic lineages in placental mammals began by the Paleocene, and perhaps as early as the Late Cretaceous. This large increase in evolutionary rates differs from patterns of overall mammal disparity, which shows no increase across the Cretaceous/Paleocene boundary. Therian mammals however do show an increase across the K/Pg. Despite high

rates of evolution among early placental mammals, it still took ~10 Ma to achieve overall disparity levels that were higher than Mesozoic levels.

Conclusion

I find evidence that mammals underwent three separate periods of rapid jaw functional trait evolution. The first of these was associated with the appearance of a number of Late Triassic mammaliaform lineages. These earliest mammaliaforms underwent rapid jaw functional trait transformations associated with the appearance of a number of new mammal clades and likely the evolution of a more mammalian jaw arrangement. They exhibit some of the highest rates of trait evolution recovered in this study.

Among crown mammals, two further periods of elevated jaw functional trait evolution are identified, suggesting two waves of crown mammalian adaptive radiation. The first is an Early – Middle Jurassic radiation of stem therian mammals. This Jurassic rate increase is associated with only a subset of the jaw functional traits included in this study, and concerns relatively few lineages.

The second is the more widely recognised placental mammal radiation, associated with a threefold increase in jaw functional traits, and increased placental ecomorphological disparity (Chapter 1, Halliday and Goswami, 2016).

Increased evolutionary rates among stem therian Jurassic mammals can be explained by the acquisition of fewer novel jaw functional traits than the

placental rate increase, indicating that the placental mammal radiation was a much more inclusive and larger-scale radiation, consistent with long-standing observations from the fossil record (e.g. Osborn, 1902, Simpson, 1937, Rose, 2006).

Thesis Conclusions

Using the largest dataset of ecomorphologically relevant jaw functional traits for fossil and modern mammals (272 fossil and 708 Pleistocene-Recent species), I show quantitatively for the first time that total mammal mandibular ecomorphological disparity was consistently low in the Mesozoic. Jaw functional disparity exceeded Mesozoic levels for the first time across the Paleocene/Eocene boundary after an approximately 10 My period of stasis during the Paleocene. Despite this lag in the timing of increase in ecomorphological disparity, increases in maximum body size and body size disparity across the Cretaceous/Paleogene (K/Pg) boundary may well have allowed mammals to explore novel niches prior to the appearance of specialised mandibular functional traits. In contrast to patterns retrieved for mammals as a whole, therian mammals show an increase in functional disparity across the K/Pg, suggesting that the Paleocene represented a time of faunal turnover and replacement for mammals, with therian mammals exploring areas of function space previously occupied by non-therian Mesozoic mammals. By the Eocene, therian mammals had begun exploring regions of function space representing ecomorphologies not occupied by and Mesozoic mammal.

The evidence that larger body sizes attained by some Cenozoic mammals in the wake of the K/Pg mass extinction may have allowed them to explore mandibular ecomorphologies that were not available to Mesozoic mammals. This suggests that mandibular ecomorphological disparity may have been

suppressed during the Mesozoic due to a constraint on their maximum body sizes. Any mammals that did realise larger sizes during the Mesozoic were too rare to fully explore large mammal function space and increase disparity. Extant and recently extinct (Pleistocene) large mammals show higher disparity that do Eocene large mammals, a pattern dominated by artiodactyls, horses, and proboscideans, suggesting that these clades continued to explore novel ecomorphologies long after the K/Pg. These later Cenozoic increases likely represent a response to Eocene/Oligocene environmental perturbations and the evolution of increasingly specialised grazing ecomorphologies driven by the proliferation of grasslands.

Despite generally low Mesozoic mandibular disparity in comparison to post-K/Pg levels, increased rates of evolution are detected along early branches of the mammaliaform clade. These increased rates likely reflect the evolution of traits associated with a mammalian-like jaw, and the initial radiation of mammal morphologies, some of which have been shown to occupy relatively disparate ecomorphologies (e.g. haramyidans) among Mesozoic species. A second period of increased mandibular functional trait evolutionary rate is detected during the Middle Jurassic, and is associated with the previously documented taxonomic and morphological diversification of stem therian mammals. This provides further evidence that mammals underwent an early and significant adaptive radiation during the Middle Jurassic, associated with the evolution of novel feeding, and likely also locomotor, ecomorphologies.

A much larger adaptive radiation is associated with the evolution of placental mammals in the latest Cretaceous or earliest Cenozoic. High

evolutionary rate are inferred along almost all placental lineages, suggesting rapid and substantial diversification early on in the history of the group, consistent with the theory of a placental mammal adaptive radiation. These increased rates are associated with an increase in therian mandibular ecomorphological disparity across the K/Pg boundary. Despite these substantial rate increases of up to three times background rate however, it still took therian, and more precisely placental, mammals approximately 10 My to explore ecomorphologies that were not present in Mesozoic faunas.

Future Directions

As with many scientific studies, no matter how successful in completing the original aims, the work presented here raises as many additional questions as it answers. Despite successfully documenting and exploring the patterns and evolutionary processes associated with the acquisition of functionally-relevant jaw ecomorphological traits through time, understanding the evolutionary patterns of one suite of ecomorphological traits still leaves questions regarding the mechanics of adaptive radiation unanswered. The acquisition of novel jaw ecomorphological traits among early Paleogene taxa is not the only way in which post-K/Pg mammals are hypothesised to have increased their disparity compared to Mesozoic forms. Early work established that novel limb ecomorphologies likely also evolved in the aftermath of the K/Pg extinction event, and these novel limb traits appear closely related to locomotor ecology (Osborn, 1902, Simpson, 1937). Therefore, a more complete understanding of overall trait evolution in mammals may be obtained by a future quantitative analysis of limb traits. There are many good arguments to suggest that these ecomorphological traits, affecting different skeletal aspects, may not evolve in unison. This is due primarily to different evolutionary pressures in response to separate functional roles. Indeed, there is already evidence for a decoupling of body size and mandibular morphological traits during the mammalian adaptive radiation (Chapter 1). During the completion of this thesis, a number of continuous character limb traits that could be used in the future to quantify

patterns of limb ecomorphological disparity through time were identified and compiled from the literature. Initial work began to collect these traits for fossil mammals throughout the time period of interest in this study, but it unfortunately became clear relatively early on that the Paleocene fossil record of mammals preserving complete long-bone elements was too poor to properly explore this question using many of the traits identified. This is not to say that these traits, and the limb data collected for Mesozoic, Eocene, and few Paleocene taxa could not be used in the future to answer a number of different evolutionary or ecological questions. In fact, much can be done with this taxonomically and temporally broad dataset. For example, previous studies have used data such as this to assess locomotor ecology in extinct mammals using modern analogues, and such studies have yielded interesting results (e.g. Chen and Wilson, 2015). Of course it is also still possible to assess differences in limb disparity between the Mesozoic periods and the Eocene. This would provide quantitative documentation of disparity both before and after the K/Pg, but would not highlight the way in which limb disparity accumulated in the immediate aftermath of the extinction event. It is possible that future discoveries of Paleocene fossils will be sufficiently well preserved to fill the gap in the data, but for now it may be more worthwhile to focus on quantifying limb disparity using a method that does not require the existence of fully-preserved long bones, such as geometric morphometric analyses of bone joint surfaces (epiphyseal shape, e.g. Walmsley et al, 2012) or from functionally relevant more robust elements (e.g. the calcaneal; Panciroli et al, 2017).

GMM and other methods of quantifying morphological change (such as orientation patch count (OPC; Wilson et al, 2012, Evans et al, 2007) could also be used to assess to what extent these proxies for feeding ecology capture the same signal.

An ambitious but worthwhile continuation of this work may be to additionally collect the continuous character jaw traits used in this study for all mammals form the Oligocene, Neogene, and Pleistocene (here only Pleistocene megafauna were included). There were a number of reasons why this study did not sample these time periods, in particular due to qualitative observations that the K/Pg radiation into novel body forms was largely over by the end-Eocene, but also dues to time constraints: the rich post-Eocene record of mammals would result in a dataset several factors larger than that produced here. However, results from the extant dataset suggest that functional disparity among larger bodied mammals did increase during this time period, and therefore inclusion of these mammals would better capture this later change in mammal jaw ecomorphology.

Perhaps the most interesting expansion of the work presented in this thesis would be to further investigate the tempo as well as mode of evolution in ecomorphological traits across the boundary. Here I tested the rate of evolution throughout the Jurassic, Cretaceous, and Eocene for jaw ecomorphological traits. Expansion of this to include a larger time scale, and also a complementary set of limb traits, would allow for a more in-depth study of how mammalian ecomorphological traits evolved through time, and how different suites of traits change in relation to one another. This would require the production of a much

larger supertree or (preferably) supermatrix including more taxa and spanning more of geological time. Further, as methods continue to develop, more robust tests for changes in mode of evolution will likely be available for multivariate data (currently the methods available rely on testing the true data against simulated datasets), which would allow for comparisons of evolutionary mode for body size (Slater, 2013) and other ecomorphological traits.

References

Alfaro ME, Santini F, Brock C, Alamillo H, Dornburg H, et al. (2009) Nine exceptional radiations plus high turnover explain species diversity in jawed vertebrates. *Proc. Natl. Acad. Sci. USA.* 106:13410–13414.

Alroy J (1998) Cope's rule and the dynamics of body mass evolution in North American fossil mammals. *Science* 280:731–734.

Alroy J (1999) The fossil record of North American mammals: evidence for a Paleocene evolutionary radiation. Syst. Biol. 48(1):107-118.

Anderson PS, Friedman M (2012) Using cladistic characters to predict functional variety: experiments using early gnathostomes. *J. Vert. Pal.* 32(6):1254-1270.

Anderson PSL, Friedman M, Ruta M (2013) Late to the Table: Diversification of Tetrapod Mandibular Biomechanics Lagged Behind the Evolution of Terrestriality. *Integrative and Comparative Biology*, Volume 53(2):197–208

Archibald DJ (2011) Extinction and Radiation. How the Fall of Dinosaurs Led to the Rise of Mammals (The Johns Hopkins University Press, Baltimore)

Archibald DJ, Deutschman DH (2001) Quantitative Analysis of the Timing of the Origin and Diversification of Extant Placental Orders *J. Mamm. Evol*. 8(2):107-124.

Aubry M-P, Berggren WA, Van Couvering JA, Ali J, Brinkhuis H, Cramer B, Kent DV, Swisher CCIII, Dupuis C, Gingerich PD, Heilmann-Clausen C, King C, Ward DJ, Knox RWO'B, Ouda K, Stott LD, Thiry M (2003) Chronostratigraphic terminology at the Paleocene/Eocene boundary. *In* Wing SL Gingerich PD Schmitz B, Thomas E (eds) Causes and Consequences of Globally Warm Climates in the Early Paleogene: *Boulder, Colorado, Geological Society of America* Special Paper 369.

Averianov AO, Archibald DJ (2016) New evidence on the stem placental mammal Paranyctoides from the Upper Cretaceous of Uzbekistan. *Palaeontologia Polonica* 67, 25–33.

Badgley C, Gingerich PD (1988) Sampling and faunal turnover in early Eocene mammals. *Palaeogeogr. Palaeoclimatol. Palaeoecol*. 63(1-3):141-157.

Baum BR (1992) Combining trees as a way of combining data sets for phylogenetic inference, and the desirability of combining gene trees. *Taxon.* 41:3–10.

Bennett CV, Upchurch P, Goin FJ, Goswami A (2018) Deep time diversity of metatherian mammals: implications for evolutionary history and fossil-record quality. *Paleobiology* 44(2):171-198.

Benson RBJ, Choiniere JN (2013) Rates of dinosaur limb evolution provide evidence for exceptional radiation in Mesozoic birds. *Proc. R. Soc. B.* 280:e20131780.

Benson BJ, Philip D.Mannion PD, Butler RJ, Upchurch P, Goswami A, Evans SE ()

Benson BJ, Philip D.Mannion PD, Butler RJ, Upchurch P, Goswami A, Evans SE (2013) Cretaceous tetrapod fossil record sampling and faunal turnover: Implications for biogeography and the rise of modern clades. 372:88-107.

Benson RBJ, Campione NE, Carrano MT, Mannion PD, Sullivan C, Upchurch P, Evans DC (2014) Rates of Dinosaur Body Mass Evolution Indicate 170 Million Years of Sustained Ecological Innovation on the Avian Stem Lineage. PLOS Biology. 12(5):e1001853

Benson RBJ, Butler RJ, Alroy J, Mannion PD, Carrano MT, Lloyd GT (2016) Near-Stasis in the Long-Term Diversification of Mesozoic Tetrapods. *PLoS Biol* 14(1):e1002359

Benson RBJ (2018) Dinosaur Macroevolution and Macroecology. *Annu. Rev. Ecol. Evol. Syst.* RIA.

Bi S, Wang Y, Guan J, Sheng X, Meng J (2014) Three new Jurassic euharamiyidan species reinforce early divergence of mammals. *Nature* 514:579–584.

Bi S, Zheng X, Wang X, Cignetti NE, Yang S, Wible JR (2018) An Early Cretaceous eutherian and the placental-marsupial dichotomy. *Nature*. 558(7710):390-395.

Bininda-Emonds ORP (2004) The Evolution of Supertrees. *TREE* 19(6):315-322.

Broderip WJ (1828) Observations on the jaw of a fossil mammiferous animal found in the Stonesfield Slate. *Zool J Lond* 3:408-412

Brusatte SL, Lloyd GT, Wang SC, Norell MA (2014) Gradual assembly of avian body plan culminated in rapid rates of evolution across the dinosaur-bird transition. *Curr. Biol*. 24:2386–92.

Calder WA (1984) Size, Function, and Life History. (Dover Publications Inc., New York)

Ciampaglio CN, Kemp M, McShea DW, (2001) Detecting changes in morphospace occupation patterns in the fossil record: characterization and analysis of measures of disparity. *Paleobiology*. 27(4):695-715.

Chen M, Wilson GP (2015) A multivariate approach to infer locomotor modes in Mesozoic mammals. *Paleobiology* 41:1-33.

Close RA, Friedman M, Lloyd GT, Benson RBJ (2015) Evidence for a Mid-Jurassic Adaptive Radiation in Mammals. *Curr. Biol.* 25(16)2137-2142.

Clyde WC, Gingerich PD (1998) Mammalian community response to the latest Paleocene thermal maximum: an isotaphonomic study in the northern Bighorn Basin, Wyoming. *Geology* 26:1011–1014.

Cooper N, Purvis A (2010) Body Size Evolution in Mammals: Complexity in tempo and mode. *Amer. Nat.* 175(6):727-738.

Croft DA, Engelman RK, Dolgushina T, Wesley G (2017) Diversity and disparity of sparassodonts (Metatheria) reveal non-analogue nature of ancient South American mammalian carnivore guilds. *Proc. R. Soc. B* 285:20172012.

Davies P, Lister AM (2001) Palaeoloxodon cypriotes, the dwarf elephant of Cyprus: size and scaling comparisons with P. falconeri (Sicily-Malta) and mainland P. antiquus. *"The World of Elephants", Rome, Proceedings*:479-480.

Dawson MR (2003) Paleogene rodents of Eurasia. In 'Distribution and migration of Tertiary mammals in Eurasia. A volume in honour of Hans De Bruijn' eds Reumer JWF, Wessels W. Deinsea 10:97-126

Delsuc F, Catzefelis FM, Stanhope MJ, Douzery EJP (2001) The evolution of armadillos, anteaters and sloths depicted by nuclear and mitochondrial

phylogenies: implications for the status of the enigmatic fossil Eurotamandua. *Proc. B.* 268(1476):1605-1615.

Dilcher D (2000) Toward a new synthesis: Major evolutionary trends in the angiosperm fossil record. *PNAS* 97(13):7030-7036.

dos Reis, Inoue J, Hasegawa M, Asher RJ, Donoghue PCJ, Yang Z (2012) Phylogenomic datasets provide both precision and accuracy in estimating the timescale of placental mammal phylogeny. *Proc. R. Soc. B.* 279:3491–3500.

Emerling CA, Delsuc F, Nachman MW (2018) Chitinase genes (*CHIA*s) provide genomic footprints of a post-Cretaceous dietary radiation in placental mammals. *Science Advances* 4(5):eaar6478.

Erwin DH (1998) The end and the beginning: recoveries from mass extinctions. *TREE* 13:344-349.

Erwin DH (2001) Lessons from the past: biotic recoveries from mass extinctions. *PNAS* 98:5399–5403.

Etienne RS, Haegeman B (2012) A Conceptual and Statistical Framework for Adaptive Radiations with a Key Role for Diversity Dependence. *The American Naturalist.* 192(4):E75-E89.

Evans AR, Wilson GP, Fortelius M, Jernvall J (2007) High-level similarity of dentitions in carnivorans and rodents. *Nature* 445:78–81.

Foote M (1992) Rarefaction analysis of morphological and taxonomic diversity. *Paleobiology* 18:17-29.

Foote M (1996) Models of morphological diversification. *Evolutionary palaeobiology,* eds Jablonski D, Erwin, DH, Lipps JH (Univ. Chicago Press, Chicago), pp 484.

Foote M (1997) The Evolution of Morphological Diversity. *Annu. Rev. Ecol. Syst.* 28:129-152.

Foote M, Hunter JP, Janis CM, Sepkoski JJ (1999) Evolutionary and preservational constraints on origins of biologic groups: divergence times of eutherian mammals. *Science*. *283*(5406):1310-1314.

Fox RC (1969) Studies of Late Cretaceous vertebrates. III. A triconodont mammal from Alberta. *Canadian Journal of Zoology* 47:1253-1256.

Franzen JL, Gingerich PD, Habersetzer J, Hurum JH, Koenigswald Wv, Smith, BH (2009) Complete Primate Skeleton from the Middle Eocene of Messel in Germany: Morphology and Paleobiology. *PLoS One* 4(5):e5723.

Gaetano, LC, Rougier GW (2011) New materials of *Argentoconodon fariasorum* (Mammaliaformes, Triconodontidae) from the Jurassic of Argentina and its bearing on triconodont phylogeny. *J. Vert. Pal.* 31:829-843.

Gervais MP (1877) Énumération de quelques ossements D'animaux Vertébrés, recueillis aux environs de Reims par M. Lemoine. *Journal de Zoologie*. 6:74-79.

Goswami A, Milne N, Wroe S (2011) Biting through constraints: cranial morphology, disparity and convergence across living and fossil carnivorous mammals. *Proc. Biol. Sci. 278*(1713):1831-1839.

Gower JC, Ross GJS (1969) Minimum Spanning Trees and Single Linkage Cluster Analysis. *J R Stat Soc Ser C Appl Stat* 18(1):54-64.

Grande L (2013) The Lost World of Fossil Lake. Snapshots from Deep Time. (The University of Chicargo Press, Chicargo & London)

Gradstein FM, Ogg JG, Schmitz MD, Ogg GM (2012) The Geologic Time Scale 2012 Volume 1(Elsevier).

Grande L (2013) The Lost world of Fossil Lake. Snapshots from Deep Time (The University of Chicago Press, Chicago and London)

Greaves WS (2012) The Mammalian Jaw, A Mechanical Analysis. (Cambridge University Press, Cambridge)

Grossnickle DM, Newham E (2016) Therian mammals experience an ecomorphological radiation during the Late Cretaceous and selective extinction at the K-Pg boundary. Proc. R. Soc. B 283:20160256.

Grossnickle DM, Polly PD (2013) Mammal disparity decreases during the Cretaceous angiosperm radiation. *Proc. Biol. Sci* 280:20132110–20132110.

Gruber G, Micklich N (2007) Messel. Treasures of the Eocene. (Hessisches Landesmuseum Darmstadt)

Hahn G, Hahn R (1998a) Neue Beobachtungen an Plagiaulacoidea (Multituberculata) des Ober-Juras 3. Der Bau der Molaren bei den Paulchoffatiidae. *Berliner geowissenschaftliche Abhandlungen E.* 28:39-84.

Hahn G, Hahn R (1998b) Neue Beobachtungen an Plagiaulacoidea (Multituberculata) des Ober-juras 4. Ein Vertreter der Albionbaataridae im Lusitanien Portugals. *Berliner geowissenschaftliche Abhandlungen E.* 28:85-89.

Halliday TJD, Goswami A (2016) Eutherian morphological disparity across the end-Cretaceous mass extinction. *Biol. J. Linn. Soc. Lond.* 118(1):152-168.

Halliday TJD, Upchurch P, Goswami A (2016) Eutherians experienced elevated evolutionary rates in the immediate aftermath of the Cretaceous–Palaeogene mass extinction. *Proc. R. Soc. B.* 283(1833):1-8.

Halliday TJD, Upchurch P, Goswami A (2017) Resolving the relationships of Paleocene placental mammals. Biol. Rev. 92:521-550.

Harmon JL et al (2010) Early bursts of body size and shape evolution are rare in comparative data. Evolution 64(8):2385-2396.

Han G, Mao F, Bi S, Wang Y, Meng J (2017) A Jurassic gliding euharamiyidan mammal with an ear of five auditory bones. *Nature* 551(7681):451-456.

Heath TA, Huelsenbeck JP, Stadler T (2014) The fossilized birth–death process for coherent calibration of divergence-time estimates PNAS 111(29):E2957-E2966.

Hoffman EA, Rowe TB (2018) Jurassic stem-mammal perinates and the origin of mammalian reproduction and growth *Nature* 561:104-108

Hooker JJ, Collinson ME, Sille NP (20014) Eocene-Oligocene mammalian faunal turnover in the Hampshire Basin, UK: Calibration to the global time scale and the major cooling event. *J. Geo. Soc.* 161(2):161-172.

Hooker JJ, Collinson ME (2012) Mammalian faunal turnover across the Paleocene-Eocene boundary in NW Europe: The roles of displacement, community evolution and environment. *Aust. J. Earth Sci*. 105(1):17-28

Hopkins MJ, Smith AB (2015) Dynamic evolutionary change in post-Paleozoic echinoids and the importance of scale when interpreting changes in rates of evolution. *Proc. Nat. Academy Sci.* 201418153.

Hopson JA, Kitching JW (2001) A probainognathian cynodont from South Africa and the phylogeny of nonmammalian cynodonts. *Bull. Mus. Comp. Zool.*156:5-35

Hu Y, Meng J, Wang Y, Li C (2005) Large Mesozoic mammals fed on young dinosaurs. *Nature* 433:149–152.

Hunt G (2007) The relative importance of directional change, random walks, and stasis in the evolution of fossil lineages. *PNAS* 104(47):18404 –18408.

Ivy LD (1990) Systematics of late Paleocene and early Eocene Rodentia (Mammalia) from the Clarks Fork Basin, Wyoming. *Contributions from the Museum of Palaeontology, University of Michigan* 28:21-70.

Jepsen GL (1937) A Paleocene Rodent, "Paramys Atavus". *Proc Am Philos Soc* 78(2): 291-301

Jablonski D (1994) Extinctions in the fossil record *Phil. Trans. R. Soc. Lond.* 344:11-17.

Jackman T, Losos JB, Larson A, de Queiroz K (1997). Phylogenetic studies of convergent adaptive radiations in Caribbean Anolis lizards. *Molecular Evolution and Adaptive Radiation* (eds) Givnish T & Systma K, (Cambridge, UK: Cambridge University Press) pp 535–557.

Janis CM, Damuth J, Theodor JM (2000) Miocene ungulates and terrestrial primary productivity: Where have all the browsers gone? *PNAS* 97(14):7899-7904.

Janis CM, Theodor JM (2014) Cranial and postcranial morphological data in ruminant phylogenetics *Zitteliana B* 32:15-31.

Jaramillo C et al (2010) Effects of Rapid Global Warming at the Paleocene-Eocene Boundary on Neotropical Vegetation *Science* 330(6006):957-961.

Jardine PE, Janis CM, Sahney S, Benton MJ (2012) Grit not grass: Concordant patterns of early origin of hypsodonty in Great Plains ungulates and Glires. *Palaeogeogr. Palaeoclimatol. Palaeoecol*. 365–366:1-10.

Ji Q, Luo Z-X, Yuan C-X, TSaabrum AR (2006) A swimming mammaliaform from the Middle Jurassic and ecomorphological diversification of early mammals. *Science* 311:1123-1127

Ji Q, Luo Z-X, Ji S-A (1999) A Chinese triconodont mammal and mosaic evolution of the mammalian skeleton. *Nature* 398:326–330.

Ji Q, Luo Z-X, Yuan C-X, Wible JR, Xhang J-P, Georgi JA (2002) The earliest known eutherian mammal. *Nature* 416:816-822.

Julien C, Escarguel G, Merceron G (2015) mvMORPH: an R package for fitting multivariate evolutionary models to morphometric data. *Methods Ecol. Evol.* 6(11):1311-1319.

Jones KE, Bielby J, Cardillo M, Fritz SA, O'Dell J, Orme CDL, Safi K, Sechrest W, Boakes EH, Carbone C, Connolly C (2009) PanTHERIA: a species-level database of life history, ecology, and geography of extant and recently extinct mammals. *Ecology*. 90(9):2648-2648.

Julien C, Aristide L, Morlon H (2018) A Penalized Likelihood Framework For High-Dimensional Phylogenetic Comparative Methods And An Application To New-World Monkeys Brain Evolution. *Systematic biology*.

Keesey TM (2018) PhyloPic. available from http://phylopic.org/

Kemp TS (2005) The Origin And Evolution of Mammals (Oxford Univ. Press, Oxford)

Kidwell SM (2001) Preservation of Species Abundance in Marine Death Assemblages *Science* 294(5544):1091-1094.

Kielan-Jaworowska Z (1975) Late Cretaceous Mammals and Dinosaurs from the Gobi Desert: Fossils excavated by the Polish-Mongolian Paleontological Expeditions of 1963–71 cast new light on primitive mammals and dinosaurs and on faunal interchange between Asia and North America. *American Scientist* 63(2):150-159.

Kielan-Jaworowska Z, Hurum JH (2001) Phylogeny and Systematics of multituberculate mammals. *Paleontology* 44:389-429.

Kielan-Jaworowska Z, Cifelli RL, Luo Z-X (2004) Mammals from the Age of Dinosaurs: Origins, Evolution, and Structure (Columbia Univ. Press, New York).

Kielan-Jaworowska Z, Nessov LA (1990) On the metatherian nature of the Deltatheroida, a sister group of the Marsupialia. *Lethaia*. 23(1):1-10.

Kielan–Jaworowska Z, Ortiz–Jaureguizar E, Vieytes C, Pascual R, Goin,FJ (2007) First ?cimolodontan multituberculate mammal from South America. *Acta Palaeontologica Polonica* 52 (2):257–262.

Kirchner JW, Weil A (2000) Delayed biological recovery from extinctions throughout the fossil record. *Nature* 404:177-180.

Korth WW, Diamond ME (2002) Review of Leptomeryx (Artiodactyla, Leptomerycidae) from the Orellan (Oligocene) of Nebraska: *Annals of the Carnegie Museum*. 71:107–129.

Krause DW et al. (2014) First cranial remains of a gondwanatherian mammal reveal remarkable mosaicism. *Nature.* 515:512–517.

Krebs B (1991) Das Skelett von *Henkelotherium guimarotae* gen. et sp. nov. (Eupantotheria, Mammalia) aus dem Oberen Jura von Portugal. *Berl Geowiss Abh A.* 133:1–110.

Krumbiegel G, Ruffle L, Haubold H (1983) Das Eozane Geiseltal (A. Ziemsen Verlag, Wittenberg Lutherstadt)

Ladeveze S, de Muizon C, Beck RMD, Germain D, Cespedes-Paz R (2011) Earliest evidence of mammalian social behaviour in the basal Tertiary of Bolivia. *Nature* 474:83-86.

Lazagabaster IA, Rowan J, Kamilar JM, Reed KE (2016) Evolution of Craniodental Correlates of Diet in African Bovidae. J. Mammal. Evol. 23(4):385-396.

Lautenschlager S, Pamela GG, Luo Z-X, Fagan MJ, Rayfield EJ (2018) The role of miniaturization in the evolution of the mammalian jaw and middle ear. *Nature* 1.

Lee MSY, Cau A, Naish D, Dyke GJ (2014) Sustained miniaturization and anatomical innovation in the dinosaurian ancestors of birds. *Science* 345:562–566.

Liu L et al (2017) Genomic evidence reveals a radiation of placental mammals uninterrupted by the KPg boundary. *PNAS* E7282–E7290.

Lillegraven JA, Kielan-Jaworowska Z, Clemens WA (1979) Mesozoic Mammals The First Two-Thirds of Mammalian History. (University of California Press, Berkeley)

Lloyd GT, Wang SC, Brusatte SL (2012) Identifying Heterogeneity in Rates of Morphological Evolution: Discrete Character Change in the Evolution of Lungfish (Sarcopterygii; Dipnoi). *Evolution* 66(2):330–348.

Losos, JB, Thorpe RS (2004) Evolutionary Diversification of Caribbean Anolis Lizards. *Adaptive Speciation* (eds) Dieckmann U, Doebeli M, Metz JAJ, Tautz D (Cambridge University Press) pp 322–344.

Lucas SG, Hunt AP (1990) The oldest mammal. *New Mexico Journal of Science* 30:41-49.

Lucas SG, Luo Z-X (1993) *Adelobasileus* from the Upper Triassic of West Texas: the oldest mammal. *J. Vert. Pal.* 13:309-334.

Luo Z-X, Cifelli RL, Kielan-Jaworowska Z (2001) Dual origin of tribosphenic mammals *Nature* 409:53–57

Luo Z-X, Ji Q, Wible JR, Yuan C-Xi (2003) An Early Cretaceous Tribosphenic Mammal and Metatherian Evolution. Science. 302(5652):1934-1940.

Luo Z-X (2007) Transformation and diversification in early mammal evolution *Nature*, 450:1011-1019.

Luo Z-X, Chen P, Li G, Chen M (2007) A new eutriconodont mammal and evolutionary development in early mammals *Nature* 446:288–293

Luo, Z-X (2007) Successive diversifications in early mammalian evolution. *In* Anderson JS, Sues H-D (eds) Major Transitions in Vertebrate Evolution (Bloomington: Indiana University Press) pp:337–391.

Luo Z-X, Yuan C-X, Meng Q-J, Ji Q (2011) A Jurassic eutherian mammal and divergence of marsupials and placentals. *Nature* 476:442–445.

Luo Z-X, Wible JR (2005) A Late Jurassic Digging Mammal and Early Mammalian Diversification. *Science* 308(5718):103-107.

Luo Z-X, Meng, Q-J, Ji Q, Liu D, Zhang Y-G, Neander AI (2015) Evolutionary development in basal mammaliaforms as revealed by a docodontan. *Science* 347(6223):760-764.

Macdonald DW (2006) The Princeton Encyclopedia of Mammals. (Windmill Books Ltd., London)

Martin T, Marugán-Lobón J, Vullo R, Martín-Abad H, Luo Z-X, Buscalioni AD (2015). A Cretaceous eutriconodont and integument evolution in early mammals. *Nature* 526:380–384.

Matthew WD (1902) The skull of *Hypisodus*, the smallest of the Artiodactyla, with a revision of the Hypertragulidae Bull. Amer. Mus. Nat. Hist. 16:311-316.

Meehan TJ, Martin LD (2004) Emended genus description and a new species of Hypisodus (Artiodactyla: Ruminanta: Hypertragulidae). *In* Lucas SG, Zeigler KE, Kondrashov PE (eds) Paleogene Mammals. *New Mexico Museum of Natural History and Sciene Bulletin.* 26:137-143.

Meng J, Hu Y, Li C, Wang Y (2006) The mammal fauna in the Early Cretaceous Jehol Biota: implications for diversity and biology of Mesozoic mammals. *Geol. J.* 41:439-463.

Meng J, Hu Y, Wang Y, Wang X, Li C (2006) A Mesozoic gliding mammal from northeastern China. *Nature* 444:889-893.

Meng J (2014) Mesozoic mammals of China: implications for phylogeny and early evolution of mammals. *Natl. Sci. Rev.* 1:521–542.

Meng Q-J, Ji Q, Zhang Y-G, Liu D, Grossnickle DM, Luo Z-X (2015) An arboreal docodont from the Jurassic and mammaliaform ecological diversification. *Science* 347(6223):764-768.

Meng Q-J, Grossnickle DM, Liu D, Zhang Y-G, Neander AI, Ji Q, Luo Z-X (2017) New gliding mammaliaformes from the Jurassic. *Nature* 548:291-296.

McKenna MC, Bell SK (1997) Classification of Mammals above the species level (Columbia University Press, New York)

Muizon C, Billet G, Argot C, Ladeveze S, Goussard F (2015) Alcidedorbignya inopinata, a basal pantodont (Placentalia, Mammalia) from the early Palaeocene of Bolivia: anatomy, phylogeny and palaeobiology. Geodiversitas 37(4):397-634.

Murphy WJ, Eizirik E, Johnson WE, Zhang YP, Ryder OA, O'Brien SJ (2001) Molecular phylogenetics and the origins of placental mammals. *Nature.* 409:614–618.

Nowak RM (2006) Walkers mammals of the world (The Johns Hopkins University Press, Baltimore)

O'Leary et al (2013) The Placental Mammal Ancestor and the Post–K-Pg Radiation of Placentals *Science* 339(6120):662-667.

Osborn HF (1902) The law of adaptive radiation. *Am. Nat.* 36:353-363.

Panciroli E, Janis C, Stockdale M, Martín-Serra A (2017) Correlates between calcaneal morphology and locomotion in extant and extinct carnivorous mammals. *Journal of Morphology*, 278:1333-1353.

Phillips, M (2015) Four mammal fossil calibrations: balancing competing palaeontological and molecular considerations. *Palaeontol. Electron*. 1–16

Pinto G, Mahler DL, Harmon LJ, Losos JB (2008) Testing the island effect in adaptive radiation: rates and patterns of morphological diversification in Caribbean and mainland Anolis lizards. *Proc. R. Soc. B.* 275:2749–2757.

Price SA, Hopkins SSB (2015) The macroevolutionary relationship between diet and body mass across mammals *Biol. J. Linnean Soc.* 115(1)173-184.

Rabosky DL, Santini F, Eastman J, Smith SA, Sidlauskas B, Chang J, Alfaro ME (2013) Rates of speciation and morphological evolution are correlated across the largest vertebrate radiation. *Nature Coms.* 4:e1958.

Radinski L (1985) Patterns in the evolution of ungulate jaw shape *Amer. Zool.* 25:303-314.

Ragan MA (1992) Phylogenetic inference based on matrix representation of trees. *Mol. Phylo. Evol.* 1:53–58.

Revell LJ (2012) phytools: An R package for phylogenetic comparative biology (and other things). *Methods Ecol. Evol.* 3:217-223.

Rich T, Vickers-Rich (2004) Chapter 3: Diversity of Early Cretaceous Mammals from Victoria, Australia. Bull. American Mus. Nat. Hist. 285:36-53.

Rohlf FJ (2018) tpsDig2, Version 1.11. Department of Ecology and Evolution, SUNY Stony Brook, Stony Brook, N.Y.

Ronquist F, Teslenko M, van der Mark P, Ayres DL, Darling A, Hohna S, Larget B, Liu L, Suchard MA, Huelsenbeck JP (2012) Mrbayes 3.2: efficient bayesian phylogenetic inference and model choice across a large model space. *Syst. Biol.* 61:539-542,

Rose KD (2006) The Beginning of the Age of Mammals (The Johns Hopkins University Press, Baltimore)

Schluter D (2000) The Ecology of Adaptive Radiation. (Oxford University Press, Oxford)

Scott WB (1891) On the Osteology of Poebrotherium: A Contribution to the Phylogeny of the Tylopoda. (Ginn & Company, USA)

Scott WB (1940) The mammalian fauna of the White River Oligocene. Part IV. Artiodactyla. Transactions of the American Philosophical Society, new series. 28:363-746.

Sepkoski JJ (1996) Patterns of Phanerozoic extinction: a perspective from global data bases, p. 31–51. *In* Walliser, O. H. (ed.),*Global Events and Event Stratigraphy*. Springer, Berlin

Sibly RM, Brown JH (2007) Effects of body size and lifestyle on evolution of mammal life histories*. Proc Natl Acad Sci USA.* 104(45):17707-12.

Simmons NB, Geisler JH (1998) Phylogenetic relationships of Icaronycteris, Archaeonycteris, Hassianycteris, and Palaeochiropteryx to extant bat lineages, with comments on the evolution of echolocation and foraging strategies in Microchiroptera. *Bulletin of the AMNH* 235:2-182.

Simpson GG (1937) The Beginning of the Age of Mammals. *Biological Reviews* 12:1-47.

Simpson GG (1944) Tempo and mode in evolution (Columbia University Press, New York City)

Simpson GG (1953) The Major Features of Evolution. (Columbia University Press, New York).

Slater GJ, Price SA, Santini F, Alfaro ME (2010) Diversity versus disparity and the radiation of modern cetaceans. *Proc. R. Soc. B.* 277(1697):3097–3104.

Slater GJ (2013) Phylogenetic evidence for a shift in the mode of mammalian body size evolution at the Cretaceous-Palaeogene boundary. Methods Ecol Evol 4(8): 734–744.

Slater GJ, Friscia AR (2018) Hierarchy, Morphology, and Adaptive Radiation: a Test of Osborn's Law in the Carnivora. https://doi.org/10.1101/285700. Preprint, posted March 20, 2018.

Sloan LC, Thomas E (1998) Global Climate of the Late Paleocene Epoch: Modeling the Circumstances Associated. Late Paleocene-early Eocene climatic and biotic events in the marine and terrestrial records.

Smith FA, et al. (2010) The evolution of maximum body size of terrestrial mammals. Science 330:1216–1219.

Soul LC, Friedman M (2015) Taxonomy and phylogeny can yield comparable results in comparative paleontological analyses. *Systematic Biology*. 64(4):608-620.

Springer MS (1997) Molecular Clocks and the Timing of the Placental and Marsupial Radiations in Relation to the Cretaceous-Tertiary Boundary. *J. Mamm. Evol.* 4(4):285-302.

Springer MS, Stanhope MJ, Madsen O, de Jong WW (2001) Molecules consolidate the placental mammal tree Author links open overlay panel. *TREE*. 19(8):430-438.

Springer MS, Murphy WJ, Eizirik E, O'Brien SJ (2003) Placental mammal diversification and the Cretaceous–Tertiary boundary. *PNAS* 100(3):1056–1061

Springer MS, Murphy WJ, Roca AL (2018) Appropriate fossil calibrations and tree constraints uphold the Mesozoic divergence of solenodons from other extant mammals. *Molecular Phylogenetics and Evolution* 121:158-165.

Stanley SM (1973) An explanation for Cope's rule. *Evolution* 27:1–26.

Stanley SM, Yang X (1987) Approximate evolutionary stasis for bivalve morphology over millions of years: a multivariate, multilineage study. *Paleobiology* 13(2):113-139.

Storch G (1996) Paleobiology of Messel Erinaceomorphs. *Palaeovertebrata* 25(2-4):215-224.

Szalay FS, Trofimov BA (1996) The Mongolian Late Cretaceous *Asiatherium*, and the early phylogeny and palaeobiogeography of Metatheria. *J. Vert. Pal.* 16:474-509.

Tarver JE et al (2015) The Interrelationships of Placental Mammals and the Limits of Phylogenetic Inference. *Genome Biol. Evol.* 8(2):330–344.

Uyeda JC, Caetano DS, Pennell MW (2015) Comparative analysis of principal components can be misleading. *Systematic Biology*. *64*(4):677-689.

Van Soest PJ (1996) Allometry and ecology of feeding behavior and digestive capacity in herbivores: a review. *Zoo Biology: Published in affiliation with the American Zoo and Aquarium Associatio*n. 15(5):455-479.

Van Valkenburgh B (1999) Major Patterns in the History of Carnivorous Mammals. *Annu. Rev. Earth Planet. Sci.* 27:463-493.

Venditti C, Meade A, Pagel M (2011) Multiple routes to mammalian diversity. *Nature*. 479:393-396.

Walmsley A, Elton S, Louys J, Bishop LC, Meloro (2012) Humeral epiphyseal shape in the felidae: The influence of phylogeny, allometry, and locomotion. *J. Morphol.* 273:1424–1438.

Wesley-Hunt GD (2005) The Morphological Diversification of Carnivores in North America. *Paleobiology* 31(1):35-55.

Wible JR, Burrows AM (2016) Does the Jurassic Agilodocodon (Mammaliaformes, Docodonta) have any exudativorous dental features? *Palaeontologia Polonica* 67:289–299.

Williamson TE, Brusatte SL, Wilson GP (2014) The origin and early evolution of metatherian mammals: the Cretaceous record. *ZooKeys* 465:1–76.

Wills MA, Briggs DEG, Fortey RA (1994) A Comparison of Cambrian and Recent Arthropods. *Paleobiology* 20(2):93-130.

Wilson GP (2013) Mammals across the K/Pg boundary in northeastern Montana, U.S.A.- dental morphology and body-size patterns reveal extinction selectivity and immigrant-fueled ecospace filling. *Paleobiology*, 39(3):429-469.

Wilson GP, Evans AR, Corfe IJ, Smits PD, Fortelius, Jernvall J (2012) Adaptive radiation of multituberculate mammals before the extinction of dinosaurs. *Nature*, 483:457-460.

Wing SL, Harrington GJ, Smith FA, Bloch JI, Boyer DM, Freeman KH (2005) Transient floral change and rapid global warming at the Paleocene-Eocene boundary *Science* 310(5750):993-996.

Wright DF (2017) Phenotypic innovation and adaptive constraints in the evolutionary radiation of Palaeozoic crinoids. *Scientific reports* 7(1):13745.

Zhang F, Crompton AW, Luo Z-X, Schaff CR (1998) Pattern of dental replacement of *Sinoconodon* and its implication for evolution of mammals. *Vertebrata PalAsiatica* 36:197-217.

Zhang H, Wang Y, Janis CM, Goodall H, Purnell MA (2017) An examination of feeding ecology in Pleistocene proboscideans from southern China (*Sinomastodon*, *Stegodon*, *Elephas*), by means of dental microwear texture analysis. Quaternary International 445:60-70.

Zheng X, Bi S, Wang X, Meng, J (2013) A new arboreal haramiyid shows the diversity of crown mammals in the Jurassic period. *Nature* 500:199-202.

Zhou C-F, Wu S, Martin T, Luo Z-X (2013) A Jurassic mammaliaform and the earliest mammalian evolutionary adaptations *Nature* 500:163-167.

Supplementary Materials

Supplementary Material S1.1

Measurements collected

The following ten continuous character measurements were collected and used to produce six ratios that serve as the mechanical traits used in this study.

CM1: Jaw length

Maximum length of the jaw, from the posterior most point of the jaw to the tip of the tooth row. The most posterior point on the jaw may consist of the angular, articulation, or coronoid. The total size of the jaw directly relates to the maximum size of food items that can be consumed.



Figure CM1: *Panthera leo* jaw, with red line indicating jaw length measure

CM2: Jaw depth

Depth of the jaw immediately posterior to the last (most posterior) tooth, usually the last molar.



Figure CM2: *Panthera leo* jaw, with red line indicating jaw width measure

CM3: Dental row length

Total length of the tooth row, from the back of the last tooth, often the ultimate molar, to the anterior margin of the most anterior tooth, often the first incisor. The length of the tooth row is the total length of the area where food can be processed.



Figure CM3: *Panthera leo* jaw, with red line indicating dental row length measure

CM4: Molar row length

Total length of the molar row, from the posterior margin of the last molar to the anterior margin of the first premolar.



Figure CM4: *Panthera leo* jaw, with red line indicating molar row length measure

CM5: Diastema length

Total length of the diastema.



Figure CM5: *Panthera leo* jaw, with red line indicating diastema length measure

CM6: Distance from condyle to coronoid

Total length of the distance from the most posterior surface of the condyle, to the tallest point on the margin of the coronoid.



Figure CM6: *Panthera leo* jaw, with red line indicating condyle to coronoid measure

CM7: Distance from condyle to middle cusp of last premolar

Total distance from the most posterior margin of the condyle to the middle cusp of the last premolar.

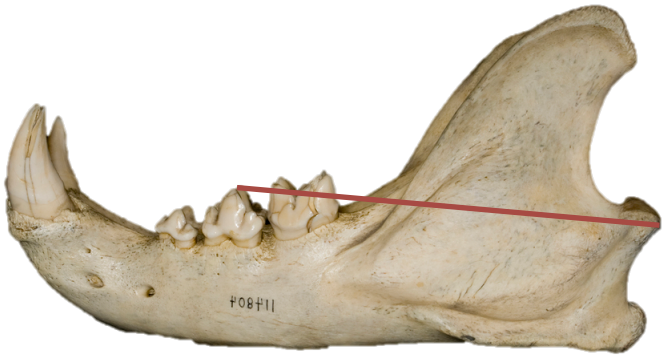


Figure CM7: *Panthera leo* jaw, with red line indicating condyle to premolar cusp measure

CM8: Coronoid height

Total length of the coronoid, from the base of the coronoid where the trough positioned anteriorly to the condyle curves upward, to the highest point on the dorsal margin of the coronoid.



Figure CM8: *Panthera leo* jaw, with red line indicating coronoid height measure

CM9: Coronoid length

Total width of the coronoid from the posterior margin to the anterior margin, in line with the point where the trough positioned anteriorly to the condyle curves upward.



Figure CM9: *Panthera leo* jaw, with red line indicating coronoid length measure

CM10: Distance from articulation to tooth row

The articular offset of the jaw is measured in a vertical line from the highest dorsal point of the articulation, the condyle, to a line drawn along the top surface of the tooth row. This line is drawn from the dorsal surface of the most proximal tooth, usually the first incisor, to the dorsal surface of the most distal tooth, usually the last molar, and extended backwards along the length of the jaw (see grey line). The cusps of teeth between the most proximal and most distal teeth may fall above or below this line. The canine often extends above this line, however the line best captures the occlusional surface of the teeth.



Figure CM10a: *Panthera leo* jaw, with grey line indicating the occlusional surface of the tooth row and red line indicating articulation offset measure



Figure CM10b: *Boselaphus tragocamelus* jaw, with grey line indicating the occlusional surface of the tooth row and red line indicating articulation offset measure

Where this measurement was taken in person using calipers, a 30cm ruler was placed along the tooth row in place of the grey line depicted below. Calipers were then used to measure from the 30cm ruler to the articulation. The vertical line measured may extend above or below the grey tooth row line (see figures 15a and 15b). In mammals, an articulation positioned above the tooth row is more frequently observed.

Traits used

The following ratios are used to capture key functional traits across mammalian jaws, and to reflect their biomechanical properties. An organism's biomechanics defines and confines it's functional abilities, and therefore can help to discriminate between different ecomorphologies.

Where appropriate (indicated in following text), proportional ratios have been arc sine transformed. This spreads out the tails of the distribution for proportions.

All data has then been z transformed. This scales all traits so that their mean is equal to 0, and allows each trait to carry equal weight in the PCA analysis.

T1: Diastema length ratio (CM5/CM3)

The diastema, the space between teeth near the front of the tooth row, has clear functional relevance and appears to be a good indicator of ecology. The diastema can be between the canine and first premolar, between the first and second premolars, or between the incisor and first premolar (where a canine is not present). A diastema positioned behind the canine is more usual in mammals. Herbivorous mammal species, including species within clades like Artiodactyla, have a large diastema. This diastema serves as a holding space for food that has been picked/grazed before it is passed backwards so that mastication can commence on the premolar/molar teeth. Hypercarnivores also have a relatively large diastema, however this space is likely not used as a holding area for torn off flesh. The diastema in hypercarnivores allows space for the upper canine to come into line with the lower canine, and allows the canines

to pierce further into carrion. Diastema length is divided by tooth row length to capture how large the diastema is relative to the overall size of the tooth row.

The diastema length ratio acts as a proportion and is therefore arc sine transformed.



Figure T1: *Panthera leo* jaw, with red lines indicating diastema length ratio (diastema length/dental row lengt)

T2: Molar row length ratio (CM4/CM3)

The molar row length ratio describes the amount of the tooth row that has been specialised for mastication. Browsers and grazers should have a larger proportion of their tooth row dedicated to this function. The molar row length ratio is calculated by dividing molar row length by dental row length.

The molar row length ratio acts as a proportion and is therefore arc sine transformed.



Figure T2: *Panthera leo* jaw, with red lines indicating molar row length ratio (molar row length/dental row length)

T3: Jaw closing mechanical advantage

The mammalian jaw can be simplified as a 2D third-order leaver. The in-leaver and out-leaver both originate from the condyle, which acts as the fulcrum (the point of rotation). The in-leaver is measured from the posterior margin of the condyle to the highest marginal point of the coronoid. The out-leaver for average jaw closing mechanical advantage is measured from the posterior margin of the condyle to the middle cusp of the last premolar. Force, provided by the m. temporalis muscle complex, is applied to the in-leaver in order to lift the out-leaver. Jaw closing mechanical advantage is calculated by dividing the condyle to coronoid length by the condyle to premolar length.

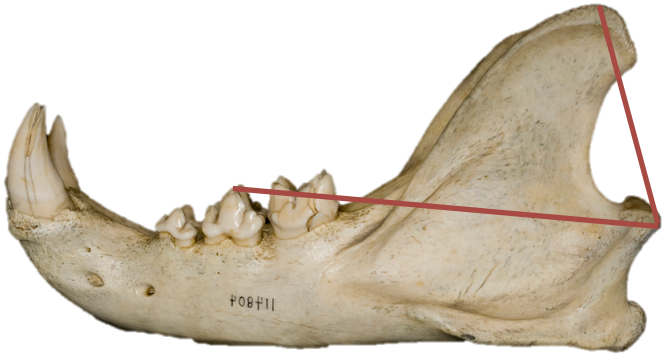


Figure T3: *Panthera leo* jaw, with red lines indicating average jaw closing mechanical advantage measure (condyle to coronoid/condyle to premolar)

T4: Jaw slenderness ratio ((CM2/CM1)*100)

This describes the stiffness of the jaw. The jaw depth measure can serve as a proxy for flexural stiffness under dorso-ventral loads (Anderson et al, 2013).

The jaw slenderness ratio is calculated by dividing jaw depth by jaw length *100.

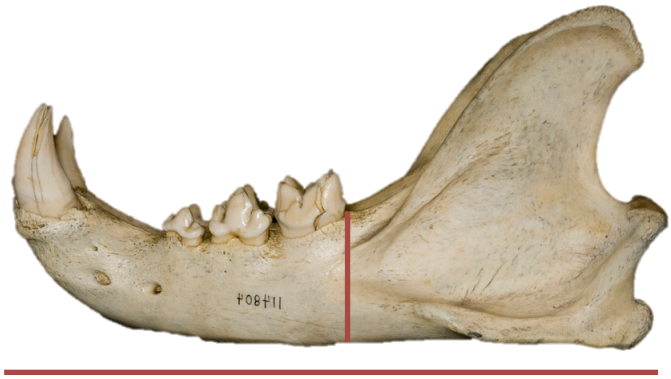


Figure T4: *Panthera leo* jaw, with red lines indicating jaw slenderness ratio (jaw depth/jaw length * 100)

T5: Coronoid slenderness ratio

The temporalis muscle attaches to the coronoid in two places. The m. temporalis pars superficialis extends from the temporal fossa on the skull to the lateral surface of the coronoid process. The m. temporalis pars profunda extends from the anterior portion/margin of the temporal fossa on the skull to the medial surface of the coronoid process on the jaw. Another muscle, the m. masseter pars profunda attaches from the medial surface of the zygomatic arch to the lower jaw along the lower margin of, or immediately below, the coronoid

process (but see wombat musculature (Sharp & Trusler, 2015)). These muscles play a role in jaw opening and closing mechanics and bite force. Differences in the size and shape of the condyle, and therefore the surface area of the muscle attachment sites, is indicative of the strength of the organisms bite. Further, the more anterioposteriorally wide the coronoid process, the more resistant it is to forces, whereas more anterioposteriorally narrow coronoid processes will withstand less force.

Coronoid height is divided by coronoid length and then times by 100 to describe the slenderness of the coronoid process, therefore capturing the robustness of the coronoid and therefore a relative measure of how much tension it can take.



Figure T5: *Panthera leo* jaw, with red lines indicating coronoid slenderness ratio ((coronoid height/coronoid length)*100)

T6: Articulation offset ratio.

The position of the articulation relative to the tooth row affects the way in which the upper and lower teeth occlude. When the articulation is in line with the tooth row (i.e. a measurement of 0), the jaw closes in a scissor-like

movement. As the articulation moves further away from the tooth row line occlusion occurs in a flatter, up and down motion, allowing all teeth to occlude at once. Broadly, carnivores have a more scissor-like occlusion to allow for a slicing action, and herbivores occlude their teeth all at once to allow for grinding of plant material.

Articulation offset ratio is calculated by dividing the distance between the jaw joint and the tooth row by jaw length.



Figure T6a: *Panthera leo* jaw, with grey line indicating the occlusional surface of the tooth row, vertical red line indicating articulation offset measure, and horizontal red line indicating jaw length. Articulation offset ratio (distance between the jaw joint and the tooth row/jaw length)



Figure T6b: *Boselaphus tragocamelus* jaw, with grey line indicating the occlusional surface of the tooth row, vertical red line indicating articulation offset measure, and horizontal red line indicating jaw length. Articulation offset ratio (distance between the jaw joint and the tooth row/jaw length)

Supplementary Material S1.2

Principle components for Chapter 1

PC1 describes 32.21% of overall variance, and correlates with (in order of significance) the length of the diastema in comparison to the length of the tooth row (T1), the length of the molar row in comparison to the length of the tooth row (T2), the slenderness of the jaw (T4), and to a lesser extent the articulation offset in comparison to the length of the jaws (T6). Mammals plotting against more positive PC1 scores have particularly slender, shallow jaws, little or no diastema and a long relative molar row, with a low articulation offset ratio. Mammals that exhibit more negative PC1 scores have an opposite suite of traits.

PC2 describes 24.98% of overall variance, and correlates with the following traits, in order of significance (Table S1.1); the articulation offset in comparison to the length of the jaw (T6), jaw closing mechanical advantage (T3), coronoid slenderness (T5), and to a lesser extent the length of the molar row in comparison to the length of the tooth row (T2). Mammals that plot more positively on PC2 have lower scores for jaw closing mechanical advantage, more anteroposteriorly slender coronoids, a larger relative articulation offset, and a longer relative molar row length.

PC3 describes 17.94% of overall variance. In order of significance, PC3 correlates well with jaw ramus slenderness (T4) and jaw closing mechanical advantage (T3), and to a lesser extent the length of the molar row in comparison to the length of the tooth row (T2). Mammals plotting more positively on PC3

have more slender, shallower jaws, a smaller mechanical advantage, and a larger molar row in comparison to the tooth row.

PC4 describes 11.84% of the variation, and correlates primarily with coronoid slenderness ratio (T5). Mammals that plot in the most positive positions on PC4 have coronoids which are more slender anterioposteriorally and more elongate dorsoventrally.

PC5 describes 7.09% of the variance. PC5 does not correlate strongly with any trait in particular, but correlates with the articulation offset ratio (T6), jaw slenderness (T4), and jaw closing mechanical advantage (T3) the most. Generally speaking, mammal species which plot more positively on PC5 have a larger relative articulation offset, a more slender jaw, and a larger jaw closing mechanical advantage.

PC6 describes 5.91% of the overall variance, but again does not correlate well with any individual trait. In order of significance, PC6 correlates best with diastema length (T1), and relative molar length (T2). Mammals plotting more positively on PC6 have, on average, a larger relative diastema, and longer relative molar row.

PC axis	Trait	Correlation	p-value
PC1	diastema.asin (T1)	-0.776649011	6.39E-56
PC1	jaw.slenderness (T4)	-0.65160064	3.87E-34
PC1	articulation.offset.ratio (T6)	-0.6061354	1.42E-28
PC1	molar.asin (T2)	0.53408426	2.18E-21
PC1	coronoid.slenderness (T5)	-0.477285029	7.98E-17
PC1	closing.ma.premolar (T3)	-0.10642074	0.080329417
PC2	closing.ma.premolar (T3)	0.683484305	1.20E-38
PC2	articulation.offset.ratio (T6)	-0.593677803	3.36E-27
PC2	molar.asin (T2)	-0.560312172	8.41E-24
PC2	coronoid.slenderness (T5)	-0.524152775	1.58E-20
PC2	diastema.asin (T1)	0.329865625	2.67E-08
PC2	jaw.slenderness (T4)	-0.003642699	0.952403012
PC3	jaw.slenderness (T4)	-0.637964207	2.27E-32
PC3	closing.ma.premolar (T3)	-0.548078895	1.19E-22
PC3	molar.asin (T2)	-0.458711405	1.66E-15
PC3	diastema.asin (T1)	0.320144989	7.11E-08
PC3	articulation.offset.ratio (T6)	-0.155132935	0.010542532
PC3	coronoid.slenderness (T5)	0.152590882	0.011899952
PC4	coronoid.slenderness (T5)	0.680934408	2.89E-38
PC4	closing.ma.premolar (T3)	0.371323045	2.76E-10
PC4	articulation.offset.ratio (T6)	-0.236628583	8.38E-05
PC4	jaw.slenderness (T4)	-0.160027894	0.008309096
PC4	diastema.asin (T1)	-0.133159571	0.028399735
PC4	molar.asin (T2)	-0.008417414	0.8902957
PC5	articulation.offset.ratio (T6)	-0.437885824	4.02E-14
PC5	jaw.slenderness (T4)	0.277136114	3.62E-06
PC5	closing.ma.premolar (T3)	-0.230993899	0.000124504
PC5	molar.asin (T2)	0.219577769	0.000269949
PC5	diastema.asin (T1)	0.139647378	0.021474371
PC5	coronoid.slenderness (T5)	0.099927659	0.100688658
PC6	molar.asin (T2)	0.266169229	8.92E-06
PC6	diastema.asin (T1)	0.263756733	1.08E-05
PC6	jaw.slenderness (T4)	-0.256888409	1.86E-05
PC6	closing.ma.premolar (T3)	0.172899888	0.004308223
PC6	articulation.offset.ratio (T6)	0.091341303	0.13365219
PC6	coronoid.slenderness (T5)	-0.022840452	0.70817212

Table S1.1. Table outlining the correlation coefficient of each principle component axis against each jaw trait submitted to the PCA. A p-value for the correlation is also presented.

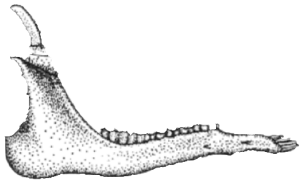
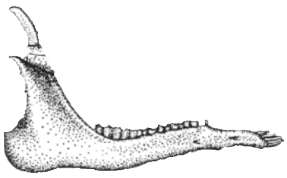
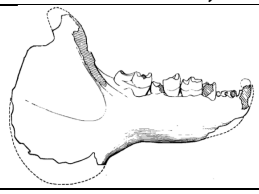
	Jaw with Most Negative PC Score	Jaw with Most Positive PC Score
PC1	***Hypisodus minimus*, Eocene**	***Megazostrodon rudnerae*, Early Jurassic**
		
PC2	***Metacheiromys dasypus*, Eocene**	***Hypisodus minimus*, Eocene**
		
PC3	***Wortmania otariidens*, Paleocene**	***Metacheiromys dasypus*, Eocene**
		
PC4	***Hypisodus minimus*, Eocene**	***Duchesneodus uintensis*, Eocene**
		
PC5	***Convallisodon convexus*, Paleocene**	***Tillodon fodiens*, Eocene**
		
PC6	***Paroodectes feisti*, Eocene**	***Metacheiromys dasypus*, Eocene**
		

Table S1.2. Table showing the extreme morphologies of the species that occupy the most extreme points recorded on each principle component axis. *Hypisodus minimus*; sketch of specimen KUVP 127574, edited from Meehan & Martin (2004). *Megazostrodon rudnerae*; reconstruction of specimen BMNH 26407, edited from Kielan-Jaworowska et al (2004). *Metacheiromys dasypus*; photograph of specimen AMNH 11718 taken by author GLB. *Wortmania otariidens*; photograph of AMNH 3394, taken from Williamson & Brusatte (2013). *Duchesneodus uintensis*; photograph of CMNH 11809, taken from Mihlbachler (2008). *Convallisodon convexus*; reconstructive sketch of IVPP V5485, taken from Chow & Qi (1978). *Tillodon fodiens*; photograph of CM 2994 (cast) taken by author GLB. *Paroodectes feisti*; photograph of jaw of HLMD-Me 7951 (cast) taken by author GLB.

Supplementary Material S1.3

Supplementary methods and discussion for Chapter 1

All four alternative methods of calculating disparity (sum of variance, sum of ranges, mean pairwise distance, mean distance from centroid) show that Cenozoic mammal disparity surpassed Mesozoic mammal disparity by the middle – late Eocene at the latest (Fig. S1.6a-d). Further, all methods recover an increase in therian mammal disparity across the K/Pg boundary, and continued increase across the Paleocene/Eocene boundary and throughout the Eocene (Fig. S1.6a-d). The discrepancies in the time it takes for disparity to exceed pre-K/Pg levels in the Eocene reflects the slightly different aspect disparity captured by the four different method used here, and can highlight different information regarding the spread of points within function space. The results of the sum of ranges through time show that the maximum range of mammals plotting in function space remains relatively low throughout the Mesozoic and across the K/Pg boundary, but rose quickly across the Paleocene/Eocene boundary and throughout the Eocene. A longer recovery period seen for the mean distance from centroid measure suggests a higher proportion of mammals with morphologies that plot closer to the centre of function space in the early part of the Cenozoic. Taken with the results of other disparity metrics, this suggests that, although the total range of function space populated increased, the proportion of the sampled population exhibiting these extreme morphologies was relatively low.

In contrast to minimum spanning tree length, the four methods presented in Fig. S1.6 suggest a possible decrease in total mammal disparity across the K/Pg boundary before a rebound and ultimately an increase during the Eocene (Figs. 1.1, S1.7a) rather than constant disparity across the boundary (Figs. S1.6-S1.7b-e). A short-term decrease in disparity could result from selective extinction of specialists as suggested in Grossnickle & Newham (2016).

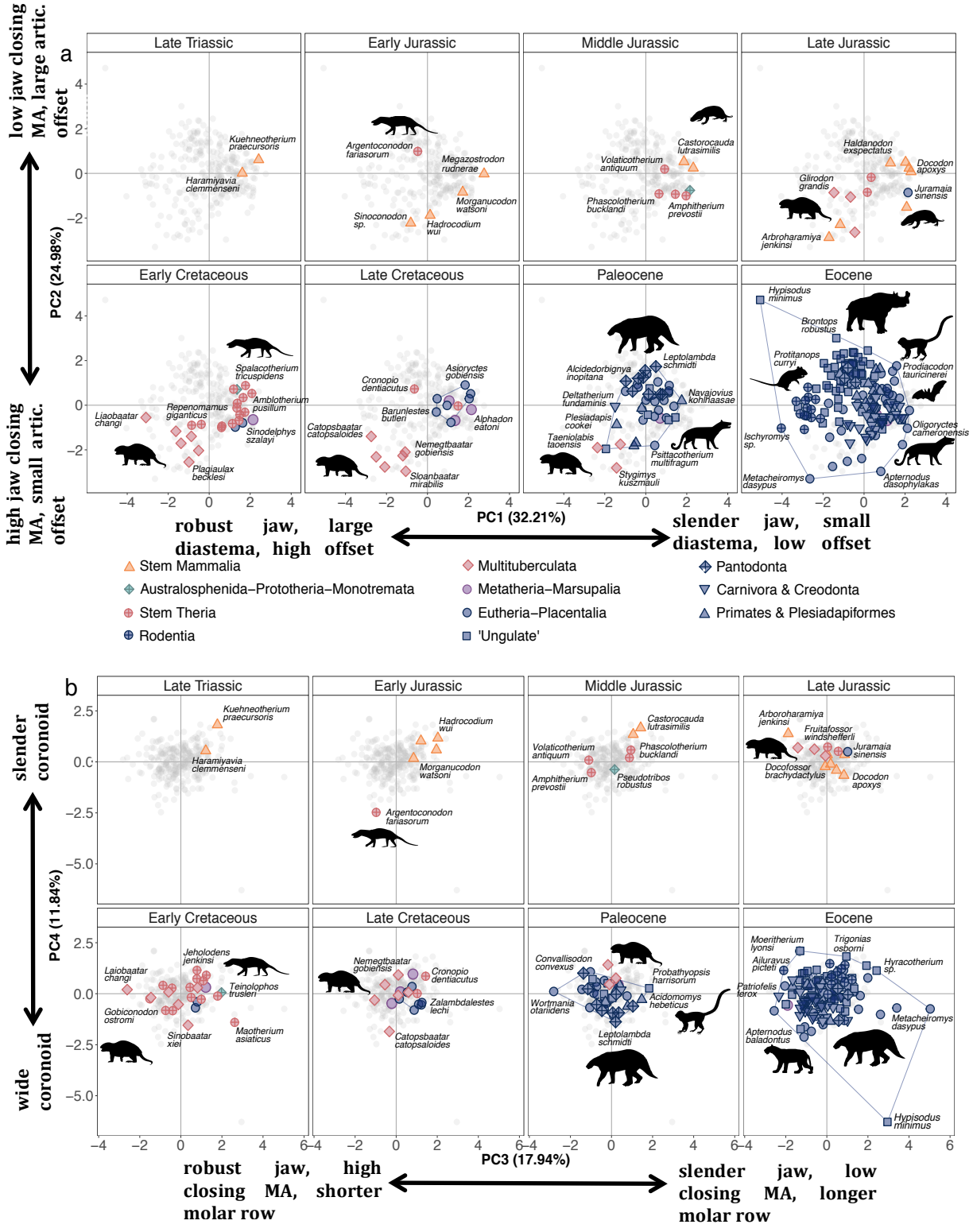


Figure S1.1. Jaw disparity function space across 8 epochs from the Late Triassic – Eocene split between (a) PC1-PC2 and (b) PC3-PC4. Mammal species, which outline the extreme regions of function space, are labelled on each panel. Different colours and symbols represent mammal clades (see key within figure). The blue polygon depicts the total spread of Eutheria-Placentalia mammals in the Late Cretaceous, Paleocene, and Eocene. The grey points represent the spread of all data points across the total study time interval.

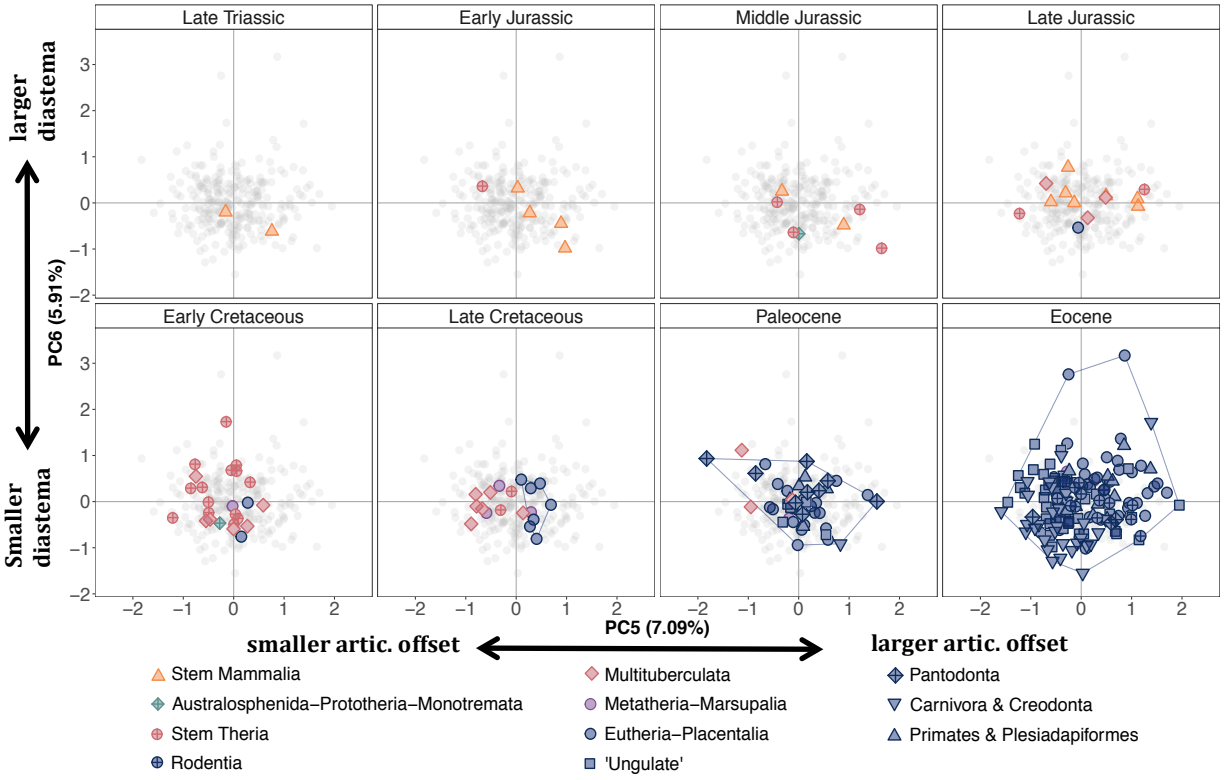


Figure S1.2. PC5-PC6 Jaw disparity function space across 8 epochs from the Late Triassic – Eocene. Different colours and symbols represent mammal clades (see key within figure). The blue polygon depicts the total spread of Eutheria-Placentalia mammals in the Late Cretaceous, Paleocene, and Eocene. The grey points represent the spread of all data points across the total study time interval.

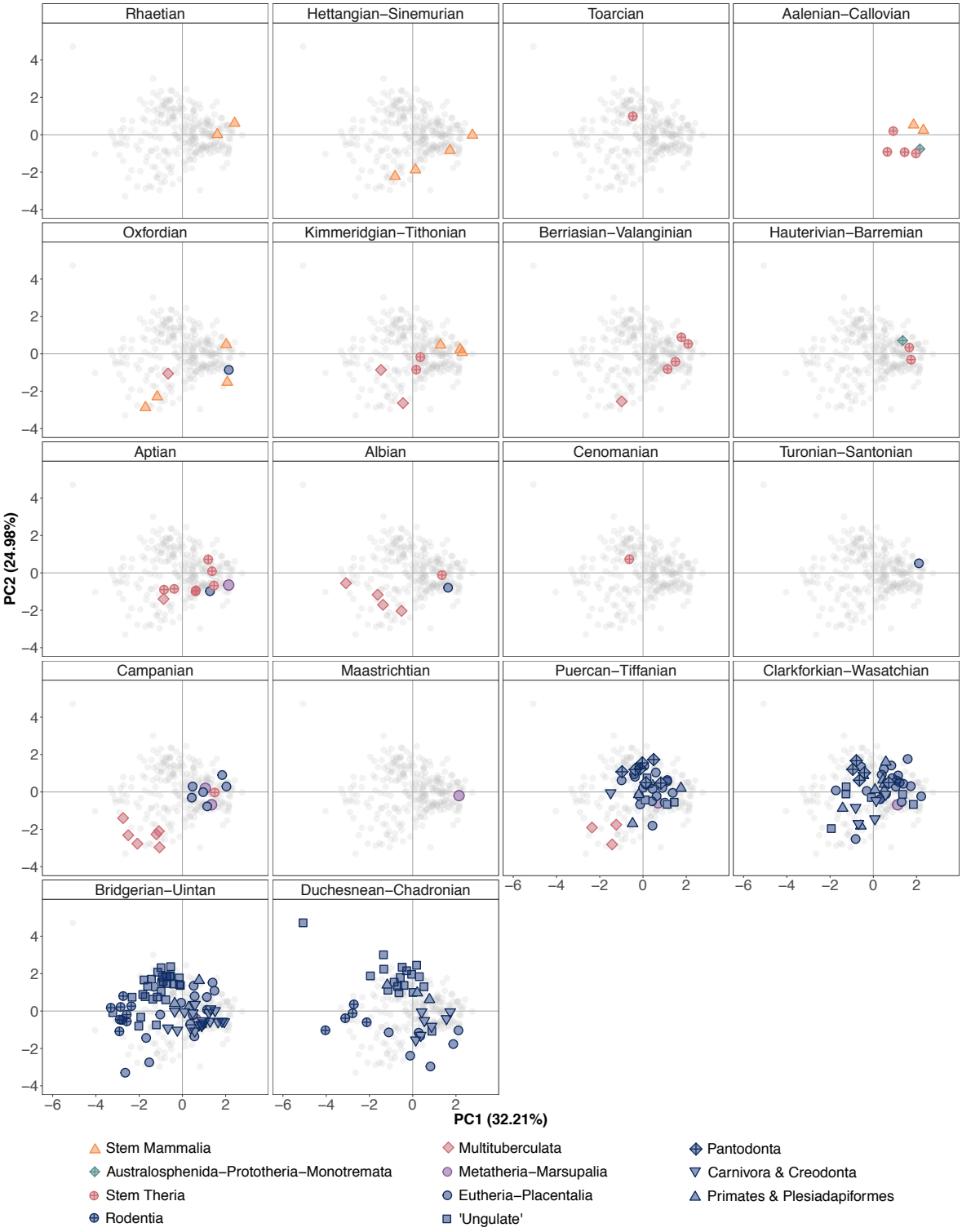


Figure S1.3. PC1-PC2 Jaw disparity function space across 18 broadly equal time bins, based on amalgamated stages (Mesozoic) and North American Land Mammal Ages (NALMA; Cenozoic) from the Rhaetian (Late Triassic) – Duchesnean-Chadronian (Eocene). Different colours and symbols represent mammal clades (see key within figure). The grey points represent the spread of all data points across the total study time interval.

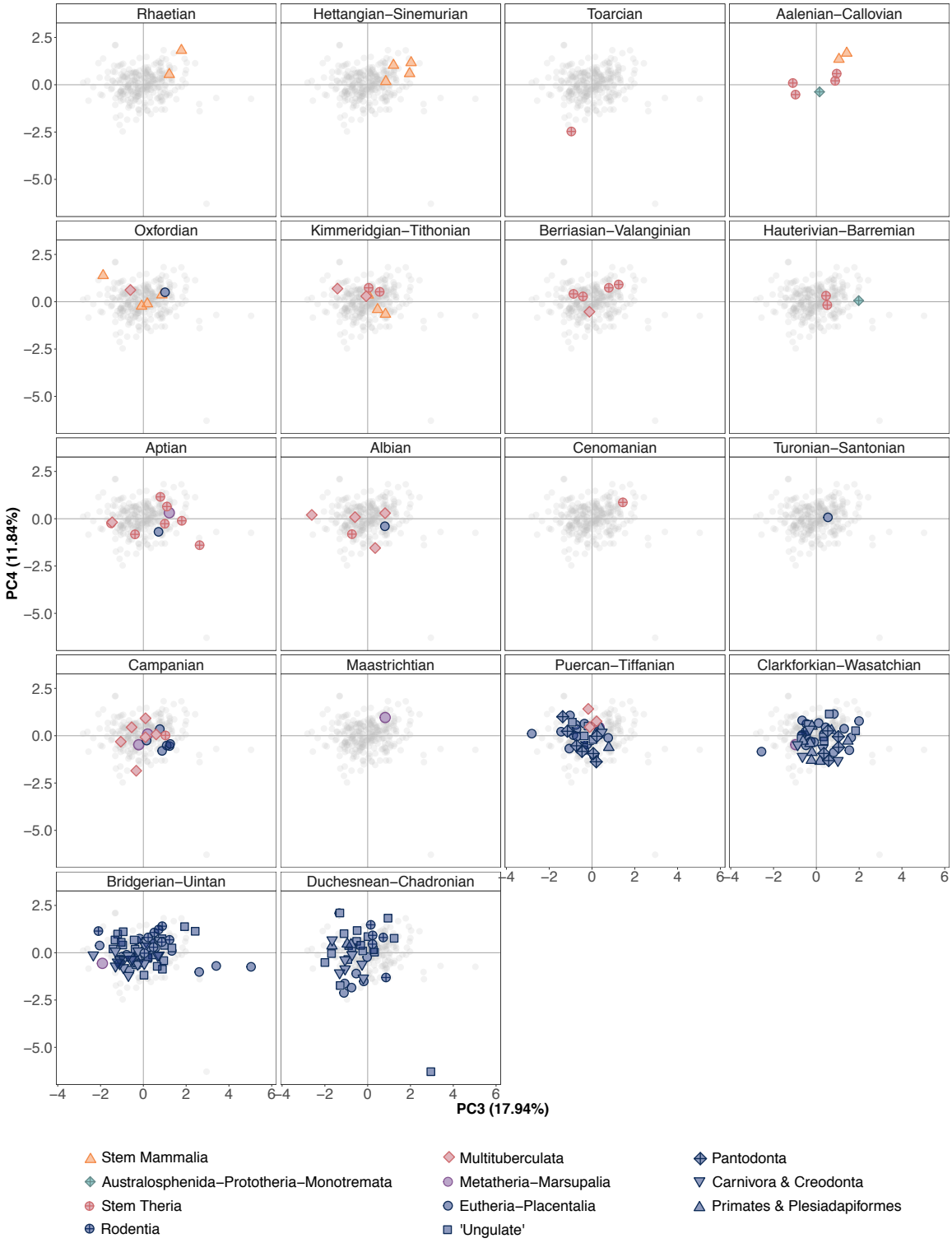


Figure S1.4. PC3-PC4 Jaw disparity function space across 18 broadly equal time bins, based on amalgamated stages (Mesozoic) and North American Land Mammal Ages (NALMA; Cenozoic) from the Rhaetian (Late Triassic) – Duchesnean-Chadronian (Eocene). Different colours and symbols represent mammal clades (see key within figure). The grey points represent the spread of all data points across the total study time interval.

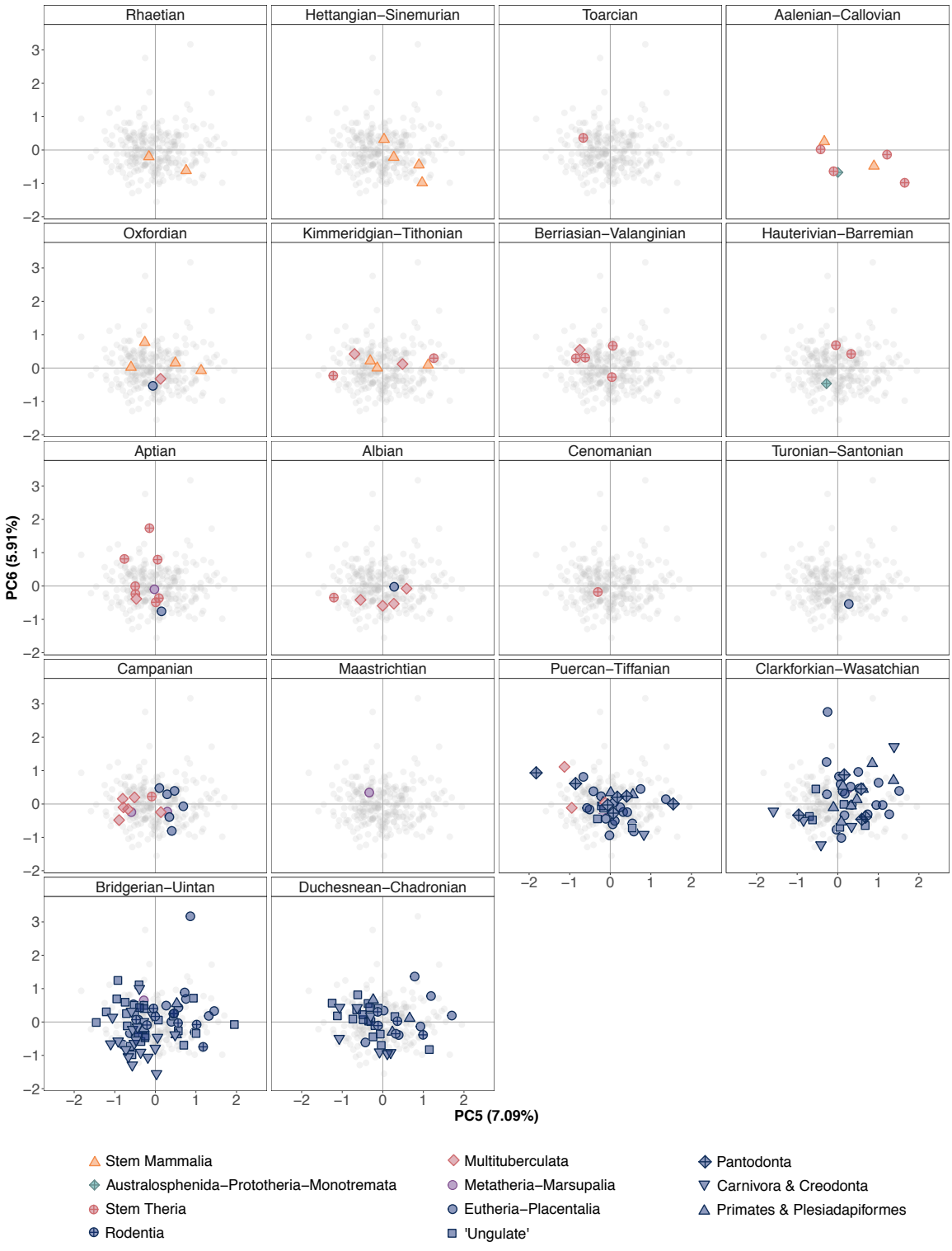


Figure S1.5. PC5-PC6 Jaw disparity function space across 18 broadly equal time bins, based on amalgamated stages (Mesozoic) and North American Land Mammal Ages (NALMA; Cenozoic) from the Rhaetian (Late Triassic) – Duchesnean-Chadronian (Eocene). Different colours and symbols represent mammal clades (see key within figure). The grey points represent the spread of all data points across the total study time interval.

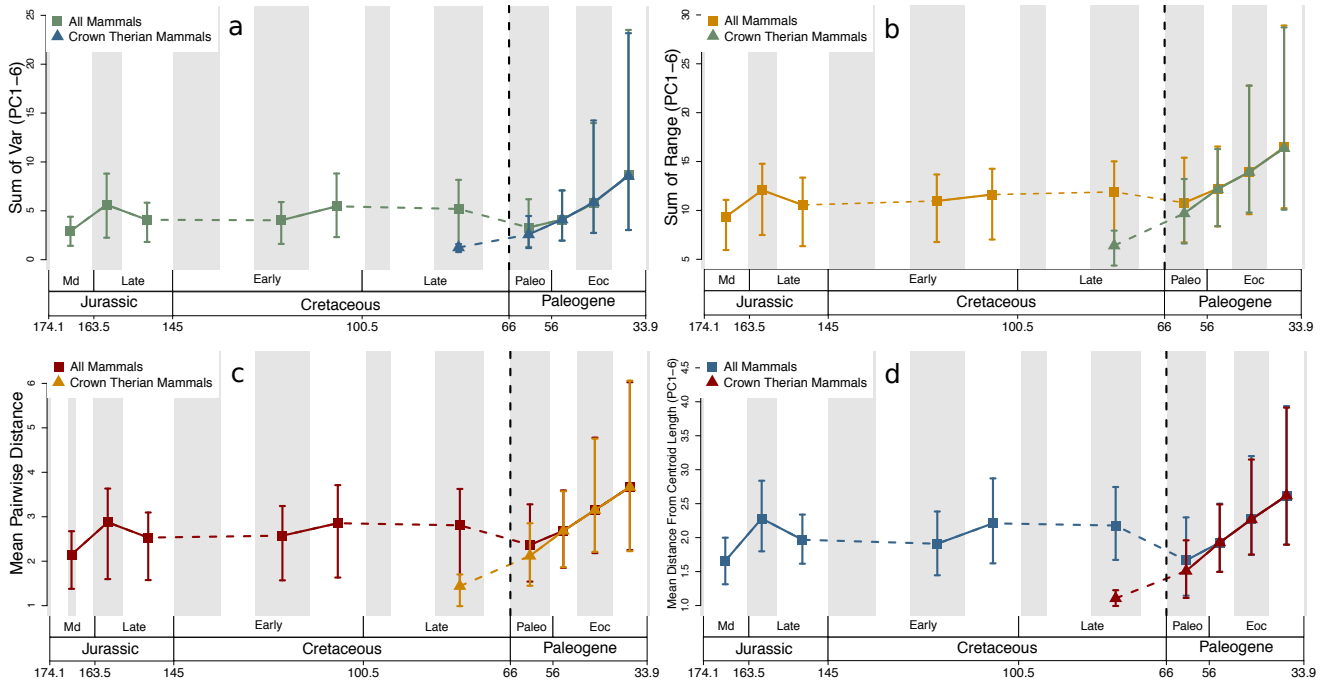


Figure S1.6. Jaw functional disparity through time, calculated using four different methods. The four methods shown here are a) sum of variance, with the green curve showing sum of variance among all mammals, and the blue showing therian mammals only, b) sum of ranges, with the orange curve showing sum of ranges among all mammals, and the green showing therian mammals only c) mean pairwise distance, with the red curve showing all mammals, and the orange showing therian mammals only and d) mean distance from centroid, with the blue curve showing all mammals, and the red showing therian mammals only. For all methods (a-d), amalgamated stages (Mesozoic) and NALMAs (Cenozoic) with six or more individuals are used as time bins (see methods). Data is rarefied (n = 6) and sampled with replacement to enable fairer comparison between bins with differing sample sizes. The 95% confidence intervals represent uncertainty produced by sampling six individuals at random with replacement across each time bin, for 5000 iterations. The points represent the mean values of these 5000 runs. A solid line indicates changes between consecutive time bins. Dashed lines indicate changes across two or more time bin boundaries. Although these curves represent rarefaction to six, total mammal disparity through time has been rarefied to fifteen (across fewer bins) across all methods and can be seen in Fig. S1.7b-e. Analysis using this higher rarefaction number recovers the same patterns across the K/Pg boundary and into the Cenozoic for all four methods.

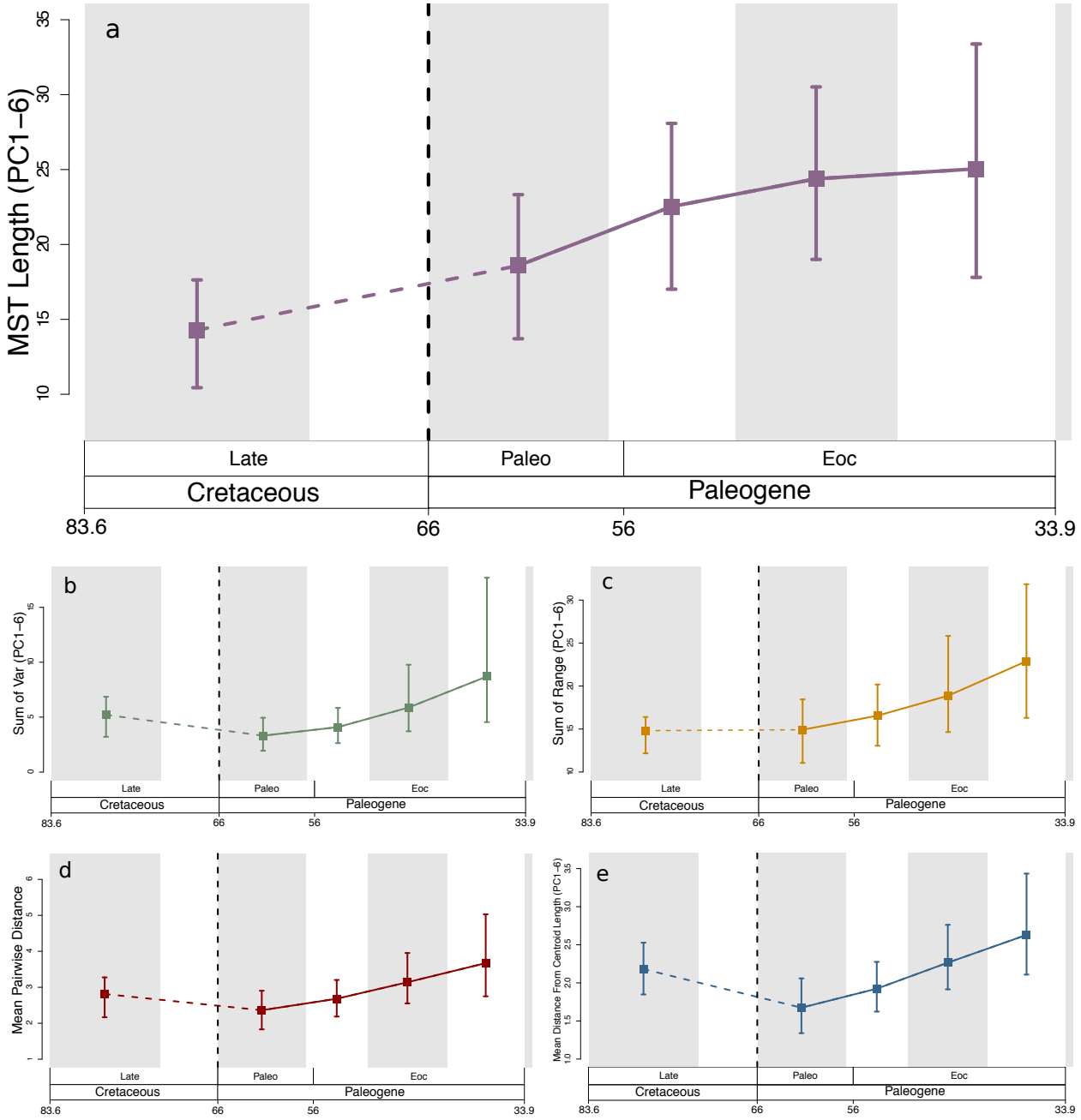


Figure S1.7. Jaw functional disparity among all mammals across the K/Pg boundary, calculated using five different methods. The five methods shown here are a) minimum spanning tree b) sum of variance, c) sum of ranges, d) mean pairwise distance, and e) mean distance from centroid. For all methods (a-e), the Campanian stage (Mesozoic) and NALMAs (Cenozoic) are used as time bins (see methods). For each disparity method, data is rarefied (n = 15) and sampled with replacement to enable fairer comparison between bins with differing sample sizes. The 95% confidence intervals represent uncertainty produced by sampling fifteen individuals at random with replacement across each time bin, for 5000 iterations. The points represent the mean values of these 5000 runs. A solid line indicates changes between consecutive time bins. Dashed lines indicate changes across two or more time bin boundaries.

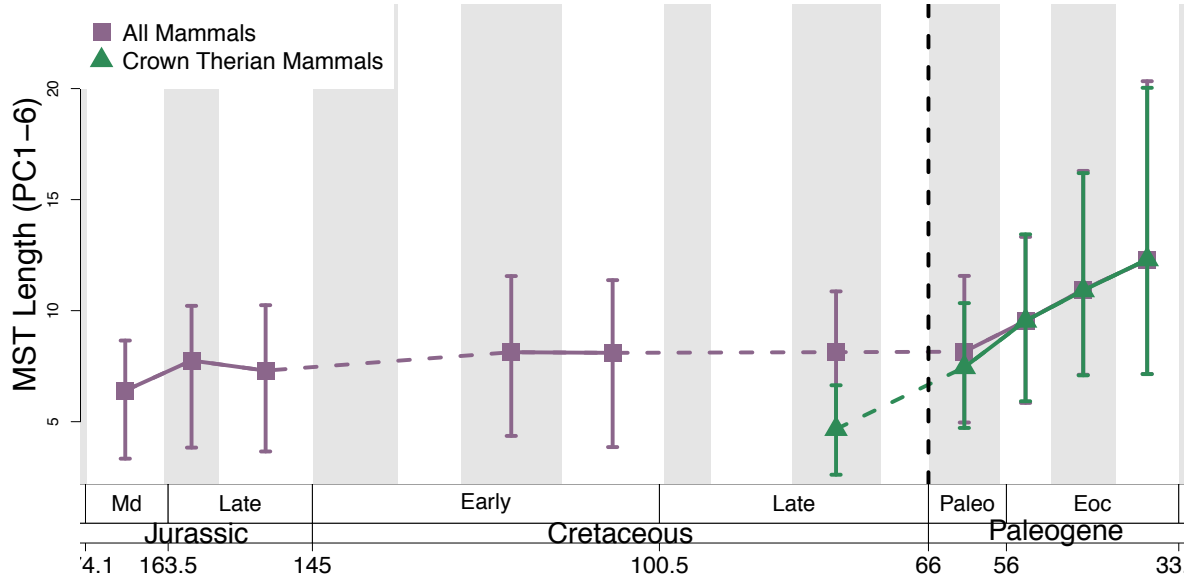


Figure S1.8. Jaw function minimum spanning tree length through time, calculated without the use of grid cells. The purple curve represents all mammals, and the green curve represents therian mammals only. Amalgamated stages (Mesozoic) and NALMAs (Cenozoic) with six or more individuals are used as time bins (see methods). Data is rarefied (n = 6) and sampled with replacement to enable fairer comparison between bins with differing sample sizes. The 95% confidence intervals represent uncertainty produced by sampling six individuals at random with replacement across each time bin, for 5000 iterations. The points represent the mean values of these 5000 runs. A solid line indicates changes between consecutive time bins. Dashed lines indicate changes across two or more time bin boundaries.

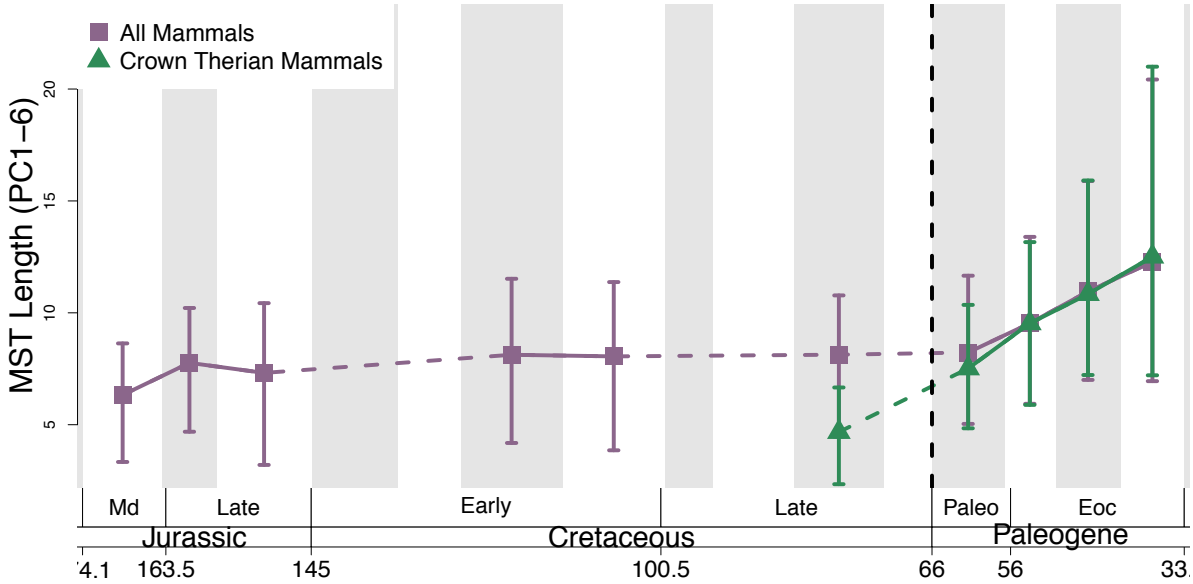


Figure S1.9. Jaw function minimum spanning tree length through time, calculated without the use of grid cells. The purple curve represents all mammals, and the green curve represents therian mammals only. Amalgamated stages (Mesozoic) and NALMAs (Cenozoic) with six or more individuals are used as time bins (see methods). Data is rarefied (n = 6) and sampled with replacement to enable fairer comparison between bins with differing sample sizes. The 95% confidence intervals represent uncertainty produced by sampling six individuals at random with replacement across each time bin, for 1000 iterations. The points represent the mean values of these 1000 runs. A solid line indicates changes between consecutive time bins. Dashed lines indicate changes across two or more time bin boundaries.

Supplementary Material S1.4

Supplementary methods for Chapter 1

Trait collection (extended)

The 10 measurements outlined in supplementary materials S1.1 were collected from fossils mammal mandibles from the Late Triassic-Eocene. These measurements were taken from mandible images in published literature, and first hand from museum and university collections. GLB visited the following 8 collections between May 2015 and April 2017 to collect mandible measurement data; OUMNH, Naturmuseum Senckenburg, Hessisches Landesmuseum Darmstadt, AMNH, Chicargo Field Museum, Carnegie Museum, Smithsonian Institution NMNH, and Johns Hopkins University (Collections curated and collected by Ken Rose).

Only terrestrial mammals were included in this study, and mammals were included at species level where possible. Where specimens identified to species level were not available, one example of the genus is included instead.

Measurements were taken from complete jaws and reasonable partial jaws. Where, for example, the anterior tip of the tooth row, or the tip of the coronoid process are missing, measurements are estimated by GLB based on knowledge of the anatomy of closely related species.

Taxonomic affiliations

Many of the older mammal clades included in this study have no living descendants or are basally branching members of living clades. Therefore phylogenetic placement and taxonomic affiliation can be challenging and sometimes multiple hypotheses for one clade or genus can exist in the literature. Where this is the case, the affiliation/placement preferred by the authors or the more commonly accepted affiliation/placement, and we outline these decisions below.

Of particular note is the placement of the clade Haramiyida. Two competing hypotheses exist. Haramiyids have been recovered as stem mammals (e.g Luo et al, 2015, Huttenlocker et al, 2018), and alternatively within Allotheria, as a sister clade to multituberculates (Kielan-Jaworowska et al, 2004) or as a paraphyletic group with the monophyletic multituberculates deriving from 'haramiyidans' (e.g. Butler, 2000, Hahn & Hahn, 2006, Averianov & Lopatin, 2011, Meng et al, 2018). For the purpose of this study, we follow the phylogenetic placement of Luo et al (2015) and assign haramiyids and euharamiyids to Stem Mammalia. We use this placement mainly because the research efforts of Luo et al (2015) were aimed primarily at addressing the descrepancies in haramiyid placement in the mammalian tree, and concluded that the clade fell within stem mammals based on detailed anatomical study. It should be noted however that truly conclusive evidence for the placement of this clade is lacking, and both hypotheses are likely to remain valid until more conclusive anatomical evidence can be found in the fossil record. Despite this, the assignment of haramiyids to stem mammals in this study does not affect our

overall conclusions regarding the timings and magnitude of the ecomorphological radiation of mammals.

A consensus on the placement of the species *Eomaia scansoria* and *Juramaia sinensis* is also lacking. Across published phylogenies, these two taxa jump between positions among the most basally branching eutherian mammals (e.g. Ji et al, 2002, Wible et al, 2009, Luo et al, 2011) and positions within Stem Theria (e.g. O'leary et al, 2013). Here, we follow a eutherian placement of these taxa (Ji et al, 2002, Wible et al, 2009, Luo et al, 2011). Including these contested species within Eutheria does not affect the disparity curves produced for therian mammals, as both *E. scansoria* and *J. sinensis* fall within time bins that pre-date bins that include sufficient numbers of therian mammals to allow for disparity to be calculated.

Finally, *Pseudotribos robustus* is here included as an Australosphenida, and is affiliated with the monotreme stem (e.g. Rauhut et al, 2002, Luo et al, 2007) (labelled Australosphenida-Prototheria-Monotremata in Figs. 1.1, S1.1-S1.5). This is in contrast to hypotheses placing either all members of Australosphenida, or a subset of species which have otherwise been affiliated with Australosphenida, closer to eutherians than to monotremes (Rich et al, 2002, Woodburne et al, 2003, Rich & Vickers-Rich, 2013). Once again, the placement of *Pseudotribos robustus* within Australosphenida does not affect our overall conclusions regarding mammal jaw disparity through time.

The choice of minimum spanning tree grid cells

The grid cells chosen in this study are 1x1 principle component unit in size. These grid cells were designed to split function space into discrete regions in order to down weigh the impact of instances where specific regions of space with atypically high numbers of taxa may dominate the disparity signal. Smaller grid cells were ruled out because the number of rarefied points. With a low rarefied sample size the use of smaller grid cells would ultimately deliver a result identical to the raw rarefied sample, because each grid cell would hold only one mammal species. The use of larger grid cells would amalgamate unnecessarily large areas of function space, merging taxa with highly distinct phenotypes. Therefore, in order to test whether the choice of grid cells used may have affected the patterns of disparity retrieved, MST length through time was also calculated without the use of grid cells. The disparity through time curves are near identical when calculating minimum spanning tree length with or without the use of grid cells. This suggests that the use of grid cells may be more important for analyses with larger sample sizes in each time bin, or where samples are not first rarefied.

Supplementary Material S2.1

Supplementary figures and tables for Chapter 2.

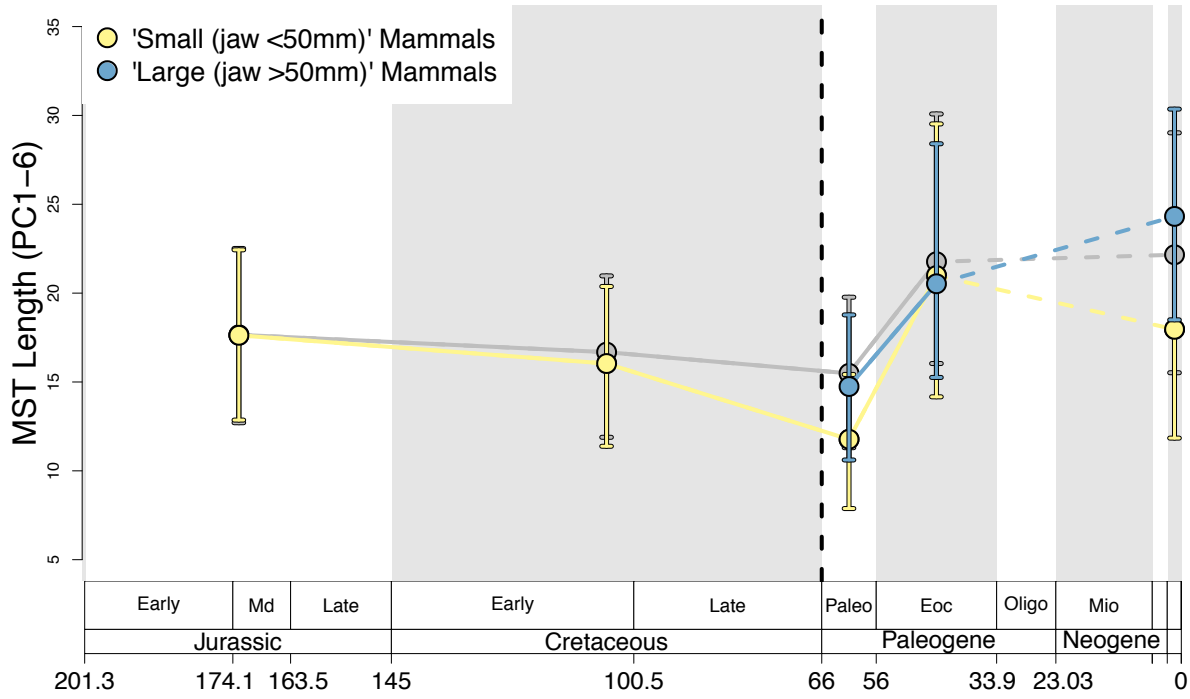


Figure S2.1. Jaw functional disparity through time, calculated as minimum spanning tree length across 5000 rarefied (n = 13) bootstrap replicates. The yellow curve depicts disparity levels through time among mammals within a small size class (defined here as any mammals that has a jaw length of 50mm or less). The blue curve shows disparity levels among mammals with a larger size class (with mammals exhibiting a jaw length of more than 50mm). The grey line depicts overall jaw functional disparity though time. A solid line connecting points indicates bin-to-bin disparity changes, while a dashed line indicates unsampled bins in between the disparity estimates.

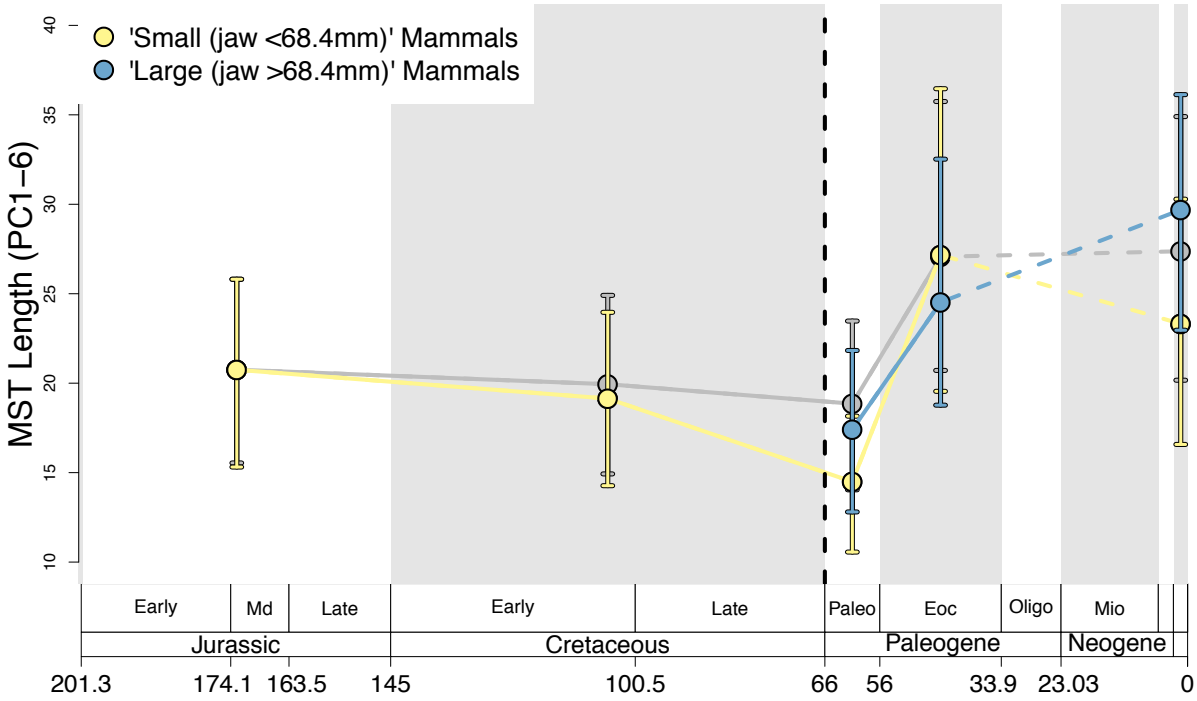


Figure S2.2. Jaw functional disparity through time, calculated as minimum spanning tree length across 5000 rarefied (n = 17) bootstrap replicates. The yellow curve depicts disparity levels through time among mammals within a small size class (defined here as any mammals that has a jaw length of 68.4mm or less). The blue curve shows disparity levels among mammals with a larger size class (with mammals exhibiting a jaw length of more than 68.4mm). The grey line depicts overall jaw functional disparity though time. A solid line connecting points indicates bin-to-bin disparity changes, while a dashed line indicates unsampled bins in between the disparity estimates.

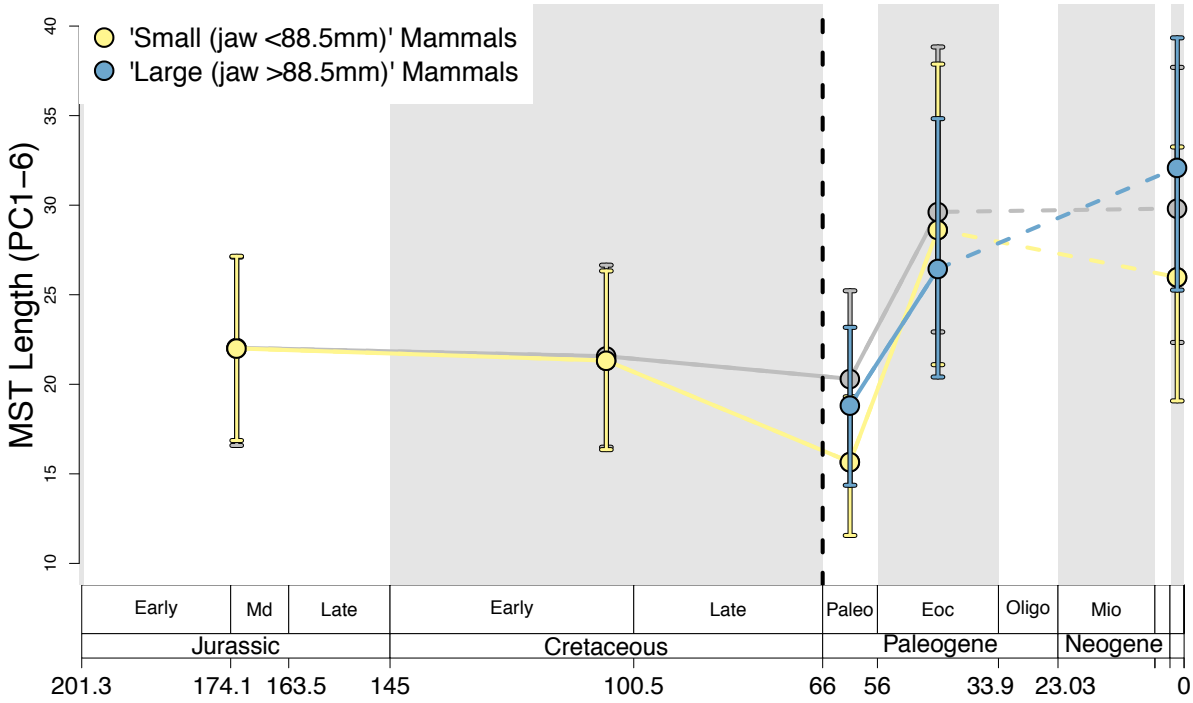


Figure S2.3. Jaw functional disparity through time, calculated as minimum spanning tree length across 5000 rarefied (n = 19) bootstrap replicates. The yellow curve depicts disparity levels through time among mammals within a small size class (defined here as any mammals that has a jaw length of 88.5mm or less). The blue curve shows disparity levels among mammals with a larger size class (with mammals exhibiting a jaw length of more than 88.5mm). The grey line depicts overall jaw functional disparity though time. A solid line connecting points indicates bin-to-bin disparity changes, while a dashed line indicates unsampled bins in between the disparity estimates.

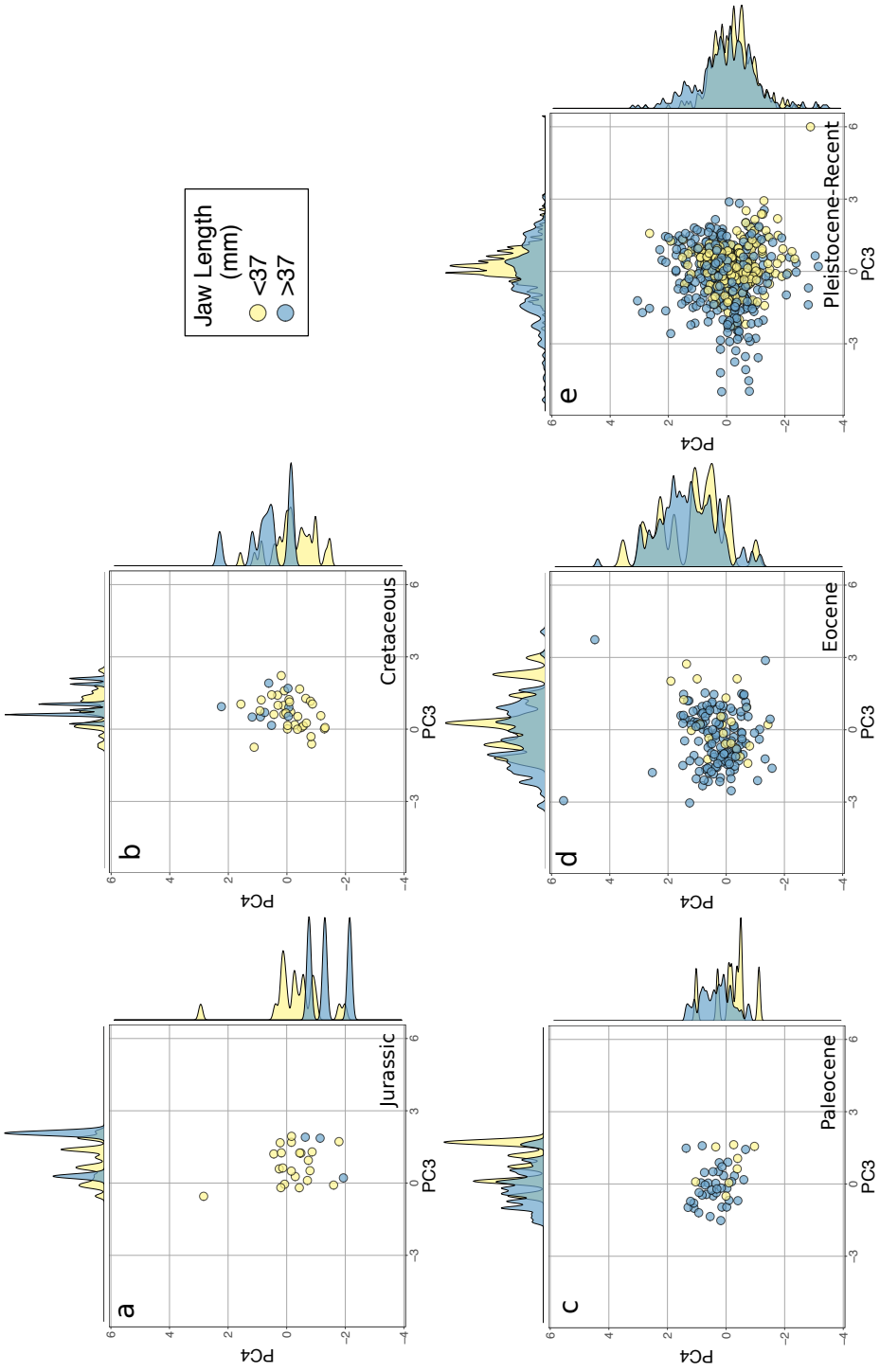


Figure S2.4. PC3-4 function space, split by Mesozoic periods, Cenozoic epoch, and the Recent, including Pleistocene megafauna. Points are coloured by size class (see legend). For this analysis, the size classes were based on mammals with jaw lengths of either below (small) or above (large) 37mm. On each function space plot, frequencies of points in each size class along PC3 (top) and PC4 (right) are shown.

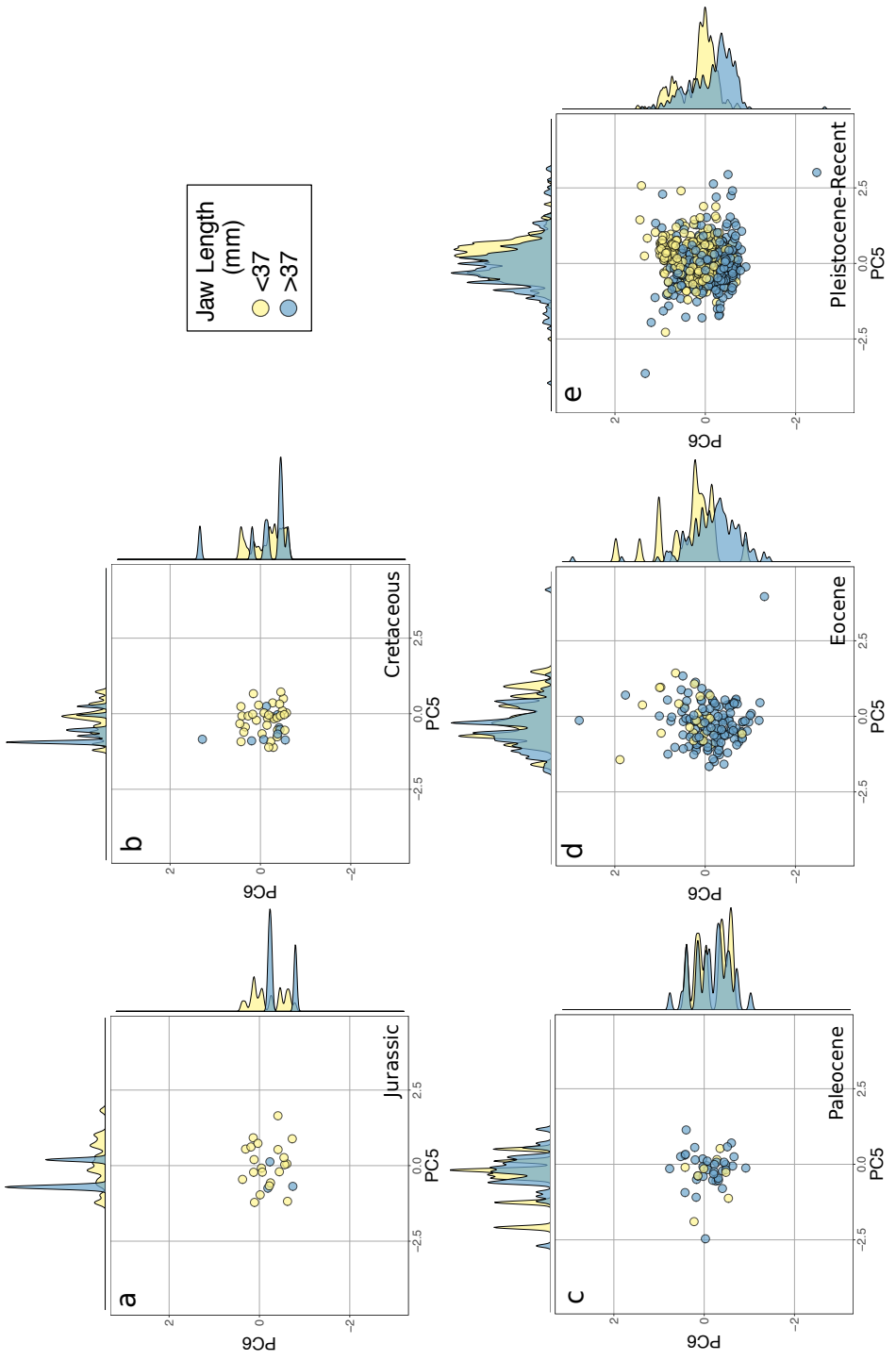


Figure S2.5. PC5-6 function space, split by Mesozoic periods, Cenozoic epoch, and the Recent, including Pleistocene megafauna. Points are coloured by size class (see legend). For this analysis, the size classes were based on mammals with jaw lengths of either below (small) or above (large) 37mm. On each function space plot, frequencies of points in each size class along PC5 (top) and PC6 (right) are shown.

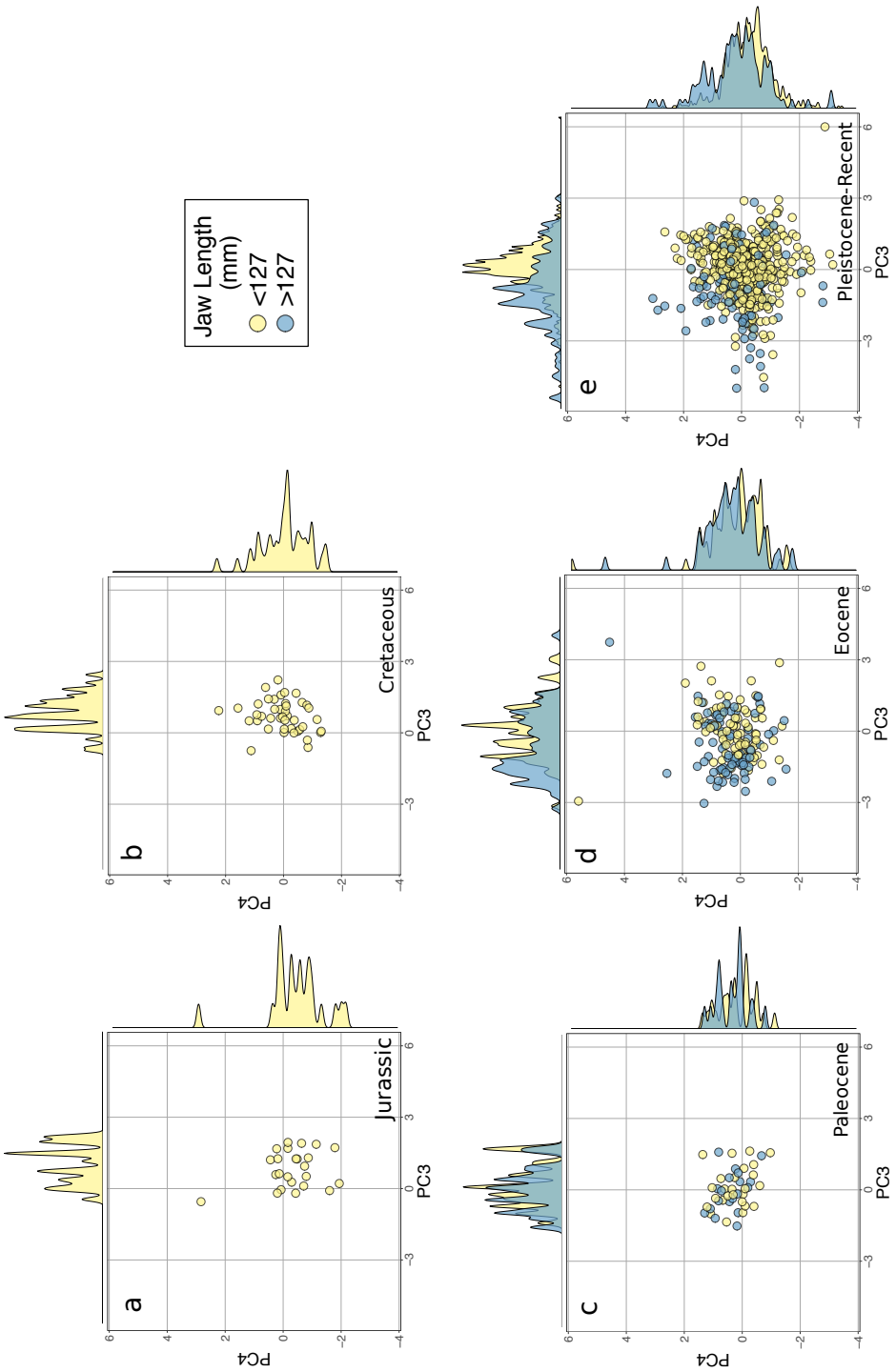


Figure S2.6. PC3-4 function space, split by Mesozoic periods, Cenozoic epoch, and the Recent, including Pleistocene megafauna. Points are coloured by size class (see legend). For this analysis, the size classes were based on mammals with jaw lengths of either below (small) or above (large) 127 mm. On each function space plot, frequencies of points in each size class along PC3 (top) and PC4 (right) are shown.

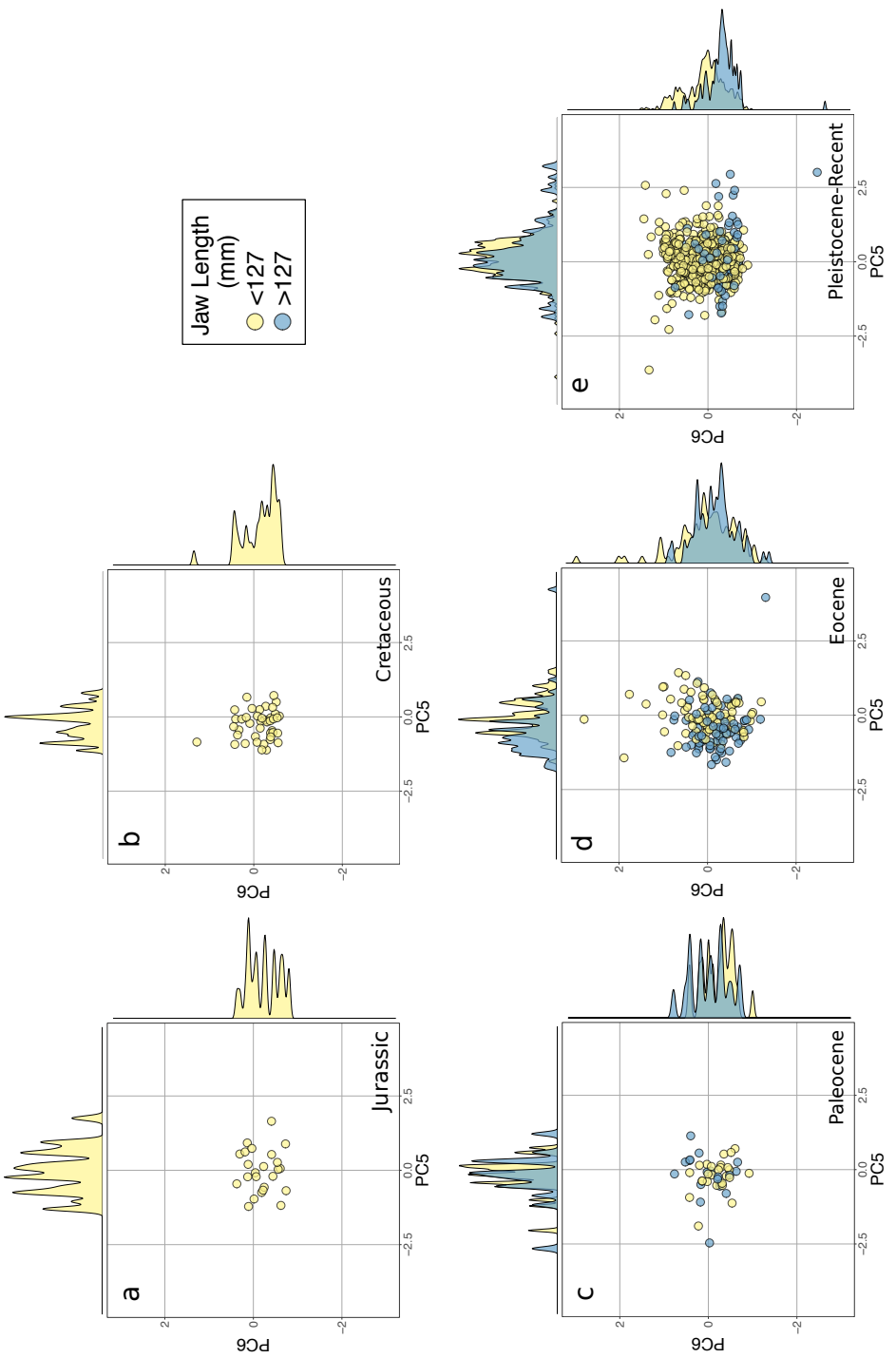


Figure S2.7. PC5-6 function space, split by Mesozoic periods, Cenozoic epoch, and the Recent, including Pleistocene megafauna. Points are coloured by size class (see legend). For this analysis, the size classes were based on mammals with jaw lengths of either below (small) or above (large) 127mm. On each function space plot, frequencies of points in each size class along PC5 (top) and PC6 (right) are shown.

Time bin (using 37mm)	PC axes	p-value	Adjusted p-value for multiple comparisons	t.test result	df	Lower 95% CI	Upper 95% CI	Mean of small mammals	Mean of large mammals
Cretaceous	PC1	0.43156072	1	0.8136	12.108	-0.6908	1.5155	0.2179	-0.1944
	PC2	**0.008317422**	0.1996181	-2.8086	32.793	-1.3355	-0.2133	-0.2795	0.4948
	PC3	0.384301549	1	-0.8967	14.716	-0.6872	0.2807	0.6677	0.8710
	PC4	**0.011496104**	0.2759065	-2.9801	11.985	-1.4100	-0.2189	-0.1390	0.6754
	PC5	**0.039573415**	0.949762	2.2613	14.511	0.0196	0.6982	-0.1866	-0.5455
	PC6	0.903958004	1	-0.1239	9.5352	-0.4681	0.4191	-0.1227	-0.0982
Paleocene	PC1	0.236421681	1	-1.2629	9.5979	-1.2181	0.3399	-0.3933	0.0457
	PC2	0.375816057	1	-0.9274	9.8633	-1.0005	0.4131	-0.0032	0.2903
	PC3	**0.020257786**	0.4861869	2.7578	9.9689	0.1670	1.5752	0.7560	-0.1150
	PC4	**0.056258002**	1	-2.1746	9.4567	-0.9996	0.0160	-0.0891	0.4026
	PC5	0.422798093	1	-0.8400	8.9316	-0.8933	0.4099	-0.4046	-0.1629
	PC6	0.976894556	1	0.0296	10.761	-0.3040	0.3123	-0.1072	-0.1113
Eocene	PC1	**0.021315504**	0.5115721	2.4267	30.641	0.1042	1.2061	0.2981	-0.3570
	PC2	0.541965767	1	-0.6151	39.753	-0.5252	0.2801	-0.0261	0.0964
	PC3	**0.020404527**	0.4897086	2.4349	33.353	0.0997	1.1106	0.2566	-0.3484
	PC4	0.450189508	1	-0.7635	35.375	-0.5070	0.2298	0.1875	0.3261
	PC5	0.140484731	1	1.5107	32.573	-0.0813	0.5497	-0.0289	-0.2631
	PC6	**0.000334132**	0.008019168	4.0119	32.329	0.2414	0.7390	0.3385	-0.1516
Pleistocene -Recent	PC1	**2.12316E-38**	5.10E-37	13.788	693.32	1.2037	1.6035	0.6742	-0.7294
	PC2	**0.009473606**	0.2273665	-2.6049	481.67	-0.4350	-0.0609	-0.1407	0.1072
	PC3	**6.65489E-09**	1.60E-07	5.8993	509.79	0.3225	0.6446	0.2064	-0.2771
	PC4	**0.000313462**	0.007523088	-3.6253	591.21	-0.3401	-0.1011	-0.1735	0.0470
	PC5	**1.02343E-05**	2.46E-04	4.4490	616.65	0.1223	0.3158	0.1797	-0.0393
	PC6	**1.83043E-20**	4.39E-19	9.5886	654.40	0.2373	0.3596	0.1759	-0.1225

Table S2.1. Results from t.tests testing for significance between small PC1-PC6 distributions and large PC1-PC6 distributions using size class division 1 (37mm). Red bold p-value scores indicate a significant difference. Black bold indicates a score very close to 0.05.

Time bin (using 50mm)	PC axes	p-value	Adjusted p-value for multiple comparisons	t.test result	df	Lower 95% CI	Upper 95% CI	Mean of small mammals	Mean of large mammals
Cretaceous	PC1	0.794435539	1	0.2731	5.6709	-1.1979	1.4941	0.1472	-0.0008
	PC2	**0.057135396**	1	-2.1821	8.9501	-1.4988	0.0276	-0.2011	0.5344
	PC3	0.99925616	1	-0.0009	5.5837	-0.7059	0.7053	0.7112	0.7115
	PC4	**0.019551897**	0.4692455	-2.9728	7.3619	-1.2820	-0.1523	-0.0498	0.6673
	PC5	0.456565374	1	0.8065	4.9997	-0.4249	0.8135	-0.2404	-0.4347
	PC6	0.789011604	1	-0.2851	4.2041	-1.0237	0.8296	-0.1290	-0.0320
Paleocene	PC1	0.84173451	1	-0.2021	21.065	-0.6540	0.5381	-0.0735	-0.0155
	PC2	0.594161803	1	-0.5396	25.406	-0.6334	0.3702	0.1446	0.2761
	PC3	0.061854354	1	1.9652	22.486	-0.0285	1.0866	0.4160	-0.1129
	PC4	0.199698361	1	-1.3321	17.712	-0.7035	0.1579	0.1212	0.3940
	PC5	0.990856924	1	-0.0115	21.195	-0.4468	0.4418	-0.2076	-0.2052
	PC6	0.625757432	1	-0.4933	26.760	-0.2886	0.1767	-0.1504	-0.0944
Eocene	PC1	0.192541655	1	1.3221	46.871	-0.1802	0.8711	0.0081	-0.3373
	PC2	**0.045648578**	1	-2.0440	56.110	-0.8555	-0.0086	-0.2547	0.1773
	PC3	**0.044865083**	1	2.0479	61.161	0.0103	0.8642	0.0798	-0.3574
	PC4	0.859707875	1	-0.1776	48.374	-0.4388	0.3675	0.2777	0.3133
	PC5	**0.000881938**	0.002116651	3.4980	60.879	0.1880	0.6898	0.1101	-0.3287
	PC6	**5.47595E-06**	0.000131423	4.9689	62.812	0.2883	0.6762	0.2938	-0.1884
Pleistocene -Recent	PC1	**2.82237E-33**	6.77E-32	12.830	569.00	1.1543	1.5716	0.5453	-0.8176
	PC2	0.441551834	1	-0.7703	379.69	-0.2920	0.1276	-0.0580	0.0241
	PC3	**1.71242E-09**	4.11E-08	6.1673	396.69	0.3784	0.7326	0.1945	-0.3609
	PC4	**0.018844386**	0.4522653	-2.3563	492.67	-0.2779	-0.0251	-0.1296	0.0219
	PC5	**0.000564218**	1.35E-02	3.4696	521.48	0.0774	0.2794	0.1466	-0.0317
	PC6	**1.58494E-25**	3.80E-24	10.977	559.80	0.2826	0.4058	0.1691	-0.1751

Table S2.2. Results from t.tests testing for significance between small PC1-PC6 distributions and large PC1-PC6 distributions using size class division 2 (50mm). Red bold p-value scores indicate a significant difference. Black bold indicates a score very close to 0.05.

Time bin (using 68.4mm)	PC axes	p-value	Adjusted p-value for multiple comparisons	t.test result	df	Lower 95% CI	Upper 95% CI	Mean of small mammals	Mean of large mammals
Cretaceous	PC1	0.642273628	1	-0.4970	4.5368	-1.5686	1.0733	0.1060	0.3536
	PC2	0.122764818	1	-1.8530	5.0260	-1.7723	0.2861	-0.1843	0.5586
	PC3	0.113929407	1	1.7161	11.079	-0.0762	0.6183	0.7371	0.4660
	PC4	**0.000930036**	0.02232086	-4.8415	8.9624	-1.3106	-0.4755	-0.0495	0.8435
	PC5	0.699477618	1	0.4196	3.4597	-0.7460	0.9928	-0.2518	-0.3752
	PC6	0.680752238	1	-0.4525	3.0945	-1.5113	1.1293	-0.1356	0.0552
Paleocene	PC1	0.758367105	1	-0.3102	31.700	-0.6246	0.4595	-0.0836	-0.0011
	PC2	0.953355158	1	0.0588	39.770	-0.4495	0.4765	0.2465	0.2330
	PC3	0.336885346	1	0.9747	32.479	-0.2803	0.7954	0.2000	-0.0574
	PC4	0.251098357	1	-1.1717	28.204	-0.5811	0.1581	0.1835	0.3951
	PC5	0.830684242	1	0.2153	37.154	-0.3424	0.4238	-0.1805	-0.2213
	PC6	0.445996145	1	-0.7695	41.068	-0.2969	0.1331	-0.1616	-0.0796
Eocene	PC1	0.444590423	1	0.7684	76.969	-0.2654	0.5990	-0.1475	-0.3143
	PC2	**0.033786422**	0.8108741	-2.1530	97.293	-0.7706	-0.0313	-0.1870	0.2139
	PC3	**0.003682209**	0.08837302	2.9639	116.75	0.1816	0.9132	0.1048	-0.4425
	PC4	0.550379149	1	-0.5994	91.233	-0.4115	0.2207	0.2421	0.3375
	PC5	**6.88441E-05**	0.001652258	4.1178	125.53	0.2261	0.6446	0.0599	-0.3754
	PC6	**0.000597247**	0.01433393	3.5712	82.128	0.1601	0.5627	0.1613	-0.2000
Pleistocene -Recent	PC1	**1.60631E-30**	3.86E-29	12.655	352.59	1.2436	1.7013	0.4375	-1.0350
	PC2	0.907356735	1	0.1164	245.13	-0.2437	0.2743	-0.0227	-0.0380
	PC3	**8.15358E-09**	1.96E-07	5.9598	260.92	0.4247	0.8440	0.1600	-0.4743
	PC4	**0.000191718**	0.004601232	-3.7743	314.51	-0.4093	-0.1288	-0.1467	0.1223
	PC5	**0.05875056**	1	1.8969	312.95	-0.0041	0.2276	0.1101	-0.0016
	PC6	**3.61766E-21**	8.68E-20	10.051	368.55	0.2738	0.4070	0.1331	-0.2072

Table S2.3. Results from t.tests testing for significance between small PC1-PC6 distributions and large PC1-PC6 distributions using size class division 3 (68.4mm). Red bold p-value scores indicate a significant difference.

Time bin (using 88.5mm)	PC axes	p-value	Adjusted p-value for multiple comparisons	t.test result	df	Lower 95% CI	Upper 95% CI	Mean of small mammals	Mean of large mammals
Paleocene	PC1	0.983191506	1	-0.0212	37.788	-0.5279	0.5170	-0.0354	-0.0299
	PC2	0.83372121	1	-0.2112	42.976	-0.5060	0.4100	0.2104	0.2584
	PC3	0.606114234	1	0.5199	38.170	-0.3901	0.6597	0.1177	-0.0170
	PC4	0.177247709	1	-1.3767	35.324	-0.5812	0.1113	0.1794	0.4144
	PC5	0.686416725	1	0.4065	42.437	-0.2980	0.4484	-0.1624	-0.2376
	PC6	0.176065124	1	-1.3763	41.650	-0.3674	0.0695	-0.1967	-0.0477
Eocene	PC1	0.949469023	1	0.0635	100.08	-0.3762	0.4011	-0.2505	-0.2629
	PC2	**0.039094732**	0.7037052	-2.0820	145.20	-0.6939	-0.0180	-0.1292	0.2267
	PC3	**0.005063535**	0.09114363	2.8433	155.69	0.1540	0.8552	0.0368	-0.4678
	PC4	0.396593368	1	-0.8504	134.17	-0.4095	0.1632	0.2335	0.3566
	PC5	**5.03338E-05**	0.000906008	4.1669	160.40	0.2245	0.6292	0.0206	-0.4062
	PC6	**0.000188925**	0.00340065	3.8656	108.69	0.1733	0.5380	0.1295	-0.2261
Pleistocene-Recent	PC1	**1.84709E-27**	3.32E-26	12.463	225.08	1.3808	1.8995	0.3738	-1.2663
	PC2	0.217730699	1	1.2370	175.16	-0.1153	0.5027	0.0136	-0.1800
	PC3	**1.03545E-07**	1.86E-06	5.5389	184.59	0.4413	0.9297	0.1281	-0.5573
	PC4	**0.000194142**	0.003493556	-3.7947	206.72	-0.4733	-0.1496	-0.1376	0.1739
	PC5	0.576859449	1	0.5588	200.00	-0.0993	0.1779	0.0874	0.0481
	PC6	**7.88399E-20**	1.42E-18	9.9087	258.71	0.2830	0.4235	0.1130	-0.2402

Table S2.4. Results from t.tests testing for significance between small PC1-PC6 distributions and large PC1-PC6 distributions using size class division 4 (88.5mm). Red bold p-value scores indicate a significant difference.

Time bin (using 127mm)	PC axes	p-value	Adjusted p-value for multiple comparisons	t.test result	df	Lower 95% CI	Upper 95% CI	Mean of small mammals	Mean of large mammals
Paleocene	PC1	0.368829719	1	-0.9082	42.858	-0.7125	0.2700	-0.1257	0.0955
	PC2	0.772982133	1	0.2909	31.137	-0.4367	0.5820	0.2688	0.1961
	PC3	0.531475111	1	0.6314	38.865	-0.3586	0.6841	0.1085	-0.0541
	PC4	0.39273473	1	-0.8635	42.059	-0.4742	0.1899	0.2552	0.3973
	PC5	0.92692393	1	0.0924	31.293	-0.3911	0.4283	-0.1980	-0.2166
	PC6	0.117497732	1	-1.6060	34.049	-0.4113	0.0481	-0.1873	-0.0057
Eocene	PC1	0.315255712	1	1.0076	147.20	-0.1649	0.5081	-0.1797	-0.3513
	PC2	**0.005898979**	0.1061816	-2.7928	151.34	-0.8040	-0.1377	-0.1362	0.3347
	PC3	**0.00094756**	0.01705608	3.3754	143.93	0.2520	0.9642	0.0196	-0.5884
	PC4	0.272041154	1	-1.1022	158.67	-0.4304	0.1220	0.2350	0.3892
	PC5	**0.000155481**	0.002798658	3.8964	129.94	0.2075	0.6356	-0.0360	-0.4576
	PC6	**0.045797806**	0.8243605	2.0135	154.06	0.0032	0.3405	0.0007	-0.1711
Pleistocene-Recent	PC1	**6.45254E-24**	1.16E-22	12.284	138.37	1.5820	2.1890	0.3064	-1.5791
	PC2	**0.016461406**	0.2963053	2.4342	115.07	0.0913	0.8894	0.0449	-0.4454
	PC3	**8.32164E-09**	1.50E-07	6.1937	121.28	0.6209	1.2042	0.1182	-0.7943
	PC4	**0.000483445**	0.00870201	-3.5818	127.80	-0.5610	-0.1617	-0.1252	0.2360
	PC5	0.505552131	1	-0.6677	123.49	-0.2371	0.1175	0.0704	0.1302
	PC6	**2.87953E-16**	5.18E-15	9.1084	163.25	0.2764	0.4294	0.0907	-0.2622

Table S2.5. Results from t.tests testing for significance between small PC1-PC6 distributions and large PC1-PC6 distributions using size class division 5 (127mm). Red bold p-value scores indicate a significant difference.

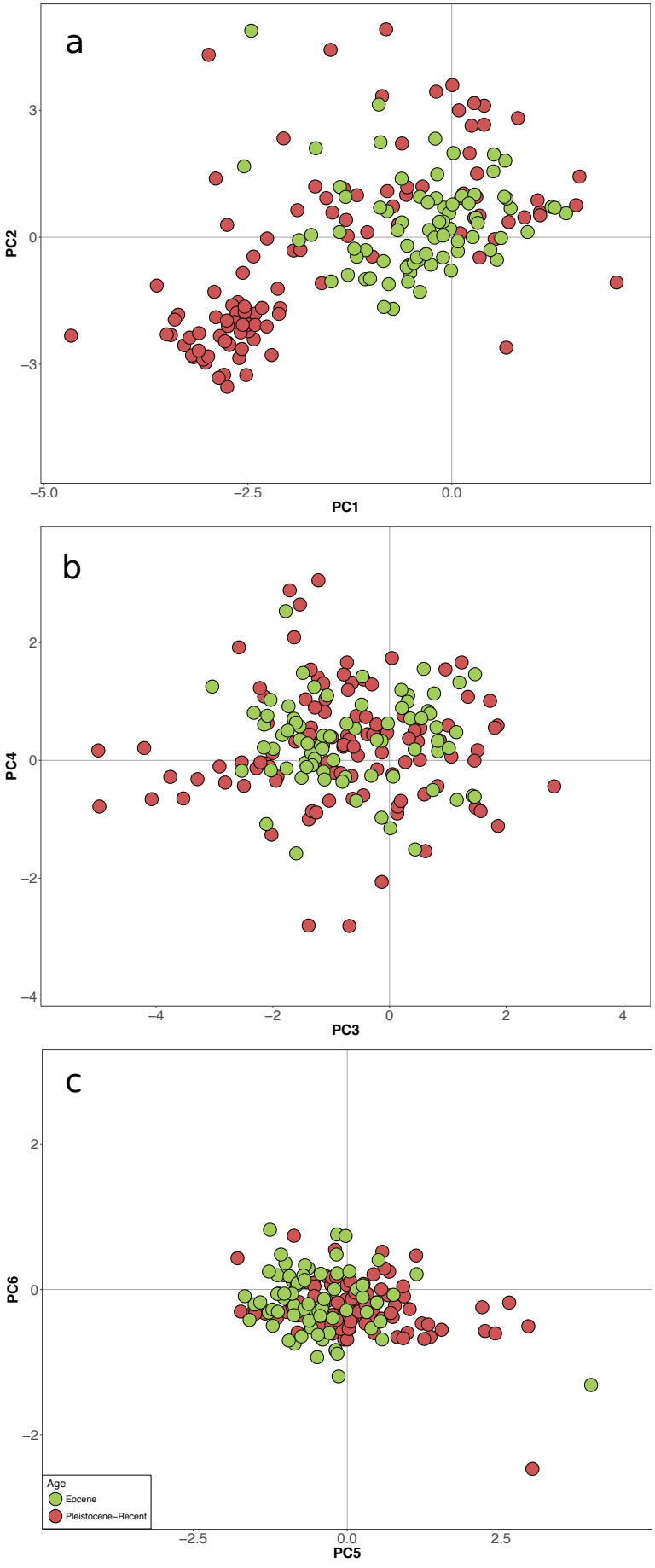


Figure S2.8. The overlap between species of Eocene (green points) and Pleistocene-Recent (red points) mammals in the large size class in (a) PC1-PC2 (b) PC3-PC4 and (c) PC5-PC6 function space. Size class division 5 was used (127mm).

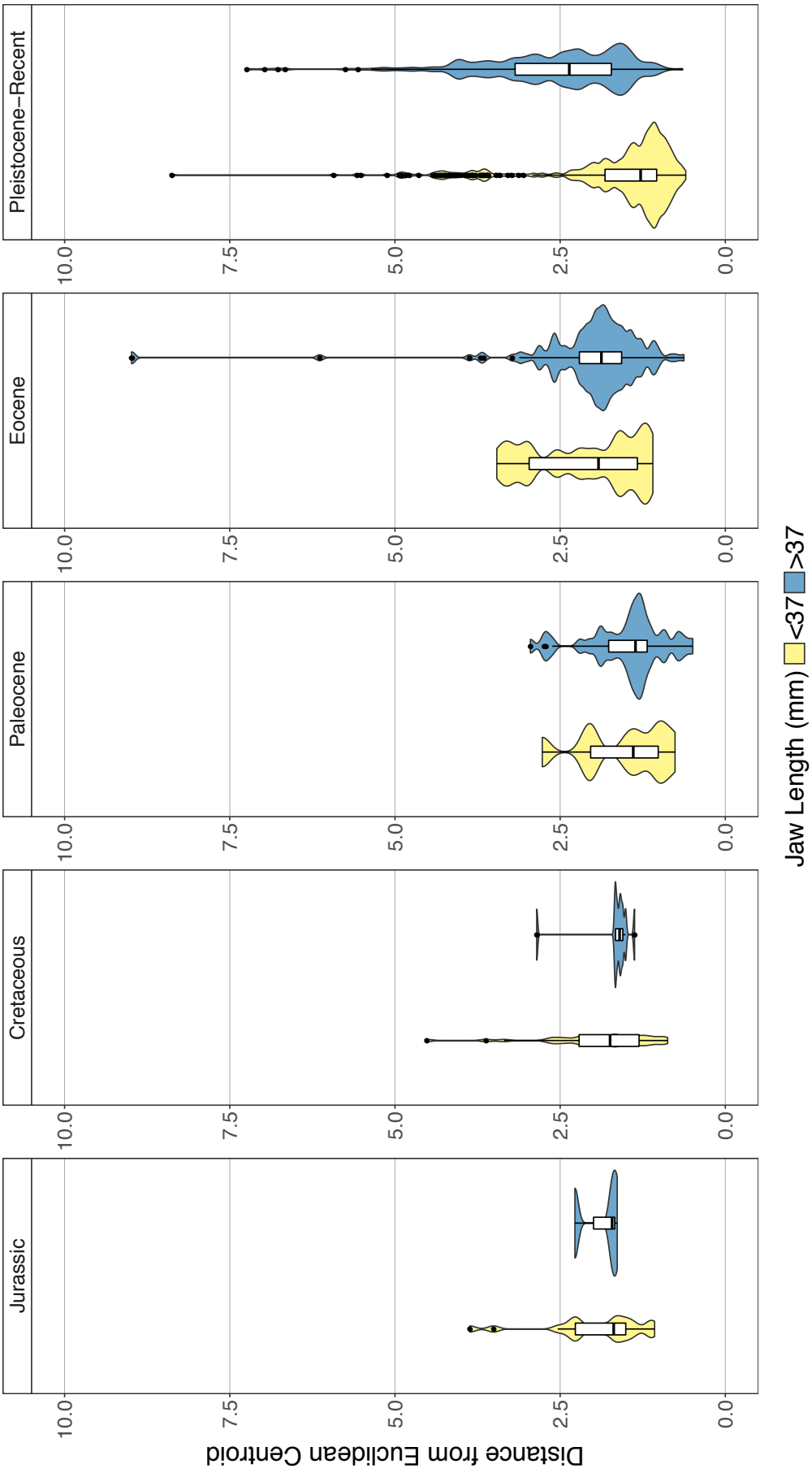


Figure S2.9. Mean distance from each size bins size class centroid through time plotted as violin plots. Small mammals (yellow) and large mammals (blue) are categorised using size class division 1 (37mm).

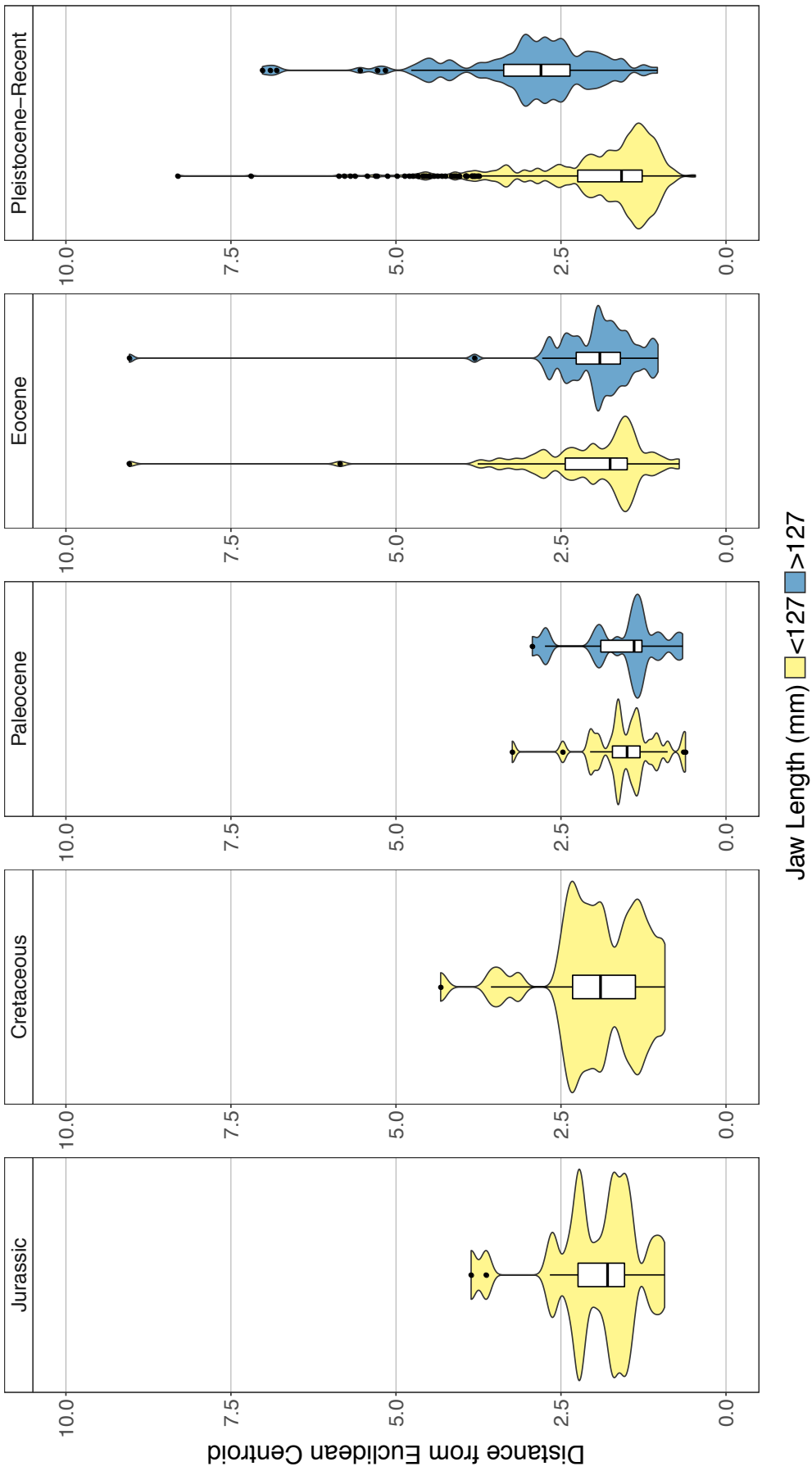


Figure S2.10. Mean distance from each size bins size class centroid through time plotted as violin plots. Small mammals (yellow) and large mammals (blue) are categorised using size class division 1 (127mm).

Size bin division	Time bin	p-value	Adjusted p-value for multiple comparisons	t.test result	df	Lower 95% CI	Upper 95% CI	Mean of small mammals	Mean of large mammals
Division 1 (37mm)	Cretaceous	0.339091057	1	0.9747	24.796	-0.2207	0.6170	1.9130	1.7148
	Paleocene	0.824617272	1	0.2279	9.3639	-0.5281	0.6472	1.5521	1.4926
	Eocene	0.867401741	1	0.1680	40.500	-0.3444	0.4069	2.0861	2.0548
	Pleistocene -Recent	**4.18559E-28**	7.53E-27	-11.485	703.93	-1.0739	-0.7603	1.6595	2.5767
Division 2 (50mm)	Cretaceous	**0.030256021**	0.5446084	2.3829	15.616	0.0468	0.8161	1.9558	1.5243
	Paleocene	0.888812062	1	-0.1416	19.951	-0.4549	0.3970	1.5285	1.5574
	Eocene	0.307908404	1	1.0307	47.028	-0.2331	0.7231	2.2418	1.9968
	Pleistocene -Recent	**3.10479E-21**	5.59E-20	-9.8330	591.14	-0.9675	-0.6453	1.7988	2.6053
Division 3 (68.4mm)	Cretaceous	**0.022369767**	0.4026558	2.9713	6.5688	0.1245	1.1625	1.9643	1.3207
	Paleocene	0.815415216	1	-0.2352	34.140	-0.4183	0.3314	1.5322	1.5756
	Eocene	0.126824094	1	1.5423	82.294	-0.0843	0.6668	2.2452	1.9539
	Pleistocene -Recent	**2.99684E-21**	5.39E-20	-10.080	365.40	-1.0471	-0.7053	1.8743	2.7506
Division 4 (88.5mm)	Paleocene	0.560726806	1	-0.5867	39.394	-0.4736	0.2605	1.4976	1.6041
	Eocene	0.225854372	1	1.2173	120.26	-0.1276	0.5350	2.1805	1.9767
	Pleistocene -Recent	**1.96177E-20**	3.53E-19	-10.179	237.82	-1.1538	-0.7796	1.9169	2.8837
Division 5 (127mm)	Paleocene	0.836778668	1	-0.2075	35.210	-0.4098	0.3337	1.5455	1.5835
	Eocene	0.711965495	1	0.3698	162.41	-0.2563	0.3745	2.0714	2.0123
	Pleistocene -Recent	**7.3135E-16**	1.32E-14	-9.1320	138.43	-1.2947	-0.8338	1.9523	3.0166

Table S2.6. Results from t.tests testing for significance between small and large mammal distance from centroid distribution for each time bin using size class divisions 1-5.

Time bin	Size bin division	p-value	Adjusted p-value for multiple comparisons	t.test result	df	Lower 95% CI	Upper 95% CI	Mean of small mammals	Mean of large mammals
Recent (with Pleistocene Removed)	Division 1 (37mm)	**6.61044E-24**	3.31E-23	-10.475	679.47	-0.9786	-0.6697	1.6595	2.4837
	Division 2 (50mm)	**5.35582E-17**	2.68E-16	-8.6480	568.49	-0.8501	-0.5354	1.7988	2.4916
	Division 3 (68.4mm)	**2.00349E-16**	1.00E-15	-8.6554	339.61	-0.8943	-0.5631	1.8743	2.6031
	Division 4 (88.5mm)	**1.40E-14**	7.00E-14	-8.2841	209.66	-0.9405	-0.5789	1.9169	2.6767
	Division 5 (127mm)	**2.64E-06**	1.32E-05	-4.9729	103.06	-0.8967	-0.3854	1.9523	2.5934

Table S2.7. Results from t.tests testing for significance between small and large mammal distance from centroid distribution for Recent mammals with the Pleistocene megafauna removed using size class divisions 1-5.

Supplementary Material S3.1

Backbone tree

Figures S3.1 is the backbone (constraint tree) used to constrain certain relationships among mammals included in the two source trees used.

Rate through time tree figures

Figures S3.2:S3.20 depict rate (shown as a colour spectrum from blue (relatively slower rates) to red (relatively faster rates)) on branches on a tree.

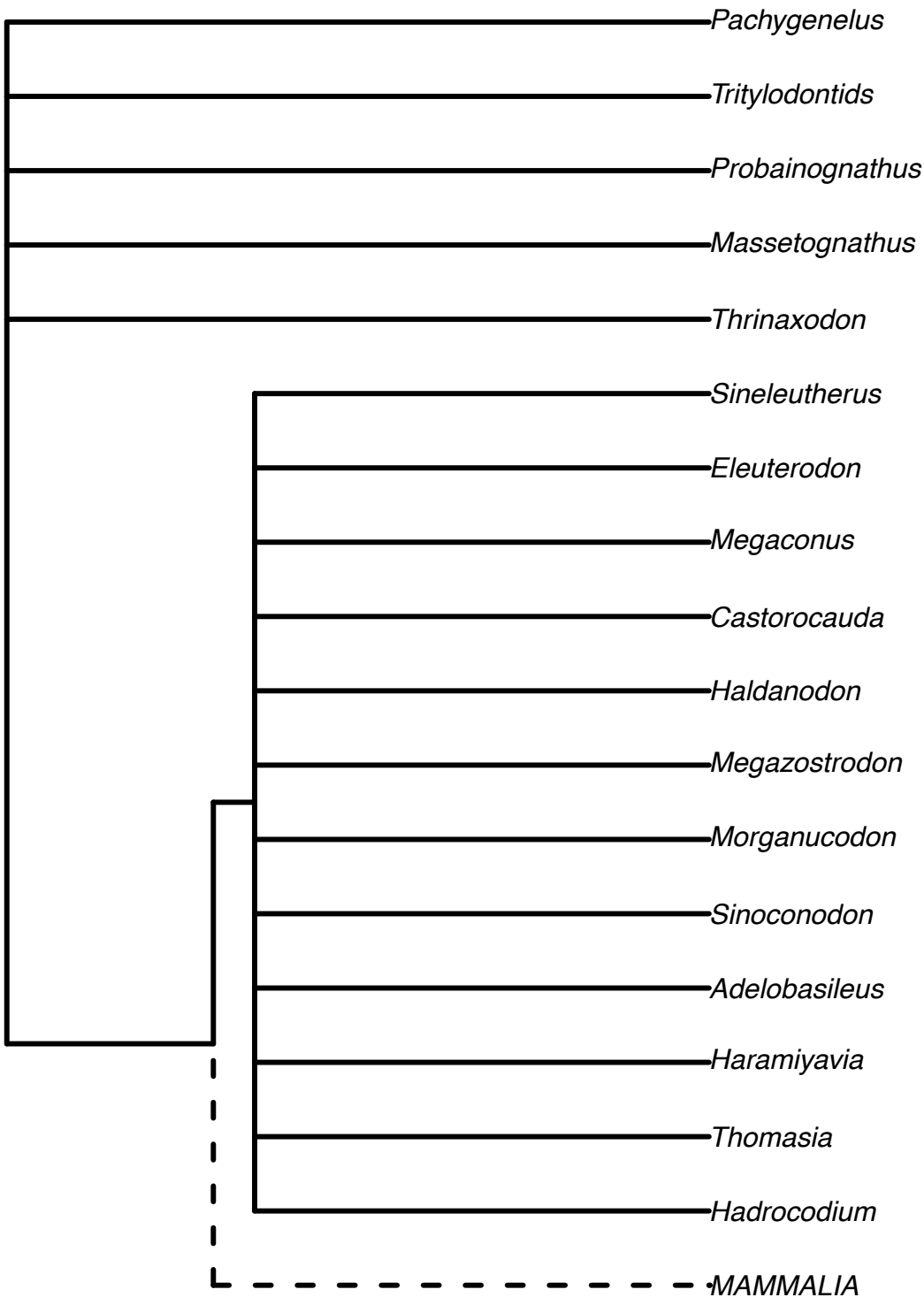


Figure S3.1a. Backbone tree part (a), consisting of mammaliaform outgroups (*Massetognathus, Thrinaxodon, Probainognathus, Tritylodontids,* and *Pachygenelus*), mammaliaformes, and their relationship to crown Mammalia.

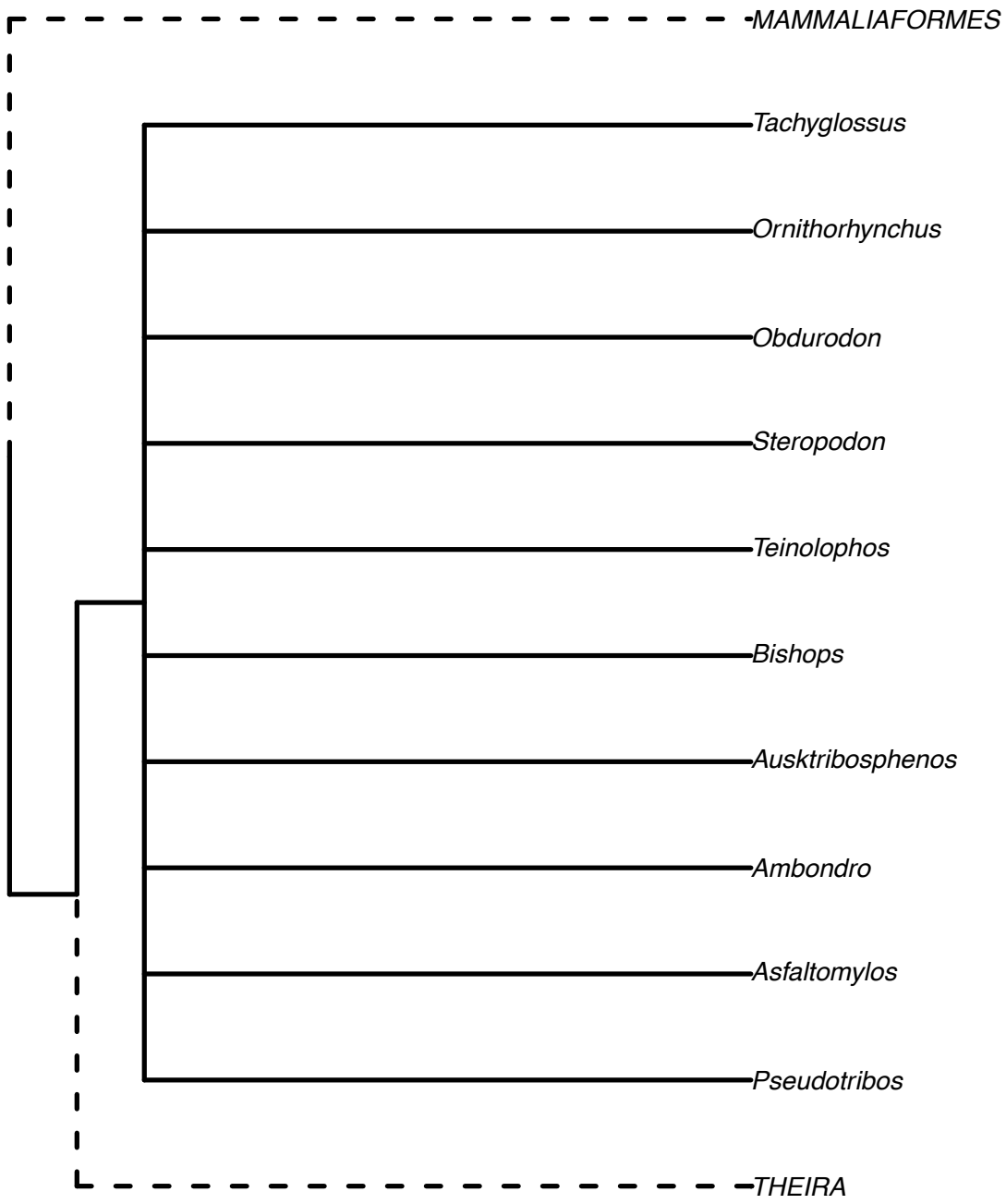


Figure S3.1b. Backbone tree continued, part (b), consisting of Ausktribosphenida-Marsupalia and their branching relationship to mammaliaformes and total-group Theria.

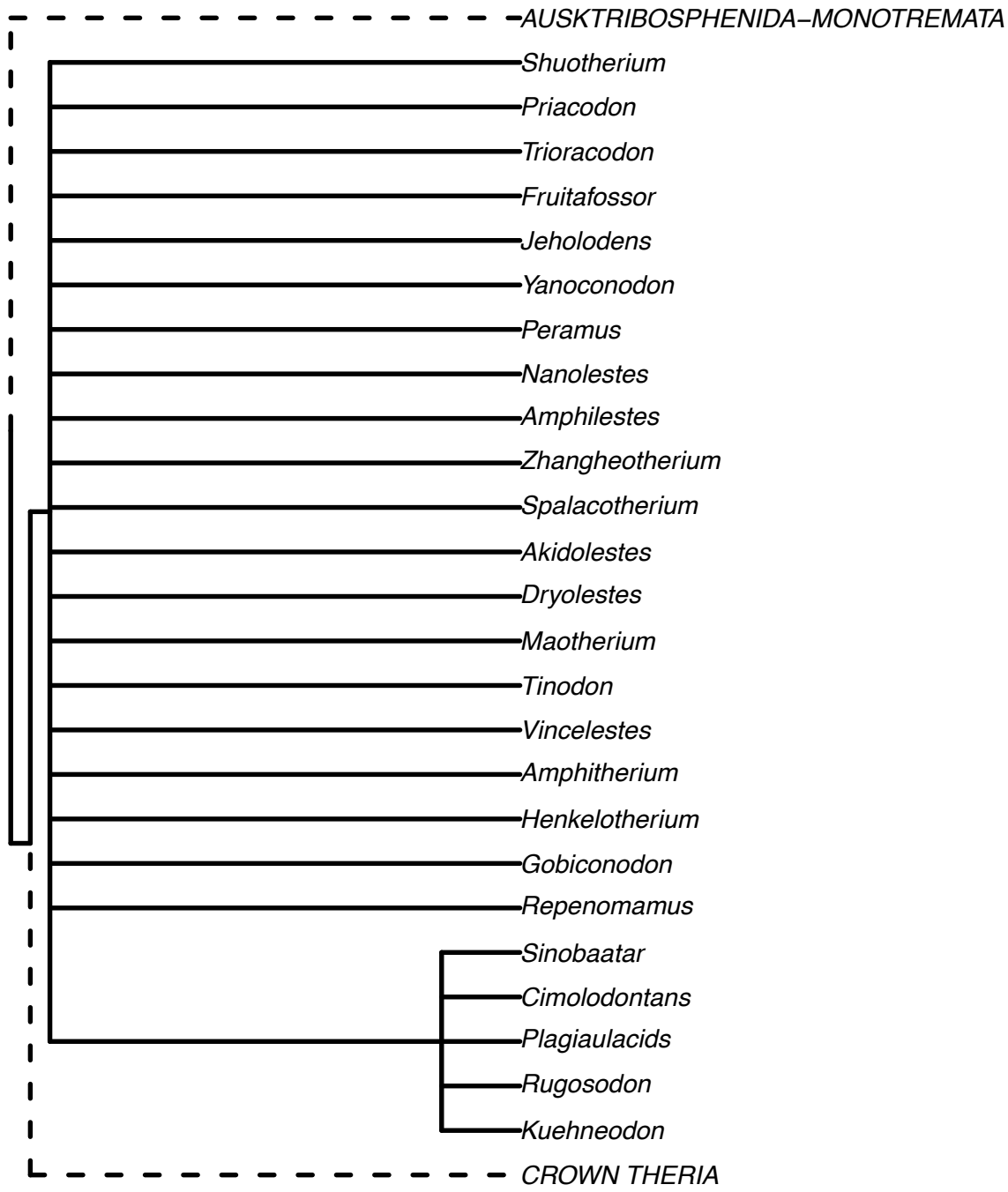


Figure S3.1c. Backbone tree part (c), showing stem Theria, and their relationship to the monoremes and to crown Theria

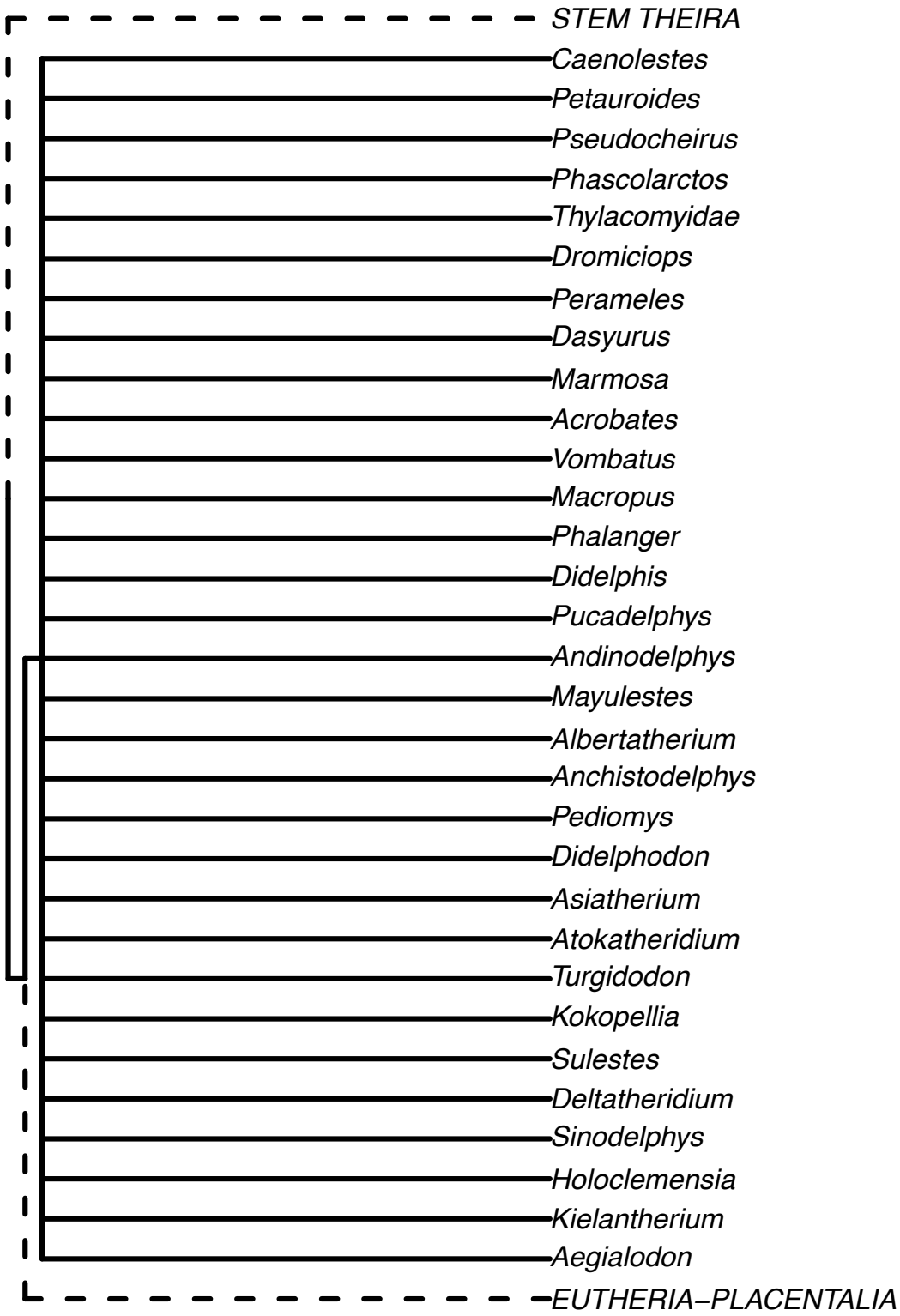


Figure S3.1d. Backbone tree, part (d), showing Metatheria-Marsupalia and their relationship to stem theria and to eutherian-placentals.

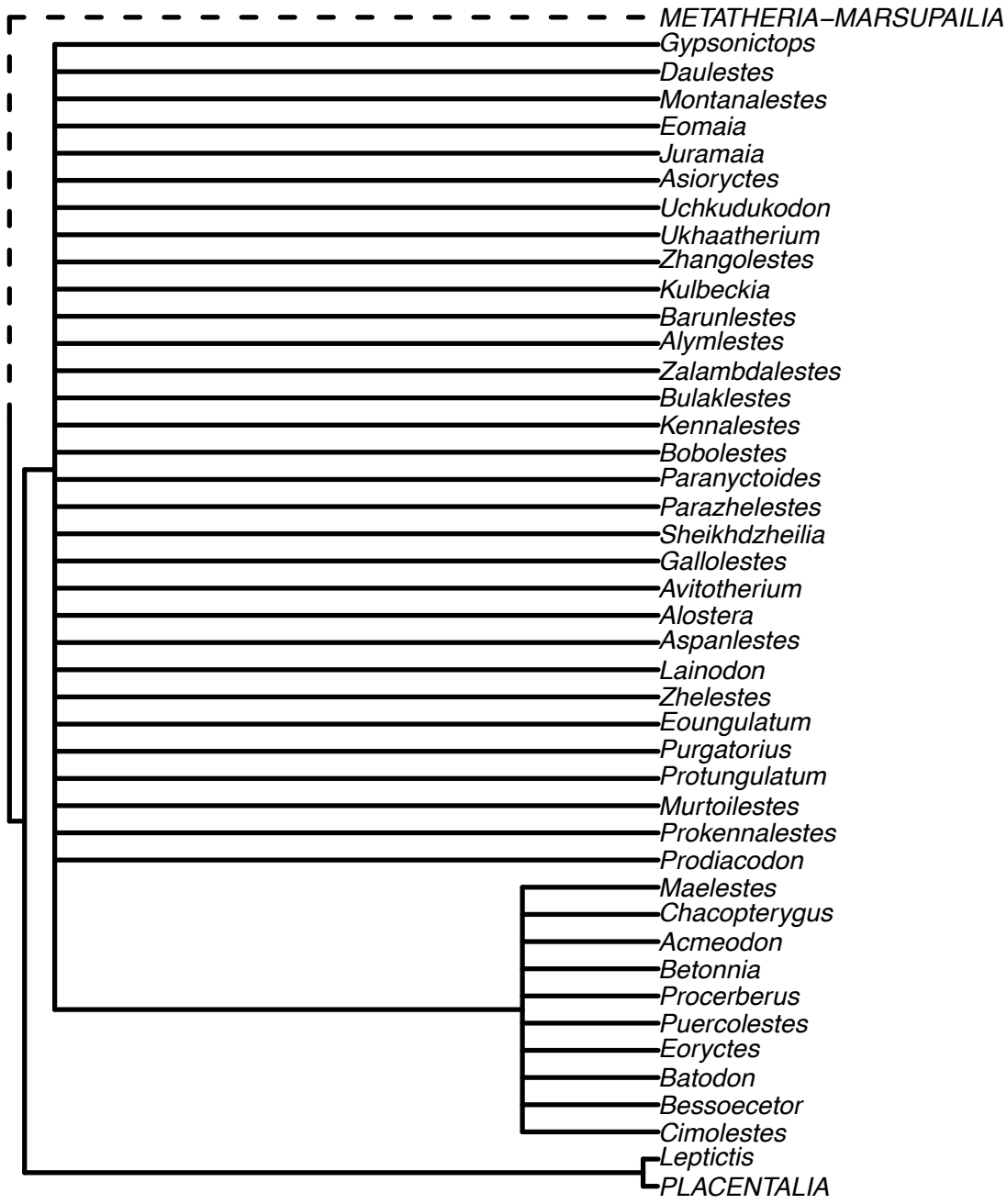


Figure S3.1e. Backbone tree, part (e), showing stem placental mammals, and their relationship to Metatheria-Marsupalia and to crown placentals.

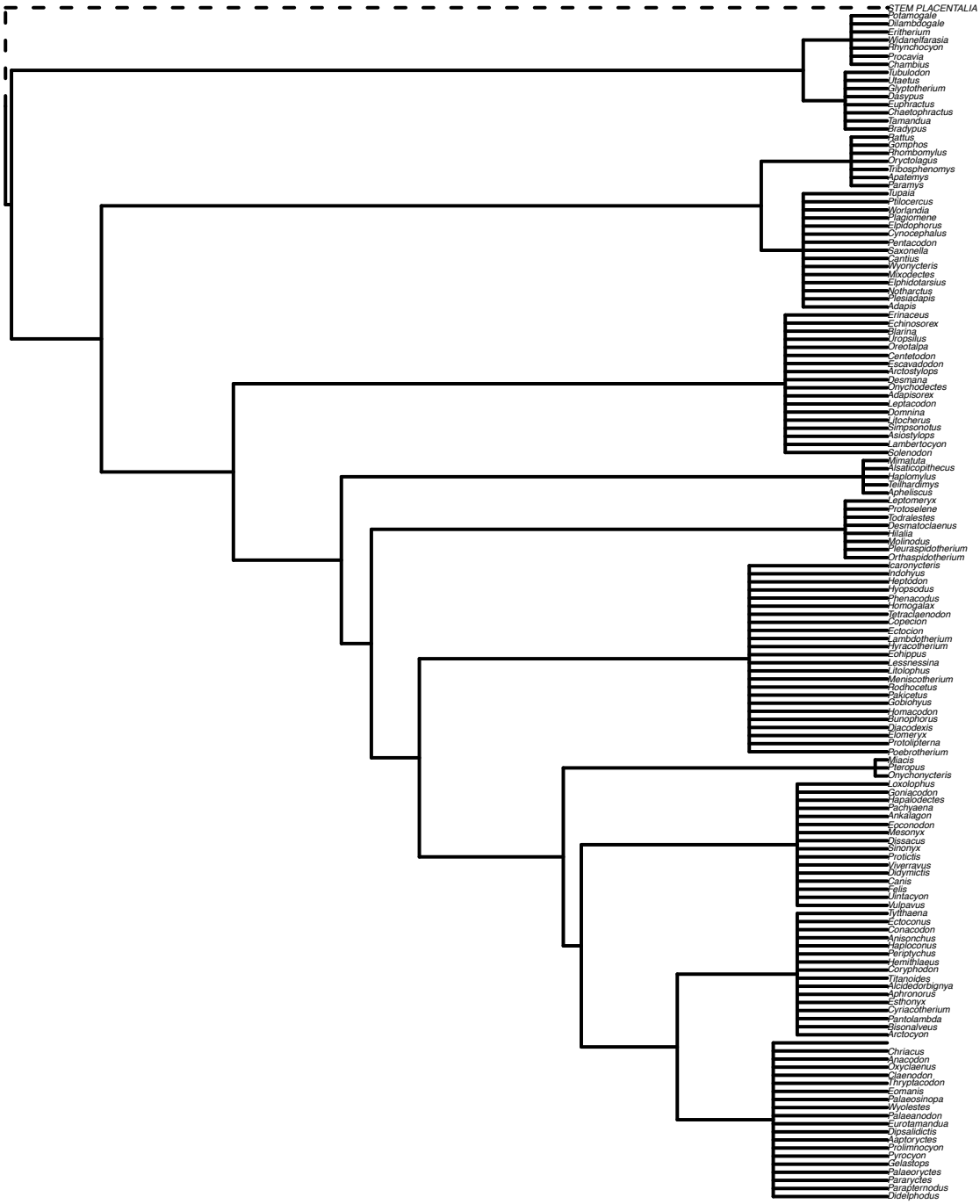


Figure S3.1f. Backbone tree, part (f), showing crow placental mammals and their relationship to stem placentals.

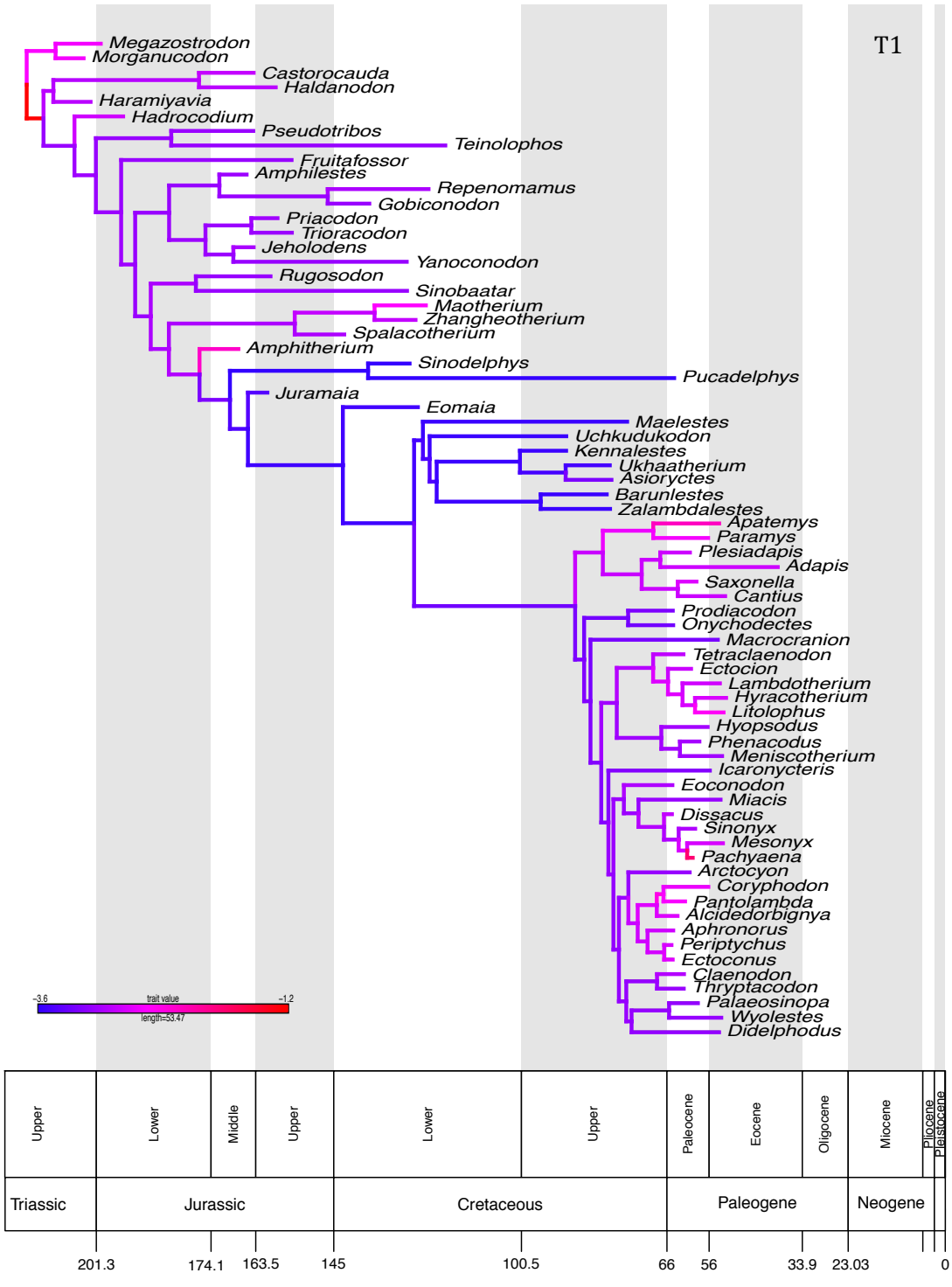


Figure S3.2. Supertree 1 showing rates of jaw functional trait change across all six PC axes through time. Warmer colours depict higher rates, and cooler colours indicate slower rates.

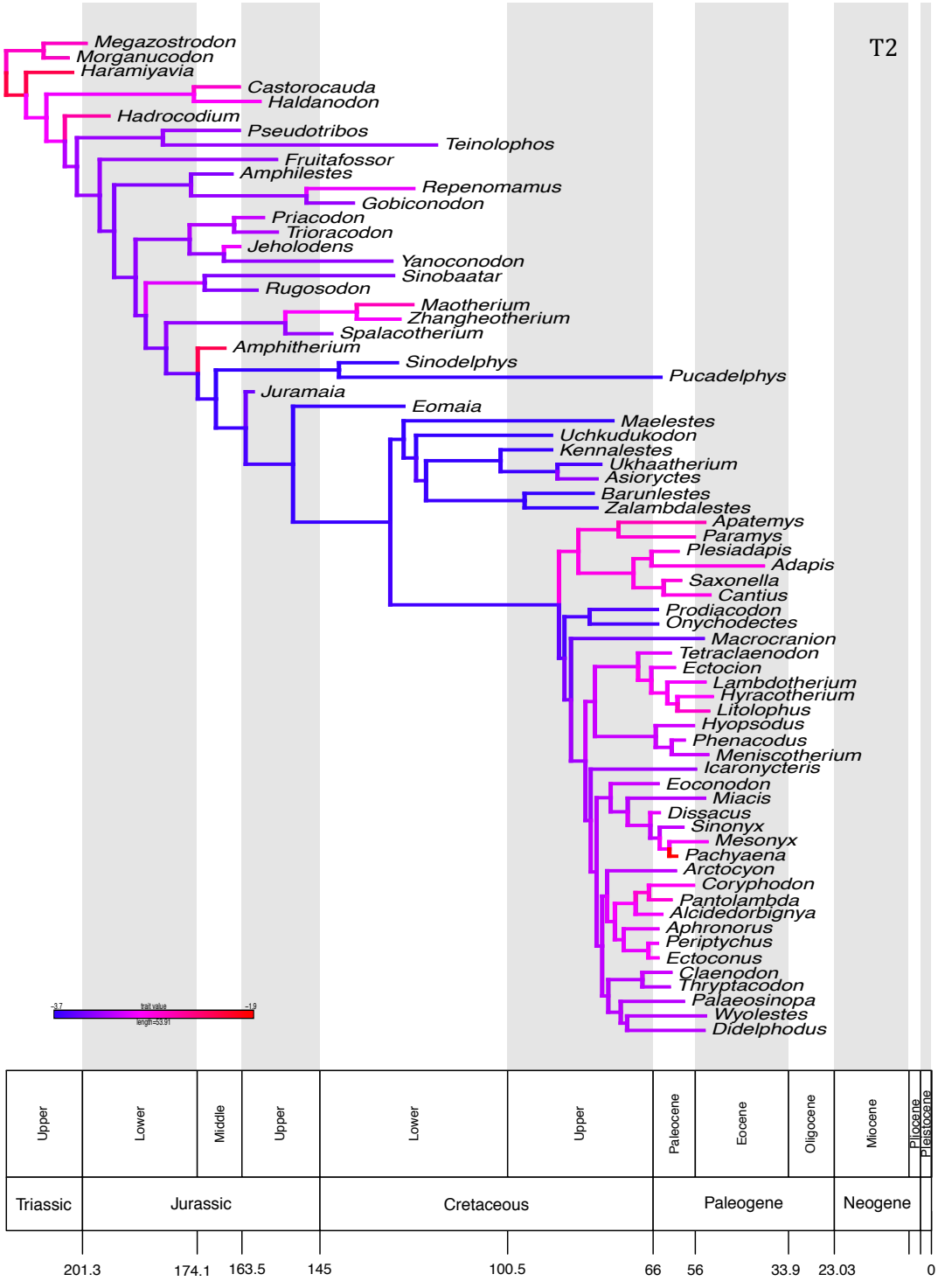


Figure S3.3. Supertree 2 showing rates of jaw functional trait change across all six PC axes through time. Warmer colours depict higher rates, and cooler colours indicate slower rates.

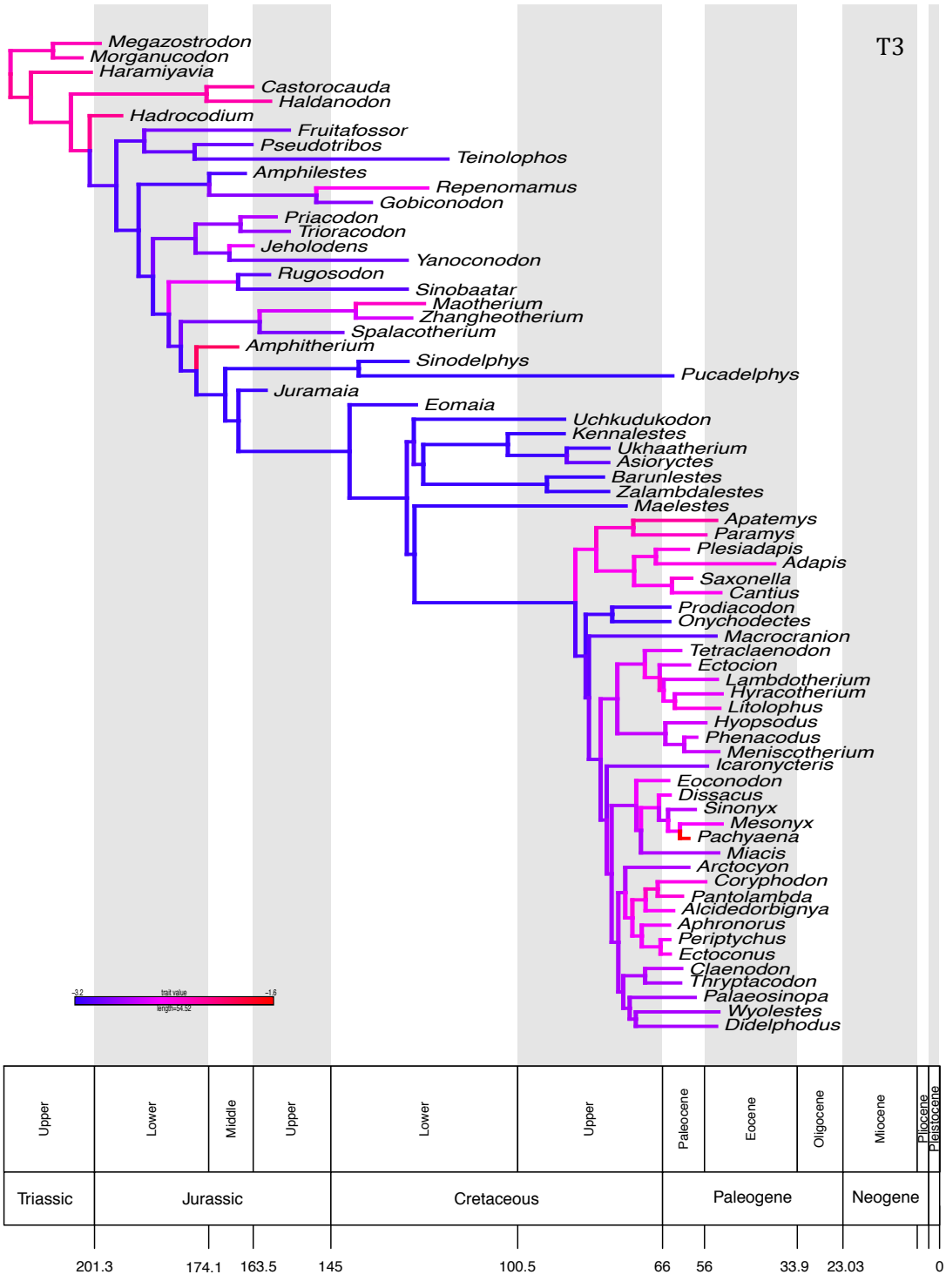


Figure S3.4. Supertree 3 showing rates of jaw functional trait change across all six PC axes through time. Warmer colours depict higher rates, and cooler colours indicate slower rates.

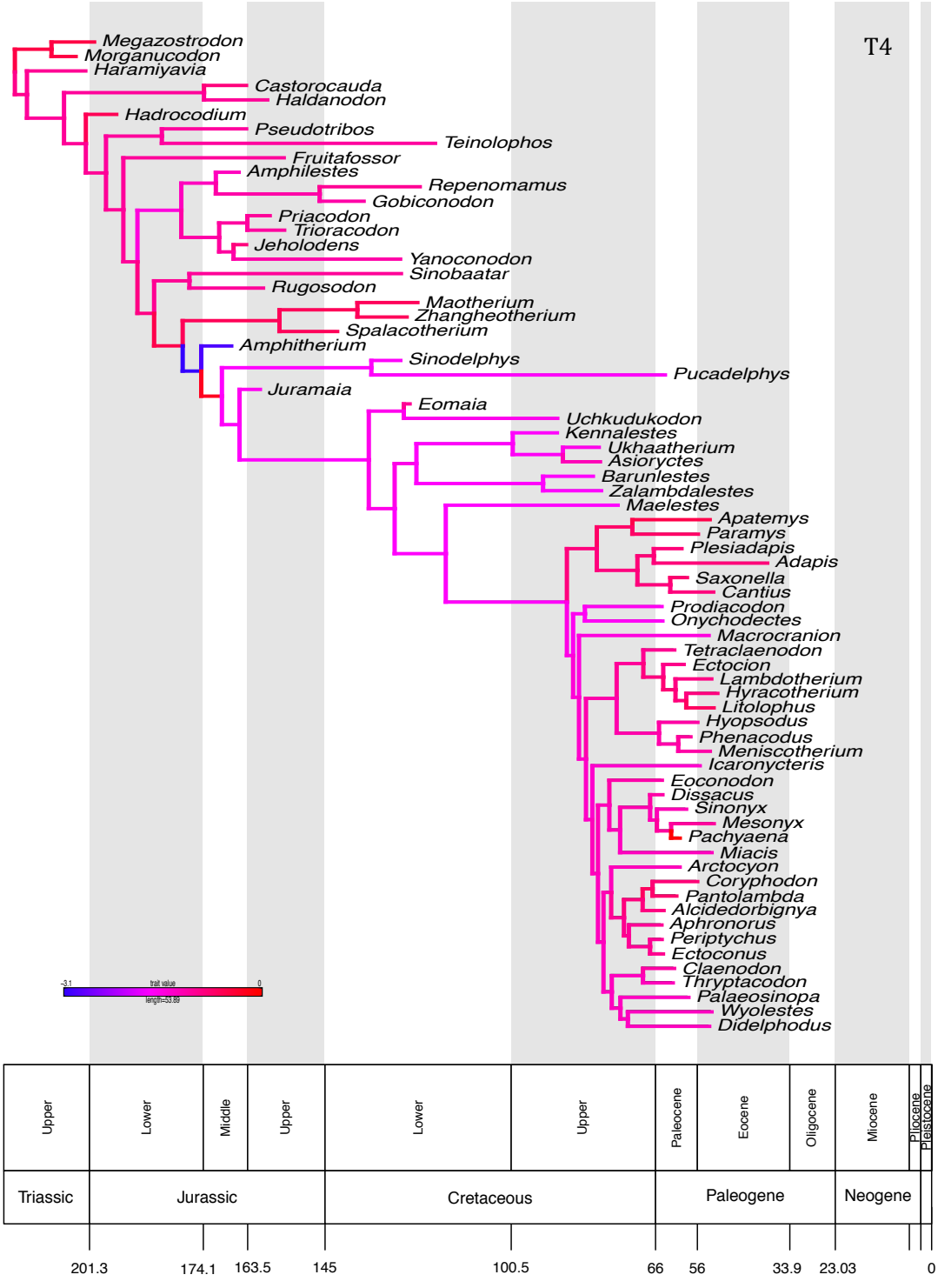


Figure S3.5. Supertree 4 showing rates of jaw functional trait change across all six PC axes through time. Warmer colours depict higher rates, and cooler colours indicate slower rates.

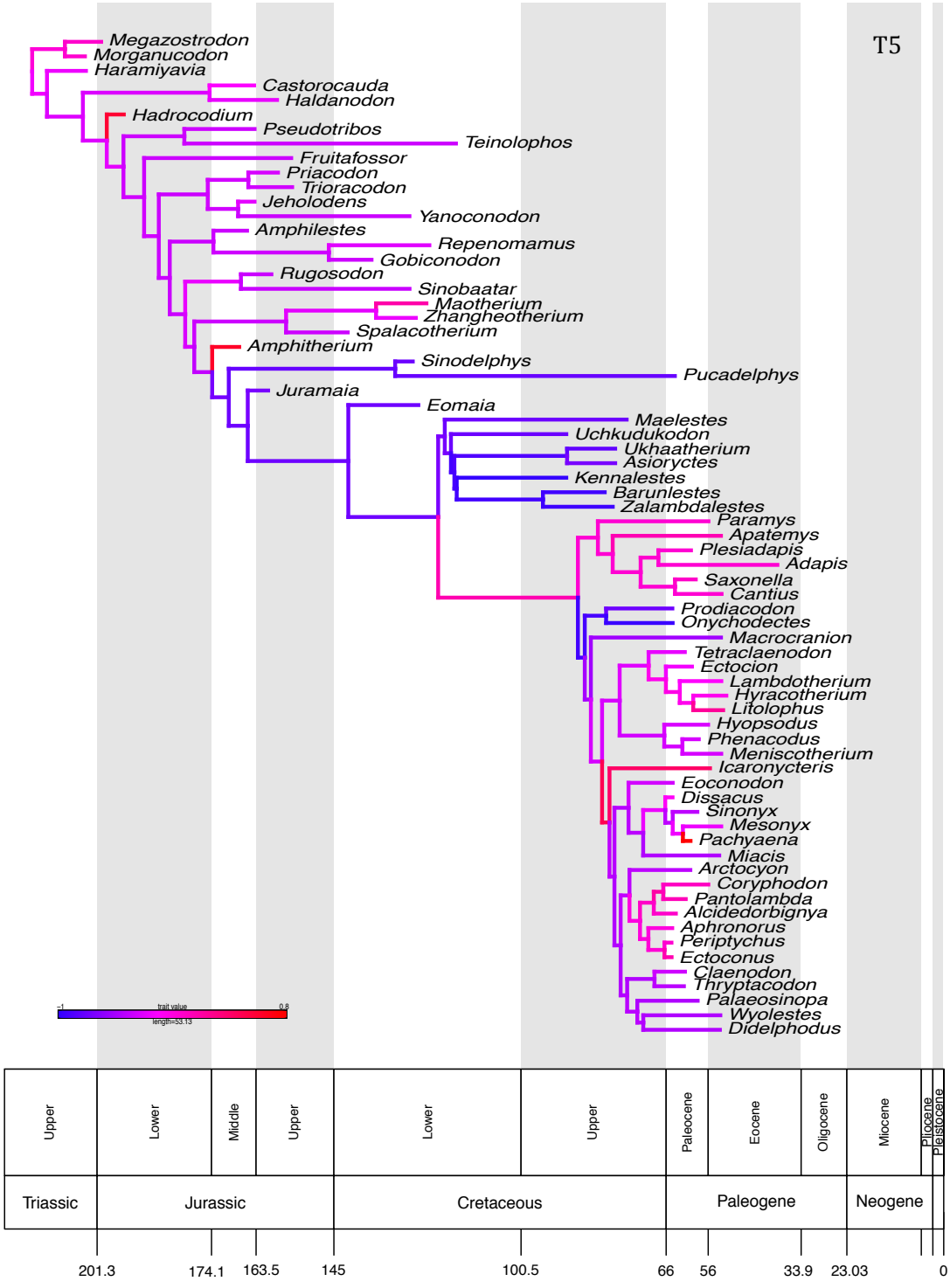


Figure S3.6. Supertree 5 showing rates of jaw functional trait change across all six PC axes through time. Warmer colours depict higher rates, and cooler colours indicate slower rates.

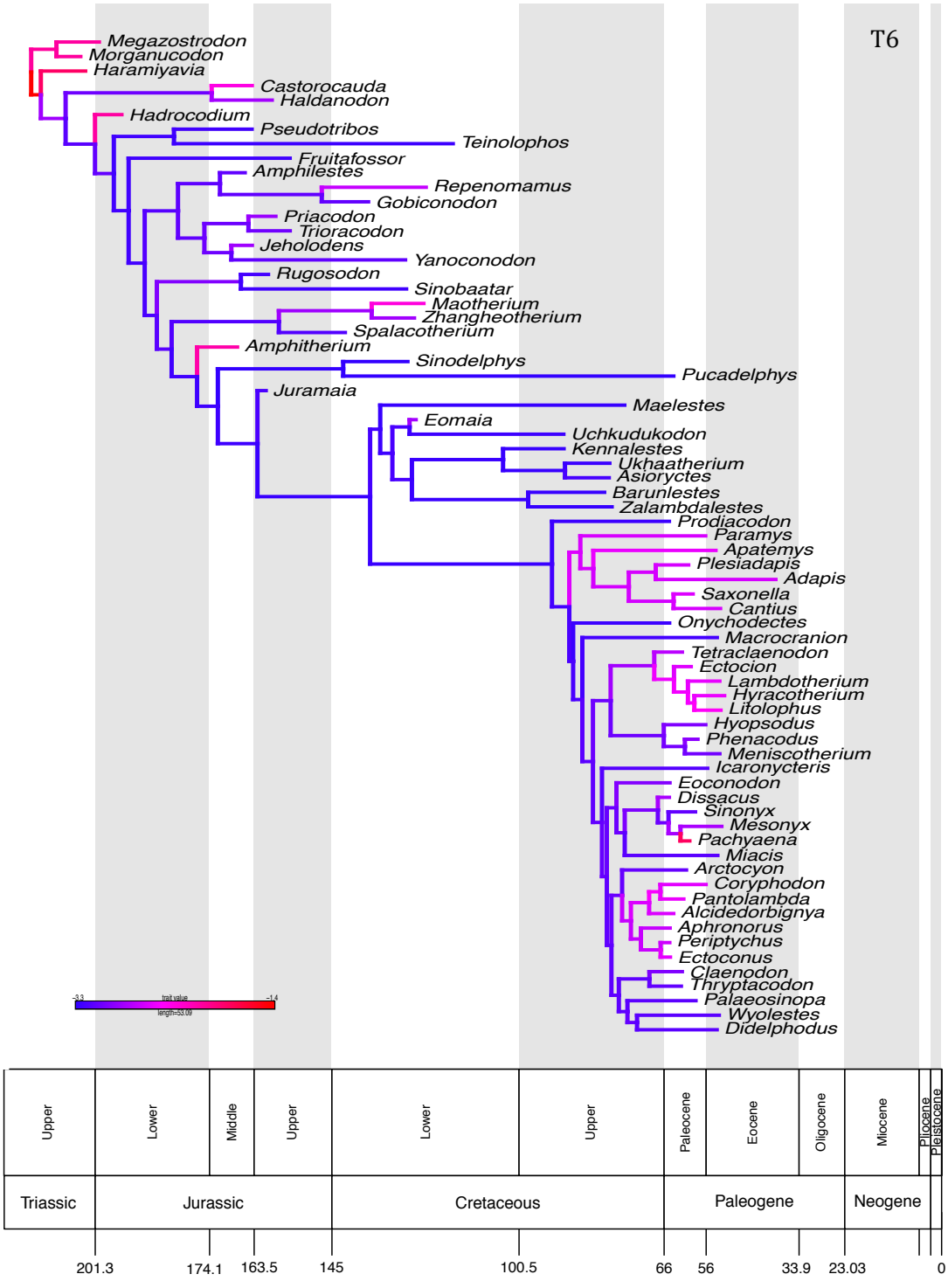


Figure S3.7. Supertree 6 showing rates of jaw functional trait change across all six PC axes through time. Warmer colours depict higher rates, and cooler colours indicate slower rates.

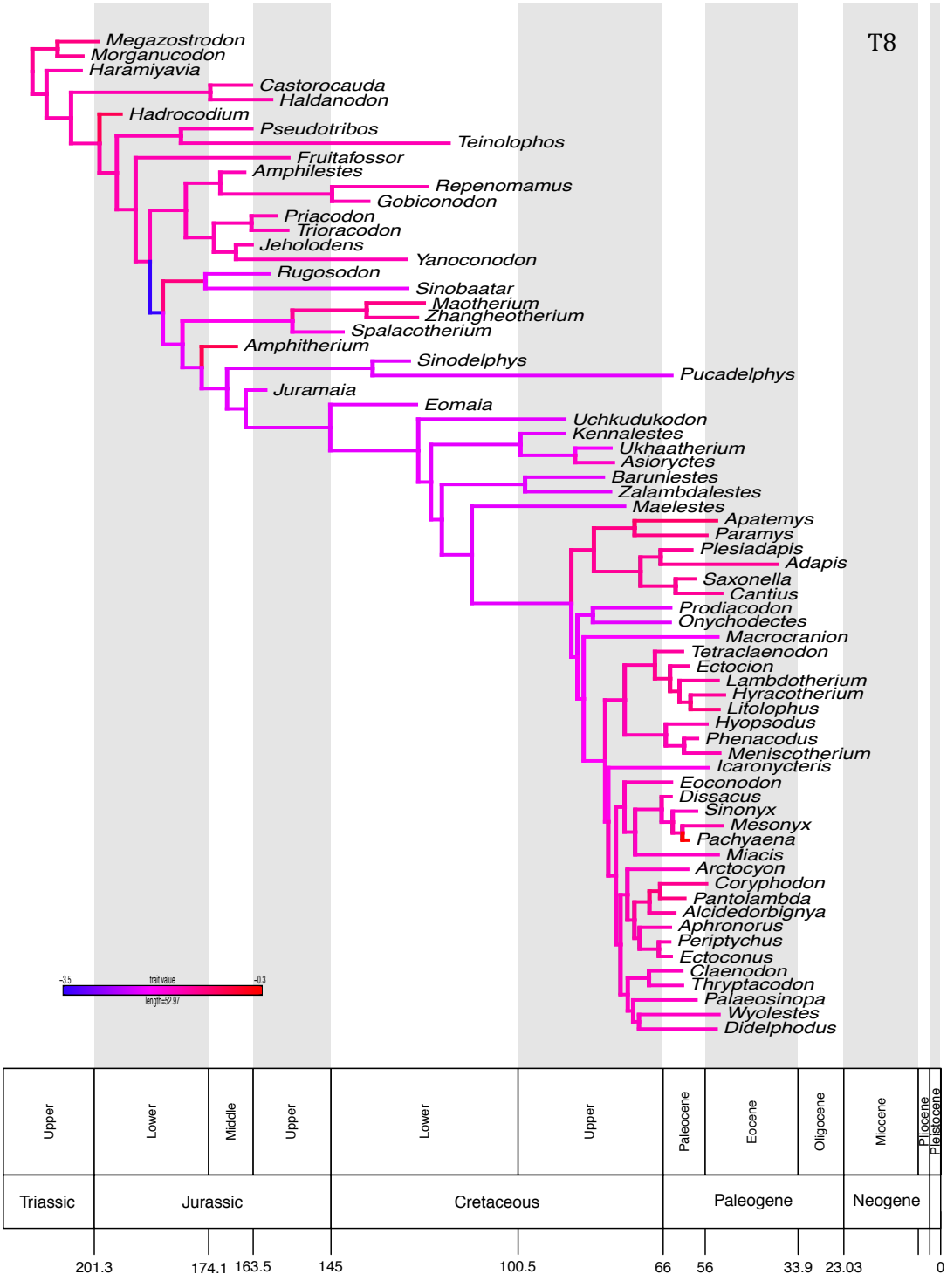


Figure S3.8. Supertree 8 showing rates of jaw functional trait change across all six PC axes through time. Warmer colours depict higher rates, and cooler colours indicate slower rates.

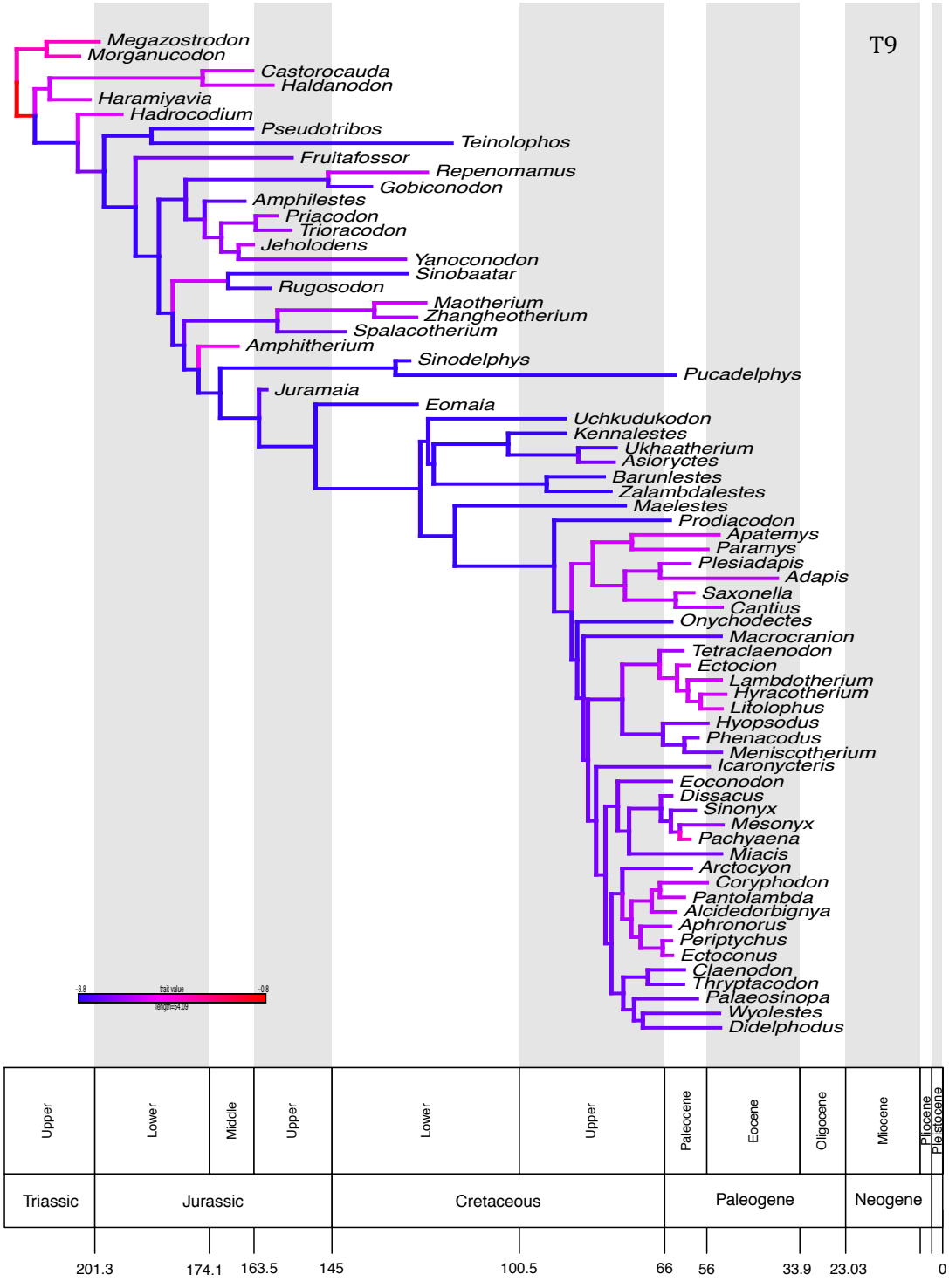


Figure S3.9. Supertree 9 showing rates of jaw functional trait change across all six PC axes through time. Warmer colours depict higher rates, and cooler colours indicate slower rates.

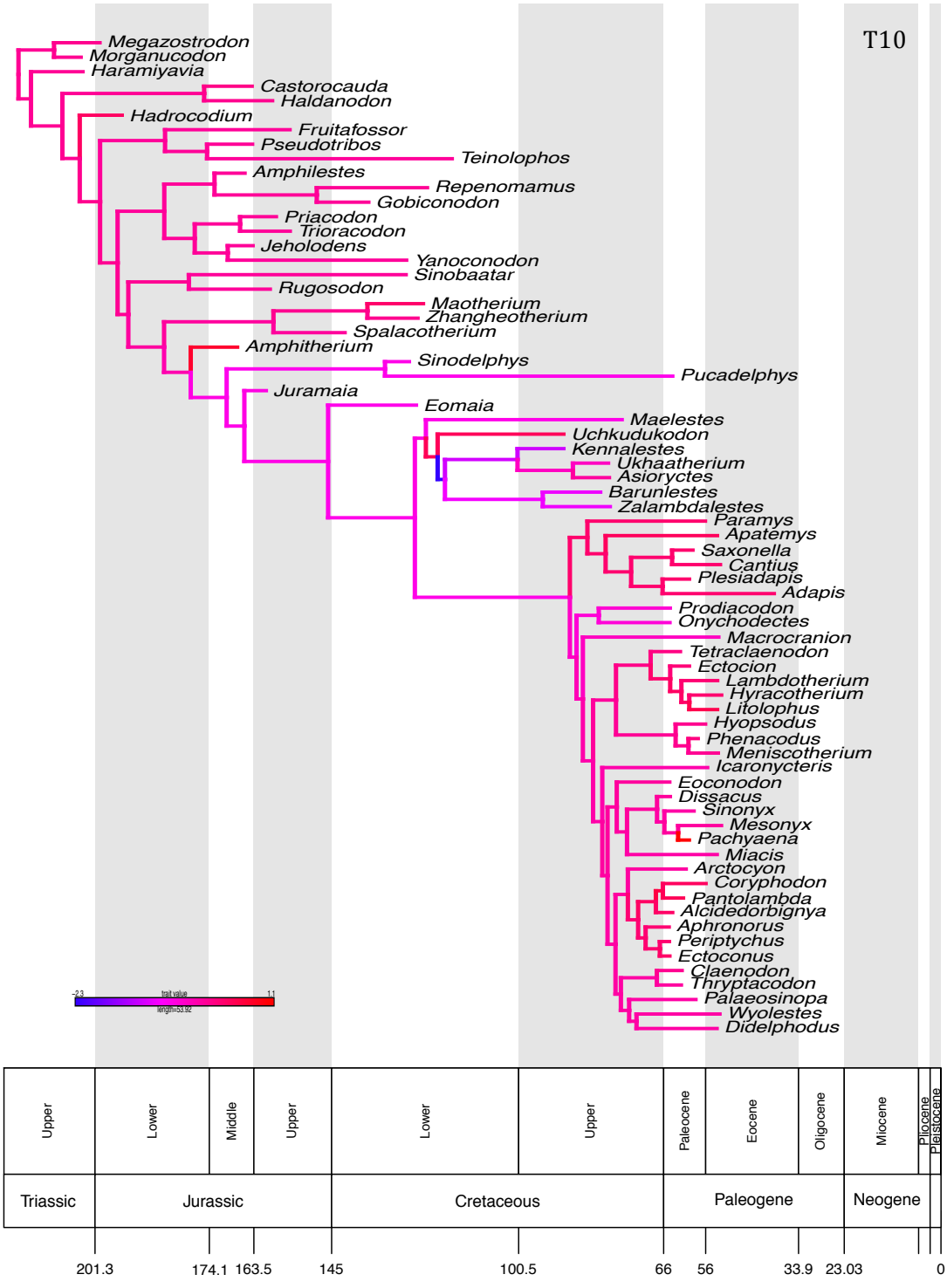


Figure S3.10. Supertree 10 showing rates of jaw functional trait change across all six PC axes through time. Warmer colours depict higher rates, and cooler colours indicate slower rates.

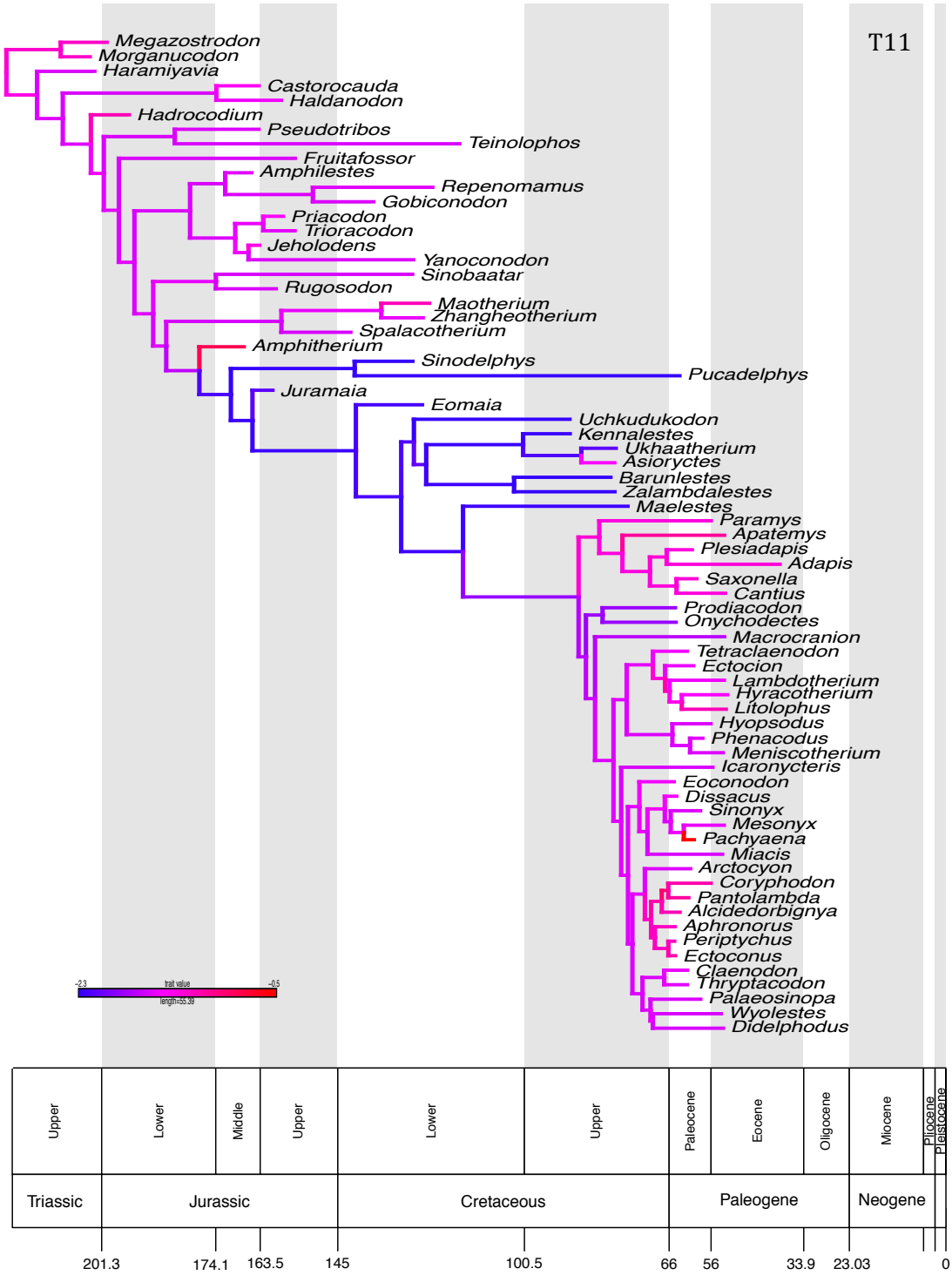


Figure S3.11. Supertree 11 showing rates of jaw functional trait change across all six PC axes through time. Warmer colours depict higher rates, and cooler colours indicate slower rates.

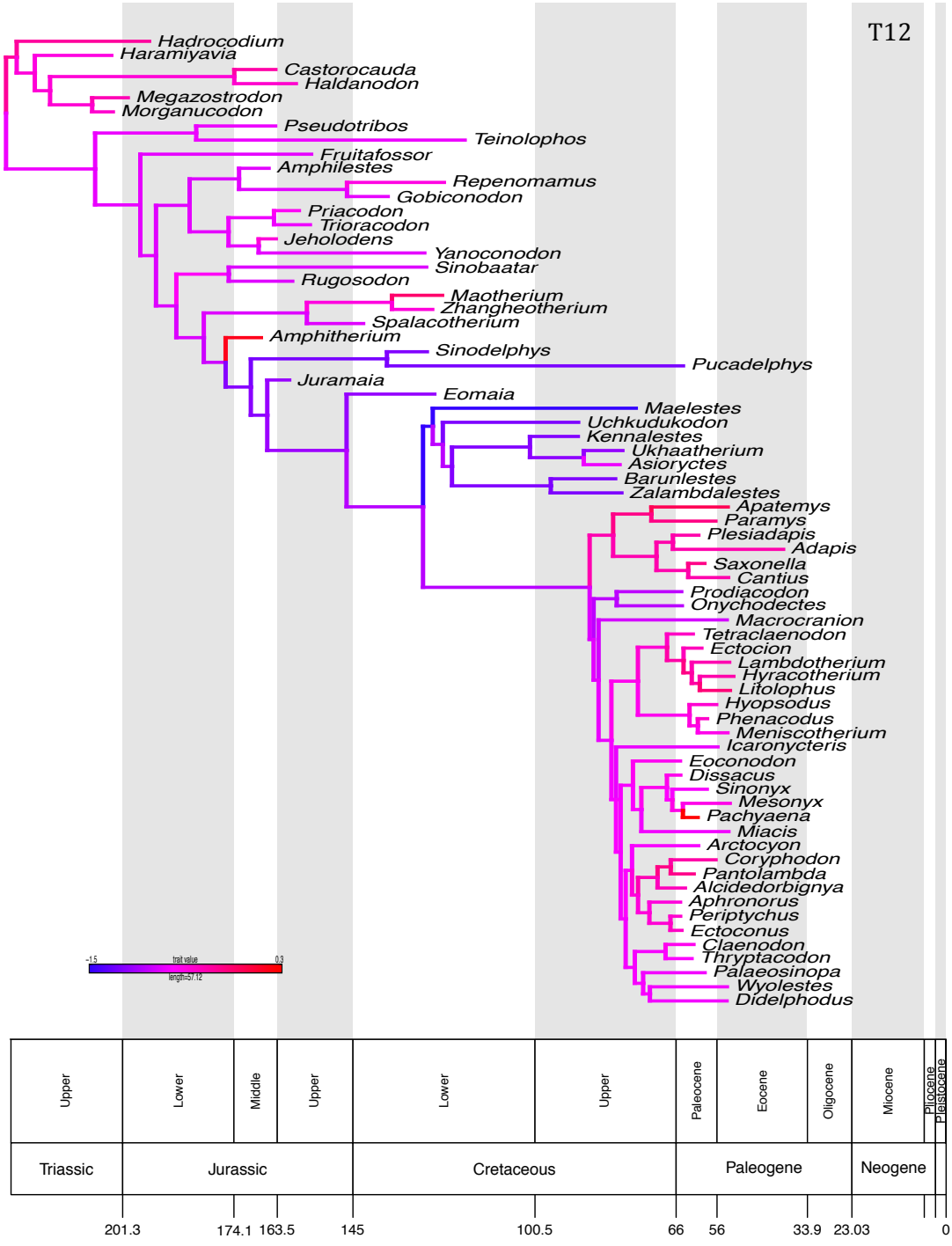


Figure S3.12. Supertree 12 showing rates of jaw functional trait change across all six PC axes through time. Warmer colours depict higher rates, and cooler colours indicate slower rates.

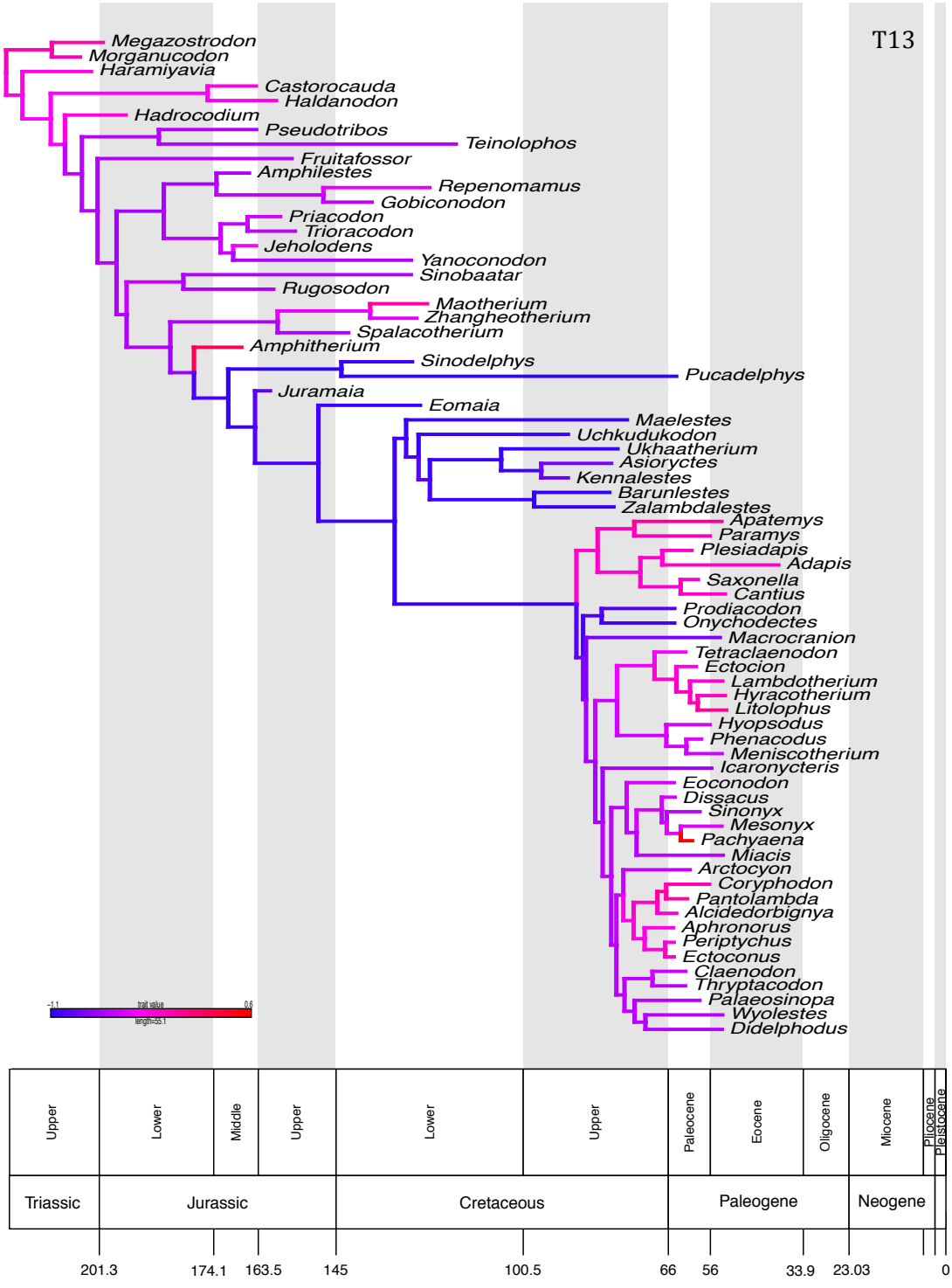


Figure S3.13. Supertree 13 showing rates of jaw functional trait change across all six PC axes through time. Warmer colours depict higher rates, and cooler colours indicate slower rates.

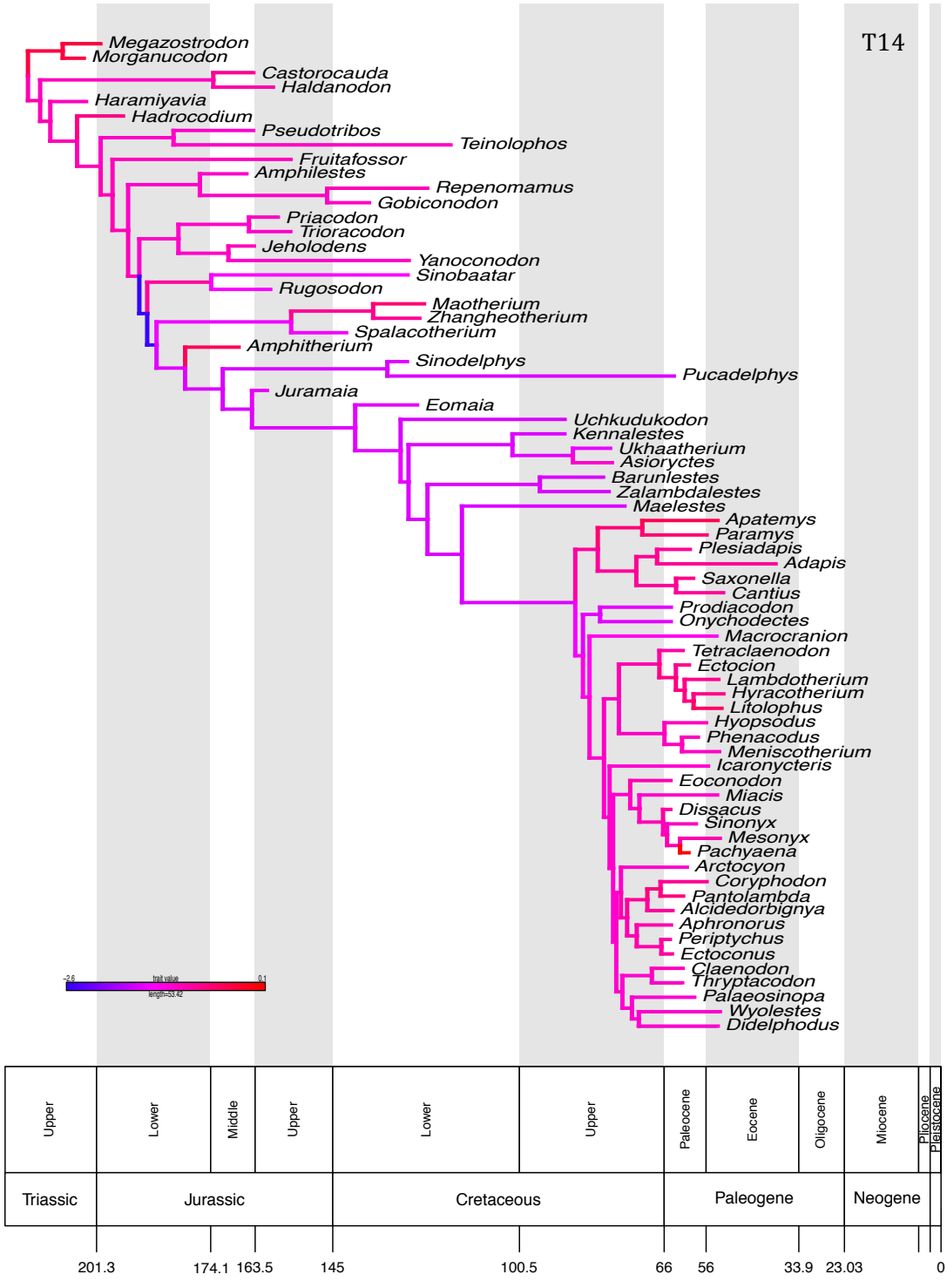


Figure S3.14. Supertree 14 showing rates of jaw functional trait change across all six PC axes through time. Warmer colours depict higher rates, and cooler colours indicate slower rates.

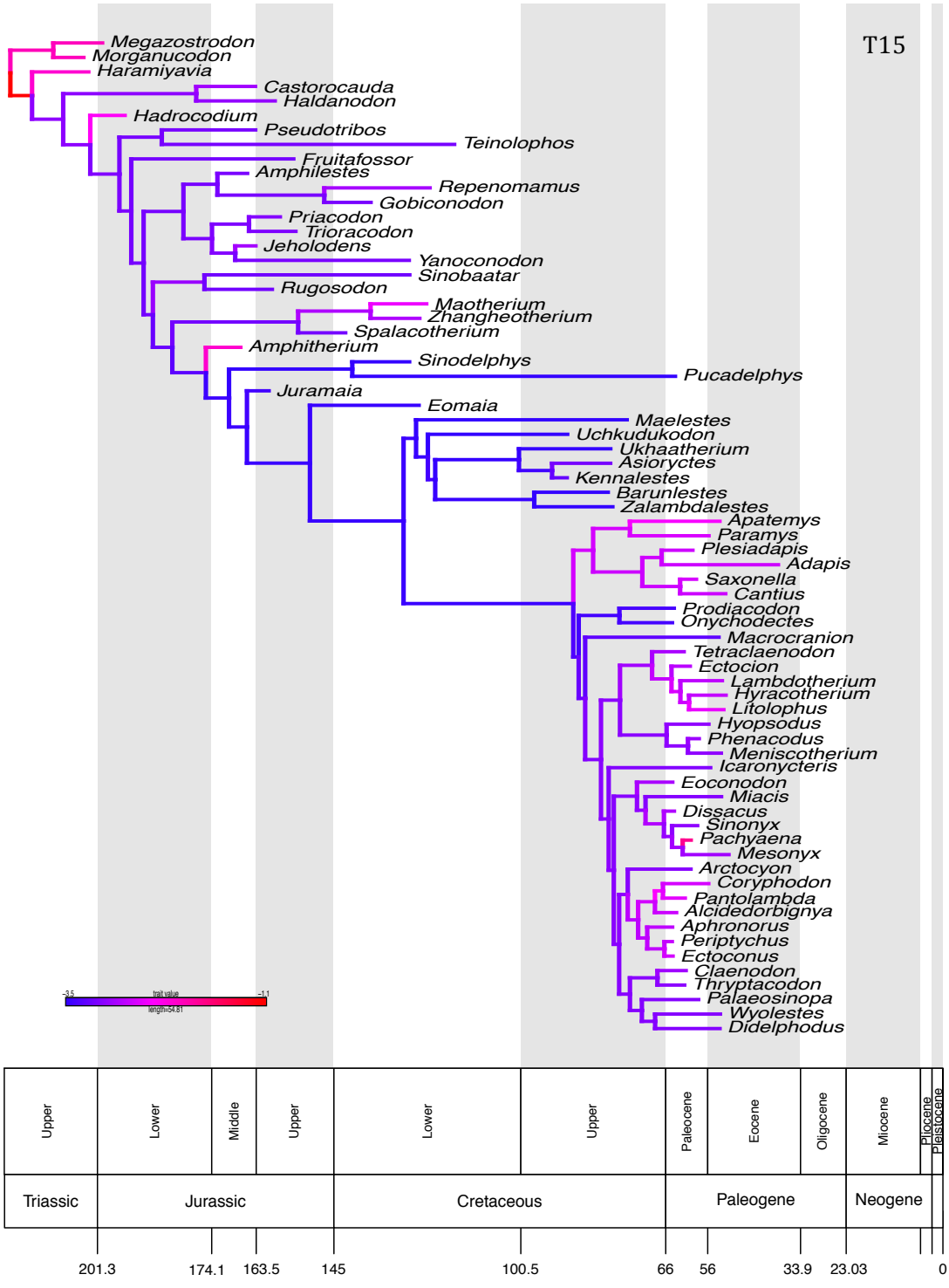


Figure S3.15. Supertree 15 showing rates of jaw functional trait change across all six PC axes through time. Warmer colours depict higher rates, and cooler colours indicate slower rates.

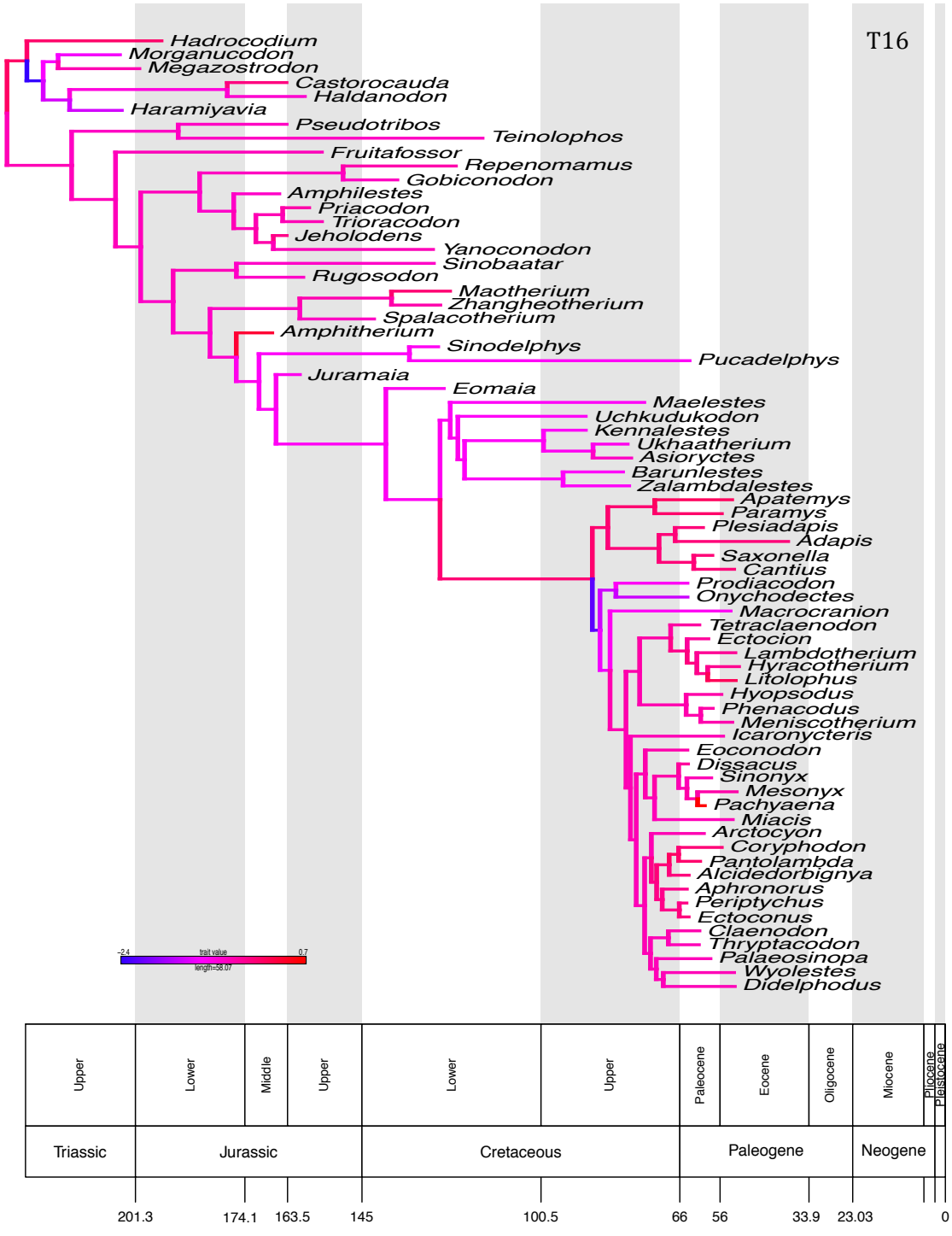


Figure S3.16. Supertree 16 showing rates of jaw functional trait change across all six PC axes through time. Warmer colours depict higher rates, and cooler colours indicate slower rates.

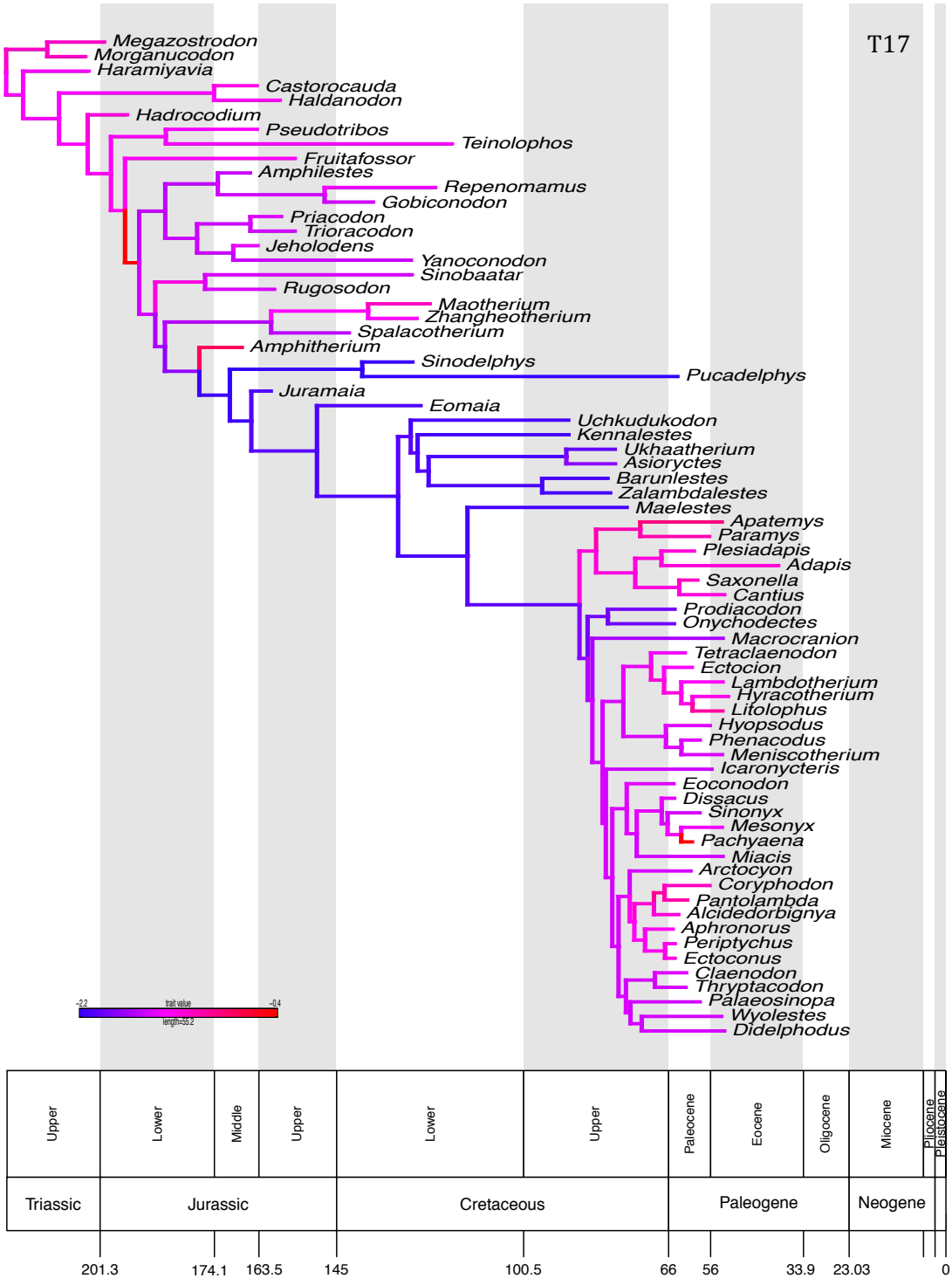


Figure S3.17. Supertree 17 showing rates of jaw functional trait change across all six PC axes through time. Warmer colours depict higher rates, and cooler colours indicate slower rates.

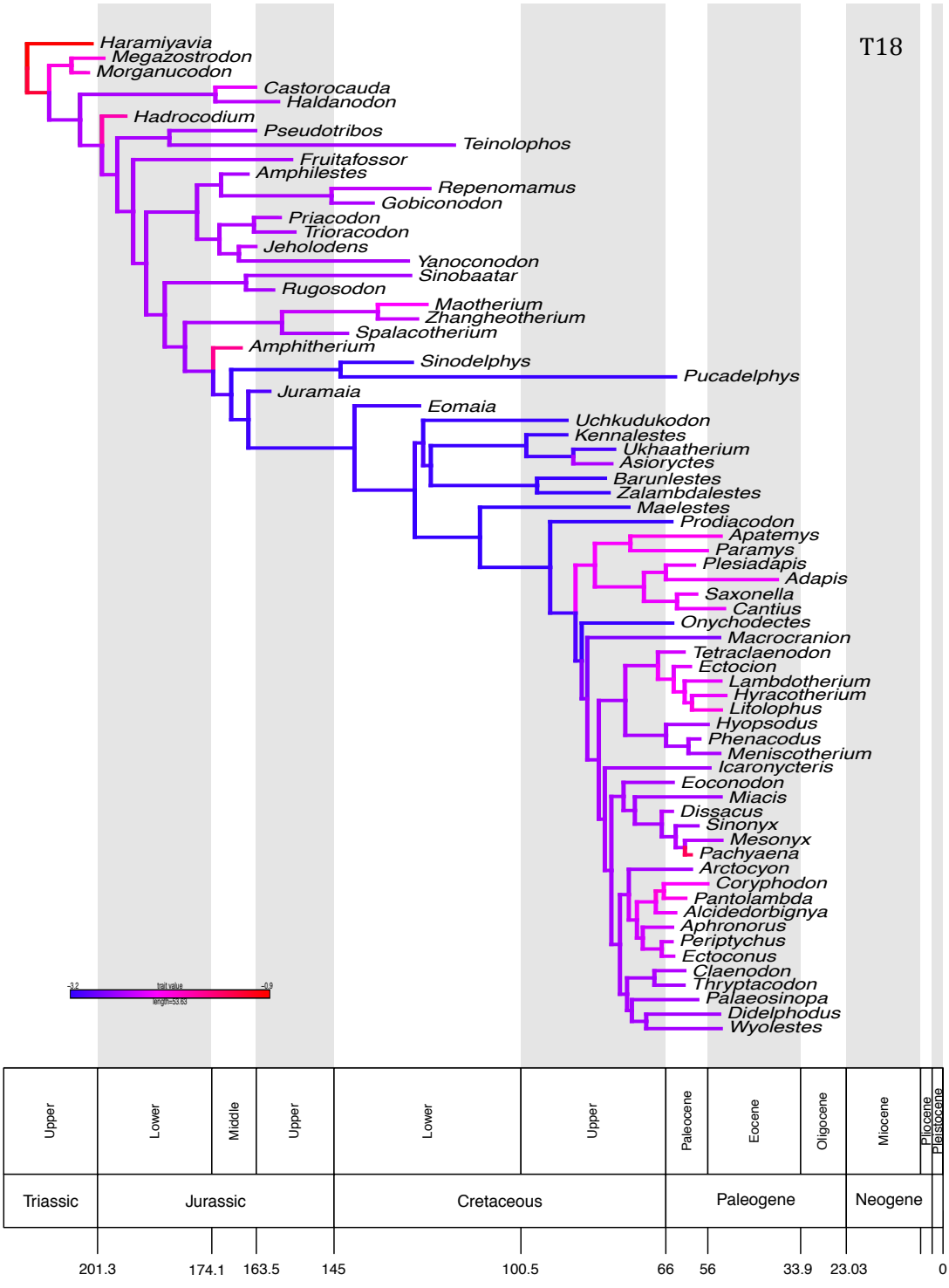


Figure S3.18. Supertree 18 showing rates of jaw functional trait change across all six PC axes through time. Warmer colours depict higher rates, and cooler colours indicate slower rates.

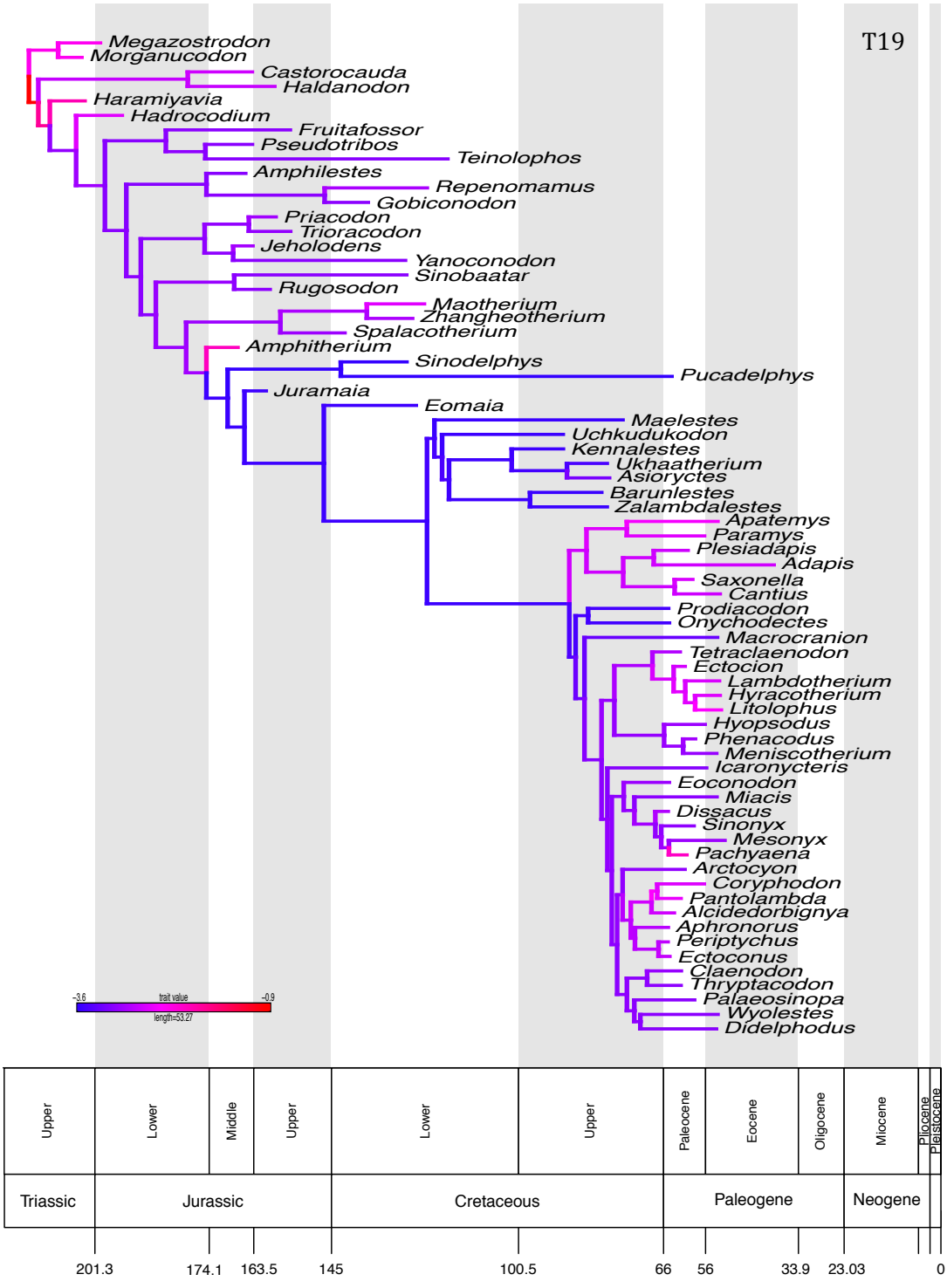


Figure S3.19. Supertree 19 showing rates of jaw functional trait change across all six PC axes through time. Warmer colours depict higher rates, and cooler colours indicate slower rates.

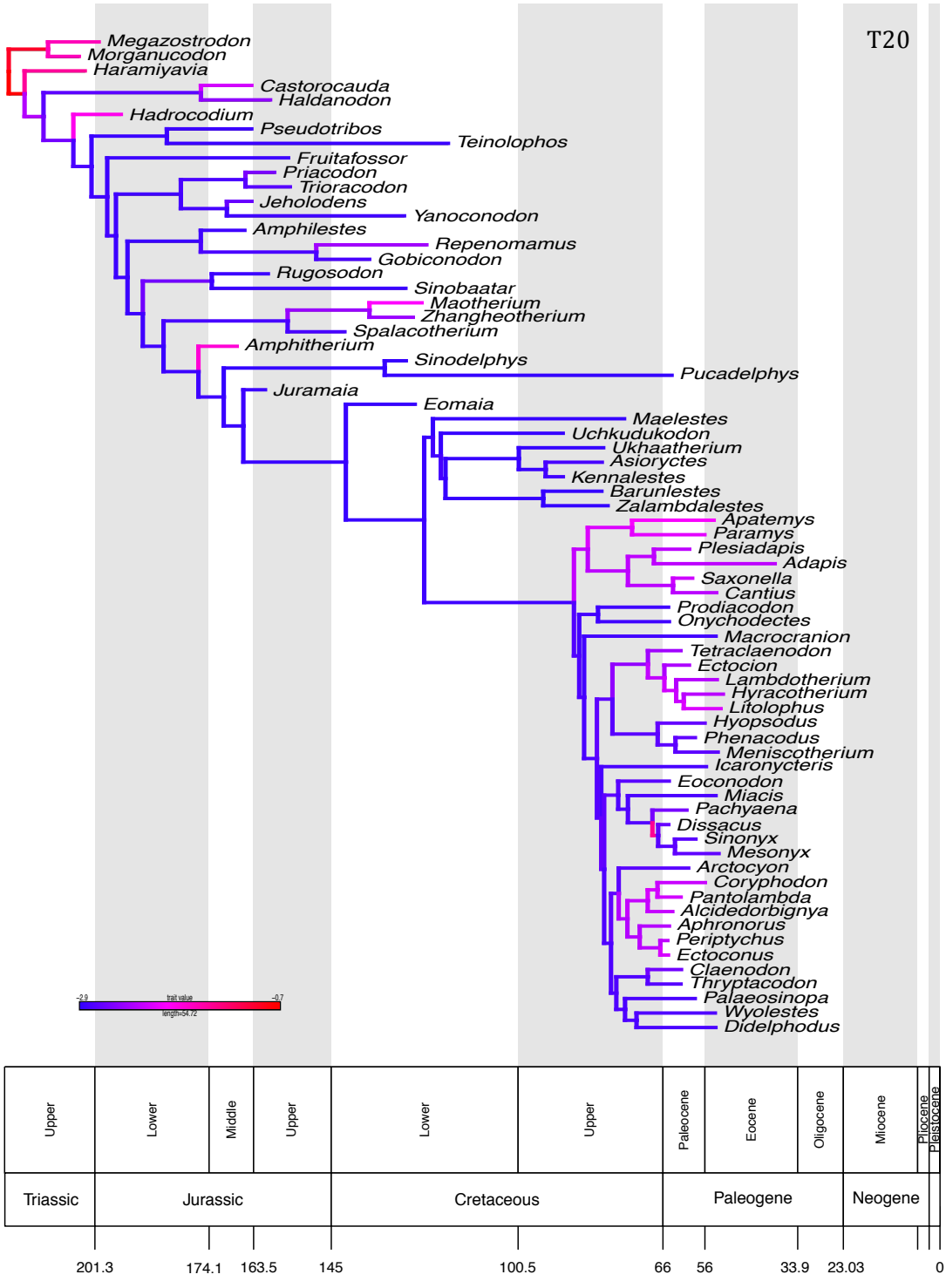


Figure S3.20. Supertree 20 showing rates of jaw functional trait change across all six PC axes through time. Warmer colours depict higher rates, and cooler colours indicate slower rates.

Supplementary References

Averianov AO, Lopatin AV (2011) Phylogeny of triconodonts and symmetrodonts and the origin of extant mammals. *Dokl. Biol. Sci.* 436:32-35.

Butler PM (2000) Review of the early allotherian mammals. *Acta Palaeontol Pol* 45:317-342.

Chow M, Qi T (1978) Paleocene Mammalian Fossils from Nomogen Formation of Inner Mongolia. *Vertebrata PalAsiatica* 16(2):77-85.

Grossnickle DM, Newham E (2016) Therian mammals experience an ecomorphological radiation during the Late Cretaceous and selective extinction at the K-Pg boundary. Proc. R. Soc. B 283:20160256.

Hahn G, Hahn R (2006) Evolutionary tendencies and systematic arrangement in the Haramiyida (Mammalia). Geol. Palaeontol. 40:173-193.

Huttenlocker AK, Grossnickle DM, Kirkland JI, Schultz JA, Luo Z-X (2018) Late-surviving stem mammal links the lowermost Cretaceous of North America and Gondwana. *Nature* 558:108-112.

Ji Q, Luo Z-X, Yuan C-X, Wible JR, Zhang J-P, Georgi JA (2002) The earliest known eutherian mammal. *Nature* 416:816–822.

Kielan-Jaworowska Z, Cifelli RL, Luo Z-X (2004) Mammals from the Age of Dinosaurs: Origins, Evolution, and Structure (Columbia Univ. Press, New York).

Luo Z-X, Gatesy SM, Jenkins Jr FA, Amaral WW, Shubin NH (2015) Mandibular and dental characteristics of Late Triassic mammaliaform Haramiyavia and their ramifications for basal mammal evolution. *PNAS* 112(51):E7101-E7109

Luo Z-X, Ji Q, Yuan C-X (2007) Convergent dental adaptations in pseudo-tribosphenic and tribosphenic mammals. *Nature* 450:93–97.

Luo Z-X, Yuan C-X, Meng Q-J, Ji Q (2011) A Jurassic eutherian mammal and divergence of marsupials and placentals. *Nature* 476:442–445.

Meehan TJ, Martin LD (2004) Emended genus description and a new species of *Hypisodus* (Artiodactyla: Ruminantia: Hypertragulidae). *Paleogene Mammals, New Mexico Museum of Natural History and Science Bulletin No. 26*, eds Lucas SG, Zeigler KE, Kondrashov PE (Authority of the State of New Mexico), pp 137-143.

Meng J, Bi S, Zheng X, Wang X (2018) Ear ossicle morphology of the Jurassic euharamiyidan *Arboroharamiya* and evolution of mammalian middle ear. *Journal of Morphology* 279(4):441-457

Mihlbachler MC (2008) Species Taxonomy, Phylogeny, and Biogeography of the Brontotheriidae (Mammalia: Perissodactyla). *Bull. Am. Mus. Nat. Hist.* 311:1-475.

O'leary MA et al (2013) The Placental Mammal Ancestor and the Post–K-Pg Radiation of Placentals. Science 339(6120):662-667.

Rauhut OWM, Martin T, Ortiz-Jaureguizar E, Puerta P (2002) A Jurassic mammal from South America. *Nature* 416:165–168.

Rich TH, Flannery TF, Trusler P, Kool L, Van Klaveren, Patricia Vickers-Rich P (2002) Evidence that monotremes and ausktribosphenids are not sistergroups, *J. Vertebr. Paleontol.* 22(2):466-469

Rich TH, Vickers-Rich P (2013) Palaeobiogeography of Mesozoic Mammals – Revisited. *Earth and Life: Global Biodiversity, Extinction Intervals and Biogeographic Perturbations through Time*, eds Talent JA (Springer, New York), pp 913-934.

Williamson TE, Brusatte SL (2013) New Specimens of the Rare Taeniodont Wortmania (Mammalia: Eutheria) from the San Juan Basin of New Mexico and Comments on the Phylogeny and Functional Morphology of "Archaic" Mammals. *PLoS One* 8(9):1-35.

Wible JR, Rougier GW, Novacek MJ, Asher RJ (2009) The eutherian mammal *Maelestes gobiensis* from the Late Cretaceous of Mongolia and the phylogeny of Cretaceous Eutheria*. Bull. Am. Mus. Nat. Hist.* 327*(*1*).*

Woodburne MO, Rich TH, Springer M (2003) The evolution of tribospheny in Mesozoic mammals. *Mol Phylogenet Evol* 28:360–385.